Optimized Waveform Relaxation Methods for Circuit Simulations

Mohammad D. Al-Khaleel

Department of Mathematics and Statistics,

McGill University, Montréal

Québec, Canada

January, 2007

A thesis submitted to the Faculty of Graduate Studies and Research

in partial fulfillment of the requirements of the degree of

Doctor of Philosophy

Your file Votre référence
ISBN: 978-0-494-32132-4
Our file Notre référence
ISBN: 978-0-494-32132-4

Abstract

Waveform Relaxation methods are very efficient and reliable methods. They have been widely used in several fields, including circuit theory, for solving large systems of ordinary differential equations and solving partial differential equations. A new approach called optimized waveform relaxation algorithms was recently introduced which greatly improved convergence by using new transmission conditions. These conditions are responsible for the exchange of information between subsystems. In this thesis, we demonstrate that the transmission conditions have a tremendous influence on the convergence of the waveform relaxation algorithms for circuit simulations. We first derive new waveform relaxation methods for a general circuit and its associated system of ordinary differential equations, and give transmission conditions with optimal performance. These optimal transmission conditions are however not convenient to use and thus we introduce approximations for them. We then determine numerically the approximate transmission conditions with the best performance of the new waveform relaxation algorithms for two model problems, and we show how much the convergence can be improved compared to the classical waveform relaxation algorithm. We then start a detailed study of optimized waveform relaxation algorithms for RC type circuits. We first analyze RC circuits of any finite size, and give optimal transmission conditions. We again propose approximations for the optimal transmission conditions which are optimized based on numerical insight. Then we choose a very small RC circuit which has only one cell and a small RC circuit which has three

cells to further study the quality of the approximations. For the very small RC circuit we show that the optimal transmission conditions are indeed local operators in time, they are first degree time derivatives which are convenient to use. However, we also propose a constant approximation of the optimal transmission conditions which is simpler to use and we prove the optimality of this approximation. For the small RC circuit we also prove the optimality of the proposed constant approximation, and find asymptotically an optimized first order approximation. We then study an infinitely large RC circuit to demonstrate that the size of the circuit does not have a major impact on the convergence of the optimized waveform relaxation methods. We recall the optimality proof for the constant approximation given in [1], and we give an asymptotic result for an optimized first order approximation. We show that results found for the infinitely large RC circuit are indeed limits of those found for the finite size RC circuit as the size of the circuit goes to infinity. We next start a detailed study of optimized waveform relaxation algorithms for transmission line type circuits. We give optimal transmission conditions which we approximate by constants. We analyze very small and small transmission line circuits, which have one cell and two cells respectively, and we find asymptotically optimized constant transmission conditions for both. We consider also an infinitely large transmission line circuit, and we give an optimized constant approximation based on an asymptotic analysis. We finally show that the systems representing the circuits considered are semi-discretizations of particular partial differential equations, and in addition, we show that the new transmission conditions introduced for the circuit problems imply the ones associated with the partial differential equations at the continuous level. We also show that the convergence factors and the solutions obtained by applying the new waveform relaxation algorithms to the partial differential equations converge to those obtained by applying the algorithms to the circuit systems. In order to demonstrate the practicality and the efficiency of the optimized waveform relaxation methods, we give numerical experiments that show the drastically improved convergence behavior.

Résumé

Les méthodes de relaxation d'ondes sont très efficaces et fiables. Elles sont utilisées avec succès dans plusieurs domaines (par exemple en théorie des circuits) pour résoudre des systèmes d'équations ordinaires ou aux dérivées partielles de grandes dimensions. Une nouvelle approche, appelée méthode de relaxation d'ondes optimisée, a été récemment introduite, elle améliore de façon remarquable la convergence en introduisant des nouvelles conditions de transmission. Ces conditions sont responsables de l'échange d'information entre les sous-systèmes. Dans cette thèse, nous démontrons que les conditions de transmission ont une influence énorme sur la convergence des algorithmes de relaxation d'ondes pour des circuit simulés. Nous développons d'abord les nouvelles méthodes de relaxation d'ondes pour un circuit général et son système d'équations différentielles ordinaires associé, et nous donnons les conditions de transmission de performance optimale. Cependant, ces conditions de transmission optimales ne sont pas commodes à utiliser et c'est ainsi que nous introduisons des approximations. Nous approximons alors numériquement les conditions de transmission à l'aide des nouveaux algorithmes de relaxation d'ondes ayant une meilleure performance, et ce pour deux problèmes types. Nous montrons de combien la convergence peut être améliorée en comparaison avec celle de l'algorithme classique de relaxation d'ondes. Nous commençons alors une étude détaillée des algorithmes optimisés de relaxation d'ondes pour des circuits RC. Nous analysons d'abord des circuits RC de n'importe quelle taille finie, et nous donnons des conditions de transmission optimales.

Sur la base de perspicacité numérique, nous proposons aussi des approximations optimisées des conditions de transmission optimales. Nous choisissons ensuite un circuit RC très petit qui a seulement une cellule et un autre petit circuit RC qui a trois cellules, et nous étudions d'avantage la qualité des approximations. Pour le circuit RC très petit, nous montrons que les conditions de transmission optimales sont en fait des opérateurs locaux en temps. Elles sont les premières dérivées par rapport au temps, qui sont très commodes à utiliser. Cependant, nous proposons également une approximation constante des conditions de transmission optimales qui est plus simple à utiliser et nous prouvons l'optimalité de cette approximation. Pour le petit circuit RC, nous prouvons également l'optimalité de l'approximation constante proposée, et trouvons asymptotiquement une approximation optimisée de premier ordre. Nous étudions alors un circuit RC infiniment grand pour démontrer que la taille du circuit n'a pas une influence importante sur la convergence des méthodes optimisées de relaxation d'ondes. Nous rappelons la preuve d'optimalité pour l'approximation constante donnée dans [1], et nous donnons un résultat asymptotique pour une approximation optimisée de premier ordre. Nous prouvons que les résultats trouvés pour le circuit RC infiniment grand sont les résultats limites de ceux trouvés pour le circuit RC fini lorsque la taille du circuit tend vers l'infini. Ensuite, nous commençons une étude détaille des algorithmes de relaxation d'ondes optimisés pour des circuits de lignes de transmission. Dans ce cas, nous donnons aussi les conditions de transmission optimales que nous approximons par des constantes. Comme précédemment, nous analysons deux circuits de lignes de transmission, un petit ayant deux cellules et un très petit n'en ayant qu'une. Pour chacun de ces circuits, nous trouvons asymptotiquement des constantes de conditions de transmissions optimisées. Nous considérons également un circuit de lignes de transmission infiniment grandes, et par une approximation basée sur une analyse asymptotique, nous donnons une constante optimisée. Nous prouvons finalement que les systèmes représentant les circuits considérés sont la semi-discrétisation d'équations différentielles partielles particulières. Nous prouvons en outre que les nouvelles conditions de transmission présentées pour les problèmes de circuit impliquent celles liées aux équations différentielles partielles continues. Nous prouvons également que les facteurs de convergence et les solutions obtenues en appliquant les nouveaux algorithmes de relaxation d'ondes aux équations différentielles partielles convergent vers ceux obtenus en appliquant les algorithmes aux systèmes de circuit. Afin de démontrer le caractère pratique et l'efficacité des méthodes optimisées de relaxation d'ondes, nous exhibons des expériences numériques qui mettent en évidence l'amélioration de la convergence.

Acknowledgments

I would like to thank my supervisor, Prof. Martin Gander, for his help, guidance, and advice during the work on this thesis. Without his contribution and insight, this humble work would not have been done. I am thankful to all professors, staff and students in the department. Special thanks to my friends, Mohammad Sababheh, Mohammad AlAkhras, Melanie Beck, Olivier Dubois, and Juan-Manuel Perez-Abarca for their valuable discussions. Many thanks to my parents, brothers, and sisters from whom I have been away during my study, for their support and encouragement.

Table of Contents

Chapter 1

Introduction

Traditional methods for solving systems of ordinary differential equations (ODEs) can become inefficient for very large systems of equations where different state variables are varying at different time rates. This is due to the fact that in applying the standard methods directly, the same method and timestep are used for every differential equation in the system. This identical discretization must be fine enough to represent all components accurately, including both the rapidly and slowly changing state variables in the system.

In the circuit domain, where we obtain large stiff systems of ODEs, many circuit solver methods have been introduced [2, 3] but the circuit simulation using these methods takes too much CPU time and too much storage to analyze a circuit. In the quest for improving the efficiency of the numerical techniques, by speeding up the solution of these large systems, and overcoming those drawbacks mentioned above, various approaches have been proposed based on partitioning and multirate techniques which are numerical methods that use different timesteps for different differential equations in the system. Indeed, by choosing for each set of differential equations in the system a maximum timestep that accurately reflects the behavior of their associated state variables, and if possible, applying a parallel process, the efficiency and performance of these methods will be greatly improved.

The idea here is to decompose the large system into smaller subsystems. Then one tries to solve each subsystem independently, with its own largest timestep. Different methods for each subsystem can be used and a full multirate integration then can be achieved. One of the most challenging problems is to know how to partition the system representing the circuit such that the natural coupling between blocks of components of the circuit is preserved, since otherwise the convergence of the iterates is likely to be very slow.

One approach for decomposing large systems is the *waveform relaxation* (WR) algorithms, which we are considering in this thesis. Waveform relaxation methods are iterative methods but to call them waveform relaxation is natural when the application area is electronics. The word relaxation arises because we use a relaxation similar to the fixed point iterative relaxation methods used to solve algebraic equations, and waveform arises since the solution sought is a function over a time interval, $t \in [t_0, T]$. The basic idea in these methods is to apply a relaxation such as the Gauss-Seidel and the Jacobi relaxations [4] directly to the system of nonlinear differential equations describing the circuit. As a consequence, the system is decomposed into decoupled subsystems of differential equations corresponding to decoupled dynamical sub-circuits. Each decoupled sub-circuit is then analyzed independently, for the entire simulation time interval by integration methods, like the backward Euler method, to obtain subsystems of nonlinear algebraic equations and Newton-Raphson iterations to linearize the subsystems of the nonlinear algebraic equations. The solutions to the sub-circuits are used to update the solutions of neighbor sub-circuits in an iterative fashion.

If we consider the initial value problem (IVP)

$$\begin{cases} \dot{\boldsymbol{y}}(t) = \boldsymbol{f}(t, \boldsymbol{y}(t)), \ t \in [t_0, T], \\ \boldsymbol{y}(t_0) = \boldsymbol{y}_0, \end{cases}$$

where $\boldsymbol{f} : \mathbb{R} \times \mathbb{R}^m \to \mathbb{R}^m$, $\boldsymbol{y} : \mathbb{R} \to \mathbb{R}^m$, $\boldsymbol{y}_0 \in \mathbb{R}^m$, then the simplest example of this approach is the Picard method which takes the form

$$\begin{cases} \dot{y}_i^{k+1}(t) = f_i(t, y_1^k(t), \ldots, y_{i-1}^k(t), y_i^k(t), y_{i+1}^k(t), \ldots, y_m^k(t)), \\ y_i^{k+1}(t_0) = y_{0,i}, \\ \qquad i = 1, 2, \ldots, m, \ t \in [t_0, T], \ k = 0, 1, \ldots \quad . \end{cases}$$

The continuous-time waveform relaxation iteration using the Jacobi relaxation, JWR, is

$$\begin{cases} \dot{y}_i^{k+1}(t) = f_i(t, y_1^k(t), \ldots, y_{i-1}^k(t), y_i^{k+1}(t), y_{i+1}^k(t), \ldots, y_m^k(t)), \\ y_i^{k+1}(t_0) = y_{0,i}, \\ \qquad i = 1, 2, \ldots, m, \ t \in [t_0, T], \ k = 0, 1, \ldots \quad , \end{cases}$$

and the continuous-time waveform relaxation iteration using the Gauss-Seidel relaxation, GWR, is

$$\begin{cases} \dot{y}_i^{k+1}(t) = f_i(t, y_1^{k+1}(t), \ldots, y_{i-1}^{k+1}(t), y_i^{k+1}(t), y_{i+1}^k(t), \ldots, y_m^k(t)), \\ y_i^{k+1}(t_0) = y_{0,i}, \\ \qquad i = 1, 2, \ldots, m, \ t \in [t_0, T], \ k = 0, 1, \ldots \quad , \end{cases}$$

with an initial approximation $\boldsymbol{y}^0(t)$, that must satisfy the initial condition $\boldsymbol{y}(t_0)$.

Table 1.1 from [5] compares the simulation time for several circuits using the circuit simulator Relax2 [6] with direct methods and Relax2 using the WR algorithm. One

Table 1.1: Simulation time for WR algorithm versus direct methods.

CPU Time for Direct Methods vs. WR for Several Industrial Circuits.

Circuit	Devices	Direct	WR
uP Control	232	90s*	45s*
CMOS Memory	621	995s*	308s*
4-bit Counter	259	540s*	299s*
Inverter Chain	250	98s**	38s**
Digital Filter	1082	1800s*	520s*
Encode-Decode	3295	5000s*	1500s*

*On VAX11/780 running Unix using Shichman-Hodges Mosfet model.
**On VAX11/780 running VMS using Yang-Chatterjee Mosfet model.

can see that less simulation time required using the WR algorithm compared to direct methods.

In fact, iterative methods for IVPs were given a firm theoretical basis in the works of Picard and Lindelöf more than one century ago. To call them Picard-Lindelöf, or Block Picard-Lindelöf iterations is therefore historically motivated. Picard [7] discussed iteration methods to study IVPs for systems of ordinary differential equations in 1893. Lindelöf showed in a paper that was published in 1894, [8], the super-linear convergence on all finite time intervals of the iteration methods that were discussed by Picard.

The WR methods were first introduced for time-domain analysis of nonlinear dynamical systems, in particular, very large-scale integrated (VLSI) circuits by Lelarasmee [9] and Lelarasmee et al. [10]. In simulating VLSI circuits, very large stiff systems are involved, but the equations fall into natural subsystems corresponding to components of the circuit. In [11] Carlin and Vochoux noted that any strong coupling between components of the circuit occurs over short time intervals. Hence, the interactions between the subsystems or sub-circuits are usually fairly brief, and in addition, they are often unidirectional. Therefore, the splitting is guided by the physicality of the problem, which allows tightly coupled nodes to be placed together in one subsystem.

As a consequence, the WR algorithms can be very efficient for problems arising from electrical network modelling. Indeed, WR techniques show the promise of becoming one of the most useful approaches for the transient analysis for VLSI MOSFET circuits and other types of circuits, due to their favorable numerical properties and their potential speed and accuracy. Due to this fact, many circuit solvers and experimental solvers have been built based on the WR techniques, e.g. [6, 12].

There are two potential advantages of the WR algorithms: The first is that each subsystem can be solved with its optimal timestep, or even with a different method independently. The second is that a massive parallelism can be obtained with the WR algorithms, since each decoupled subsystem can be solved in parallel. The JWR algorithm given above is a parallel process, since each subsystem can be solved independently in parallel. The GWR algorithm is not a parallel process, it is inherently sequential, since y_{i+1}^{k+1} can not be calculated until y_i^{k+1} has been calculated. This can however be remedied by using an appropriate coloring strategy for realistic problems from VLSI design.

A good study and survey of these algorithms with emphasis on simulation of VLSI circuits as written by White et al. [5], and by White and Sangiovanni-Vincentelli [13].

The convergence theory of the linear WR methods was put on a mathematical basis by Miekkala and Nevanlinna [14, 15], and Nevanlinna [16, 17, 18]. They considered the linear problem

$$\dot{x}(t) + Ax(t) = f(t),\ x(0) = x_0, \tag{1.1}$$

and thus for an (M, N) splitting of the $m \times m$ complex matrix A, $A = M - N$, a general WR algorithm is given by the iteration scheme

$$\dot{x}^k(t) + Mx^k(t) = Nx^{k-1}(t) + f(t),\ x^k(0) = x_0. \tag{1.2}$$

Miekkala and Nevanlinna wrote the sequence of iterates $x^1(t), x^2(t), \ldots,$ of (1.2) in a fixed-point iterative form as

$$x^k(t) = \mathcal{K}x^{k-1}(t) + g(t),$$

where the convolution iteration operator $\mathcal{K}$ and the kernel function r are given by

$$\mathcal{K}u(t) := \int_0^t r(t-s)u(s)\,ds, \qquad r(t) := e^{-tM}N,$$

and g is given by

$$g(t) := e^{-tM}x_0 + \int_0^t e^{-(t-s)M}f(s)\,ds.$$

If $x(t)$ is the solution of (1.1) and $x^k(t)$ is the solution of (1.2), and if

$$\varepsilon^k(t) = x(t) - x^k(t),$$

then

$$\varepsilon^k(t) = \mathcal{K}^k \varepsilon^0(t).$$

Miekkala and Nevanlinna showed that the convolution operator $\mathcal{K}$ and its resolvent are bounded,

$$\|\mathcal{K}^k\| \leq \frac{(CT)^k}{k!}, \qquad \|(\mathcal{K} - \lambda I)^{-1}\| \leq |\lambda| e^{CT/|\lambda|},$$

for all $\lambda \neq 0$ and some constant C, and thus the spectral radius of $\mathcal{K}$,

$$\rho(\mathcal{K}) := \lim_{k \to \infty} \|\mathcal{K}^k\|^{\frac{1}{k}}$$

satisfies $\rho(\mathcal{K}) = 0$ in the space of uniform convergence on a bounded time interval $[0, T]$. In order to cope with large values for T, and to see the dependence on the splitting, since $\rho(\mathcal{K}) = 0$ on $[0, T]$ and no information about the effect of the splitting on the actual convergence rate would be obtained, they introduced an exponentially weighted norm of the form

$$\|x\|_T := \sup_{[0,T]} \|e^{-\alpha t} x(t)\|, \; \alpha \geq 0$$

in which $\mathcal{K}$ would become a contraction, where $\|\cdot\|$ is any fixed norm in $\mathbb{C}^m$. Assuming $\|r(t)\| \leq Ce^{-\alpha t}$, and $0 \leq t \leq T \leq \infty$, Nevanlinna [16] showed that for $\alpha > 0$

$$\|\mathcal{K}^k\|_T \leq \left(\frac{C}{\alpha}\right)^k \frac{\Gamma_{\alpha T}(k)}{\Gamma(k)},$$

where

$$\Gamma_\gamma(s) = \int_0^\gamma e^{-\tau} \tau^{s-1} \, d\tau$$

is the incomplete Γ-function. If $\frac{C}{\alpha} < 1$, then the iteration converges uniformly, since $\Gamma_\gamma(s) \longrightarrow \Gamma(s)$ as $\gamma \longrightarrow \infty$.

Convergence of the nonlinear WR methods was first analyzed in [9, 10], and then extended in [5, 13]. Studies in [9, 10] used the most general formulation of a system of nonlinear differential equations. They considered the dynamical system

$$F(\dot{y}, y, u) = 0,$$
$$E(y(0) - y_0) = 0,$$

where $y(t) \in \mathbb{R}^m$ is the vector of unknowns at time $t \in [0, T]$, $u : \mathbb{R} \longrightarrow \mathbb{R}^r$ are the input waveforms to the system, piecewise continuous functions, $y_0 \in \mathbb{R}^m$ is the initial value of y, $F : \mathbb{R}^m \times \mathbb{R}^m \times \mathbb{R}^r \longrightarrow \mathbb{R}^m$ is a continuous function, and $E \in \mathbb{R}^{n \times m}$, $n \leq m$ is a matrix of rank n such that $Ey(t)$ is the state of the system at time t. The less general form that was considered in [5, 13], in which many practical problems, in particular circuit simulation can be described, is

$$c(y(t), u(t))\dot{y}(t) = f(y(t), u(t)), \; y(0) = y_0, \; t \in [0, T], \tag{1.3}$$

where $y \in \mathbb{R}^m$ represents the circuit waveforms, and $u \in \mathbb{R}^r$ are again the input waveforms, which are piecewise continuous. The inverse $c(y, u)^{-1}$ is assumed to exist and uniformly bounded with respect to y and u. The function f is assumed to be Lipschitz continuous with respect to y for all $u \in \mathbb{R}^r$, where Lipschitz continuous is defined by

Definition 1.1. The function $f(x, y)$, where $f : \mathbb{R}^n \times \mathbb{R}^m \longrightarrow \mathbb{R}^m$ is called Lipschitz continuous or is said to satisfy a Lipschitz condition with respect to y if there exists a constant $L > 0$ such that

$$\|f(x, y) - f(x, z)\| \leq L\|y - z\|, \quad \forall x \in \mathbb{R}^n, \quad \forall y, \; z \in \mathbb{R}^m.$$

The smallest such L is called the Lipschitz constant.

These conditions guarantee a unique solution to (1.3).

It was proved in [9, 10] that the waveform iteration based on either Gauss-Seidel or Jacobi splitting applied to (1.3) will converge in the continuous-time domain from an arbitrary initial guess, if $c(y, u)$ is diagonally dominant and independent of y. The result was generalized by White et al. [5] in the following theorem.

Theorem 1.2. *If in addition to the assumptions associated with (1.3), $c(y, u)$ is strictly diagonally dominant for all $y(t)$ and for all $u(t)$ and is Lipschitz continuous with respect to y for all u, then the sequence of waveforms $\{y^k\}$ generated by the Gauss-Seidel or Jacobi waveform relaxation algorithm converges uniformly on all bounded time intervals $[0, T]$.*

Proof. See [5]. □

The following theorem is a general convergence theorem for WR algorithms, in the sense that more general splitting functions, not only Gauss-Seidel or Jacobi splittings as in Theorem 1.2, can be used. It also gives bounds on the growth of errors in terms of the initial error.

Theorem 1.3. *Consider the general differential equation*

$$\dot{y}(t) = f(y(t)),\ f : \mathbb{R}^m \to \mathbb{R}^m,\ t \in [0, T],$$
$$y(0) = y_0,$$

and assume there is a splitting characterized by the function $F(y, z)$ where F satisfies

$$F(y, y) = f(y),\ F : \mathbb{R}^m \times \mathbb{R}^m \to \mathbb{R}^m,$$

where F is Lipschitz continuous with respect to both arguments. Then the WR scheme

$$\dot{y}^k(t) = F(y^k, y^{k-1}),\ y^k(0) = y_0,$$

converges uniformly on all finite intervals $[0, T]$ with

$$\|\varepsilon^k\|_T \leq \frac{(L_2 T)^k}{k!} e^{L_1 T} \|\varepsilon^0\|_T,\ \varepsilon^k(t) = y^k(t) - y(t),$$

where L_1 and L_2 are the Lipschitz constants associated with the first and the second argument of F, respectively.

Proof. See [19]. □

One of the classical approaches in solving partial differential equations (PDEs) in parallel is to discretize the equations in space and then applying a WR algorithm to the large system of ODEs obtained from the spatial discretization, see [20] for a formulation using discretized subdomains. Abandoning the idea of subsystems, efficient WR algorithms of multigrid type have been introduced, see [21, 22, 23, 24]. The WR algorithms have been extended to time dependent PDEs in [25] and independently in [26] directly at the continuous level without discretization. It was shown that the coupling between subdomains in physical space using Dirichlet transmission conditions at the artificial subdomain interfaces corresponds to using a classical WR algorithm. Recent work in PDEs shows that the classical transmission conditions are far from optimal [27]. Much better performance can be obtained if additional information is exchanged in the transmission conditions. Several attempts have been made before to improve the subsystem transmission conditions for WR with different types of circuit overlap schemes, e.g. [28, 29, 30] to improve the transmission of information across the interface.

Gander and Ruehli [31] introduced a new class of methods which improves the performance over the classical WR algorithms with little computational overhead. These methods are called *optimized* WR algorithms since they include an optimization process. The optimization concerns the transmission conditions which are responsible for the exchange of the information between the neighboring subsystems. The new transmission conditions proposed in [31], which transmit a combination of voltages and currents between the subsystems, greatly enhance the performance of the method and lead to a faster and much more uniform overall convergence in few iterations, as

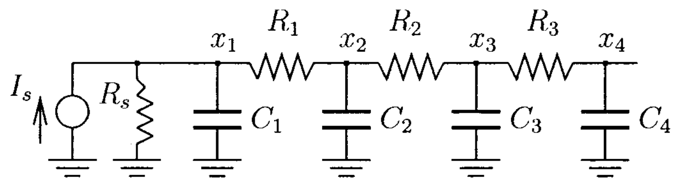

Figure 1.1: A small RC circuit.

it has been demonstrated for diffusive circuits in [31], and for a small transmission line circuit in [32].

In [31] Gander and Ruehli considered the small RC circuit given in Figure 1.1, which we choose here to introduce general concepts and discuss the notation that we will be using.

Circuit equations are usually specified in terms of the modified nodal analysis equations (MNA) [3], in the form $\mathbf{C}\dot{\boldsymbol{x}}(t) + \mathbf{G}\boldsymbol{x}(t) = \mathbf{B}\boldsymbol{u}(t)$, where $\mathbf{C}$ contains the reactive elements, $\mathbf{G}$ the other elements, while $\mathbf{B}$ is the input selector matrix, and $\boldsymbol{u}(t)$ are the forcing functions. For the model problems we are analyzing we can rewrite the MNA circuit equations in tridiagonal form

$$\dot{\boldsymbol{x}} = \begin{bmatrix} b_1 & c_1 & & & \\ a_1 & b_2 & c_2 & & \\ & a_2 & b_3 & c_3 & \\ & & a_3 & b_4 & \ddots \\ & & & \ddots & \ddots \end{bmatrix} \boldsymbol{x} + \boldsymbol{f}, \tag{1.4}$$

and the solution is sought for a given initial condition $\boldsymbol{x}(0) = \boldsymbol{x}^0$. The values a_i, b_i, and c_i for $i = 1, 2, \ldots$ are given by the circuit. Note that, in general, the system (1.4) is not tridiagonal, but for the RC and transmission line type circuits we are studying in what follows, we have tridiagonal systems.

To find the entries a_i, b_i, and c_i we use Ohm's law which says that the relation between the current I and the voltage v through a resistance R is given by $I = \frac{v}{R}$.

The current through a capacitor C is given by $I = C\frac{dv}{dt}$, where $\frac{dv}{dt}$ is the derivative of the voltage with respect to the time t. The voltage across an inductor L is given by $v = L\frac{dI}{dt}$, where $\frac{dI}{dt}$ is the derivative of the current with respect to the time t. Kirchhoff's current law is used as well, which says that at each node in the circuit the algebraic sum of all currents equals zero, which is equivalent to saying that the sum of all entering currents equals the sum of all leaving currents. The voltage is measured in volts, the current in amperes, the capacitance in farads, the resistance in ohms, the inductance in henrys, and the time in seconds [33].

Let us consider now the RC circuit in Figure 1.1. To derive the circuit equations, we use the laws we have explained above. For instance, at the node x_1 we have

$$I_s = C_1\dot{x}_1 + \frac{x_1}{R_s} + \frac{x_1 - x_2}{R_1},$$

and after simplifying we get

$$\dot{x}_1 = -\left(\frac{1}{R_s} + \frac{1}{R_1}\right)\frac{1}{C_1}x_1 + \frac{1}{R_1C_1}x_2 + \frac{I_s}{C_1}.$$

At the second node x_2 we have

$$\frac{x_2 - x_1}{R_1} + C_2\dot{x}_2 + \frac{x_2 - x_3}{R_2} = 0,$$

which implies

$$\dot{x}_2 = -\left(\frac{1}{R_1} + \frac{1}{R_2}\right)\frac{1}{C_2}x_2 + \frac{1}{R_1C_2}x_1 + \frac{1}{R_2C_2}x_3.$$

The other equations at the other nodes can be found similarly. Thus, the circuit equations are of the form

$$\dot{\boldsymbol{x}} = \begin{bmatrix} b_1 & c_1 & & \\ a_1 & b_2 & c_2 & \\ & a_2 & b_3 & c_3 \\ & & a_3 & b_4 \end{bmatrix} \boldsymbol{x} + \boldsymbol{f}, \tag{1.5}$$

where the entries in the tridiagonal matrix are given by

$$a_i = \frac{1}{R_i C_{i+1}}, \quad b_i = \begin{cases} -(\frac{1}{R_s} + \frac{1}{R_1})\frac{1}{C_1}, & i = 1 \\ -(\frac{1}{R_{i-1}} + \frac{1}{R_i})\frac{1}{C_i}, & i = 2, 3, \\ -\frac{1}{R_{i-1}C_i}, & i = 4 \end{cases} \quad c_i = \frac{1}{R_i C_i}.$$

Here the resistor values R_i and R_s and the capacitors C_i are strictly positive constants. The source term on the right hand side is given by $\boldsymbol{f}(t) = (I_s(t)/C_1, 0, 0, 0)^T$ for some source function $I_s(t)$, and we are also given the initial voltage values $\boldsymbol{x}(0) = (v_1^0, v_2^0, v_3^0, v_4^0)^T$ at the time $t = 0$.

We are analyzing two types of partitioning: The first one is what we call partitioning *without overlap* and the second one we call partitioning *with overlap*. To illustrate this concept, we consider the system of differential equations given in (1.5). We partition the system into two subsystems, and we call the unknowns in the first subsystem $\boldsymbol{u}$ and in the second subsystem $\boldsymbol{w}$. The partitioning without overlap is illustrated by

$$\begin{pmatrix} \dot{u}_1 \\ \dot{u}_2 \\ \dot{w}_1 \\ \dot{w}_2 \end{pmatrix} = \left[\begin{array}{cc|cc} b_1 & c_1 & & \\ a_1 & b_2 & c_2 & \\ \hline & a_2 & b_3 & c_3 \\ & & a_3 & b_4 \end{array}\right] \left(\begin{array}{c|c} u_1 & \\ u_2 & w_0 \\ u_3 & w_1 \\ & w_2 \end{array}\right) + \begin{pmatrix} f_1 \\ f_2 \\ f_3 \\ f_4 \end{pmatrix},$$

where the solid lines indicate the two subsystems we will obtain and the unknowns for each subsystem. Note that, without overlap here is in the matrix sense not in the real life. This will be however shown in Chapter 5. For the partitioning with overlap, we have

$$\begin{pmatrix} \dot{\boldsymbol{u}} \\ \dot{\boldsymbol{w}} \end{pmatrix} = \left[\begin{array}{c|c|cc} b_1 & c_1 & & \\ \hline a_1 & b_2 & c_2 & \\ \hline & a_2 & b_3 & c_3 \\ & & a_3 & b_4 \end{array}\right] \left(\begin{array}{c|c} u_1 & w_0 \\ u_2 & w_1 \\ u_3 & w_2 \\ & w_3 \end{array}\right) + \begin{pmatrix} f_1 \\ f_2 \\ f_3 \\ f_4 \end{pmatrix},$$

where the solid lines indicate again the two subsystems we will obtain and the unknowns for each subsystem. Note that one could also split differently. The splitting without overlap leads to the two subsystems

$$
\begin{aligned}
\begin{pmatrix} \dot{u}_1 \\ \dot{u}_2 \end{pmatrix} &= \begin{bmatrix} b_1 & c_1 \\ a_1 & b_2 \end{bmatrix} \begin{pmatrix} u_1 \\ u_2 \end{pmatrix} + \begin{pmatrix} f_1 \\ f_2 \end{pmatrix} + \begin{pmatrix} 0 \\ c_2 u_3 \end{pmatrix}, \\
\begin{pmatrix} \dot{w}_1 \\ \dot{w}_2 \end{pmatrix} &= \begin{bmatrix} b_3 & c_3 \\ a_3 & b_4 \end{bmatrix} \begin{pmatrix} w_1 \\ w_2 \end{pmatrix} + \begin{pmatrix} f_3 \\ f_4 \end{pmatrix} + \begin{pmatrix} a_2 w_0 \\ 0 \end{pmatrix},
\end{aligned}
\tag{1.6}
$$

and with overlap we obtain the two subsystems

$$
\begin{aligned}
\begin{pmatrix} \dot{u}_1 \\ \dot{u}_2 \end{pmatrix} &= \begin{bmatrix} b_1 & c_1 \\ a_1 & b_2 \end{bmatrix} \begin{pmatrix} u_1 \\ u_2 \end{pmatrix} + \begin{pmatrix} f_1 \\ f_2 \end{pmatrix} + \begin{pmatrix} 0 \\ c_2 u_3 \end{pmatrix}, \\
\begin{pmatrix} \dot{w}_1 \\ \dot{w}_2 \\ \dot{w}_3 \end{pmatrix} &= \begin{bmatrix} b_2 & c_2 & \\ a_2 & b_3 & c_3 \\ & a_3 & b_4 \end{bmatrix} \begin{pmatrix} w_1 \\ w_2 \\ w_3 \end{pmatrix} + \begin{pmatrix} f_2 \\ f_3 \\ f_4 \end{pmatrix} + \begin{pmatrix} a_1 w_0 \\ 0 \\ 0 \end{pmatrix}.
\end{aligned}
\tag{1.7}
$$

Now using for (1.6) the classical transmission conditions

$$
u_3^{k+1} = w_1^k, \quad w_0^{k+1} = u_2^k, \tag{1.8}
$$

we get from (1.6) the classical WR algorithm

$$
\begin{aligned}
\dot{\boldsymbol{u}}^{k+1} &= \begin{bmatrix} b_1 & c_1 \\ a_1 & b_2 \end{bmatrix} \boldsymbol{u}^{k+1} + \begin{pmatrix} f_1 \\ f_2 \end{pmatrix} + \begin{pmatrix} 0 \\ c_2 w_1^k \end{pmatrix}, \\
\dot{\boldsymbol{w}}^{k+1} &= \begin{bmatrix} b_3 & c_3 \\ a_3 & b_4 \end{bmatrix} \boldsymbol{w}^{k+1} + \begin{pmatrix} f_3 \\ f_4 \end{pmatrix} + \begin{pmatrix} a_2 u_2^k \\ 0 \end{pmatrix},
\end{aligned}
\tag{1.9}
$$

with corresponding initial conditions $\boldsymbol{u}^{k+1}(0) = (v_1^0, v_2^0)^T$ and $\boldsymbol{w}^{k+1}(0) = (v_3^0, v_4^0)^T$, which was analyzed in [31]. To start the WR iteration, we need to specify two initial waveforms $u_2^0(t)$ and $w_1^0(t)$ for $t \in [0,T]$. For (1.7) we get

$$\begin{aligned}
\dot{\boldsymbol{u}}^{k+1} &= \begin{bmatrix} b_1 & c_1 \\ a_1 & b_2 \end{bmatrix} \boldsymbol{u}^{k+1} + \begin{pmatrix} f_1 \\ f_2 \end{pmatrix} + \begin{pmatrix} 0 \\ c_2 w_1^k \end{pmatrix}, \\
\dot{\boldsymbol{w}}^{k+1} &= \begin{bmatrix} b_2 & c_2 & \\ a_2 & b_3 & c_3 \\ & a_3 & b_4 \end{bmatrix} \boldsymbol{w}^{k+1} + \begin{pmatrix} f_2 \\ f_3 \\ f_4 \end{pmatrix} + \begin{pmatrix} a_1 u_2^k \\ 0 \\ 0 \end{pmatrix}.
\end{aligned} \tag{1.10}$$

The new transmission conditions that were introduced in [31] are given by

$$(u_3^{k+1} - u_2^{k+1}) + \alpha u_3^{k+1} = (w_1^k - w_0^k) + \alpha w_1^k, \quad (w_1^{k+1} - w_0^{k+1}) + \beta w_0^{k+1} = (u_3^k - u_2^k) + \beta u_2^k. \tag{1.11}$$

By comparing the new transmission conditions with (1.8), we also exchange the voltages u_3 and w_0. However, they are multiplied with a weighting factor α while the difference between the voltages $(u_3 - u_2)$ insures that the currents are also taken into account, since the currents could be written as $\alpha^{-1}(u_3 - u_2)$, where α can be considered as a resistor.

The new WR algorithm using the new transmission conditions (1.11) and considering the case without overlap (1.6), is given in [31] as

$$\begin{aligned}
\dot{\boldsymbol{u}}^{k+1} &= \begin{bmatrix} b_1 & c_1 \\ a_1 & b_2 + \frac{c_2}{\alpha+1} \end{bmatrix} \boldsymbol{u}^{k+1} + \begin{pmatrix} f_1 \\ f_2 \end{pmatrix} + \begin{pmatrix} 0 \\ c_2 w_1^k - \frac{c_2}{\alpha+1} w_0^k \end{pmatrix}, \\
\dot{\boldsymbol{w}}^{k+1} &= \begin{bmatrix} b_3 - \frac{a_2}{\beta-1} & c_3 \\ a_3 & b_4 \end{bmatrix} \boldsymbol{w}^{k+1} + \begin{pmatrix} f_3 \\ f_4 \end{pmatrix} + \begin{pmatrix} a_2 u_2^k + \frac{a_2}{\beta-1} u_3^k \\ 0 \end{pmatrix},
\end{aligned} \tag{1.12}$$

where the values u_3^k and w_0^k are determined by the transmission conditions (1.11).

Our analysis of the above WR algorithms is based on the Fourier and Laplace transforms [34]. Using the Laplace transform allows us to easily obtain explicit formulas for the solutions, since we are studying linear IVPs, and the coefficients of the equations are constants.

Let h be a complex-valued function defined on the real line such that $|h|$ is (at least improperly) integrable on every finite interval, and

$$\int_{-\infty}^{\infty} |h(t)|\, dt < \infty.$$

The integral

$$\hat{h}(\omega) := \mathcal{F}(h(t)) = \int_{-\infty}^{\infty} h(t)e^{-i\omega t}\, dt$$

then exists for all real ω. The function $\hat{h}$ is called the Fourier transform of h.

The Laplace transform for a function h is denoted by

$$\hat{h}(s) := \mathcal{L}(h(t)) = \int_{0}^{\infty} h(t)e^{-st}\, dt, \quad s \in \mathbb{C}.$$

If the function h is piecewise continuous on every finite interval in the range $t \geq 0$, and satisfies $|h(t)| \leq Me^{\gamma t}$ for all $t \geq 0$ and for some constants γ and M, then the Laplace transform of $h(t)$ exists for all $\Re(s) > \gamma$.

Now consider the function g which is defined for all real t and identically zero for $t < 0$, where $g \in L^1(\mathbb{R})$. Since $g(t) = 0$ for $t < 0$, we have

$$\hat{g}(\omega) = \mathcal{F}(g(t)) = \int_{-\infty}^{\infty} g(t)e^{-i\omega t}\, dt = \int_{0}^{\infty} g(t)e^{-i\omega t}\, dt = \mathcal{L}(g(t))|_{s=i\omega} = \hat{g}(s)|_{s=i\omega},$$

and moreover, we have for all $\eta \geq 0$,

$$|e^{-\eta t}g(t)| \leq |g(t)|,$$

and hence,

$$\int_{-\infty}^{\infty} |e^{-\eta t}g(t)|\, dt \leq \int_{-\infty}^{\infty} |g(t)|\, dt < \infty.$$

Therefore, for $G(t) := e^{-\eta t}g(t)$, $\eta \geq 0$, we have $G \in L^1(\mathbb{R})$, and its Fourier transform is given by

$$\hat{G}(\omega) := \mathcal{F}(G(t)) = \int_{-\infty}^{\infty} e^{-\eta t}g(t)e^{-i\omega t}\, dt.$$

If $s = \eta + i\omega$, $\eta \geq 0$, then the Laplace transform $\hat{g} = \mathcal{L}(g)$ may be written as

$$\hat{g}(\eta + i\omega) = \int_{-\infty}^{\infty} e^{-\eta t}g(t)e^{-i\omega t}\, dt = \int_{-\infty}^{\infty} g(t)e^{-st}\, dt,$$

and thus as a function of ω may be considered as the Fourier transform of the function $G(t)$ whose integral over $(-\infty, \infty)$ converges absolutely. Therefore, Laplace transforms are also Fourier transforms and this connects the Fourier analysis to Laplace transform theory.

Parseval's formula [34],

$$\int_{-\infty}^{\infty} |h(t)|^2 \, dt = \frac{1}{2\pi} \int_{-\infty}^{\infty} |\hat{h}(\omega)|^2 \, d\omega,$$

holds in the space $L^2(\mathbb{R})$ of functions h satisfying

$$\int_{-\infty}^{\infty} |h(t)|^2 \, dt < \infty,$$

where the integral is a Lebesgue integral. Therefore, assuming $g \in L^2(\mathbb{R})$, we have $G \in L^2(\mathbb{R})$, and by Parseval's formula, we have

$$\|e^{-\eta t} g(t)\|_2 = \frac{1}{\sqrt{2\pi}} \|\hat{G}(\omega)\|_2 = \frac{1}{\sqrt{2\pi}} \|\hat{g}(\eta + i\omega)\|_2.$$

In the analysis of the convergence, it also suffices to consider the homogeneous problem where the initial conditions and the source terms are zero, $\boldsymbol{x}(0) = \mathbf{0}$ and $\boldsymbol{f}(t) = \mathbf{0}$. This is due to the fact that in the k^{th} iteration, the difference between the exact solution $\boldsymbol{x}(t)$ and the iterates $\boldsymbol{x}^k(t)$, which we call the error $\boldsymbol{\varepsilon}^k(t) = \boldsymbol{x}(t) - \boldsymbol{x}^k(t)$, satisfies a homogeneous linear system of differential equations with homogeneous initial conditions.

It was shown in [31] that applying the Laplace transform to the homogeneous case of (1.9) implies $\hat{u}_2^{2k} = (\rho_{cla})^k \, \hat{u}_2^0$, and $\hat{w}_1^{2k} = (\rho_{cla})^k \, \hat{w}_1^0$, with the convergence factor ρ_{cla} given by

$$\rho_{cla}(s, \boldsymbol{a}, \boldsymbol{b}, \boldsymbol{c}) = \frac{c_2(s - b_1)}{(s - b_1)(s - b_2) - a_1 c_1} \cdot \frac{a_2(s - b_4)}{(s - b_3)(s - b_4) - a_3 c_3}, \quad s = \eta + i\omega. \tag{1.13}$$

Moreover, it was shown that the convergence factor for the new WR algorithm (1.12) is

$$\begin{aligned} \rho_{opt}(s, \boldsymbol{a}, \boldsymbol{b}, \boldsymbol{c}, \alpha, \beta) \;\; = \;\; & -\tfrac{c_2(s-b_1)(\beta-1)+(s-b_1)(s-b_2)-a_1c_1}{((s-b_3)(s-b_4)-a_3c_3)(\beta-1)+a_2(s-b_4)} \\ & \cdot \tfrac{-a_2(s-b_4)(\alpha+1)+(s-b_3)(s-b_4)-a_3c_3}{((s-b_1)(s-b_2)-a_1c_1)(\alpha+1)+c_2(b_1-s)}, \end{aligned} \tag{1.14}$$

and as before $\hat{u}_2^{2k} = (\rho_{opt})^k \hat{u}_2^0$, and $\hat{w}_1^{2k} = (\rho_{opt})^k \hat{w}_1^0$. If we now consider the relation $\hat{u}_2^{2k}(s) = (\rho(s))^k \hat{u}_2^0$, where $s = \eta + i\omega$, $\eta \geq 0$ from above, and $\rho(s)$ is some convergence factor, then we have

$$\begin{aligned} \int_{-\infty}^{\infty} |\hat{u}_2^{2k}(\eta+i\omega)|^2 d\omega &= \int_{-\infty}^{\infty} |\rho^k(\eta+i\omega)\hat{u}_2^0(\eta+i\omega)|^2 d\omega \\ &\leq \left(\max_{\omega\in\mathbb{R},\eta\geq 0} |\rho(\eta+i\omega)|\right)^{2k} \int_{-\infty}^{\infty} |\hat{u}_2^0(\eta+i\omega)|^2 d\omega. \end{aligned}$$

Now, by Parseval's formula we get

$$\|e^{-\eta t}u_2^{2k}(t)\|_2 \leq \left(\max_{\eta\geq 0} |\rho(s)|\right)^k \|e^{-\eta t}u_2^0(t)\|_2,$$

which implies with the weighted norm $\|\cdot\|_\eta := \|e^{-\eta t}\cdot\|_2$

$$\|u_2^{2k}(t)\|_\eta \leq \left(\max_{\eta\geq 0} |\rho(s)|\right)^k \|u_2^0(t)\|_\eta. \tag{1.15}$$

Therefore, the convergence in the frequency domain ω implies the convergence in the time domain t, and by using Laplace transform we will be able to analyze convergence in the exponentially weighted norm for $\eta > 0$, or in the L^2 norm if $\eta = 0$. Note that, for convergence for all time, we need $|\rho(s)| < 1$.

The optimal values of α and β in the new transmission conditions can be derived from the convergence factor (1.14), and are given by

$$\alpha := \frac{-a_3c_3}{(s-b_4)a_2} + \frac{s-b_3}{a_2} - 1, \quad \beta := \frac{a_1c_1}{(s-b_1)c_2} - \frac{s-b_2}{c_2} + 1, \quad s \in \mathbb{C}, \tag{1.16}$$

where the new WR algorithm converges in two iterations for this choice of parameters, independently of the initial guess for the waveforms [31].

In [1] the optimal choice (1.16) which corresponds to a nonlocal operator in time because of the s^{-1} behavior, was used to get an optimal WR algorithm, where a transformation was used to make the optimal symbols α and β local operators in time. The transmission conditions were multiplied by $(s-b_4)$ and $(s-b_1)$ respectively. This led to second degree polynomials in $s \in \mathbb{C}$, which correspond to second degree derivatives in the transmission conditions. This required implementations of second degree time derivatives which only require local information.

However, Gander and Ruehli proposed a constant approximation of the optimal choice for α and β in [31], since in general the optimal symbols can not be transformed to local operators in time as in [1]. In addition, the constant approximation leads to a very practical algorithm.

Assuming α and β are constants, for fast convergence we want $|\rho_{opt}| \ll 1$, and this leads to the min-max problem

$$\min_{\alpha,\beta}\left(\max_{\Re(s)\geq 0}|\rho_{opt}(s,\boldsymbol{a},\boldsymbol{b},\boldsymbol{c},\alpha,\beta)|\right), \tag{1.17}$$

which we need to solve.

The first step in the optimization is to ensure that the convergence factor ρ_{opt} is an analytic function in the right half of the complex plane, $s = \eta + i\omega$, $\eta > 0$, which was proved in [31] using the following theorem.

Theorem 1.4. *If $f, g : \mathbb{C} \to \mathbb{C}$ are analytic on $U \subset \mathbb{C}$, then the quotient f/g is analytic on the open subset of $z \in U$ such that $g(z) \neq 0$.*

Proof. See [35]. □

Next, since the convergence factor ρ_{opt} is analytic in the right half of the complex plane, the maximum of the modulus of ρ_{opt} is attained on the boundary, by the maximum principle for complex analytic functions which is stated in the following theorem.

Theorem 1.5. *Let R be the region consisting of a simple closed curve C and its interior, and let $f(s)$ be analytic and not identically constant in R. Then the maximum value of $|f(s)|$ in R occurs on the boundary C. If $f(s)$ has no zero in R, then $|f(s)|$ also attains its minimum in R on the boundary C.*

Proof. See [36]. □

Indeed, Theorems 1.4 and 1.5 will be used throughout the analysis in this thesis in order to solve optimization problems of the form (1.17).

Gander and Ruehli [31] showed that the maximum of the modulus of the convergence factor ρ_{opt} is attained on the boundary at $\eta = 0$, and in addition, they showed that $|\rho_{opt}|$ for $s = i\omega$ depends on ω^2 only, and thus it suffices to optimize for nonnegative frequencies, $\omega \geq 0$. They then chose $\beta = -\alpha$ to keep the optimization simpler, and they showed numerically that the solution of the min-max problem occurs when the convergence factor at $\omega = 0$ and at $\omega = \omega_{max}$ are balanced, and they used the equation

$$|\rho_{opt}(\alpha^*, 0)| = |\rho_{opt}(\alpha^*, \omega_{max})|$$

to determine the optimized parameter α^*. In the numerical example they gave, where they chose $\omega_{max} = \infty$, they found $\alpha^* = 1$, and from the similarity assumption above they obtained $\beta^* = -1$, which leads to the result given in Figure 1.2, where the error is plotted as a function of the iterations.

In this thesis, we analyze and prove the optimality of the constant approximation proposed by Gander and Ruehli in [31].

In [1] a time scaling was used to simplify the optimization process which we will need in the analysis, and it is defined as follows: assume we have the system

$$\frac{d\boldsymbol{x}}{dt} = \begin{bmatrix} \ddots & \ddots & \ddots & & & \\ & a & b & a & & \\ & & a & b & a & \\ & & & \ddots & \ddots & \ddots \end{bmatrix} \boldsymbol{x}.$$

If we replace the pair x and t with x and τ, where $\tau := \alpha t$ for a positive real number α, then $\frac{d\boldsymbol{x}}{d\tau} = \frac{1}{\alpha}\frac{d\boldsymbol{x}}{dt}$, hence if we take $\alpha := a$, and substitute for $\frac{d\boldsymbol{x}}{dt}$ from above, we get

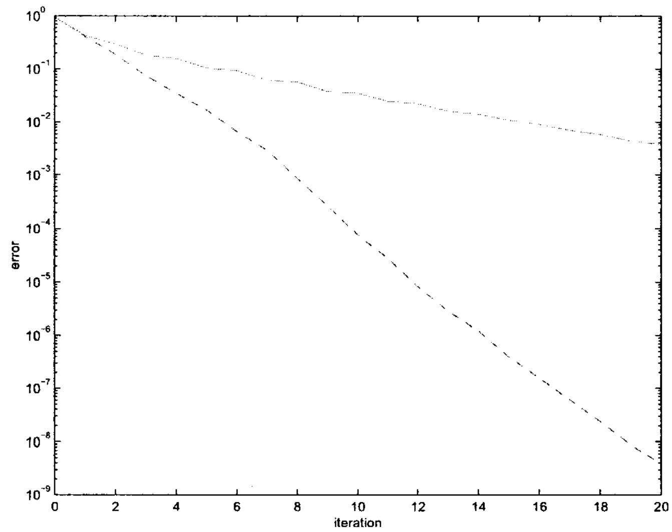

Figure 1.2: Convergence behavior of classical (solid line) versus optimized (dashed) WR methods.

the system

$$\frac{d\boldsymbol{x}}{d\tau} = \begin{bmatrix} \ddots & \ddots & \ddots & & & \\ & \tilde{a} & \tilde{b} & \tilde{a} & & \\ & & \tilde{a} & \tilde{b} & \tilde{a} & \\ & & & \ddots & \ddots & \ddots \end{bmatrix} \boldsymbol{x},$$

where $\tilde{b} = \frac{b}{a}$, $\tilde{a} = 1$ and if $a > 0$, $b < 0$, and $|b| \geq 2a$, then $\tilde{b} = -2c^2$ for $c \geq 1$. Furthermore, the Laplace transform of $h(\alpha t)$ is given by $\frac{1}{\alpha}\hat{h}(\frac{s}{\alpha})$, so with this scaling the Laplace transform parameter $s = \eta + i\omega$ becomes $\tilde{s} = \frac{\eta}{a} + i\frac{\omega}{a} = \tilde{\eta} + i\tilde{\omega}$.

This thesis is organized as follows. In Chapter 2, we analyze a general circuit and its system of ODEs, where we use an algebraic approach to find optimal transmission conditions which lead to optimal WR methods. We propose approximations for the optimal transmission conditions, and we give numerical experiments to show the feasibility of the optimized WR algorithms and the better convergence over the classical WR algorithm. Chapter 3 contains the analysis and results for the convergence of the classical and the new WR methods for RC type circuits using the partitioning without overlap to get subsystems of the same size. We start by analyzing the finite size circuit given in Figure 3.1, where we give results for any RC circuit of finite size n. We then consider the very small and small RC circuits given in Figures 3.7 and 1.1 respectively, and we find more general results for these two particular finite size RC circuits, and we compare them with those found for the RC circuit of size n. We also show that results found for the finite size RC circuit converge to those found for the infinitely large RC circuit in Figure 3.19 as n goes to infinity. Approximations by local operators in time for the optimal parameters are introduced in this chapter. We propose approximations of order zero, which means approximations with constants independent of s, and approximations of order one, which means approximations that are linear in s which lead to better convergence than the constant approximations. A simple choice is to use low frequency approximations based on Taylor expansions about $s = 0$. To get better approximations, optimization problems of the type (1.17) are formulated and analyzed. The optimality is formally proved for some cases, whereas we use asymptotic analysis for other cases which leads to approximate solutions of the optimization problems. Each section ends with numerical experiments. In Chapter 4, we study very small, small, and infinitely large transmission line circuits as given in Figures 4.1, 4.8 and 4.17 respectively. We also analyze the convergence of the classical and the new WR methods, where we use first the partitioning without overlap and then we introduce the partitioning with overlap to get subsystems of the same size, and we focus on the optimized transmission conditions by solving min-max problems. We propose here approximations of order zero, and we use asymptotic analysis to obtain approximate solutions for the optimization problems. At the end of each section we give numerical experiments. In Chapter 5, we discuss the connections between circuit problems and semi-discretized PDEs. Finally, we give the conclusions.

Chapter 2

Analysis for a General Circuit

In this chapter we analyze the classical WR algorithm and we introduce an optimal WR algorithm for a general circuit and its corresponding linear system of ODEs,

$$\dot{\boldsymbol{u}} = A\boldsymbol{u} + \boldsymbol{f}. \tag{2.1}$$

The algebraic approach of Schur complements [37] is used to obtain the optimal transmission conditions. Note that a realistic circuit does not have every node connected to every other node; its graph is in general significantly less dense, and such circuits can be partitioned into block tridiagonal subsystems by partitioning the circuit vertically into subcircuits $S_1, S_2, \ldots, S_N$ as shown in Figure 2.1, where the information is exchanged only between neighboring subsystems. We consider a Jacobi type iteration here, but the Gauss-Seidel case is similar.

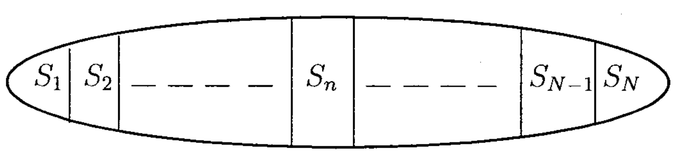

Figure 2.1: Decomposition of the circuit into vertical strips.

2.1 The WR Algorithms with Overlap

To determine the WR algorithms with overlap, we consider a partition of (2.1) into two blocks with a common interface,

$$\begin{pmatrix} \dot{\boldsymbol{u}}_{1i} \\ \dot{\boldsymbol{u}}_{\Gamma} \\ \dot{\boldsymbol{u}}_{2i} \end{pmatrix} = \begin{bmatrix} A_{1i} & C_1 & \\ B_2 & A_\Gamma & B_1 \\ & C_2 & A_{2i} \end{bmatrix} \begin{bmatrix} \boldsymbol{u}_{1i} \\ \boldsymbol{u}_{\Gamma} \\ \boldsymbol{u}_{2i} \end{bmatrix} + \begin{bmatrix} \boldsymbol{f}_{1i} \\ \boldsymbol{f}_{\Gamma} \\ \boldsymbol{f}_{2i} \end{bmatrix}, \tag{2.2}$$

where the matrices A_{1i} and A_{2i} correspond to the interior unknowns, and A_Γ to the interface unknowns. We also need an initial condition $\boldsymbol{u}(0) = \boldsymbol{u}_0$. Note that partitions into multiple subsystems are also possible.

Splitting (2.2) into two separate subsystems with a common interface leads to

$$\begin{aligned} \begin{pmatrix} \dot{\boldsymbol{u}}_{1i} \\ \dot{\boldsymbol{u}}_{1\Gamma} \end{pmatrix} &= \begin{bmatrix} A_{1i} & C_1 \\ B_2 & A_\Gamma \end{bmatrix} \begin{bmatrix} \boldsymbol{u}_{1i} \\ \boldsymbol{u}_{1\Gamma} \end{bmatrix} + \begin{bmatrix} \boldsymbol{f}_{1i} \\ \boldsymbol{f}_\Gamma + B_1 \boldsymbol{u}_{1\Gamma+1} \end{bmatrix}, \\ \begin{pmatrix} \dot{\boldsymbol{u}}_{2\Gamma} \\ \dot{\boldsymbol{u}}_{2i} \end{pmatrix} &= \begin{bmatrix} A_\Gamma & B_1 \\ C_2 & A_{2i} \end{bmatrix} \begin{bmatrix} \boldsymbol{u}_{2\Gamma} \\ \boldsymbol{u}_{2i} \end{bmatrix} + \begin{bmatrix} \boldsymbol{f}_\Gamma + B_2 \boldsymbol{u}_{2\Gamma-1} \\ \boldsymbol{f}_{2i} \end{bmatrix}. \end{aligned} \tag{2.3}$$

Using the classical transmission conditions

$$\boldsymbol{u}_{1\Gamma+1}^{k+1} = \boldsymbol{u}_{2i}^{k}, \quad \boldsymbol{u}_{2\Gamma-1}^{k+1} = \boldsymbol{u}_{1i}^{k}, \tag{2.4}$$

the classical WR algorithm is given by

$$\begin{aligned} \begin{pmatrix} \dot{\boldsymbol{u}}_{1i}^{k+1} \\ \dot{\boldsymbol{u}}_{1\Gamma}^{k+1} \end{pmatrix} &= \begin{bmatrix} A_{1i} & C_1 \\ B_2 & A_\Gamma \end{bmatrix} \begin{bmatrix} \boldsymbol{u}_{1i}^{k+1} \\ \boldsymbol{u}_{1\Gamma}^{k+1} \end{bmatrix} + \begin{bmatrix} \boldsymbol{f}_{1i} \\ \boldsymbol{f}_\Gamma + B_1 \boldsymbol{u}_{2i}^{k} \end{bmatrix}, \\ \begin{pmatrix} \dot{\boldsymbol{u}}_{2\Gamma}^{k+1} \\ \dot{\boldsymbol{u}}_{2i}^{k+1} \end{pmatrix} &= \begin{bmatrix} A_\Gamma & B_1 \\ C_2 & A_{2i} \end{bmatrix} \begin{bmatrix} \boldsymbol{u}_{2\Gamma}^{k+1} \\ \boldsymbol{u}_{2i}^{k+1} \end{bmatrix} + \begin{bmatrix} \boldsymbol{f}_\Gamma + B_2 \boldsymbol{u}_{1i}^{k} \\ \boldsymbol{f}_{2i} \end{bmatrix}. \end{aligned} \tag{2.5}$$

The Laplace transform applied to (2.2) and (2.3) for $s \in \mathbb{C}$ with the initial condition $\boldsymbol{u}(0) = (\boldsymbol{u}_{1i0}, \boldsymbol{u}_{\Gamma 0}, \boldsymbol{u}_{2i0})^T$ implies after simplifying

$$\begin{bmatrix} sI - A_{1i} & -C_1 & \\ -B_2 & sI - A_\Gamma & -B_1 \\ & -C_2 & sI - A_{2i} \end{bmatrix} \begin{bmatrix} \hat{\boldsymbol{u}}_{1i} \\ \hat{\boldsymbol{u}}_{\Gamma} \\ \hat{\boldsymbol{u}}_{2i} \end{bmatrix} = \begin{bmatrix} \hat{\boldsymbol{f}}_{1i} \\ \hat{\boldsymbol{f}}_{\Gamma} \\ \hat{\boldsymbol{f}}_{2i} \end{bmatrix} + \begin{bmatrix} \boldsymbol{u}_{1i0} \\ \boldsymbol{u}_{\Gamma 0} \\ \boldsymbol{u}_{2i0} \end{bmatrix}, \tag{2.6}$$

and

$$\left[\begin{array}{cc} sI - A_{1i} & -C_1 \\ -B_2 & sI - A_\Gamma \end{array}\right]\left[\begin{array}{c} \hat{\boldsymbol{u}}_{1i} \\ \hat{\boldsymbol{u}}_{1\Gamma} \end{array}\right] = \left[\begin{array}{c} \hat{\boldsymbol{f}}_{1i} \\ \hat{\boldsymbol{f}}_\Gamma + B_1 \hat{\boldsymbol{u}}_{1\Gamma+1} \end{array}\right] + \left[\begin{array}{c} \boldsymbol{u}_{1i0} \\ \boldsymbol{u}_{1\Gamma 0} \end{array}\right],$$
$$\left[\begin{array}{cc} sI - A_\Gamma & -B_1 \\ -C_2 & sI - A_{2i} \end{array}\right]\left[\begin{array}{c} \hat{\boldsymbol{u}}_{2\Gamma} \\ \hat{\boldsymbol{u}}_{2i} \end{array}\right] = \left[\begin{array}{c} \hat{\boldsymbol{f}}_\Gamma + B_2 \hat{\boldsymbol{u}}_{2\Gamma-1} \\ \hat{\boldsymbol{f}}_{2i} \end{array}\right] + \left[\begin{array}{c} \boldsymbol{u}_{2\Gamma 0} \\ \boldsymbol{u}_{2i0} \end{array}\right]. \tag{2.7}$$

Therefore, the classical WR algorithm (2.5) in the frequency domain is given by

$$\left[\begin{array}{cc} sI - A_{1i} & -C_1 \\ -B_2 & sI - A_\Gamma \end{array}\right]\left[\begin{array}{c} \hat{\boldsymbol{u}}_{1i}^{k+1} \\ \hat{\boldsymbol{u}}_{1\Gamma}^{k+1} \end{array}\right] = \left[\begin{array}{c} \hat{\boldsymbol{f}}_{1i} \\ \hat{\boldsymbol{f}}_\Gamma + B_1 \hat{\boldsymbol{u}}_{2i}^{k} \end{array}\right] + \left[\begin{array}{c} \boldsymbol{u}_{1i0} \\ \boldsymbol{u}_{1\Gamma 0} \end{array}\right],$$
$$\left[\begin{array}{cc} sI - A_\Gamma & -B_1 \\ -C_2 & sI - A_{2i} \end{array}\right]\left[\begin{array}{c} \hat{\boldsymbol{u}}_{2\Gamma}^{k+1} \\ \hat{\boldsymbol{u}}_{2i}^{k+1} \end{array}\right] = \left[\begin{array}{c} \hat{\boldsymbol{f}}_\Gamma + B_2 \hat{\boldsymbol{u}}_{1i}^{k} \\ \hat{\boldsymbol{f}}_{2i} \end{array}\right] + \left[\begin{array}{c} \boldsymbol{u}_{2\Gamma 0} \\ \boldsymbol{u}_{2i0} \end{array}\right]. \tag{2.8}$$

At convergence, eliminating the unknowns $\hat{\boldsymbol{u}}_{2i}$ in the first subsystem in (2.8) gives

$$\begin{aligned} &\left[\begin{array}{cc} sI - A_{1i} & -C_1 \\ -B_2 & sI - A_\Gamma - B_1(sI - A_{2i})^{-1}C_2 \end{array}\right]\left[\begin{array}{c} \hat{\boldsymbol{u}}_{1i} \\ \hat{\boldsymbol{u}}_{1\Gamma} \end{array}\right] \\ &\qquad = \left[\begin{array}{c} \hat{\boldsymbol{f}}_{1i} \\ \hat{\boldsymbol{f}}_\Gamma + B_1(sI - A_{2i})^{-1}(\hat{\boldsymbol{f}}_{2i} + \boldsymbol{u}_{2i0}) \end{array}\right] + \left[\begin{array}{c} \boldsymbol{u}_{1i0} \\ \boldsymbol{u}_{1\Gamma 0} \end{array}\right], \end{aligned}$$

and $\hat{\boldsymbol{f}}_{2i}$ can be expressed in terms of the unknowns in the second subsystem,

$$\hat{\boldsymbol{f}}_{2i} = (sI - A_{2i})\hat{\boldsymbol{u}}_{2i} - C_2 \hat{\boldsymbol{u}}_{2\Gamma} - \boldsymbol{u}_{2i0}.$$

Similarly we eliminate the unknowns $\hat{\boldsymbol{u}}_{1i}$ in the second subsystem, and we obtain the iterations

$$
\begin{aligned}
&\begin{bmatrix} sI - A_{1i} & -C_1 \\ -B_2 & sI - A_\Gamma - B_1(sI - A_{2i})^{-1}C_2 \end{bmatrix} \begin{bmatrix} \hat{\boldsymbol{u}}_{1i}^{k+1} \\ \hat{\boldsymbol{u}}_{1\Gamma}^{k+1} \end{bmatrix} \\
&\qquad = \begin{bmatrix} \hat{\boldsymbol{f}}_{1i} \\ \hat{\boldsymbol{f}}_\Gamma + B_1\hat{\boldsymbol{u}}_{2i}^k - B_1(sI - A_{2i})^{-1}C_2\hat{\boldsymbol{u}}_{2\Gamma}^k \end{bmatrix} + \begin{bmatrix} \boldsymbol{u}_{1i0} \\ \boldsymbol{u}_{1\Gamma 0} \end{bmatrix}, \\
&\begin{bmatrix} sI - A_\Gamma - B_2(sI - A_{1i})^{-1}C_1 & -B_1 \\ -C_2 & sI - A_{2i} \end{bmatrix} \begin{bmatrix} \hat{\boldsymbol{u}}_{2\Gamma}^{k+1} \\ \hat{\boldsymbol{u}}_{2i}^{k+1} \end{bmatrix} \\
&\qquad = \begin{bmatrix} \hat{\boldsymbol{f}}_\Gamma + B_2\hat{\boldsymbol{u}}_{1i}^k - B_2(sI - A_{1i})^{-1}C_1\hat{\boldsymbol{u}}_{1\Gamma}^k \\ \hat{\boldsymbol{f}}_{2i} \end{bmatrix} + \begin{bmatrix} \boldsymbol{u}_{2\Gamma 0} \\ \boldsymbol{u}_{2i0} \end{bmatrix}.
\end{aligned}
\tag{2.9}
$$

We show next that the new WR algorithm (2.9) converges in two iterations. By linearity, it suffices to analyze the homogeneous problem where $\boldsymbol{f}(t) = \boldsymbol{0}$ and $\boldsymbol{u}(0) = \boldsymbol{0}$.

Proposition 2.1. *The new WR algorithm (2.9) converges in two iterations independently of the initial waveforms.*

Proof. From the first equation in the first subsystem and the second equation in the second subsystem in (2.9) we obtain, respectively,

$$
\begin{aligned}
\hat{\boldsymbol{u}}_{1i}^{k+1} &= (sI - A_{1i})^{-1}C_1\hat{\boldsymbol{u}}_{1\Gamma}^{k+1}, \\
\hat{\boldsymbol{u}}_{2i}^{k+1} &= (sI - A_{2i})^{-1}C_2\hat{\boldsymbol{u}}_{2\Gamma}^{k+1}.
\end{aligned}
$$

Now, in the first iteration we have

$$
\begin{aligned}
\hat{\boldsymbol{u}}_{1i}^{1} &= (sI - A_{1i})^{-1}C_1\hat{\boldsymbol{u}}_{1\Gamma}^{1}, \\
\hat{\boldsymbol{u}}_{2i}^{1} &= (sI - A_{2i})^{-1}C_2\hat{\boldsymbol{u}}_{2\Gamma}^{1}.
\end{aligned}
\tag{2.10}
$$

From the first and second subsystems in (2.9), in the second iteration we get after some algebra

$$
\begin{aligned}
(sI - A_\Gamma - B_1(sI - A_{2i})^{-1}C_2 - B_2(sI - A_{1i})^{-1}C_1)\hat{\boldsymbol{u}}_{1\Gamma}^2 &= B_1\hat{\boldsymbol{u}}_{2i}^1 - B_1(sI - A_{2i})^{-1}C_2\hat{\boldsymbol{u}}_{2\Gamma}^1, \\
(sI - A_\Gamma - B_2(sI - A_{1i})^{-1}C_1 - B_1(sI - A_{2i})^{-1}C_2)\hat{\boldsymbol{u}}_{2\Gamma}^2 &= B_2\hat{\boldsymbol{u}}_{1i}^1 - B_2(sI - A_{1i})^{-1}C_1\hat{\boldsymbol{u}}_{1\Gamma}^1.
\end{aligned}
\tag{2.11}
$$

Now substituting $\hat{\boldsymbol{u}}_{2i}^1$ and $\hat{\boldsymbol{u}}_{1i}^1$ from (2.10) into the first and second equations in (2.11) respectively, implies

$$(sI - A_\Gamma - B_1(sI - A_{2i})^{-1}C_2 - B_2(sI - A_{1i})^{-1}C_1)\hat{\boldsymbol{u}}_{1\Gamma}^2 = \mathbf{0},$$
$$(sI - A_\Gamma - B_2(sI - A_{1i})^{-1}C_1 - B_1(sI - A_{2i})^{-1}C_2)\hat{\boldsymbol{u}}_{2\Gamma}^2 = \mathbf{0}.$$

Therefore, $\hat{\boldsymbol{u}}_{1\Gamma}^2$ and $\hat{\boldsymbol{u}}_{2\Gamma}^2$ are identically zero, independently of the guess for the initial waveforms. □

This convergence is optimal, since the resulting waveforms in each subsystem depend in general also on the source term $\boldsymbol{f}_j$ in the other subsystem. Therefore, the minimum number of iterations needed for convergence for any WR algorithm with two subsystems is two: a first iteration where each subsystem incorporates the information of its source term $\boldsymbol{f}_j$ into its waveforms and then transmits this information to the neighboring subsystem, and a second iteration to incorporate this transmitted information about $\boldsymbol{f}_j$ from the neighboring subsystem into its own waveforms. Therefore, the optimal transmission conditions with overlap are given by

$$\begin{aligned} \hat{\boldsymbol{u}}_{1\Gamma+1}^{k+1} - (sI - A_{2i})^{-1}C_2\hat{\boldsymbol{u}}_{1\Gamma}^{k+1} &= \hat{\boldsymbol{u}}_{2i}^{k} - (sI - A_{2i})^{-1}C_2\hat{\boldsymbol{u}}_{2\Gamma}^{k}, \\ \hat{\boldsymbol{u}}_{2\Gamma-1}^{k+1} - (sI - A_{1i})^{-1}C_1\hat{\boldsymbol{u}}_{2\Gamma}^{k+1} &= \hat{\boldsymbol{u}}_{1i}^{k} - (sI - A_{1i})^{-1}C_1\hat{\boldsymbol{u}}_{1\Gamma}^{k}. \end{aligned} \tag{2.12}$$

To find the iteration matrix of the classical WR algorithm, we consider the two subsystems in (2.8), and by linearity, we again consider the homogeneous problem where $\boldsymbol{f}(t) = \mathbf{0}$ and $\boldsymbol{u}(0) = \mathbf{0}$. From the equations at the interface we obtain

$$(sI - A_\Gamma)\hat{\boldsymbol{u}}_{1\Gamma}^{k+1} - B_2\hat{\boldsymbol{u}}_{1i}^{k+1} = B_1\hat{\boldsymbol{u}}_{2i}^{k},$$
$$(sI - A_\Gamma)\hat{\boldsymbol{u}}_{2\Gamma}^{k+1} - B_1\hat{\boldsymbol{u}}_{2i}^{k+1} = B_2\hat{\boldsymbol{u}}_{1i}^{k}.$$

We then substitute from (2.8) for $\hat{\boldsymbol{u}}_{1i}$ and $\hat{\boldsymbol{u}}_{2i}$ above to get after simplifying,

$$\begin{aligned} \hat{\boldsymbol{u}}_{1\Gamma}^{k+1} &= (sI - A_\Gamma - B_2(sI - A_{1i})^{-1}C_1)^{-1}B_1(sI - A_{2i})^{-1}C_2\hat{\boldsymbol{u}}_{2\Gamma}^{k}, \\ \hat{\boldsymbol{u}}_{2\Gamma}^{k+1} &= (sI - A_\Gamma - B_1(sI - A_{2i})^{-1}C_2)^{-1}B_2(sI - A_{1i})^{-1}C_1\hat{\boldsymbol{u}}_{1\Gamma}^{k}. \end{aligned} \tag{2.13}$$

Inserting the second equation into the first one in (2.13) at iteration k leads to a relation over two steps of the classical WR algorithm,

$$\hat{\boldsymbol{u}}_{1\Gamma}^{k+1} = X_1 X_2 \hat{\boldsymbol{u}}_{1\Gamma}^{k-1},$$

and inserting the first one into the second one at iteration k implies

$$\hat{\boldsymbol{u}}_{2\Gamma}^{k+1} = X_2 X_1 \hat{\boldsymbol{u}}_{2\Gamma}^{k-1},$$

where

$$X_1 = (sI - A_\Gamma - B_2(sI - A_{1i})^{-1}C_1)^{-1}B_1(sI - A_{2i})^{-1}C_2,$$
$$X_2 = (sI - A_\Gamma - B_1(sI - A_{2i})^{-1}C_2)^{-1}B_2(sI - A_{1i})^{-1}C_1.$$

By induction we obtain $\hat{\boldsymbol{u}}_{1\Gamma}^{2k} = (X_1X_2)^k \hat{\boldsymbol{u}}_{1\Gamma}^0$ and $\hat{\boldsymbol{u}}_{2\Gamma}^{2k} = (X_2X_1)^k \hat{\boldsymbol{u}}_{2\Gamma}^0$. Therefore, the iteration matrix is given by

$$G_{cla}(s) = \begin{pmatrix} X_1X_2 & \mathbf{0} \\ \mathbf{0} & X_2X_1 \end{pmatrix}. \tag{2.14}$$

The spectral radius $\rho(G_{cla})$ of the iteration matrix G_{cla}, which is defined by

$$\rho(G_{cla}) = \max_j |\lambda_j(G_{cla})|,$$

where λ_j are the eigenvalues of G_{cla}, is a fixed function of the system or circuit elements in the classical WR algorithm as is evident from (2.14). Thus the algorithm does not have any adjustable parameters like the new WR algorithm below.

Using the new transmission conditions

$$\begin{aligned} \boldsymbol{u}_{1\Gamma+1}^{k+1} + \boldsymbol{\alpha} C_2 \boldsymbol{u}_{1\Gamma}^{k+1} &= \boldsymbol{u}_{2i}^{k} + \boldsymbol{\alpha} C_2 \boldsymbol{u}_{2\Gamma}^{k}, \\ \boldsymbol{u}_{2\Gamma-1}^{k+1} + \boldsymbol{\beta} C_1 \boldsymbol{u}_{2\Gamma}^{k+1} &= \boldsymbol{u}_{1i}^{k} + \boldsymbol{\beta} C_1 \boldsymbol{u}_{1\Gamma}^{k}, \end{aligned} \tag{2.15}$$

where we introduced the weighting factors $\boldsymbol{\alpha}$ and $\boldsymbol{\beta}$ which are square matrices or possibly linear operators in time, the new WR algorithm is

$$\begin{aligned} \begin{pmatrix} \dot{\boldsymbol{u}}_{1i}^{k+1} \\ \dot{\boldsymbol{u}}_{1\Gamma}^{k+1} \end{pmatrix} &= \begin{bmatrix} A_{1i} & C_1 \\ B_2 & A_\Gamma - B_1\boldsymbol{\alpha}C_2 \end{bmatrix} \begin{bmatrix} \boldsymbol{u}_{1i}^{k+1} \\ \boldsymbol{u}_{1\Gamma}^{k+1} \end{bmatrix} + \begin{bmatrix} \boldsymbol{f}_{1i} \\ \boldsymbol{f}_\Gamma + B_1\boldsymbol{u}_{2i}^k + B_1\boldsymbol{\alpha}C_2\boldsymbol{u}_{2\Gamma}^k \end{bmatrix}, \\ \begin{pmatrix} \dot{\boldsymbol{u}}_{2\Gamma}^{k+1} \\ \dot{\boldsymbol{u}}_{2i}^{k+1} \end{pmatrix} &= \begin{bmatrix} A_\Gamma - B_2\boldsymbol{\beta}C_1 & B_1 \\ C_2 & A_{2i} \end{bmatrix} \begin{bmatrix} \boldsymbol{u}_{2\Gamma}^{k+1} \\ \boldsymbol{u}_{2i}^{k+1} \end{bmatrix} + \begin{bmatrix} \boldsymbol{f}_\Gamma + B_2\boldsymbol{u}_{1i}^k + B_2\boldsymbol{\beta}C_1\boldsymbol{u}_{1\Gamma}^k \\ \boldsymbol{f}_{2i} \end{bmatrix}. \end{aligned} \tag{2.16}$$

We will next look for the iteration matrix of the new WR algorithm (2.16). We consider again the homogenous problem. Applying the Laplace transform to (2.16) implies

$$\begin{bmatrix} sI - A_{1i} & -C_1 \\ -B_2 & sI - A_\Gamma + B_1\boldsymbol{\alpha}C_2 \end{bmatrix}\begin{bmatrix} \hat{\boldsymbol{u}}_{1i}^{k+1} \\ \hat{\boldsymbol{u}}_{1\Gamma}^{k+1} \end{bmatrix} = \begin{bmatrix} \mathbf{0} \\ B_1\hat{\boldsymbol{u}}_{2i}^{k} + B_1\boldsymbol{\alpha}C_2\hat{\boldsymbol{u}}_{2\Gamma}^{k} \end{bmatrix},$$
$$\begin{bmatrix} sI - A_\Gamma + B_2\boldsymbol{\beta}C_1 & -B_1 \\ -C_2 & sI - A_{2i} \end{bmatrix}\begin{bmatrix} \hat{\boldsymbol{u}}_{2\Gamma}^{k+1} \\ \hat{\boldsymbol{u}}_{2i}^{k+1} \end{bmatrix} = \begin{bmatrix} B_2\hat{\boldsymbol{u}}_{1i}^{k} + B_2\boldsymbol{\beta}C_1\hat{\boldsymbol{u}}_{1\Gamma}^{k} \\ \mathbf{0} \end{bmatrix}. \tag{2.17}$$

The equations at the interface are given by

$$-B_2\hat{\boldsymbol{u}}_{1i}^{k+1} + (sI - A_\Gamma + B_1\boldsymbol{\alpha}C_2)\hat{\boldsymbol{u}}_{1\Gamma}^{k+1} = B_1\hat{\boldsymbol{u}}_{2i}^{k} + B_1\boldsymbol{\alpha}C_2\hat{\boldsymbol{u}}_{2\Gamma}^{k},$$
$$-B_1\hat{\boldsymbol{u}}_{2i}^{k+1} + (sI - A_\Gamma + B_2\boldsymbol{\beta}C_1)\hat{\boldsymbol{u}}_{2\Gamma}^{k+1} = B_2\hat{\boldsymbol{u}}_{1i}^{k} + B_2\boldsymbol{\beta}C_1\hat{\boldsymbol{u}}_{1\Gamma}^{k}.$$

Substituting above from (2.17) for $\hat{\boldsymbol{u}}_{1i}$ and $\hat{\boldsymbol{u}}_{2i}$ implies after simplifying,

$$\hat{\boldsymbol{u}}_{1\Gamma}^{k+1} = (sI - A_\Gamma + B_1\boldsymbol{\alpha}C_2 - B_2(sI - A_{1i})^{-1}C_1)^{-1}(B_1(sI - A_{2i})^{-1}C_2 + B_1\boldsymbol{\alpha}C_2)\hat{\boldsymbol{u}}_{2\Gamma}^{k},$$
$$\hat{\boldsymbol{u}}_{2\Gamma}^{k+1} = (sI - A_\Gamma + B_2\boldsymbol{\beta}C_1 - B_1(sI - A_{2i})^{-1}C_2)^{-1}(B_2(sI - A_{1i})^{-1}C_1 + B_2\boldsymbol{\beta}C_1)\hat{\boldsymbol{u}}_{1\Gamma}^{k}. \tag{2.18}$$

Now, inserting the second equation into the first one in (2.18) at iteration k implies a relation over two iteration steps,

$$\hat{\boldsymbol{u}}_{1\Gamma}^{k+1} = \tilde{X}_1\tilde{X}_2\hat{\boldsymbol{u}}_{1\Gamma}^{k-1}.$$

Similarly, inserting the first equation into the second one at iteration k we get

$$\hat{\boldsymbol{u}}_{2\Gamma}^{k+1} = \tilde{X}_2\tilde{X}_1\hat{\boldsymbol{u}}_{2\Gamma}^{k-1},$$

and by induction we find, as before, $\hat{\boldsymbol{u}}_{1\Gamma}^{2k} = (\tilde{X}_1\tilde{X}_2)^k\hat{\boldsymbol{u}}_{1\Gamma}^{0}$ and $\hat{\boldsymbol{u}}_{2\Gamma}^{2k} = (\tilde{X}_2\tilde{X}_1)^k\hat{\boldsymbol{u}}_{2\Gamma}^{0}$. Therefore, the iteration matrix for the new WR algorithm is given by

$$G_{opt}(s, \boldsymbol{\alpha}, \boldsymbol{\beta}) = \begin{pmatrix} \tilde{X}_1\tilde{X}_2 & \mathbf{0} \\ \mathbf{0} & \tilde{X}_2\tilde{X}_1 \end{pmatrix}, \tag{2.19}$$

where $\tilde{X}_1$ and $\tilde{X}_2$ are

$$\tilde{X}_1 := (sI - A_\Gamma + B_1\boldsymbol{\alpha}C_2 - B_2(sI - A_{1i})^{-1}C_1)^{-1}(B_1(sI - A_{2i})^{-1}C_2 + B_1\boldsymbol{\alpha}C_2),$$
$$\tilde{X}_2 := (sI - A_\Gamma + B_2\boldsymbol{\beta}C_1 - B_1(sI - A_{2i})^{-1}C_2)^{-1}(B_2(sI - A_{1i})^{-1}C_1 + B_2\boldsymbol{\beta}C_1).$$

From the iteration matrix (2.19) one can derive the optimal values of the parameters $\boldsymbol{\alpha}$ and $\boldsymbol{\beta}$ as given in the following theorem.

Theorem 2.1 (Optimal Convergence). *The new WR algorithm (2.16) converges in two iterations if*

$$\boldsymbol{\alpha}_{opt} := -(sI - A_{2i})^{-1}, \quad \boldsymbol{\beta}_{opt} := -(sI - A_{1i})^{-1}, \tag{2.20}$$

independently of the initial waveforms $\hat{\boldsymbol{u}}_{1\Gamma}^0$ *and* $\hat{\boldsymbol{u}}_{2\Gamma}^0$.

Proof. The iteration matrix vanishes if we insert (2.20) into G_{opt} given by (2.19). Hence, $\hat{\boldsymbol{u}}_{1\Gamma}^2$ and $\hat{\boldsymbol{u}}_{2\Gamma}^2$ are identically zero, independently of $\hat{\boldsymbol{u}}_{1\Gamma}^0$ and $\hat{\boldsymbol{u}}_{2\Gamma}^0$. □

This result shows that the optimal values of the parameters $\boldsymbol{\alpha}$ and $\boldsymbol{\beta}$ in the transmission conditions (2.15) lead to the optimal transmission conditions shown earlier in (2.12). We observe that the optimal values in (2.20) are not just parameters, but the Laplace transform of operators in time since they depend on s, and moreover, they have a matrix inverse, and thus they are expensive to implement. Therefore, an approximation of the best possible transmission conditions will be proposed, which will lead to a very practical algorithm. We next introduce the WR algorithms without overlap.

2.2 The WR Algorithms without Overlap

To determine the WR algorithms without overlap, we now consider a partition of (2.1) into two blocks without a common interface

$$\begin{pmatrix} \dot{\boldsymbol{u}}_{11} \\ \dot{\boldsymbol{u}}_{22} \end{pmatrix} = \begin{bmatrix} A_1 & B \\ C & A_2 \end{bmatrix} \begin{bmatrix} \boldsymbol{u}_{11} \\ \boldsymbol{u}_{22} \end{bmatrix} + \begin{bmatrix} \boldsymbol{f}_{11} \\ \boldsymbol{f}_{22} \end{bmatrix}, \tag{2.21}$$

with an initial condition $\boldsymbol{u}(0) = (\boldsymbol{u}_{110}, \boldsymbol{u}_{220})^T$.

A general partition into two blocks is given by

$$\begin{aligned} \dot{\boldsymbol{u}}_{11} &= A_1\boldsymbol{u}_{11} + B\boldsymbol{u}_{12} + \boldsymbol{f}_{11}, \\ \dot{\boldsymbol{u}}_{22} &= A_2\boldsymbol{u}_{22} + C\boldsymbol{u}_{21} + \boldsymbol{f}_{22}. \end{aligned} \tag{2.22}$$

Using the classical transmission conditions

$$\boldsymbol{u}_{12}^{k+1} = \boldsymbol{u}_{22}^{k}, \quad \boldsymbol{u}_{21}^{k+1} = \boldsymbol{u}_{11}^{k},$$

the classical WR algorithm is

$$\begin{aligned} \dot{\boldsymbol{u}}_{11}^{k+1} &= A_1\boldsymbol{u}_{11}^{k+1} + B\boldsymbol{u}_{22}^{k} + \boldsymbol{f}_{11}, \\ \dot{\boldsymbol{u}}_{22}^{k+1} &= A_2\boldsymbol{u}_{22}^{k+1} + C\boldsymbol{u}_{11}^{k} + \boldsymbol{f}_{22}. \end{aligned} \tag{2.23}$$

The Laplace transform applied to (2.21) and (2.22) implies after simplifying

$$\begin{bmatrix} sI - A_1 & -B \\ -C & sI - A_2 \end{bmatrix} \begin{bmatrix} \hat{\boldsymbol{u}}_{11} \\ \hat{\boldsymbol{u}}_{22} \end{bmatrix} = \begin{bmatrix} \hat{\boldsymbol{f}}_{11} \\ \hat{\boldsymbol{f}}_{22} \end{bmatrix} + \begin{bmatrix} \boldsymbol{u}_{110} \\ \boldsymbol{u}_{220} \end{bmatrix}, \tag{2.24}$$

and

$$\begin{aligned} (sI - A_1)\hat{\boldsymbol{u}}_{11} &= B\hat{\boldsymbol{u}}_{12} + \hat{\boldsymbol{f}}_{11} + \boldsymbol{u}_{110}, \\ (sI - A_2)\hat{\boldsymbol{u}}_{22} &= C\hat{\boldsymbol{u}}_{21} + \hat{\boldsymbol{f}}_{22} + \boldsymbol{u}_{220}. \end{aligned} \tag{2.25}$$

The classical WR algorithm in the frequency domain is now given by

$$\begin{aligned} (sI - A_1)\hat{\boldsymbol{u}}_{11}^{k+1} &= B\hat{\boldsymbol{u}}_{22}^{k} + \hat{\boldsymbol{f}}_{11} + \boldsymbol{u}_{110}, \\ (sI - A_2)\hat{\boldsymbol{u}}_{22}^{k+1} &= C\hat{\boldsymbol{u}}_{11}^{k} + \hat{\boldsymbol{f}}_{22} + \boldsymbol{u}_{220}. \end{aligned} \tag{2.26}$$

Similar to the WR algorithms with overlap, at convergence, eliminating the unknowns $\hat{\boldsymbol{u}}_{22}$ in the first subsystem in (2.26) gives

$$(sI - A_1 - B(sI - A_2)^{-1}C)\hat{\boldsymbol{u}}_{11} = \hat{\boldsymbol{f}}_{11} + B(sI - A_2)^{-1}(\hat{\boldsymbol{f}}_{22} + \boldsymbol{u}_{220}) + \boldsymbol{u}_{110},$$

and $\hat{\boldsymbol{f}}_{22}$ can be expressed in terms of the unknowns in the second subsystem,

$$\hat{\boldsymbol{f}}_{22} = (sI - A_2)\hat{\boldsymbol{u}}_{22} - C\hat{\boldsymbol{u}}_{21} - \boldsymbol{u}_{220}.$$

Similarly also eliminating the unknowns $\hat{\boldsymbol{u}}_{11}$ in the second subsystem we obtain the iterations

$$\begin{aligned}(sI - A_1 - B(sI - A_2)^{-1}C)\hat{\boldsymbol{u}}_{11}^{k+1} &= \hat{\boldsymbol{f}}_{11} + B\hat{\boldsymbol{u}}_{22}^{k} - B(sI - A_2)^{-1}C\hat{\boldsymbol{u}}_{21}^{k} + \boldsymbol{u}_{110},\\ (sI - A_2 - C(sI - A_1)^{-1}B)\hat{\boldsymbol{u}}_{22}^{k+1} &= \hat{\boldsymbol{f}}_{22} + C\hat{\boldsymbol{u}}_{11}^{k} - C(sI - A_1)^{-1}B\hat{\boldsymbol{u}}_{12}^{k} + \boldsymbol{u}_{220}.\end{aligned} \tag{2.27}$$

We next show that the new WR algorithm (2.27) converges in two iterations. Therefore, the optimal transmission conditions without overlap are

$$\begin{aligned}\hat{\boldsymbol{u}}_{12}^{k+1} - (sI - A_2)^{-1}C\hat{\boldsymbol{u}}_{11}^{k+1} &= \hat{\boldsymbol{u}}_{22}^{k} - (sI - A_2)^{-1}C\hat{\boldsymbol{u}}_{21}^{k},\\ \hat{\boldsymbol{u}}_{21}^{k+1} - (sI - A_1)^{-1}B\hat{\boldsymbol{u}}_{22}^{k+1} &= \hat{\boldsymbol{u}}_{11}^{k} - (sI - A_1)^{-1}B\hat{\boldsymbol{u}}_{12}^{k}.\end{aligned} \tag{2.28}$$

Note that the optimal transmission conditions without overlap are similar to those with overlap, they have however different matrices. We again consider below the homogeneous problem.

Proposition 2.2. *The new WR algorithm (2.27) converges in two iterations independently of the initial waveforms.*

Proof. In the first iteration we have

$$\begin{aligned}(sI - A_1 - B(sI - A_2)^{-1}C)\hat{\boldsymbol{u}}_{11}^{1} &= B\hat{\boldsymbol{u}}_{22}^{0} - B(sI - A_2)^{-1}C\hat{\boldsymbol{u}}_{21}^{0},\\ (sI - A_2 - C(sI - A_1)^{-1}B)\hat{\boldsymbol{u}}_{22}^{1} &= C\hat{\boldsymbol{u}}_{11}^{0} - C(sI - A_1)^{-1}B\hat{\boldsymbol{u}}_{12}^{0}.\end{aligned}$$

From the first equation above together with the first transmission condition in (2.28) we get

$$\hat{\boldsymbol{u}}_{11}^{1} = (sI - A_1)^{-1}B\hat{\boldsymbol{u}}_{12}^{1}. \tag{2.29}$$

Similarly, from the second equation together with the second transmission condition in (2.28) we obtain

$$\hat{\boldsymbol{u}}_{22}^{1} = (sI - A_2)^{-1}C\hat{\boldsymbol{u}}_{21}^{1}. \tag{2.30}$$

Now substituting from (2.29) and (2.30) into the subsystems in (2.27) in the second iteration implies

$$\begin{aligned}(sI - A_1 - B(sI - A_2)^{-1}C)\hat{\boldsymbol{u}}_{11}^{2} &= \boldsymbol{0},\\ (sI - A_2 - C(sI - A_1)^{-1}B)\hat{\boldsymbol{u}}_{22}^{2} &= \boldsymbol{0}.\end{aligned}$$

Hence, $\hat{\boldsymbol{u}}_{11}^2$ and $\hat{\boldsymbol{u}}_{22}^2$ are identically zero, independently of the guess for the initial waveforms. □

To find the iteration matrix of the classical WR algorithm we consider the homogeneous problem of (2.26). From the first and second equations in (2.26) we obtain

$$\begin{aligned}\hat{\boldsymbol{u}}_{11}^{k+1} &= (sI - A_1)^{-1}B\hat{\boldsymbol{u}}_{22}^{k},\\ \hat{\boldsymbol{u}}_{22}^{k+1} &= (sI - A_2)^{-1}C\hat{\boldsymbol{u}}_{11}^{k}.\end{aligned}$$

Inserting the second equation into the first one above we get a relation over two iteration steps of the classical WR algorithm,

$$\hat{\boldsymbol{u}}_{11}^{k+1} = (sI - A_1)^{-1}B(sI - A_2)^{-1}C\hat{\boldsymbol{u}}_{11}^{k-1},$$

and inserting the first one into the second one implies

$$\hat{\boldsymbol{u}}_{22}^{k+1} = (sI - A_2)^{-1}C(sI - A_1)^{-1}B\hat{\boldsymbol{u}}_{22}^{k-1}.$$

By induction we obtain

$$\begin{aligned}\hat{\boldsymbol{u}}_{11}^{2k} &= ((sI - A_1)^{-1}B(sI - A_2)^{-1}C)^k\hat{\boldsymbol{u}}_{11}^{0},\\ \hat{\boldsymbol{u}}_{22}^{2k} &= ((sI - A_2)^{-1}C(sI - A_1)^{-1}B)^k\hat{\boldsymbol{u}}_{22}^{0}.\end{aligned}$$

Therefore, the iteration matrix is given by

$$G_{cla}(s) = \begin{pmatrix} (sI - A_1)^{-1}B(sI - A_2)^{-1}C & \mathbf{0} \\ \mathbf{0} & (sI - A_2)^{-1}C(sI - A_1)^{-1}B \end{pmatrix}. \tag{2.31}$$

Using the new transmission conditions

$$\begin{aligned}\boldsymbol{u}_{12}^{k+1} + \boldsymbol{\alpha}C\boldsymbol{u}_{11}^{k+1} &= \boldsymbol{u}_{22}^{k} + \boldsymbol{\alpha}C\boldsymbol{u}_{21}^{k},\\ \boldsymbol{u}_{21}^{k+1} + \boldsymbol{\beta}B\boldsymbol{u}_{22}^{k+1} &= \boldsymbol{u}_{11}^{k} + \boldsymbol{\beta}B\boldsymbol{u}_{12}^{k},\end{aligned} \tag{2.32}$$

the new WR algorithm is

$$\begin{aligned}\dot{\boldsymbol{u}}_{11}^{k+1} &= (A_1 - B\boldsymbol{\alpha}C)\boldsymbol{u}_{11}^{k+1} + B\boldsymbol{u}_{22}^{k} + B\boldsymbol{\alpha}C\boldsymbol{u}_{21}^{k} + \boldsymbol{f}_{11},\\ \dot{\boldsymbol{u}}_{22}^{k+1} &= (A_2 - C\boldsymbol{\beta}B)\boldsymbol{u}_{22}^{k+1} + C\boldsymbol{u}_{11}^{k} + C\boldsymbol{\beta}B\boldsymbol{u}_{12}^{k} + \boldsymbol{f}_{22}.\end{aligned} \tag{2.33}$$

The Laplace transform applied to the homogeneous problem of (2.33) implies

$$\begin{aligned}(sI - A_1 + B\boldsymbol{\alpha}C)\hat{\boldsymbol{u}}_{11}^{k+1} &= B\hat{\boldsymbol{u}}_{22}^{k} + B\boldsymbol{\alpha}C\hat{\boldsymbol{u}}_{21}^{k},\\ (sI - A_2 + C\boldsymbol{\beta}B)\hat{\boldsymbol{u}}_{22}^{k+1} &= C\hat{\boldsymbol{u}}_{11}^{k} + C\boldsymbol{\beta}B\hat{\boldsymbol{u}}_{12}^{k}.\end{aligned} \tag{2.34}$$

From the first equation in (2.34) and the first transmission condition in (2.32) we get

$$B\hat{\boldsymbol{u}}_{12}^{k+1} = (sI - A_1)\hat{\boldsymbol{u}}_{11}^{k+1}.$$

Now, substituting from above at iteration k into the second equation in (2.34), we obtain after simplifying,

$$\hat{\boldsymbol{u}}_{22}^{k+1} = (sI - A_2 + C\boldsymbol{\beta}B)^{-1}C(I + \boldsymbol{\beta}(sI - A_1))\hat{\boldsymbol{u}}_{11}^{k}. \tag{2.35}$$

Similarly, from the second equation in (2.34) and the second transmission condition in (2.32) we get

$$C\hat{\boldsymbol{u}}_{21}^{k+1} = (sI - A_2)\hat{\boldsymbol{u}}_{22}^{k+1},$$

and substituting at iteration k into the first equation in (2.34), we obtain after simplifying,

$$\hat{\boldsymbol{u}}_{11}^{k+1} = (sI - A_1 + B\boldsymbol{\alpha}C)^{-1}B(I + \boldsymbol{\alpha}(sI - A_2))\hat{\boldsymbol{u}}_{22}^{k}. \tag{2.36}$$

By inserting (2.35) into (2.36) at iteration k we obtain a relation over two iteration steps,

$$\hat{\boldsymbol{u}}_{11}^{k+1} = \overline{X}_1\overline{X}_2\hat{\boldsymbol{u}}_{11}^{k-1}.$$

Similarly, by inserting (2.36) into (2.35) at iteration k we get

$$\hat{\boldsymbol{u}}_{22}^{k+1} = \overline{X}_2\overline{X}_1\hat{\boldsymbol{u}}_{22}^{k-1},$$

and by induction we find, as before, $\hat{\boldsymbol{u}}_{11}^{2k} = (\overline{X}_1\overline{X}_2)^k\hat{\boldsymbol{u}}_{11}^{0}$ and $\hat{\boldsymbol{u}}_{22}^{2k} = (\overline{X}_2\overline{X}_1)^k\hat{\boldsymbol{u}}_{22}^{0}$. Therefore, the iteration matrix for the new WR algorithm is given by

$$G_{opt}(s, \boldsymbol{\alpha}, \boldsymbol{\beta}) = \begin{pmatrix} \overline{X}_1\overline{X}_2 & \mathbf{0} \\ \mathbf{0} & \overline{X}_2\overline{X}_1 \end{pmatrix}, \tag{2.37}$$

where $\overline{X}_1$ and $\overline{X}_2$ are

$$\overline{X}_1 := (sI - A_1 + B\boldsymbol{\alpha}C)^{-1}B(I + \boldsymbol{\alpha}(sI - A_2)),$$
$$\overline{X}_2 := (sI - A_2 + C\boldsymbol{\beta}B)^{-1}C(I + \boldsymbol{\beta}(sI - A_1)).$$

The optimal values of the parameters $\boldsymbol{\alpha}$ and $\boldsymbol{\beta}$ are given in the following theorem.

Theorem 2.2 (Optimal Convergence). *The new WR algorithm (2.33) converges in two iterations if*

$$\boldsymbol{\alpha}_{opt} := -(sI - A_2)^{-1}, \quad \boldsymbol{\beta}_{opt} := -(sI - A_1)^{-1}, \tag{2.38}$$

independently of the initial waveforms $\hat{\boldsymbol{u}}_{11}^0$ *and* $\hat{\boldsymbol{u}}_{22}^0$.

Proof. The proof is similar to the proof of Theorem 2.1. □

This result shows again that the optimal values of the parameters $\boldsymbol{\alpha}$ and $\boldsymbol{\beta}$ in the transmission conditions (2.32) lead to the optimal transmission conditions shown earlier in (2.28). Note that the optimal choice found here is similar to the one found for the case with overlap, where we see that it is not just a parameter, but the Laplace transform of an operator in time since it depends on s, and in addition, it has a matrix inverse.

2.3 Optimization Process of the New WR Algorithm

We consider here the WR algorithm without overlap, the case with overlap can be treated similarly. The optimal values in (2.38) can be approximated by constant matrices $\boldsymbol{\alpha}$ and $\boldsymbol{\beta}$ to get a practical optimized WR algorithm. The simplest constant matrix approximation is obtained by using a Taylor expansion about $s = 0$, which leads to

$$\boldsymbol{\alpha}_T = A_2^{-1}, \quad \boldsymbol{\beta}_T = A_1^{-1}.$$

This low frequency approximation was motivated by the concrete case of RC circuits we analyze in detail in Chapter 3, where high frequencies converge fast, and low frequencies converge slowly. In addition, choosing another expansion point would lead to complex matrices, and hence the algorithm would then need to be implemented in complex arithmetic, a significant drawback. There are however better choices than the ones based on expansions, as we will show in the next paragraph. Note that this low frequency approximation exists whenever the matrices A_1 and A_2 are non-singular matrices. In case that one of the matrices A_1 and A_2 is singular one might decompose the system at a different row to get different matrices, which might lead to non-singular matrices A_1 and A_2, and thus obtain a low frequency approximation.

Another possibility is to choose the approximation by just constants $\alpha \in \mathbb{R}$ and $\beta \in \mathbb{R}$ for the optimal choice in (2.38). An optimization process then allows us to reduce the spectral radius of the iteration matrix in order to obtain faster convergence. Mathematically, we want $\rho(G_{opt}) \ll 1$, which leads to the min-max problem

$$\min_{\alpha,\beta}\left(\max_{j}|\lambda_j(G_{opt}(s,\alpha,\beta))|\right),\ s=\eta+i\omega, \tag{2.39}$$

where $\lambda_j(G_{opt})$ are the eigenvalues of the iteration matrix G_{opt}. To find the solution of the min-max problem (2.39) in its full generality, we need to resort to numerical methods. We use a multidimensional unconstrained nonlinear routine (Nelder-Mead). We will however analyze concrete cases in Chapters 3 and 4.

2.4 Multiple Subsystems

In the previous sections we analyzed WR algorithms by splitting the linear system into two subsystems. However, in realistic applications the circuit needs to be partitioned into multiple subsystems. We partition here the circuit into N subsystems without overlap, with corresponding solutions $\boldsymbol{u}_{nn}$, $n = 1, 2, \ldots, N$. We analyze the homogeneous problem because of the linearity as before, and we consider the system of ODEs

$$\dot{\boldsymbol{u}} = \begin{bmatrix} A_1 & B_1 & & & & \\ C_1 & A_2 & B_2 & & & \\ & C_2 & A_3 & B_3 & & \\ & & \ddots & \ddots & \ddots & \\ & & & C_{N-2} & A_{N-1} & B_{N-1} \\ & & & & C_{N-1} & A_N \end{bmatrix} \boldsymbol{u}.$$

Using the new transmission conditions

$$\begin{aligned} &\boldsymbol{u}_{12}^{k+1} + \boldsymbol{\alpha}_1 C_1 \boldsymbol{u}_{11}^{k+1} = \boldsymbol{u}_{22}^{k} + \boldsymbol{\alpha}_1 C_1 \boldsymbol{u}_{21}^{k}, \\ &\boldsymbol{u}_{nn-1}^{k+1} + \boldsymbol{\beta}_{n-1} B_{n-1} \boldsymbol{u}_{nn}^{k+1} = \boldsymbol{u}_{n-1n-1}^{k} + \boldsymbol{\beta}_{n-1} B_{n-1} \boldsymbol{u}_{n-1n}^{k}, \ n = 2, 3, \ldots, N-1, \\ &\boldsymbol{u}_{nn+1}^{k+1} + \boldsymbol{\alpha}_n C_n \boldsymbol{u}_{nn}^{k+1} = \boldsymbol{u}_{n+1n+1}^{k} + \boldsymbol{\alpha}_n C_n \boldsymbol{u}_{n+1n}^{k}, \ n = 2, 3, \ldots, N-1, \\ &\boldsymbol{u}_{NN-1}^{k+1} + \boldsymbol{\beta}_{N-1} B_{N-1} \boldsymbol{u}_{NN}^{k+1} = \boldsymbol{u}_{N-1N-1}^{k} + \boldsymbol{\beta}_{N-1} B_{N-1} \boldsymbol{u}_{N-1N}^{k}, \end{aligned} \tag{2.40}$$

the new WR algorithm with N subsystems without overlap is given by

$$\begin{aligned} \dot{\boldsymbol{u}}_{11}^{k+1} &= (A_1 - B_1 \boldsymbol{\alpha}_1 C_1) \boldsymbol{u}_{11}^{k+1} + B_1 \boldsymbol{u}_{22}^{k} + B_1 \boldsymbol{\alpha}_1 C_1 \boldsymbol{u}_{21}^{k}, \\ &\vdots \\ \dot{\boldsymbol{u}}_{nn}^{k+1} &= (A_n - C_{n-1} \boldsymbol{\beta}_{n-1} B_{n-1} - B_n \boldsymbol{\alpha}_n C_n) \boldsymbol{u}_{nn}^{k+1} \\ &\quad + C_{n-1} \boldsymbol{u}_{n-1n-1}^{k} + C_{n-1} \boldsymbol{\beta}_{n-1} B_{n-1} \boldsymbol{u}_{n-1n}^{k} + B_n \boldsymbol{u}_{n+1n+1}^{k} + B_n \boldsymbol{\alpha}_n C_n \boldsymbol{u}_{n+1n}^{k}, \\ &\qquad n = 2, 3, \ldots, N-1, \\ &\vdots \\ \dot{\boldsymbol{u}}_{NN}^{k+1} &= (A_N - C_{N-1} \boldsymbol{\beta}_{N-1} B_{N-1}) \boldsymbol{u}_{NN}^{k+1} + C_{N-1} \boldsymbol{u}_{N-1N-1}^{k} + C_{N-1} \boldsymbol{\beta}_{N-1} B_{N-1} \boldsymbol{u}_{N-1N}^{k}, \end{aligned} \tag{2.41}$$

where n represents the subsystem number. Note that we are studying here the algorithm without overlap, the one with overlap can be treated similarly.

Theorem 2.3 (Optimal Convergence for N Subsystems). *The new WR algo-*

rithm with N subsystems (2.41) converges in N iterations if

$$\begin{aligned}\boldsymbol{\beta}_1 &= -(sI - A_1)^{-1}, \\ \boldsymbol{\beta}_n &= -(sI - A_n + C_{n-1}\boldsymbol{\beta}_{n-1}B_{n-1})^{-1}, \; n = 2, 3, \ldots, N-1,\end{aligned} \tag{2.42}$$

and

$$\begin{aligned}\boldsymbol{\alpha}_n &= -(sI - A_{n+1} + B_{n+1}\boldsymbol{\alpha}_{n+1}C_{n+1})^{-1}, \; n = 1, 2, \ldots, N-2, \\ \boldsymbol{\alpha}_{N-1} &= -(sI - A_N)^{-1},\end{aligned} \tag{2.43}$$

independently of the initial waveforms, assuming that the matrices are invertible.

Proof. We apply first the Laplace transform to each subsystem. Now in the first iteration, we have

$$(sI - A_1 + B_1\boldsymbol{\alpha}_1 C_1)\hat{\boldsymbol{u}}_{11}^1 = B_1(\hat{\boldsymbol{u}}_{22}^0 + \boldsymbol{\alpha}_1 C_1 \hat{\boldsymbol{u}}_{21}^0),$$

and from the first transmission condition in (2.40), we obtain

$$(sI - A_1)\hat{\boldsymbol{u}}_{11}^1 = B_1 \hat{\boldsymbol{u}}_{12}^1.$$

Assuming the matrix $(sI - A_1)$ is invertible leads to

$$\hat{\boldsymbol{u}}_{11}^1 = (sI - A_1)^{-1} B_1 \hat{\boldsymbol{u}}_{12}^1. \tag{2.44}$$

In the second iteration from the second subsystem, we have

$$(sI - A_2 + C_1\boldsymbol{\beta}_1 B_1 + B_2\boldsymbol{\alpha}_2 C_2)\hat{\boldsymbol{u}}_{22}^2 = C_1\hat{\boldsymbol{u}}_{11}^1 + C_1\boldsymbol{\beta}_1 B_1 \hat{\boldsymbol{u}}_{12}^1 + B_2(\hat{\boldsymbol{u}}_{33}^1 + \boldsymbol{\alpha}_2 C_2 \hat{\boldsymbol{u}}_{32}^1).$$

Substituting above from (2.44) for $\hat{\boldsymbol{u}}_{11}^1$, and using the third transmission condition in (2.40) for $n = 2$, together with $\boldsymbol{\beta}_1 = -(sI - A_1)^{-1}$, we find

$$(sI - A_2 + C_1\boldsymbol{\beta}_1 B_1)\hat{\boldsymbol{u}}_{22}^2 = B_2 \hat{\boldsymbol{u}}_{23}^2,$$

and assuming the matrix $(sI - A_2 + C_1\boldsymbol{\beta}_1 B_1)$ is invertible we get

$$\hat{\boldsymbol{u}}_{22}^2 = (sI - A_2 + C_1\boldsymbol{\beta}_1 B_1)^{-1} B_2 \hat{\boldsymbol{u}}_{23}^2. \tag{2.45}$$

Now in the third iteration from the third subsystem we have

$$(sI - A_3 + C_2\boldsymbol{\beta}_2 B_2 + B_3\boldsymbol{\alpha}_3 C_3)\hat{\boldsymbol{u}}_{33}^3 = C_2\hat{\boldsymbol{u}}_{22}^2 + C_2\boldsymbol{\beta}_2 B_2\hat{\boldsymbol{u}}_{23}^2 + B_3(\hat{\boldsymbol{u}}_{44}^2 + \boldsymbol{\alpha}_3 C_3\hat{\boldsymbol{u}}_{43}^2).$$

We substitute above from (2.45) for $\hat{\boldsymbol{u}}_{22}^2$, then using the third transmission condition in (2.40) for $n = 3$, together with (2.42) for $n = 2$, we get

$$(sI - A_3 + C_2\boldsymbol{\beta}_2 B_2)\hat{\boldsymbol{u}}_{33}^3 = B_3\hat{\boldsymbol{u}}_{34}^3.$$

Assuming the matrix $(sI - A_3 + C_2\boldsymbol{\beta}_2 B_2)$ is invertible implies

$$\hat{\boldsymbol{u}}_{33}^3 = (sI - A_3 + C_2\boldsymbol{\beta}_2 B_2)^{-1} B_3\hat{\boldsymbol{u}}_{34}^3. \tag{2.46}$$

By induction we obtain

$$\hat{\boldsymbol{u}}_{nn}^n = (sI - A_n + C_{n-1}\boldsymbol{\beta}_{n-1} B_{n-1})^{-1} B_n\hat{\boldsymbol{u}}_{nn+1}^n,\ n = 2, 3, \ldots, N-1, \tag{2.47}$$

where

$$\boldsymbol{\beta}_1 = -(sI - A_1)^{-1},$$
$$\boldsymbol{\beta}_n = -(sI - A_n + C_{n-1}\boldsymbol{\beta}_{n-1} B_{n-1})^{-1},\ n = 2, 3, \ldots, N-1.$$

Thus in the iteration $N-1$, form the subsystem $N-1$ we have

$$\hat{\boldsymbol{u}}_{N-1N-1}^{N-1} = (sI - A_{N-1} + C_{N-2}\boldsymbol{\beta}_{N-2} B_{N-2})^{-1} B_{N-1}\hat{\boldsymbol{u}}_{N-1N}^{N-1}. \tag{2.48}$$

Now in the N^{th} iteration, from the N^{th} subsystem we get

$$(sI - A_N + C_{N-1}\boldsymbol{\beta}_{N-1} B_{N-1})\hat{\boldsymbol{u}}_{NN}^N = C_{N-1}\hat{\boldsymbol{u}}_{N-1N-1}^{N-1} + C_{N-1}\boldsymbol{\beta}_{N-1} B_{N-1}\hat{\boldsymbol{u}}_{N-1N}^{N-1}.$$

Substituting above from (2.48) for $\hat{\boldsymbol{u}}_{N-1N-1}^{N-1}$, and using (2.42) for $n = N-1$, we get

$$(sI - A_N + C_{N-1}\boldsymbol{\beta}_{N-1} B_{N-1})\hat{\boldsymbol{u}}_{NN}^N = \mathbf{0}.$$

Assuming $(sI - A_N + C_{N-1}\boldsymbol{\beta}_{N-1} B_{N-1})$ is invertible we have

$$\hat{\boldsymbol{u}}_{NN}^N = \mathbf{0}.$$

Now we apply a similar argument in the other direction. In the first iteration, we obtain from the N^{th} subsystem

$$(sI - A_N + C_{N-1}\boldsymbol{\beta}_{N-1}B_{N-1})\hat{\boldsymbol{u}}^1_{NN} = C_{N-1}(\hat{\boldsymbol{u}}^0_{N-1N-1} + \boldsymbol{\beta}_{N-1}B_{N-1}\hat{\boldsymbol{u}}^0_{N-1N}).$$

Using the last transmission condition in (2.40) implies

$$\hat{\boldsymbol{u}}^1_{NN} = (sI - A_N)^{-1}C_{N-1}\hat{\boldsymbol{u}}^1_{NN-1}. \tag{2.49}$$

Now in the second iteration, from the subsystem $N-1$ we get

$$\begin{aligned}(sI - A_{N-1} + C_{N-2}\boldsymbol{\beta}_{N-2}B_{N-2} + B_{N-1}\boldsymbol{\alpha}_{N-1}C_{N-1})\hat{\boldsymbol{u}}^2_{N-1N-1} = \\ C_{N-2}(\hat{\boldsymbol{u}}^1_{N-2N-2} + \boldsymbol{\beta}_{N-2}B_{N-2}\hat{\boldsymbol{u}}^1_{N-2N-1}) + B_{N-1}\hat{\boldsymbol{u}}^1_{NN} + B_{N-1}\boldsymbol{\alpha}_{N-1}C_{N-1}\hat{\boldsymbol{u}}^1_{NN-1}.\end{aligned}$$

Substituting above from (2.49) for $\hat{\boldsymbol{u}}^1_{NN}$, together with $\boldsymbol{\alpha}_{N-1} = -(sI - A_N)^{-1}$ implies

$$\begin{aligned}(sI - A_{N-1} + C_{N-2}\boldsymbol{\beta}_{N-2}B_{N-2} + B_{N-1}\boldsymbol{\alpha}_{N-1}C_{N-1})\hat{\boldsymbol{u}}^2_{N-1N-1} = \\ C_{N-2}(\hat{\boldsymbol{u}}^1_{N-2N-2} + \boldsymbol{\beta}_{N-2}B_{N-2}\hat{\boldsymbol{u}}^1_{N-2N-1}).\end{aligned}$$

Now using the second transmission condition in (2.40) for $n = N-1$, we obtain

$$(sI - A_{N-1} + B_{N-1}\boldsymbol{\alpha}_{N-1}C_{N-1})\hat{\boldsymbol{u}}^2_{N-1N-1} = C_{N-2}\hat{\boldsymbol{u}}^2_{N-1N-2}.$$

Assuming the matrix $(sI - A_{N-1} + B_{N-1}\boldsymbol{\alpha}_{N-1}C_{N-1})$ is invertible we get

$$\hat{\boldsymbol{u}}^2_{N-1N-1} = (sI - A_{N-1} + B_{N-1}\boldsymbol{\alpha}_{N-1}C_{N-1})^{-1}C_{N-2}\hat{\boldsymbol{u}}^2_{N-1N-2}.$$

By induction we have

$$\hat{\boldsymbol{u}}^{N-n+1}_{nn} = (sI - A_n + B_n\boldsymbol{\alpha}_nC_n)^{-1}C_{n-1}\hat{\boldsymbol{u}}^{N-n+1}_{nn-1},\ n = N-1, N-2, \ldots, 2, \tag{2.50}$$

where

$$\begin{aligned}\boldsymbol{\alpha}_n &= -(sI - A_{n+1} + B_{n+1}\boldsymbol{\alpha}_{n+1}C_{n+1})^{-1},\ n = 1, 2, \ldots, N-2,\\ \boldsymbol{\alpha}_{N-1} &= -(sI - A_N)^{-1}.\end{aligned}$$

In the N^{th} iteration, from the first subsystem we get

$$(sI - A_1 + B_1\boldsymbol{\alpha}_1 C_1)\hat{\boldsymbol{u}}_{11}^N = B_1\hat{\boldsymbol{u}}_{22}^{N-1} + B_1\boldsymbol{\alpha}_1 C_1\hat{\boldsymbol{u}}_{21}^{N-1}.$$

Now substituting above from (2.50) for $\hat{\boldsymbol{u}}_{22}^{N-1}$, together with $\boldsymbol{\alpha}_1$ from (2.43) we get

$$(sI - A_1 + B_1\boldsymbol{\alpha}_1 C_1)\hat{\boldsymbol{u}}_{11}^N = \mathbf{0},$$

and assuming the matrix $(sI - A_1 + B_1\boldsymbol{\alpha}_1 C_1)$ is invertible we obtain

$$\hat{\boldsymbol{u}}_{11}^N = \mathbf{0}.$$

Therefore, we have shown that $\hat{\boldsymbol{u}}_{11}^N$ and $\hat{\boldsymbol{u}}_{NN}^N$ are identically zero independently of the guess for the initial waveforms.

Now, from (2.47) and (2.50) we get

$$\begin{aligned}
\hat{\boldsymbol{u}}_{nn}^n - (sI - A_n + C_{n-1}\boldsymbol{\beta}_{n-1}B_{n-1})^{-1}B_n\hat{\boldsymbol{u}}_{nn+1}^n &= \mathbf{0},\\
\hat{\boldsymbol{u}}_{nn}^{N-n+1} - (sI - A_n + B_n\boldsymbol{\alpha}_n C_n)^{-1}C_{n-1}\hat{\boldsymbol{u}}_{nn-1}^{N-n+1} &= \mathbf{0},
\end{aligned}$$

for $n = 2, 3, \ldots, N-1$, which means we are propagating zero transmission conditions from both sides, and thus the unknowns in the middle are also zero. □

This convergence result is again optimal, since the solution of the last subsystem depends on the source terms in the first subsystem and vice versa. If information is exchanged only between neighboring subsystems, as in the classical JWR, then it can propagate by one subsystem at most for each iteration. Hence, there are at least N iterations required to transmit the information across N sequential subsystems.

2.5 Numerical Experiments

We now show three examples for which we find numerically the optimized parameters, and we use them to illustrate the remarkable improvement in convergence of the optimized WR algorithm over the classical one. We choose here the WR algorithms without overlap and with two subsystems.

We start by a random example to show that the optimized WR algorithm works well with an arbitrary linear system of differential equations, whereas the classical WR algorithm has difficulties to converge. The system of ODEs we consider is given by

$$\dot{\boldsymbol{x}} = A\boldsymbol{x} + \boldsymbol{f},$$

where the matrix A is given by

$$A = \begin{bmatrix} -31.7460 & -1.5873 & 0 & -2 & 0 \\ 202.0202 & -0.1010 & -202.0202 & 0 & 0 \\ 0 & 1.5873 & 0 & -1.5873 & 1 \\ 1 & 0 & 202.0202 & -0.1010 & -202.0202 \\ 0 & -2 & 0 & 1.5873 & -31.7460 \end{bmatrix}.$$

The source term is given by $\boldsymbol{f}(t) = (I_s(t)/C, 0, 0, 0, 0)^T$, where $I_s(t) = 10t$ for $0 < t < 0.1$ and $I_s(t) = 1$ for $t \geq 0.1$, and $C = 0.63$. We choose a zero initial condition and random initial waveforms. The analysis time interval is $[0, T]$, with $T = 1$. We use for the numerical computations the backward Euler method, with a time step of $\Delta t = 1/100$. We first give an example of $\rho(G_{cla})$ as a function of ω and η on the top of Figure 2.2. In Figure 2.2, we also give $\rho(G_{opt})$ as a function of ω and η, at the bottom using the numerically optimized parameters $\alpha^* = -0.0389$ and $\beta^* = -0.0445$ on the left hand side, and on the right hand side, using the Taylor approximation $\boldsymbol{\alpha}_T = A_2^{-1}$ and $\boldsymbol{\beta}_T = A_1^{-1}$. One can observe that $\rho(G_{opt})$ with the numerically optimized parameters is more uniform than $\rho(G_{opt})$ with the Taylor approximation, and than $\rho(G_{cla})$ which takes values bigger than one. To illustrate the difference in convergence between the two WR algorithms, we show the error as a function of the iterations in Figure 2.3. The better convergence of the optimized WR algorithm over

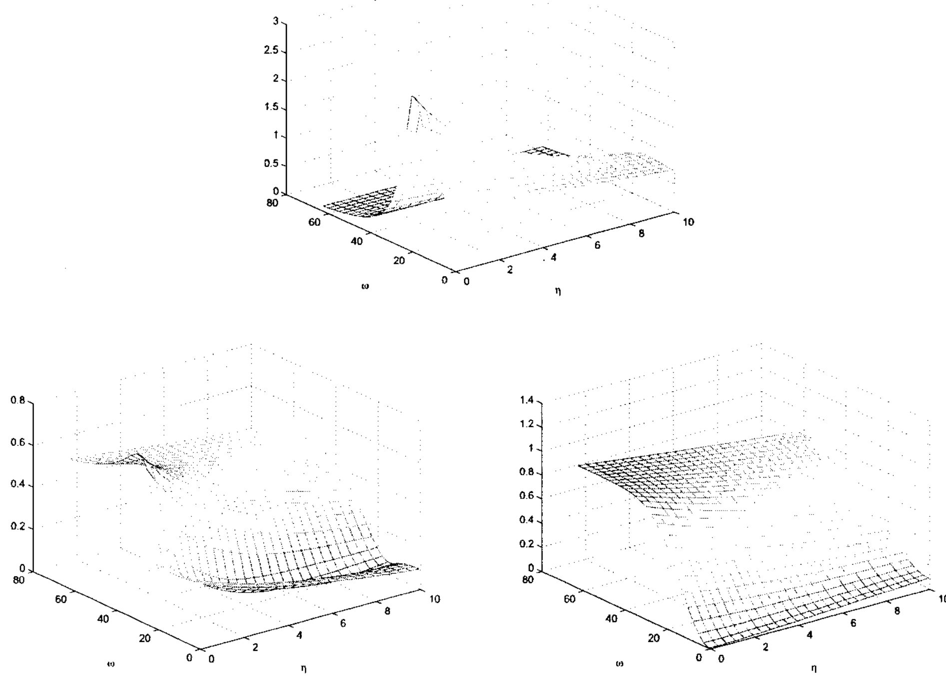

Figure 2.2: Top: classical spectral radius $\rho(G_{cla}(\omega))$. Bottom: optimized spectral radius $\rho(G_{opt}(\omega, \alpha^*, \beta^*))$ on the left, and on the right $\rho(G_{opt}(\omega, \boldsymbol{\alpha}_T, \boldsymbol{\beta}_T))$.

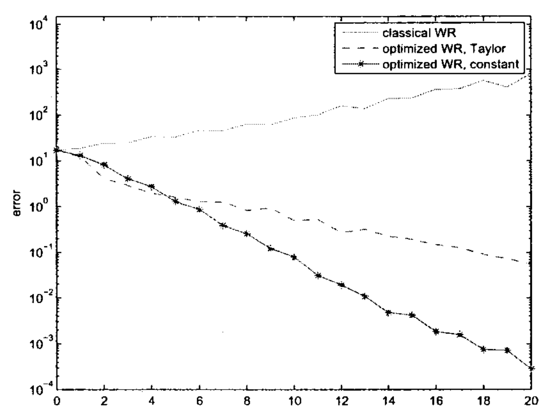

Figure 2.3: Convergence behavior of the classical versus optimized WR algorithms.

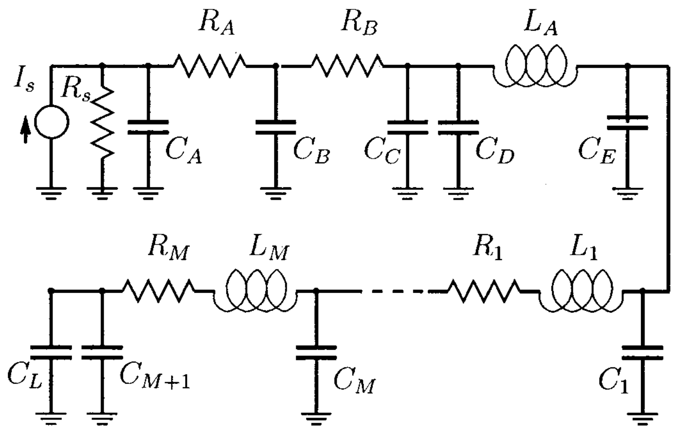

Figure 2.4: A general realistic circuit.

the classical one is evident from this comparison where the classical WR algorithm is not even converging. We also observe that the optimized WR algorithm with the optimized constant approximation has a better convergence than the one with the Taylor approximation.

We give as a second example the circuit given in Figure 2.4. The equations of the circuit, where we choose $M = 4$, are given by

$$\dot{\boldsymbol{x}} = \begin{bmatrix} b_1 & c_1 & & & \\ a_1 & b_2 & c_2 & & \\ & a_2 & b_3 & \ddots & \\ & & \ddots & \ddots & c_{12} \\ & & & a_{12} & b_{13} \end{bmatrix} \boldsymbol{x} + \boldsymbol{f}, \tag{2.51}$$

with the vector of unknown waveforms $\boldsymbol{x} = (v_1, v_2, v_3, i_1, v_4, i_2, v_5, i_3, v_6, i_4, v_7, i_5, v_8)^T$, where v_j corresponds to a nodal capacitive voltage and i_j corresponds to an inductance current. The entries in the matrix are given by

$$a_1 = \frac{1}{R_A C_B},\ a_2 = \frac{1}{R_B C_{C+D}},\ a_3 = \frac{1}{L_A},\ a_4 = \frac{1}{C_{E+1}},\ a_5 = \frac{1}{L_1},\ a_6 = \frac{1}{C_2},$$
$$a_7 = \frac{1}{L_2},\ a_8 = \frac{1}{C_3},\ a_9 = \frac{1}{L_3},\ a_{10} = \frac{1}{C_4},\ a_{11} = \frac{1}{L_4},\ a_{12} = \frac{1}{C_{5+L}},$$

$$b_1 = -(\frac{1}{R_s} + \frac{1}{R_A})\frac{1}{C_A},\ b_2 = -(\frac{1}{R_A} + \frac{1}{R_B})\frac{1}{C_B},\ b_3 = -\frac{1}{R_B C_{C+D}},$$
$$b_4 = 0,\ b_5 = 0,\ b_i = \begin{cases} -\frac{R_{(i/2)-2}}{L_{(i/2)-2}}, & i = 6, 8, 10, 12, \\ 0, & i = 7, 9, 11, 13, \end{cases}$$

$$c_1 = \frac{1}{R_A C_A},\ c_2 = \frac{1}{R_B C_B},\ c_3 = -\frac{1}{C_{C+D}},\ c_4 = -\frac{1}{L_A},\ c_5 = -\frac{1}{C_{E+1}},\ c_6 = -\frac{1}{L_1},$$
$$c_7 = -\frac{1}{C_2},\ c_8 = -\frac{1}{L_2},\ c_9 = -\frac{1}{C_3},\ c_{10} = -\frac{1}{L_3},\ c_{11} = -\frac{1}{C_4},\ c_{12} = -\frac{1}{L_4},$$

where $C_{C+D} = C_C + C_D$, and similarly for the other capacitors. The source on the right hand side is the 13×1 vector $\boldsymbol{f}(t) = (I_s(t)/C_A, 0, 0, \ldots, 0)^T$. For the input current source we use an input step function with an amplitude of $I_s(t) = 33.33$ mA and a rise time of 0.05 ns. The circuit parameters that we use are

$$R_s = 0.03 \text{ kOhms},\ C_A = C_B = C_C = 0.08 \text{ pF},\ R_A = R_B = 0.012 \text{ kOhms},$$
$$C_D = C_E = 0.25 \text{ pF},\ L_A = 0.001\ \mu\text{H},\ C_L = 0.25 \text{ pF},\ C_5 = 0.25 \text{ pF}.$$

The part from L_1 to L_M and C_1 to C_M represent a transmission line which we choose to be of 1 cm length and 4 sections. The total capacitance is $C = 2$ pF/cm, the total inductance is $L = 0.0005\ \mu$H/cm, and the total resistance is $R = 0.0001$ kOhms/cm. Since the total resistance for resistors connected in series is obtained by adding their values, and the same holds for inductors connected in series, we have $R_1 = R_2 = R_3 = R_4 = 0.0001/4$ kOhms, and $L_1 = L_2 = L_3 = L_4 = 0.0005/4\ \mu$H. In addition, the total capacitance of capacitors connected in parallel is obtained by adding their values, and thus we have $C_1 = C_2 = C_3 = C_4 = 2/4$ pF. We choose a zero initial condition and random initial waveforms. The analysis time interval is $[0, T]$, with $T = 5$. We use again for the numerical computations the backward Euler method, with a time step of $\Delta t = 1/20$. In Figure 2.5 on the top, we give $\rho(G_{cla})$ as a function of ω and

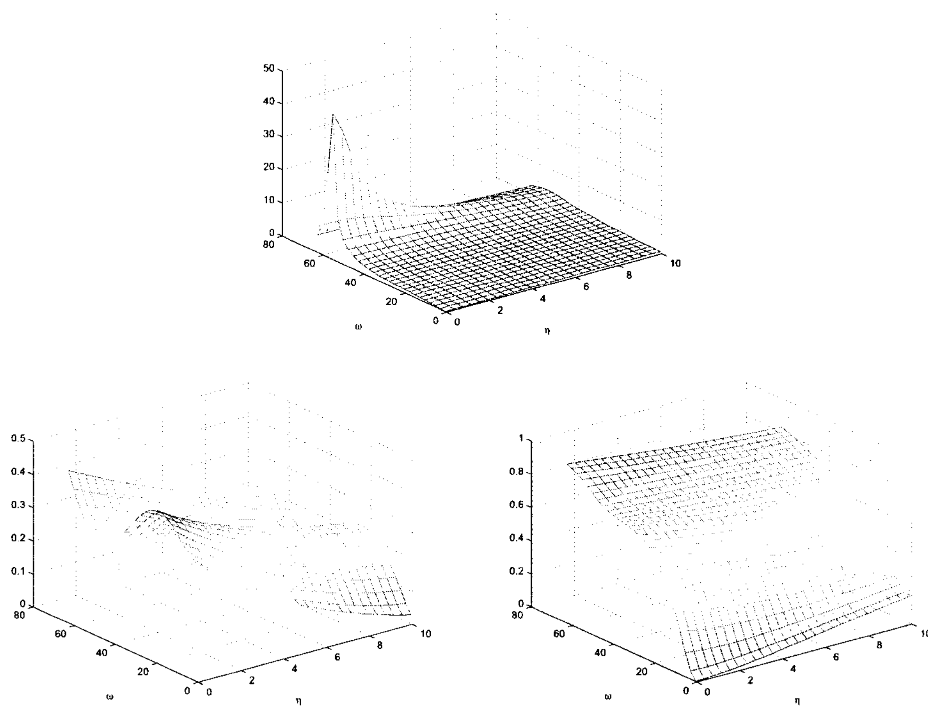

Figure 2.5: Top: classical spectral radius $\rho(G_{cla}(\omega))$. Bottom: optimized spectral radius $\rho(G_{opt}(\omega, \alpha^*, \beta^*))$ on the left, and on the right $\rho(G_{opt}(\omega, \boldsymbol{\alpha}_T, \boldsymbol{\beta}_T))$.

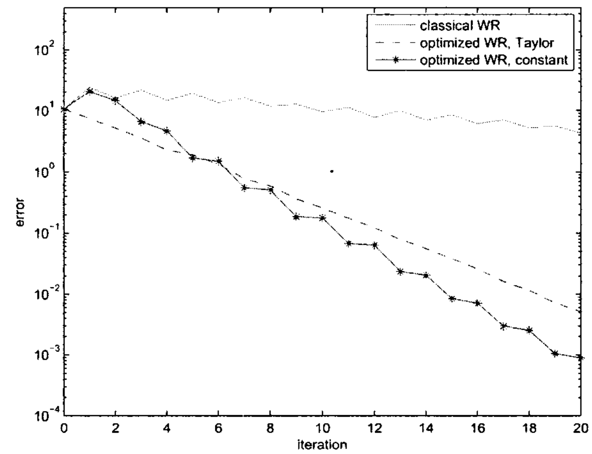

Figure 2.6: Convergence behavior of the classical versus optimized WR algorithms.

η. At the bottom we give $\rho(G_{opt})$ as a function of ω and η, using the numerically optimized parameters $\alpha^* = -0.0141$ and $\beta^* = -0.0158$ on the left hand side, and on the right hand side, using the Taylor approximation $\boldsymbol{\alpha}_T = A_2^{-1}$ and $\boldsymbol{\beta}_T = A_1^{-1}$. We observe here as well that $\rho(G_{opt})$ with the optimized constant approximation is more uniform than $\rho(G_{opt})$ with the Taylor approximation, and than $\rho(G_{cla})$ which takes values bigger than one. To illustrate the difference in convergence between the two WR algorithms we again show the error as a function of the iterations in Figure 2.6. The optimized WR algorithm shows a better convergence than the classical one which has difficulties to converge.

In order to show that the new algorithm works well for a full matrix we analyze the circuit given in Figure 2.7. The equations of the circuit are given by

$$\dot{\boldsymbol{x}} = \begin{bmatrix} b_1 & c_{12} & c_{13} & c_{14} \\ a_{12} & b_2 & c_{23} & c_{24} \\ a_{13} & a_{23} & b_3 & c_{34} \\ a_{14} & a_{24} & a_{34} & b_4 \end{bmatrix} \boldsymbol{x} + \boldsymbol{f}, \tag{2.52}$$

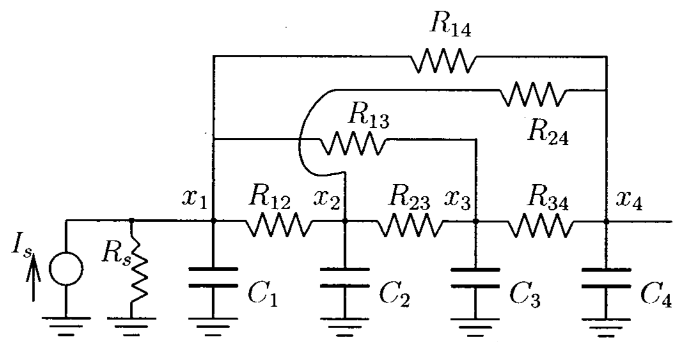

Figure 2.7: Circuit with full matrix.

where the entries in the matrix are

$$a_{12} = \frac{1}{R_{12}C_2},\ a_{13} = \frac{1}{R_{13}C_3},\ a_{23} = \frac{1}{R_{23}C_3},\ a_{14} = \frac{1}{R_{14}C_4},\ a_{24} = \frac{1}{R_{24}C_4},\ a_{34} = \frac{1}{R_{34}C_4},$$
$$b_1 = -(\tfrac{1}{R_s} + \tfrac{1}{R_{12}} + \tfrac{1}{R_{13}} + \tfrac{1}{R_{14}})\tfrac{1}{C_1},\ b_2 = -(\tfrac{1}{R_{12}} + \tfrac{1}{R_{23}} + \tfrac{1}{R_{24}})\tfrac{1}{C_2},$$
$$b_3 = -(\tfrac{1}{R_{13}} + \tfrac{1}{R_{23}} + \tfrac{1}{R_{34}})\tfrac{1}{C_3},\ b_4 = -(\tfrac{1}{R_{14}} + \tfrac{1}{R_{24}} + \tfrac{1}{R_{34}})\tfrac{1}{C_4},$$
$$c_{12} = \frac{1}{R_{12}C_1},\ c_{13} = \frac{1}{R_{13}C_1},\ c_{14} = \frac{1}{R_{14}C_1},\ c_{23} = \frac{1}{R_{23}C_2},\ c_{24} = \frac{1}{R_{24}C_2},\ c_{34} = \frac{1}{R_{34}C_3}.$$

The source on the right hand side is given by $\boldsymbol{f}(t) = (I_s(t)/C_1, 0, 0, 0)^T$, and for the input current source we use here an input step function with an amplitude of $I_s(t) = 1$ mA and a rise time of 1 ns. The circuit parameters that we use are

$$R_s = R_{12} = R_{23} = R_{34} = R_{13} = R_{14} = R_{24} = 0.5 \text{ Ohms},$$
$$C_1 = C_2 = C_3 = C_4 = 0.6 \text{ pF}.$$

We choose a zero initial condition and random initial waveforms. The analysis time interval is $[0, 10]$. We use again for the numerical computations the backward Euler method, with a time step of $\Delta t = 1/10$. In Figure 2.8 we again give $\rho(G_{cla})$ as a function of ω and η on the top. At the bottom we give $\rho(G_{opt})$ as a function of ω and η, using the numerically optimized parameters $\alpha^* = -0.0928$ and $\beta^* = -0.0945$ on the left hand side, and on the right hand side, using the Taylor approximation $\boldsymbol{\alpha}_T = A_2^{-1}$ and $\boldsymbol{\beta}_T = A_1^{-1}$. In Figure 2.9 we again plot the error as a function of the iterations which shows that the new algorithm works well and better than the classical one for full matrices as well.

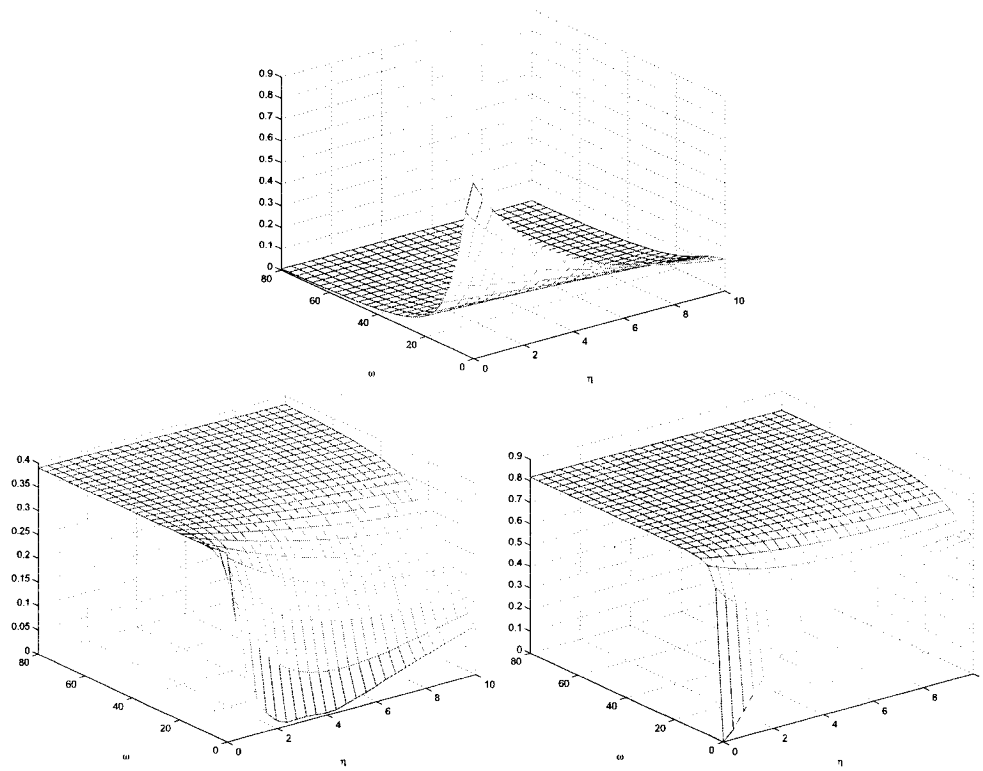

Figure 2.8: Top: classical spectral radius $\rho(G_{cla}(\omega))$. Bottom: optimized spectral radius $\rho(G_{opt}(\omega, \alpha^*, \beta^*))$ on the left, and on the right $\rho(G_{opt}(\omega, \boldsymbol{\alpha}_T, \boldsymbol{\beta}_T))$.

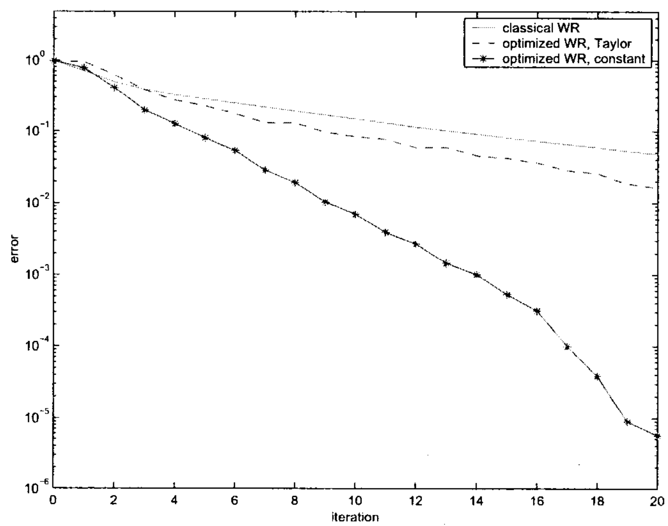

Figure 2.9: Convergence behavior of the classical versus optimized WR algorithms.

Chapter 3

RC Type Circuits

In this chapter, we analyze the classical WR algorithm, an optimal WR algorithm, and optimized WR algorithms for RC type circuits. The circuit equations are derived as in the introduction, see (1.4). The results we obtain for this type of RC circuits will be of a great interest when we have a general circuit which consists of many complicated parts that are connected to each other by such type of circuits. Indeed, we can decompose this general circuit into smaller and simpler subcircuits by applying a partitioning at the RC circuits. In other words, we look for RC type circuits in the general circuit which might have nonlinear components, and we partition there since we know how to do the partitioning for the RC circuit with an excellent performance using the results from this chapter. We start with finite size RC type circuits, and then we study an infinitely large circuit. In both cases, we investigate and analyze the convergence of the WR algorithms. We are analyzing a Jacobi type iteration here, but the Gauss-Seidel case could be analyzed similarly.

3.1 Any finite size RC Type Circuit

In this section, we consider any finite size RC type circuit as shown in Figure 3.1. The system we obtain from this circuit is of size $n \times n$, where n is the number of nodal capacitive voltages in the circuit. We assume that n is an even number for the analysis below, $n = 2j$, $j = 1, 2, \ldots$. This means that there is an even number of capacitors in the circuit given in Figure 3.1, where at each one we have a nodal voltage as an unknown. By decomposing the system representing the finite size circuit in the middle at row j into two subsystems, we get two subsystems of the same size. The odd case can be analyzed similarly. The equations for the RC circuit of size n are given by

$$\dot{\boldsymbol{x}} = \begin{bmatrix} b_1 & c_1 & & & \\ a_1 & b_2 & c_2 & & \\ & \ddots & \ddots & \ddots & \\ & & a_{n-2} & b_{n-1} & c_{n-1} \\ & & & a_{n-1} & b_n \end{bmatrix} \boldsymbol{x} + \boldsymbol{f}, \tag{3.1}$$

where the entries in the tridiagonal matrix are

$$\begin{cases} a_i = \frac{1}{R_i C_{i+1}}, & \\ c_i = \frac{1}{R_i C_i}, & i = 1, 2, \ldots n-1, \end{cases} \qquad b_i = \begin{cases} -(\frac{1}{R_s} + \frac{1}{R_1})\frac{1}{C_1}, & i = 1 \\ -(\frac{1}{R_{i-1}} + \frac{1}{R_i})\frac{1}{C_i}, & i = 2, 3, \ldots n-1, \\ -\frac{1}{R_{i-1} C_i}, & i = n \end{cases}$$

and the resistor values R_i and R_s, and the capacitors C_i are strictly positive constants. The source term on the right hand side is given by the $n \times 1$ vector $\boldsymbol{f} = (I_s(t)/C_1, 0, 0, 0, \ldots, 0)^T$, for some source function $I_s(t)$, and we are also given the initial voltage values $\boldsymbol{x}(0) = (v_1^0, v_2^0, v_3^0, v_4^0, \ldots, v_n^0)^T$ at the time $t = 0$.

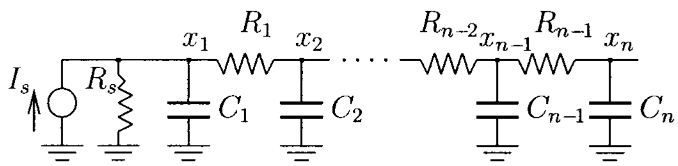

Figure 3.1: A finite size RC circuit.

We partition the system (3.1) at row j into two subsystems,

$$\begin{aligned}
\dot{\boldsymbol{u}} &= \begin{bmatrix} b_1 & c_1 & & & \\ a_1 & b_2 & c_2 & & \\ & \ddots & \ddots & \ddots & \\ & & a_{j-2} & b_{j-1} & c_{j-1} \\ & & & a_{j-1} & b_j \end{bmatrix} \begin{pmatrix} u_1 \\ u_2 \\ \vdots \\ u_j \end{pmatrix} + \begin{pmatrix} 0 \\ 0 \\ \vdots \\ c_j u_{j+1} \end{pmatrix} + \begin{pmatrix} f_1 \\ f_2 \\ \vdots \\ f_j \end{pmatrix}, \\
\dot{\boldsymbol{w}} &= \begin{bmatrix} b_{j+1} & c_{j+1} & & & \\ a_{j+1} & b_{j+2} & c_{j+2} & & \\ & \ddots & \ddots & \ddots & \\ & & a_{2j-2} & b_{2j-1} & c_{2j-1} \\ & & & a_{2j-1} & b_{2j} \end{bmatrix} \begin{pmatrix} w_1 \\ w_2 \\ \vdots \\ w_j \end{pmatrix} + \begin{pmatrix} a_j w_0 \\ 0 \\ \vdots \\ 0 \end{pmatrix} + \begin{pmatrix} f_{j+1} \\ f_{j+2} \\ \vdots \\ f_{2j} \end{pmatrix},
\end{aligned} \tag{3.2}$$

where we call the unknown voltages in subsystem one $\boldsymbol{u}(t)$, and in subsystem two $\boldsymbol{w}(t)$. The classical WR algorithm applied to (3.1), using the classical transmission conditions

$$u_{j+1}^{k+1} = w_1^k, \quad w_0^{k+1} = u_j^k, \tag{3.3}$$

is given by

$$\dot{\boldsymbol{u}}^{k+1} = \begin{bmatrix} b_1 & c_1 & & & \\ a_1 & b_2 & c_2 & & \\ & \ddots & \ddots & \ddots & \\ & & a_{j-2} & b_{j-1} & c_{j-1} \\ & & & a_{j-1} & b_j \end{bmatrix} \begin{pmatrix} u_1 \\ u_2 \\ \vdots \\ u_j \end{pmatrix}^{k+1} + \begin{pmatrix} 0 \\ 0 \\ \vdots \\ c_j w_1^k \end{pmatrix} + \begin{pmatrix} f_1 \\ f_2 \\ \vdots \\ f_j \end{pmatrix},$$

$$\dot{\boldsymbol{w}}^{k+1} = \begin{bmatrix} b_{j+1} & c_{j+1} & & & \\ a_{j+1} & b_{j+2} & c_{j+2} & & \\ & \ddots & \ddots & \ddots & \\ & & a_{2j-2} & b_{2j-1} & c_{2j-1} \\ & & & a_{2j-1} & b_{2j} \end{bmatrix} \begin{pmatrix} w_1 \\ w_2 \\ \vdots \\ w_j \end{pmatrix}^{k+1} + \begin{pmatrix} a_j u_j^k \\ 0 \\ \vdots \\ 0 \end{pmatrix} + \begin{pmatrix} f_{j+1} \\ f_{j+2} \\ \vdots \\ f_{2j} \end{pmatrix}, \tag{3.4}$$

with initial voltage values $\boldsymbol{u}(0) = (v_1^0, v_2^0, \ldots, v_j^0)^T$, and $\boldsymbol{w}(0) = (v_{j+1}^0, v_{j+2}^0, \ldots, v_{2j}^0)^T$. To start the WR algorithm, we need to specify two initial waveforms $u_j^0(t)$ and $w_1^0(t)$, for $t \in [0, T]$.

In [31] Gander and Ruehli proposed new transmission conditions, which are given for any finite RC circuit by

$$\begin{aligned} (u_{j+1}^{k+1} - u_j^{k+1}) + \alpha u_{j+1}^{k+1} &= (w_1^k - w_0^k) + \alpha w_1^k, \\ (w_1^{k+1} - w_0^{k+1}) + \beta w_0^{k+1} &= (u_{j+1}^k - u_j^k) + \beta u_j^k. \end{aligned} \tag{3.5}$$

The new transmission conditions (3.5), comparing with (3.3), also exchange the voltages u_{j+1} and w_0, but they are multiplied with weighting factors α and β, respectively. The voltage differences between the nodal voltages $(u_{j+1} - u_j)$ and $(w_1 - w_0)$ insure that the currents are also taken into account in the transmission conditions since we could write the currents as $\alpha^{-1}(u_{j+1} - u_j)$ and $\beta^{-1}(w_1 - w_0)$ where α and β can be viewed as resistors. Therefore, the new transmission conditions attempt to transmit voltages as well as currents at the interfaces between the subsystems during the iteration, instead of only voltage values like the classical transmission conditions. Gander and Ruehli proved in [31] that the converged solution of the new WR algorithm with transmission conditions (3.5) is identical to the converged solution of the classical WR algorithm with transmission conditions (3.3), if $(\alpha + 1)(\beta - 1) + 1 \neq 0$. Using the new transmission conditions, the new WR algorithm is given by

$$\dot{\boldsymbol{u}}^{k+1} = \begin{bmatrix} b_1 & c_1 & & & \\ a_1 & b_2 & c_2 & & \\ & \ddots & \ddots & \ddots & \\ & & a_{j-2} & b_{j-1} & c_{j-1} \\ & & & a_{j-1} & b_j + \frac{c_j}{\alpha+1} \end{bmatrix} \begin{pmatrix} u_1 \\ u_2 \\ \vdots \\ u_j \end{pmatrix}^{k+1} + \begin{pmatrix} 0 \\ 0 \\ \vdots \\ c_j w_1^k - \frac{c_j}{\alpha+1} w_0^k \end{pmatrix} + \begin{pmatrix} f_1 \\ f_2 \\ \vdots \\ f_j \end{pmatrix},$$

$$\dot{\boldsymbol{w}}^{k+1} = \begin{bmatrix} b_{j+1} - \frac{a_j}{\beta-1} & c_{j+1} & & & \\ a_{j+1} & b_{j+2} & c_{j+2} & & \\ & \ddots & \ddots & \ddots & \\ & & a_{2j-2} & b_{2j-1} & c_{2j-1} \\ & & & a_{2j-1} & b_{2j} \end{bmatrix} \begin{pmatrix} w_1 \\ w_2 \\ \vdots \\ w_j \end{pmatrix}^{k+1} + \begin{pmatrix} a_j u_j^k + \frac{a_j}{\beta-1} u_{j+1}^k \\ 0 \\ \vdots \\ 0 \end{pmatrix} + \begin{pmatrix} f_{j+1} \\ f_{j+2} \\ \vdots \\ f_{2j} \end{pmatrix}, \tag{3.6}$$

where we start with initial waveforms $u_j^0(t)$, $u_{j+1}^0(t)$, $w_1^0(t)$, and $w_0^0(t)$, for $t \in [0, T]$, which must satisfy the initial conditions, and for the next iterations, the values u_{j+1}^k, and w_0^k are determined by the transmission conditions (3.5).

In order to keep the analysis and the optimization process we are solving simpler, we consider here the simplifying assumptions

$$c_i = a_i = a_1 = a, \ \text{for } i = 1, 2, \ldots, n-1, \ b_i = b_1 = b, \ \text{for } i = 1, 2, \ldots, n. \tag{3.7}$$

Indeed, this is a justified choice since we have circuits where the subsystems or subcircuits have very similar electrical properties on both sides of the partitioning boundary as we can observe in Figure 3.1. For the infinitely large circuit in Section 3.4, the circuit element values are given to be the same for all internal circuit elements to simplify the computations as well.

As stated in the introduction, we analyze the homogeneous problem, and we use the Laplace transform for the convergence study of the linear circuits considered here. The Laplace transform for $s \in \mathbb{C}$ of (3.2), with the simplifying assumptions (3.7), is given by

$$
\begin{aligned}
s\hat{\boldsymbol{u}} &= \begin{bmatrix} b & a & & & \\ a & b & a & & \\ & \ddots & \ddots & \ddots & \\ & & a & b & a \\ & & & a & b \end{bmatrix} \begin{pmatrix} \hat{u}_1 \\ \hat{u}_2 \\ \vdots \\ \hat{u}_j \end{pmatrix} + \begin{pmatrix} 0 \\ 0 \\ \vdots \\ a\hat{u}_{j+1} \end{pmatrix}, \\
s\hat{\boldsymbol{w}} &= \begin{bmatrix} b & a & & & \\ a & b & a & & \\ & \ddots & \ddots & \ddots & \\ & & a & b & a \\ & & & a & b \end{bmatrix} \begin{pmatrix} \hat{w}_1 \\ \hat{w}_2 \\ \vdots \\ \hat{w}_j \end{pmatrix} + \begin{pmatrix} a\hat{w}_0 \\ 0 \\ \vdots \\ 0 \end{pmatrix}.
\end{aligned}
\tag{3.8}
$$

The following lemmas are needed to find the convergence factors of the classical and optimal WR algorithms in closed form.

Lemma 3.1. *Let S_1, S_2, and S_3 be given by*

$$
\begin{aligned}
S_1 &:= (s-b) \sum_{r=1}^{\lfloor \frac{k+2}{2} \rfloor} (-1)^{r+1} \binom{k-r+1}{r-1} (s-b)^{k-2r+2} a^{2r-2}, \\
S_2 &:= -a^2 \sum_{r=1}^{\lfloor \frac{k+1}{2} \rfloor} (-1)^{r+1} \binom{k-r}{r-1} (s-b)^{k-2r+1} a^{2r-2}, \\
S_3 &:= \sum_{r=1}^{\lfloor \frac{k+3}{2} \rfloor} (-1)^{r+1} \binom{k-r+2}{r-1} (s-b)^{k-2r+3} a^{2r-2},
\end{aligned}
$$

where k is any integer greater than or equal to 1, and for any real number t, we have denoted above $\lfloor t \rfloor = l$, where l is the unique integer such that $l \le t < l+1$. Then

$$S_1 + S_2 = S_3.$$

Proof. If k is even, then $k = 2\ell$, $\ell = 1, 2, \ldots$, and $\lfloor \frac{k+3}{2} \rfloor = \ell + 1$, $\lfloor \frac{k+2}{2} \rfloor = \ell + 1$, and

$\lfloor \frac{k+1}{2} \rfloor = \ell$, and we write S_1, S_2, and S_3 as

$$\begin{aligned} S_1 &:= (s-b)^{k+1} + \sum_{r=2}^{\ell+1} (-1)^{r+1} \tbinom{k-r+1}{r-1} (s-b)^{k-2r+3} a^{2r-2}, \\ S_2 &:= -\sum_{r=1}^{\ell} (-1)^{r+1} \tbinom{k-r}{r-1} (s-b)^{k-2r+1} a^{2r}, \\ S_3 &:= (s-b)^{k+1} + \sum_{r=2}^{\ell+1} (-1)^{r+1} \tbinom{k-r+2}{r-1} (s-b)^{k-2r+3} a^{2r-2}. \end{aligned} \tag{3.9}$$

For any $r = j$, where $1 < j \leq \ell + 1$, the summands in S_1 and S_3 are, respectively,

$$\begin{aligned} &(-1)^{j+1} \tbinom{k-j+1}{j-1} (s-b)^{k-2j+3} a^{2j-2}, \\ &(-1)^{j+1} \tbinom{k-j+2}{j-1} (s-b)^{k-2j+3} a^{2j-2}, \end{aligned}$$

and for any $r = j-1$, $1 < j \leq \ell + 1$, the summand in S_2 is

$$(-1)^{j+1} \binom{k-j+1}{j-2} (s-b)^{k-2j+3} a^{2j-2}.$$

Therefore, we have the same powers, and we only need to show that the sum of the coefficients in the summands in S_2 for $r = j-1$, and in S_1 for $r = j$, $1 < j \leq \ell + 1$, is equal to the coefficient in the summand in S_3 for $r = j$. This is true due to the binomial coefficients property

$$\binom{n}{k+1} + \binom{n}{k} = \binom{n+1}{k+1},$$

which implies

$$\binom{k-j+1}{j-1} + \binom{k-j+1}{j-2} = \binom{k-j+2}{j-1},$$

for $1 < j \leq \ell + 1$. The summand in S_2 for $r = 1$, or $j = 2$, is already considered above, since for S_2, we considered $r = j-1$, and $1 < j \leq \ell + 1$, so for $r = 1$, we only have the summand in S_1 and in S_3. From (3.9), for $r = 1$, the summand in S_1 is $(s-b)^{k+1}$, and it is the same expression we obtain from the summand in S_3 for $r = 1$, and this finishes the proof for k even.

Now, if k is odd, then $k = 2\ell - 1$, $\ell = 1, 2, \ldots$, and $\lfloor \frac{k+3}{2} \rfloor = \ell + 1$, $\lfloor \frac{k+2}{2} \rfloor = \ell$, and $\lfloor \frac{k+1}{2} \rfloor = \ell$, and we write S_1, S_2, and S_3 as

$$\begin{aligned} S_1 &:= (s-b)^{k+1} + \sum_{r=2}^{\ell} (-1)^{r+1} \binom{k-r+1}{r-1} (s-b)^{k-2r+3} a^{2r-2}, \\ S_2 &:= -\sum_{r=1}^{\ell-1} (-1)^{r+1} \binom{k-r}{r-1} (s-b)^{k-2r+1} a^{2r} + (-1)^{\ell+2} a^{2\ell}, \\ S_3 &:= (s-b)^{k+1} + \sum_{r=2}^{\ell} (-1)^{r+1} \binom{k-r+2}{r-1} (s-b)^{k-2r+3} a^{2r-2} + (-1)^{\ell+2} a^{2\ell}. \end{aligned} \tag{3.10}$$

Showing that $S_1 + S_2 = S_3$ is similar to the case where k is even, but here, we have $1 < j < \ell + 1$, instead of $1 < j \le \ell + 1$, since the last value for r in S_1 is $r = \ell$, whereas it was $\ell + 1$ for k even. Therefore, we only need to show equality between the summands in S_3 for $r = j = \ell + 1$, and in S_2 for $r = j - 1 = \ell$. As is evident from (3.10), the summand in S_3 for $r = \ell + 1$ is equal to the summand in S_2 for $r = \ell$. $\square$

Lemma 3.2. *For the systems in (3.8), for any $1 \le m \le j$, $j = 1, 2, \ldots$, $\hat{u}_m$ is given by*

$$\hat{u}_m = \frac{a \sum_{r=1}^{\lfloor \frac{m+1}{2} \rfloor} (-1)^{r+1} \binom{m-r}{r-1} (s-b)^{m-2r+1} a^{2r-2}}{\sum_{r=1}^{\lfloor \frac{m+2}{2} \rfloor} (-1)^{r+1} \binom{m-r+1}{r-1} (s-b)^{m-2r+2} a^{2r-2}} \hat{u}_{m+1}, \tag{3.11}$$

and $\hat{w}_{j-m+1}$ is given by

$$\hat{w}_{j-m+1} = \frac{a \sum_{r=1}^{\lfloor \frac{m+1}{2} \rfloor} (-1)^{r+1} \binom{m-r}{r-1} (s-b)^{m-2r+1} a^{2r-2}}{\sum_{r=1}^{\lfloor \frac{m+2}{2} \rfloor} (-1)^{r+1} \binom{m-r+1}{r-1} (s-b)^{m-2r+2} a^{2r-2}} \hat{w}_{j-m}, \tag{3.12}$$

where $\lfloor . \rfloor$ is the integer defined in Lemma 3.1.

Proof. The proof is by induction. For $m = 1$, from the first subsystem in (3.8), we have

$$\hat{u}_1 = \frac{a}{s-b} \hat{u}_2,$$

which is the same as we obtain by using (3.11) for $m = 1$, so relation (3.11) holds for $m = 1$. We thus assume that (3.11) holds for $m = k$, i.e.

$$\hat{u}_k = \frac{a \sum_{r=1}^{\lfloor \frac{k+1}{2} \rfloor} (-1)^{r+1} \binom{k-r}{r-1} (s-b)^{k-2r+1} a^{2r-2}}{\sum_{r=1}^{\lfloor \frac{k+2}{2} \rfloor} (-1)^{r+1} \binom{k-r+1}{r-1} (s-b)^{k-2r+2} a^{2r-2}} \hat{u}_{k+1}.$$

Now we need to show that (3.11) also holds for $m = k+1$. The equation for $m = k+1$ from the first subsystem in (3.8) is

$$s\hat{u}_{k+1} = a\hat{u}_k + b\hat{u}_{k+1} + a\hat{u}_{k+2},$$

which implies, after substituting $\hat{u}_k$ from (3.11) for $m = k$, and simplifying,

$$X\hat{u}_{k+1} = Y\hat{u}_{k+2},$$

where

$$\begin{aligned} X &:= (s-b) \sum_{r=1}^{\lfloor \frac{k+2}{2} \rfloor} (-1)^{r+1} \binom{k-r+1}{r-1} (s-b)^{k-2r+2} a^{2r-2} \\ &\quad - a^2 \sum_{r=1}^{\lfloor \frac{k+1}{2} \rfloor} (-1)^{r+1} \binom{k-r}{r-1} (s-b)^{k-2r+1} a^{2r-2}, \\ Y &:= a \sum_{r=1}^{\lfloor \frac{k+2}{2} \rfloor} (-1)^{r+1} \binom{k-r+1}{r-1} (s-b)^{k-2r+2} a^{2r-2}. \end{aligned}$$

Hence, $\hat{u}_{k+1} = \frac{Y}{X}\hat{u}_{k+2}$. The numerator of the expression in (3.11) for $m = k+1$ is equal to Y, so we only need to show that the denominator of (3.11) for $m = k+1$ is equal to X, and this is proved in Lemma 3.1. Therefore, relation (3.11) holds for $m = k+1$, and the proof by induction is complete. The proof of relation (3.12) is similar. □

We analyze now the convergence factor of the classical WR algorithm (3.4), with the simplifying assumptions (3.7).

Theorem 3.1. *The convergence factor $\rho_{cla(j)}$ of the classical WR algorithm (3.4), with $n = 2j$, $j = 1, 2, \dots$, and the simplifying assumptions (3.7) is given by*

$$\rho_{cla(j)}(s,a,b) = \left(\frac{1}{\lambda_j}\right)^2, \quad \lambda_j = \frac{\sum_{r=1}^{\lfloor \frac{j+2}{2} \rfloor} (-1)^{r+1} \binom{j-r+1}{r-1} (s-b)^{j-2r+2} a^{2r-2}}{a \sum_{r=1}^{\lfloor \frac{j+1}{2} \rfloor} (-1)^{r+1} \binom{j-r}{r-1} (s-b)^{j-2r+1} a^{2r-2}}. \tag{3.13}$$

Proof. The proof is by induction. The last equation in the first subsystem in (3.4), after taking Laplace transform and considering the homogeneous problem, for $j = 1$, is given by

$$s\hat{u}_1^{k+1} = b\hat{u}_1^{k+1} + a\hat{w}_1^k,$$

which implies

$$\hat{u}_1^{k+1} = \frac{1}{\lambda_1}\hat{w}_1^k, \tag{3.14}$$

where

$$\lambda_1 = \frac{s-b}{a},$$

which is λ_j in (3.13) for $j = 1$. Similarly, we find for the second subsystem from the first equation,

$$\hat{w}_1^{k+1} = \frac{1}{\lambda_1}\hat{u}_1^k. \tag{3.15}$$

Inserting (3.15) at step k into (3.14) implies

$$\hat{u}_1^{k+1} = \rho_{cla(1)}(s,a,b)\hat{u}_1^{k-1},$$

with convergence factor $\rho_{cla(1)}$ of the classical WR algorithm given by

$$\rho_{cla(1)}(s,a,b) = \left(\frac{1}{\lambda_1}\right)^2,$$

where λ_1 is given in (3.13) for $j = 1$. Now for $j > 1$, the last equation in the first subsystem is given by

$$s\hat{u}_j^{k+1} = a\hat{u}_{j-1}^{k+1} + b\hat{u}_j^{k+1} + a\hat{w}_1^k.$$

Using Lemma 3.2 to substitute for $\hat{u}_{j-1}^{k+1}$, and simplifying, we get

$$\hat{u}_j^{k+1} = \frac{1}{\lambda_j}\hat{w}_1^k, \tag{3.16}$$

where $\lambda_j = \frac{N_j}{D_j}$, and N_j, D_j are given by

$$N_j = (s-b)\sum_{r=1}^{\lfloor\frac{j+1}{2}\rfloor}(-1)^{r+1}\binom{j-r}{r-1}(s-b)^{j-2r+1}a^{2r-2} - a^2\sum_{r=1}^{\lfloor\frac{j}{2}\rfloor}(-1)^{r+1}\binom{j-r-1}{r-1}(s-b)^{j-2r}a^{2r-2},$$
$$D_j = a\sum_{r=1}^{\lfloor\frac{j+1}{2}\rfloor}(-1)^{r+1}\binom{j-r}{r-1}(s-b)^{j-2r+1}a^{2r-2},$$

and using Lemma 3.1, we obtain

$$\lambda_j = \frac{N_j}{D_j} = \frac{\sum_{r=1}^{\lfloor\frac{j+2}{2}\rfloor}(-1)^{r+1}\binom{j-r+1}{r-1}(s-b)^{j-2r+2}a^{2r-2}}{a\sum_{r=1}^{\lfloor\frac{j+1}{2}\rfloor}(-1)^{r+1}\binom{j-r}{r-1}(s-b)^{j-2r+1}a^{2r-2}},$$

as given in (3.13). Note also that $N_j = (s-b)N_{j-1} - aD_{j-1}$, and $D_j = aN_{j-1}$. Similarly, we find for the second subsystem from the first equation,

$$\hat{w}_1^{k+1} = \frac{1}{\lambda_j}\hat{u}_j^k. \tag{3.17}$$

Inserting (3.17) at step k into (3.16), we get

$$\hat{u}_j^{k+1} = \rho_{cla(j)}(s,a,b)\hat{u}_j^{k-1},$$

with convergence factor $\rho_{cla(j)}$ of the classical WR algorithm given by

$$\rho_{cla(j)}(s,a,b) = \left(\frac{1}{\lambda_j}\right)^2,$$

where λ_j is given in (3.13). The same result holds for $\hat{w}_1^{k+1}$, and by induction we find $\hat{u}_j^{2k} = (\rho_{cla(j)})^k\hat{u}_j^0$, and $\hat{w}_1^{2k} = (\rho_{cla(j)})^k\hat{w}_1^0$. □

For convergence as is given in (1.15), we need that $|\rho_{cla(j)}(s,a,b)| < 1$ for $\Re(s) > 0$, and for fast convergence, the modulus of $\rho_{cla(j)}$ should be much smaller than 1,

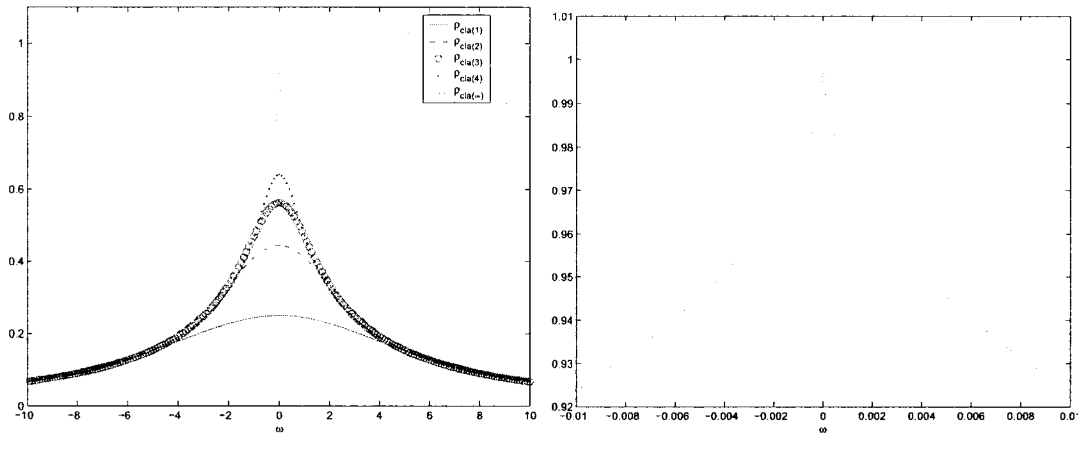

Figure 3.2: Convergence factor $|\rho_{cla(j)}|$ for different values of j on the left, and on the right, a zoom around the maximum of $|\rho_{cla(\infty)}|$.

$|\rho_{cla(j)}| \ll 1$. However, the convergence factor $|\rho_{cla(j)}|$ is a fixed function of the circuit parameters in the classical WR algorithm, and thus the algorithm does not have any adjustable parameters like the new WR algorithm we discuss below. We can only analyze for the classical WR algorithm if the convergence test $|\rho_{cla(j)}| < 1$ is satisfied. It is shown in Sections 3.2 and 3.3 for the very small, $j = 1$, and small, $j = 2$, RC circuits that this convergence test is satisfied. For the infinitely large RC circuit, $j = \infty$, in Section 3.4, it is shown that $|\rho_{cla(j)}| < 1$ for all ω and $|b| > 2a$, $|\rho_{cla(j)}| < 1$ for $\omega \neq 0$ and $|b| = 2a$, and for the case $\omega = 0$ and $|b| = 2a$, the maximum of $|\rho_{cla(j)}|$ is one, and the convergence test $|\rho_{cla(j)}| < 1$ is not satisfied. An example of the classical convergence factor as a function of ω for different values of j, with $|b| = 2a$, is given in Figure 3.2. We observe from Figure 3.2 that the modulus of the convergence factor for finite j is less than one, and it becomes bigger and bigger around $\omega = 0$ as we increase the size of the circuit, and as noted above, for the infinitely large circuit the convergence factor is one at $\omega = 0$.

Let us now consider the new WR algorithm (3.6), and look for the convergence factor with the simplifying assumptions (3.7).

Theorem 3.2. *The convergence factor of the new WR algorithm (3.6), with $n = 2j$, $j = 1, 2, \dots$, and the simplifying assumptions (3.7) is given by*

$$\rho_{opt(j)}(s, a, b, \alpha, \beta) = \frac{(\alpha+1) - \lambda_j}{(\alpha+1)\lambda_j - 1} \cdot \frac{(\beta-1) + \lambda_j}{(\beta-1)\lambda_j + 1}, \tag{3.18}$$

where λ_j is given in (3.13).

Proof. The proof is similar to the proof of Theorem 3.1. For $j = 1$, from the last equation in the first subsystem in (3.6), after taking the Laplace transform as we did in the classical case, and considering the homogeneous problem, after some algebra, we obtain

$$\hat{u}_1^{k+1} = F_1(\hat{w}_1^k(\alpha+1) - \hat{w}_0^k), \quad F_1 = \frac{a}{(s-b)(\alpha+1) - a}, \tag{3.19}$$

and similarly from the first equation of the second subsystem, we get

$$\hat{w}_1^{k+1} = F_2(\hat{u}_1^k(\beta-1) + \hat{u}_2^k), \quad F_2 = \frac{a}{(s-b)(\beta-1) + a}. \tag{3.20}$$

Next, we want to obtain the convergence factor for the optimal WR algorithm in closed form. We need to find a relation between $\hat{u}_1^{k+1}$ and $\hat{w}_1^k$ from (3.19), and similarly a relation between $\hat{w}_1^{k+1}$ and $\hat{u}_1^k$ from (3.20). Using the second transmission condition in (3.5), for $j = 1$, we find, together with (3.20),

$$\hat{w}_0^{k+1} = \left(\frac{1}{(\beta-1)F_2} - \frac{1}{\beta-1}\right)\hat{w}_1^{k+1},$$

and using this result at step k in (3.19), we find for the first subsystem

$$\hat{u}_1^{k+1} = F_1\left(\alpha + 1 - \frac{1}{(\beta-1)F_2} + \frac{1}{\beta-1}\right)\hat{w}_1^k. \tag{3.21}$$

With a similar manipulation for the second subsystem, we find

$$\hat{w}_1^{k+1} = F_2\left(\frac{1}{(\alpha+1)F_1} + \frac{1}{\alpha+1} + \beta - 1\right)\hat{u}_1^k. \tag{3.22}$$

Finally, by inserting (3.22) at iteration k into (3.21), we get a relation over two iteration steps,

$$\hat{u}_1^{k+1} = \rho_{opt(1)}(s, a, b, \alpha, \beta)\hat{u}_1^{k-1},$$

with convergence factor of the optimal WR algorithm given by

$$\rho_{opt(1)}(s,a,b,\alpha,\beta) = \frac{(\alpha+1)-\lambda_1}{(\alpha+1)\lambda_1-1}\cdot\frac{(\beta-1)+\lambda_1}{(\beta-1)\lambda_1+1},$$

where λ_1 is given in (3.13) for $j=1$. Now for $j>1$, the last equation in the first subsystem in (3.8) is given by

$$s\hat{u}_j = a\hat{u}_{j-1} + b\hat{u}_j + a\hat{u}_{j+1},$$

and using Lemmas 3.2 and 3.1, we get

$$\frac{\sum_{r=1}^{\lfloor\frac{j+2}{2}\rfloor}(-1)^{r+1}\binom{j-r+1}{r-1}(s-b)^{j-2r+2}a^{2r-2}}{\sum_{r=1}^{\lfloor\frac{j+1}{2}\rfloor}(-1)^{r+1}\binom{j-r}{r-1}(s-b)^{j-2r+1}a^{2r-2}}\hat{u}_j = a\hat{u}_{j+1}. \tag{3.23}$$

Now inserting the iterations, and substituting $\hat{u}_{j+1}^{k+1}$ from the first transmission condition in (3.5) into (3.23), which is basically the last equation in the first subsystem in (3.6) after taking Laplace transform and considering the homogeneous problem, we get

$$\left(X-\frac{a}{\alpha+1}\right)\hat{u}_j^{k+1} = \frac{a}{\alpha+1}(\hat{w}_1^k - \hat{w}_0^k + \alpha\hat{w}_1^k),$$

where

$$X := \frac{\sum_{r=1}^{\lfloor\frac{j+2}{2}\rfloor}(-1)^{r+1}\binom{j-r+1}{r-1}(s-b)^{j-2r+2}a^{2r-2}}{\sum_{r=1}^{\lfloor\frac{j+1}{2}\rfloor}(-1)^{r+1}\binom{j-r}{r-1}(s-b)^{j-2r+1}a^{2r-2}},$$

and after simplifying, we get

$$\hat{u}_j^{k+1} = F_1(\hat{w}_1^k - \hat{w}_0^k + \alpha\hat{w}_1^k), \quad F_1 := \frac{aX_1}{(\alpha+1)X_2 - aX_1}, \tag{3.24}$$

where

$$X_1 := \sum_{r=1}^{\lfloor\frac{j+1}{2}\rfloor}(-1)^{r+1}\binom{j-r}{r-1}(s-b)^{j-2r+1}a^{2r-2},$$
$$X_2 := \sum_{r=1}^{\lfloor\frac{j+2}{2}\rfloor}(-1)^{r+1}\binom{j-r+1}{r-1}(s-b)^{j-2r+2}a^{2r-2}.$$

Similarly, from the second subsystem, we obtain

$$\hat{w}_1^{k+1} = F_2(\hat{u}_{j+1}^k - \hat{u}_j^k + \beta\hat{u}_j^k), \quad F_2 := \frac{aX_1}{(\beta-1)X_2 + aX_1}, \tag{3.25}$$

where X_1 and X_2 are as given above. Again, we need to derive a relation between $\hat{u}_j^{k+1}$ and $\hat{w}_1^k$ from (3.24), and similarly a relation between $\hat{w}_1^{k+1}$ and $\hat{u}_j^k$ from (3.25) to obtain the convergence factor for the optimal WR algorithm in closed form.

Using the second transmission condition in (3.5), together with (3.25), we find

$$\hat{w}_0^{k+1} = \left(\frac{1}{(\beta-1)F_2} - \frac{1}{\beta-1}\right)\hat{w}_1^{k+1},$$

and using this result at step k in (3.24) we find for the first subsystem

$$\hat{u}_j^{k+1} = F_1\left(\alpha + 1 - \frac{1}{(\beta-1)F_2} + \frac{1}{\beta-1}\right)\hat{w}_1^k. \tag{3.26}$$

With a similar manipulation for the second subsystem, we obtain

$$\hat{w}_1^{k+1} = F_2\left(\frac{1}{(\alpha+1)F_1} + \frac{1}{\alpha+1} + \beta - 1\right)\hat{u}_j^k. \tag{3.27}$$

Finally, by inserting (3.27) at iteration k into (3.26), we get a relation over two iteration steps of the optimal WR algorithm,

$$\hat{u}_j^{k+1} = F_1F_2\left(\alpha + 1 - \frac{1}{(\beta-1)F_2} + \frac{1}{\beta-1}\right)\left(\frac{1}{(\alpha+1)F_1} + \frac{1}{\alpha+1} + \beta - 1\right)\hat{u}_j^{k-1},$$

and after simplifying,

$$\hat{u}_j^{k+1} = \rho_{opt(j)}(s, a, b, \alpha, \beta)\hat{u}_j^{k-1},$$

where the convergence factor $\rho_{opt(j)}$ is given by

$$\rho_{opt(j)}(s, a, b, \alpha, \beta) = \frac{(\alpha+1) - \lambda_j}{(\alpha+1)\lambda_j - 1} \cdot \frac{(\beta-1) + \lambda_j}{(\beta-1)\lambda_j + 1},$$

and λ_j is given in (3.13). The same result also holds for the second subsystem and by induction we find, as before, $\hat{u}_j^{2k} = (\rho_{opt(j)})^k \hat{u}_j^0$, and $\hat{w}_1^{2k} = (\rho_{opt(j)})^k \hat{w}_1^0$. □

From the convergence factor (3.18) we can derive the optimal values of the parameters α and β as in the following theorem.

Theorem 3.3 (Optimal Convergence). *The new WR algorithm (3.6) converges in two iterations, independently of the initial waveforms $\hat{u}_j^0$ and $\hat{w}_1^0$, if*

$$\alpha := \alpha_{opt(j)} = \lambda_j - 1, \quad \beta := \beta_{opt(j)} = 1 - \lambda_j,\ j = 1, 2, \ldots, \tag{3.28}$$

and hence $\beta_{opt(j)} = -\alpha_{opt(j)}$.

Proof. The convergence factor vanishes if we insert (3.28) into $\rho_{opt(j)}$ given by (3.18). Hence, $\hat{u}_j^2$ and $\hat{w}_1^2$ are identically zero, independently of $\hat{u}_j^0$ and $\hat{w}_1^0$. □

We observe that the optimal choice (3.28) is not just a parameter, but the Laplace transform of a linear operator in time, since it depends on s. Since we have a rational function in s, the optimal transmission conditions correspond to nonlocal operators in time. They require integral operators which can not be avoided in general and are expensive to use, since they would require convolutions in the transmission conditions. This is true for more general circuits as well, therefore, approximations of the best transmission conditions are proposed. In Figure 3.3, we show the modulus of the optimal choice of α and β (3.28) as a function of η and ω for the cases $j = 1$ and $j = 2$, where we choose $a = \frac{200}{63}$ and $b = -2a$ from typical RC circuit parameters.

To further analyze the convergence factor (3.18), we assume for simplicity that $\beta = -\alpha$ motivated by the optimal choice (3.28) with the simplifying assumptions (3.7), where we have $\beta_{opt(j)} = -\alpha_{opt(j)}$, and that the circuits considered here behave identical on both sides of the cut. This leads to the convergence factor

$$\rho_{opt(j)}(s, a, b, \alpha) = \left(\frac{(\alpha + 1) - \lambda_j}{(\alpha + 1)\lambda_j - 1} \right)^2, \tag{3.29}$$

and λ_j is given in (3.13).

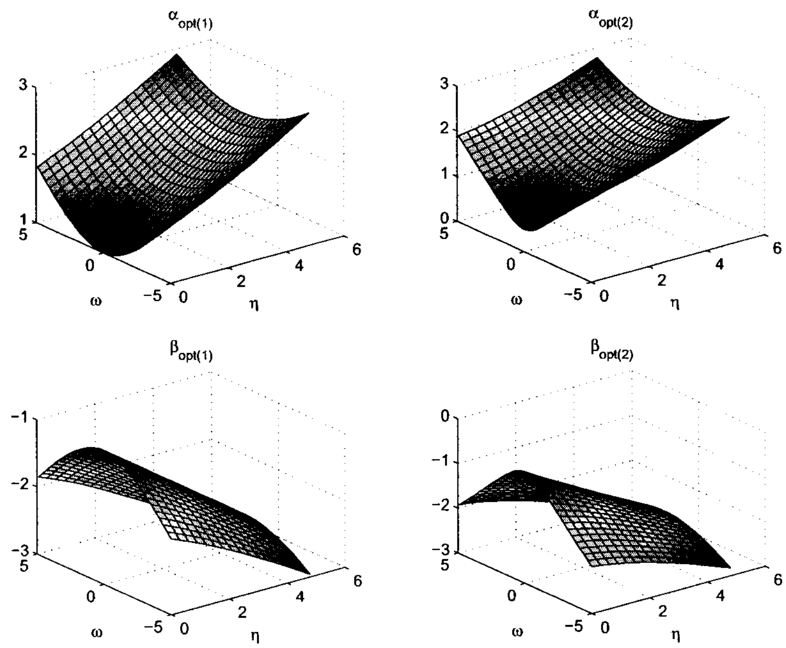

Figure 3.3: $|\alpha_{opt(j)}|$ and $|\beta_{opt(j)}|$ for $j = 1$ and $j = 2$.

We now study λ_j in (3.13) in more detail. As we have seen in the proof of Theorem 3.1, $\lambda_1 = \frac{s-b}{a}$, and for $j > 1$, $N_j = (s-b)N_{j-1} - aD_{j-1}$, and $D_j = aN_{j-1}$, and

$$\lambda_j = \frac{N_j}{D_j} = \frac{(s-b)N_{j-1} - aD_{j-1}}{aN_{j-1}} = \frac{s-b}{a} - \frac{D_{j-1}}{N_{j-1}} = \frac{s-b}{a} - \frac{1}{\lambda_{j-1}}.$$

Hence, we get the recurrence relation

$$\begin{aligned} \lambda_1 &= \tfrac{s-b}{a}, \\ \lambda_{j+1} &= \lambda_1 - \tfrac{1}{\lambda_j},\ j \geq 1. \end{aligned} \tag{3.30}$$

In the following Theorem we prove convergence of the sequence (3.30).

Theorem 3.4. *For s in the right half of the complex plane, $s = \eta + i\omega$, $\eta > 0$, and $|b| \geq 2a$, the sequence*

$$\begin{aligned} \lambda_1 &= \tfrac{s-b}{a}, \\ \lambda_{j+1} &= \lambda_1 - \tfrac{1}{\lambda_j},\ j \geq 1, \end{aligned}$$

converges to the limit

$$\lambda_+ = \frac{s - b + \sqrt{(s-b)^2 - 4a^2}}{2a}, \tag{3.31}$$

as j goes to infinity.

Proof. Let $\lambda_j = \frac{y_j(\lambda_1)}{z_j(\lambda_1)}$. Then

$$\lambda_{j+1} = \lambda_1 - \frac{z_j(\lambda_1)}{y_j(\lambda_1)} = \frac{\lambda_1 y_j(\lambda_1) - z_j(\lambda_1)}{y_j(\lambda_1)},$$

and hence, we have

$$\begin{aligned} z_{j+1}(\lambda_1) &= y_j(\lambda_1), \\ y_{j+1}(\lambda_1) &= \lambda_1 y_j(\lambda_1) - z_j(\lambda_1) = \lambda_1 y_j(\lambda_1) - y_{j-1}(\lambda_1). \end{aligned}$$

Now, we write the above equations in the system

$$\begin{pmatrix} y_{j+1}(\lambda_1) \\ y_j(\lambda_1) \end{pmatrix} = \begin{pmatrix} \lambda_1 & -1 \\ 1 & 0 \end{pmatrix} \begin{pmatrix} y_j(\lambda_1) \\ y_{j-1}(\lambda_1) \end{pmatrix} = \begin{pmatrix} \lambda_1 & -1 \\ 1 & 0 \end{pmatrix}^j \begin{pmatrix} y_1 \\ y_0 \end{pmatrix}.$$

The eigenvalues of the matrix

$$\begin{pmatrix} \lambda_1 & -1 \\ 1 & 0 \end{pmatrix}, \quad \lambda_1 = \frac{s-b}{a}, \tag{3.32}$$

in the system above are given by

$$\lambda_\pm = \frac{s - b \pm \sqrt{(s-b)^2 - 4a^2}}{2a},$$

where $|\lambda_+| > 1$ and $|\lambda_-| < 1$ in the right half of the complex plane, $s = \eta + i\omega$, $\eta > 0$, for $|b| \geq 2a$, see [31]. Therefore, we have two distinct eigenvalues, and hence the matrix in (3.32) is diagonalizable, and can be written as

$$\begin{pmatrix} \lambda_1 & -1 \\ 1 & 0 \end{pmatrix} = P \begin{pmatrix} \lambda_+ & 0 \\ 0 & \lambda_- \end{pmatrix} P^{-1},$$

where P is an invertible matrix, which has the corresponding eigenvectors as its column vectors. By forming the matrix P, and using $y_1 = s - b$ and $y_0 = a$, we can find σ_1 and σ_2 by direct calculations, such that

$$\begin{pmatrix} y_{j+1}(\lambda_1) \\ y_j(\lambda_1) \end{pmatrix} = P \begin{pmatrix} \lambda_+^j & 0 \\ 0 & \lambda_-^j \end{pmatrix} P^{-1} \begin{pmatrix} y_1 \\ y_0 \end{pmatrix} = \begin{pmatrix} \sigma_1 \lambda_+^{j+1} + \sigma_2 \lambda_-^{j+1} \\ \sigma_1 \lambda_+^j + \sigma_2 \lambda_-^j \end{pmatrix}.$$

Hence,

$$\lambda_{j+1} = \frac{y_{j+1}}{z_{j+1}} = \frac{y_{j+1}}{y_j} = \frac{\sigma_1 \lambda_+^{j+1} + \sigma_2 \lambda_-^{j+1}}{\sigma_1 \lambda_+^j + \sigma_2 \lambda_-^j},$$

and since $|\lambda_+| > 1$ and $|\lambda_-| < 1$, we have, as j goes to infinity,

$$\lim_{j \to \infty} \lambda_{j+1} = \lambda_+.$$

Note that the exact values for σ_1 and σ_2 are not really needed for the result above. □

In fact, we will see later in Section 3.4, that the limit λ_+ which is found here is the same λ_+ which is found in the circuit of infinite size, and hence we have proved that λ_j for any finite size circuit, $n = 2j$, $j = 1, 2, \ldots$, converges to λ_+ for the infinitely large circuit as j goes to infinity.

For the case $j = 1$, we get the very small RC circuit case which will be discussed in Section 3.2, and for $j = 2$, we get the small RC circuit case which will be discussed in Section 3.3. Assuming that the optimal choice for α given in (3.28) is approximated by a constant $\alpha_{(j)}$, the simplest way to obtain a constant approximation is to use a Taylor expansion about $s = 0$, which corresponds to a low frequency approximation. Note that for low frequencies the classical convergence factor behaves worst as one can observe from Figure 3.2. The low frequency constant approximation for the optimal choice given in (3.28) is

$$\alpha_{(j)T} = \frac{\sum_{r=1}^{\lfloor \frac{j+2}{2} \rfloor} (-1)^{r+1} \binom{j-r+1}{r-1} (-b)^{j-2r+2} a^{2r-2}}{a \sum_{r=1}^{\lfloor \frac{j+1}{2} \rfloor} (-1)^{r+1} \binom{j-r}{r-1} (-b)^{j-2r+1} a^{2r-2}} - 1, \quad \beta_{(j)T} = -\alpha_{(j)T}. \tag{3.33}$$

As an example, for $j = 1$, $j = 2$, $j = 3$, and $j = 4$ we get

$$\alpha_{(1)T} = \frac{-b}{a} - 1,\ \alpha_{(2)T} = \frac{a^2-b^2}{ab} - 1,\ \alpha_{(3)T} = \frac{b(2a^2-b^2)}{a(b^2-a^2)} - 1,\ \alpha_{(4)T} = \frac{a^2(3b^2-a^2)-b^4}{ab(b^2-2a^2)} - 1.$$

To find a better constant approximation, assuming $\beta_{(j)} = -\alpha_{(j)}$, we need to solve the min-max problem

$$\min_{\alpha_{(j)}} \left(\max_{\Re(s)\geq 0} |\rho_{opt(j)}(s, a, b, \alpha_{(j)})| \right), \tag{3.34}$$

where $\alpha_{(j)}$ is the only optimization parameter left. In Sections 3.2 and 3.3 for the very small, $j = 1$, small, $j = 2$, RC circuits respectively, we prove that the solution of the min-max problem (3.34), with constant approximation of the optimal choice of α occurs when the convergence factor at $\omega = 0$ and at $\omega = \omega_{max} \to \infty$ are balanced. Therefore, we use the equation

$$|\rho_{opt(j)}(0, \alpha^*_{(j)})| = \lim_{\omega\to\infty} |\rho_{opt(j)}(\omega, \alpha^*_{(j)})|$$

to determine the optimized parameter $\alpha^*_{(j)}$. Similar thing is shown for the infinitely large RC circuit in Section 3.4, where we use the equation

$$|\rho_{opt(j)}(\omega_{min}, \alpha^*_{(j)})| = \lim_{\omega\to\infty} |\rho_{opt(j)}(\omega, \alpha^*_{(j)})|, \tag{3.35}$$

and ω_{min} is a minimal frequency relevant to the problem, to determine the optimized parameter $\alpha^*_{(j)}$, since the limit of the maximum of the convergence factor is one as $\omega \to 0$ if $|b| = 2a$ which often holds for RC type circuits. For any finite $j > 2$, we have to rely on numerical calculations only due to the complexity of the polynomials and the min-max problems we obtain. On the left hand side of Figure 3.4 we show the function $|\rho_{opt(j)}(\omega, \alpha)|$ for $j = 3$ on the top, and for $j = 4$ at the bottom, where we choose $a = \frac{200}{63}$ and $b = -2a$ form typical RC circuit parameters. We observe that the solution of the min-max problem occurs when the convergence factor at $\omega = 0$ and at $\omega = \omega_{max}$ are balanced. In this example, for $j = 3$ we obtain $\alpha^*_{(3)} = 1.215$, and for $j = 4$ we obtain $\alpha^*_{(4)} = 1$, which leads to the convergence factors shown on

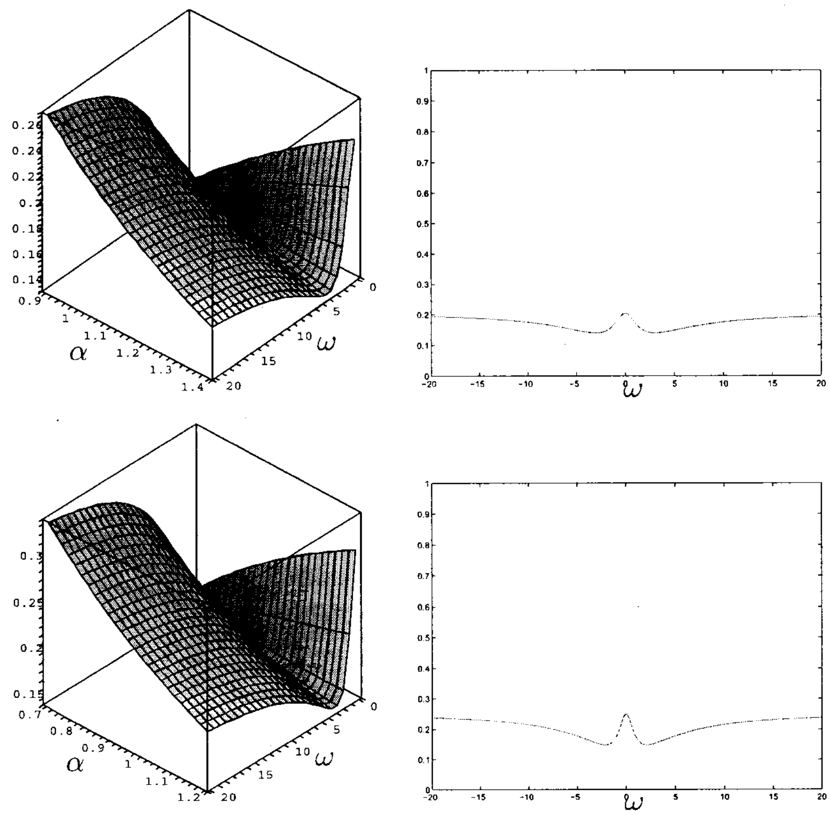

Figure 3.4: Top, left: convergence factor $|\rho_{opt(3)}(\omega, \alpha)|$, and right: optimized convergence factor $|\rho_{opt(3)}(\omega, \alpha^*_{(3)})|$. Bottom, left: convergence factor $|\rho_{opt(4)}(\omega, \alpha)|$, and right: optimized convergence factor $|\rho_{opt(4)}(\omega, \alpha^*_{(4)})|$.

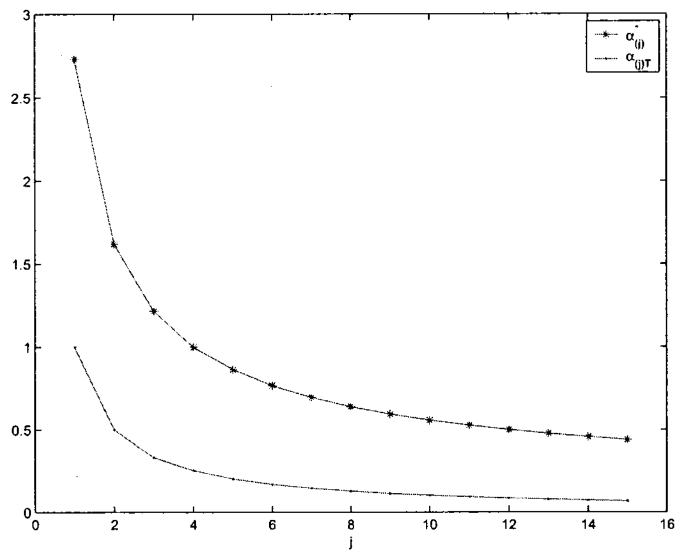

Figure 3.5: Optimized $\alpha^*_{(j)}$ versus $\alpha_{(j)T}$.

the right hand side of Figure 3.4. In Figure 3.5 we compare the optimized $\alpha^*_{(j)}$ with the Taylor approximation $\alpha_{(j)T}$, where we plot them as functions of j.

We state the following result as a suggestion for applications for finite $j > 2$ based on the numerical experiments we have done. If we approximate the optimal parameter α by a constant, and assume that the value of λ_j, $j = 1, 2, \ldots$ in (3.13), with $s = i\omega$, $\omega \geq 0$, at $\omega = 0$, is denoted by λ_{j0}, which is a real value since $\omega = 0$, then as for the cases $j = 1$ and $j = 2$ in Sections 3.2 and 3.3 respectively, we have

$$|\rho_{opt(j)}(0, \alpha_{(j)})| = \left|\frac{\alpha_{(j)} + 1 - \lambda_{j0}}{(\alpha_{(j)} + 1)\lambda_{j0} - 1}\right|^2 = \left(\frac{\alpha_{(j)} + 1 - \lambda_{j0}}{(\alpha_{(j)} + 1)\lambda_{j0} - 1}\right)^2 := R_{j0}.$$

Now, since the numerator in λ_j is of a degree higher than the denominator by one, we have

$$|\lim_{\omega \to \infty} \rho_{opt(j)}(i\omega, \alpha_{(j)})| = \left(\frac{1}{\alpha_{(j)} + 1}\right)^2 := R_{j\infty}.$$

By solving the equation $R_{j0} = R_{j\infty}$, we will get the solutions $\alpha_{(j)} = 0,\ -2,\ \lambda_{j0} \pm \sqrt{\lambda_{j0}^2 - 1} - 1$. The solution which gives the right optimized constant approximation

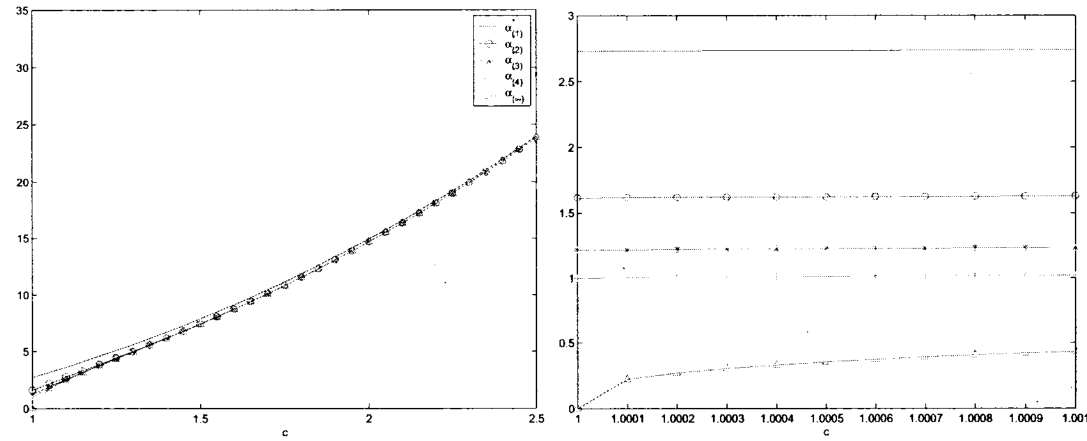

Figure 3.6: Optimized constant approximation $\alpha^*_{(j)}$ for different j on the left, and a zoom on the right.

is

$$\alpha^*_{(j)} := \lambda_{j0} + \sqrt{\lambda_{j0}^2 - 1} - 1, \; j = 1, 2, \dots. \tag{3.36}$$

This result is formally proved for the cases $j = 1$ and $j = 2$ in Subsections 3.2.3, 3.3.3 respectively. For the infinitely large circuit with $|b| \geq 2a$ and $\omega = \omega_{min}$ a similar result is found as we will see in Subsection 3.4.3. We show in Figure 3.6 the optimized constant approximation $\alpha^*_{(j)}$ given in (3.36) for different j as a function of the circuit parameter $c = \sqrt{\frac{-b}{2a}}$, where $-b \geq 2a$ for RC type circuits, and $-b = 2a$ often holds. We observe that the values become closer and closer as c becomes bigger and bigger. Note that $\alpha^*_{(j)}$ is equal to zero for $j = \infty$ and $c = 1$ i.e. $-b = 2a$, as one can see from (3.36) since $\lambda_j = \lambda_+ = 1$ for $j = \infty$, $\omega = 0$, and $c = 1$. However, as noted earlier, the limit of the maximum of the convergence factor is one as $\omega \to 0$ if $|b| = 2a$, and we use equation (3.35) to find $\alpha^*_{(j)}$ for $j = \infty$, where we take $\omega = \omega_{min}$. Note also that $\rho_{opt(\infty)}$ is the same as ρ_{optL} from Section 3.4. For $\omega_{min} = \frac{\pi}{20}$ and $\omega_{max} = 20\pi$, we find the value $\alpha^*_{(\infty)} = 0.7346$, which will be shown in Subsection 3.4.3 for the infinitely large circuit case.

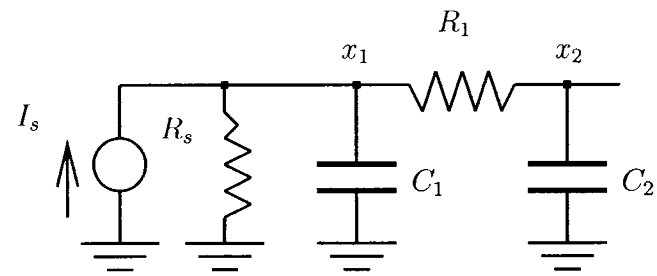

Figure 3.7: A very small RC circuit.

3.2 A Very Small RC Type Circuit Model

A very simple RC type circuit, which we call the extra small RC circuit, is given in Figure 3.7. We confirm here the results we found in Section 3.1 for $j = 1$, and we also prove our practical suggestion given in (3.36) for this case. Indeed, this extra small problem could easily be solved, but interest is in the large scale case, and by studying the simple case we will gain insight for the larger ones. In addition, we are studying this really simple circuit, because it will be of interest in a case where we have two large circuits which are joined or connected with just a simple circuit like this one.

The circuit equations are specified in the form of (1.4) as

$$\dot{\boldsymbol{x}} = \begin{bmatrix} b_1 & c_1 \\ a_1 & b_2 \end{bmatrix} \boldsymbol{x} + \boldsymbol{f}, \tag{3.37}$$

where the entries in the tridiagonal matrix are given by

$$a_1 = \frac{1}{R_1 C_2}, \quad b_i = \begin{cases} -(\frac{1}{R_s} + \frac{1}{R_1})\frac{1}{C_1}, & i = 1, \\ -\frac{1}{R_1 C_2}, & i = 2, \end{cases} \quad c_1 = \frac{1}{R_1 C_1}.$$

The source term on the right hand side is given by $\boldsymbol{f} = (I_s(t)/C_1, 0)^T$, for some source function $I_s(t)$, and we are also given the initial voltage values $\boldsymbol{x}(0) = (v_1^0, v_2^0)^T$ at the time $t = 0$.

3.2.1 The Classical WR Algorithm

We analyze here the classical WR algorithm for the extra small circuit shown in Figure 3.7, which has only two nodes. We keep the entries in the system representing the circuit without the simplifying assumptions given in (3.7), to get more general results for the case $j = 1$. We partition the circuit into two sub-circuits, which contain only one equation each for this case. We call the unknown voltage in equation one $u_1(t)$ and in equation two $w_1(t)$. The classical WR algorithm applied to (3.37) is given by

$$\begin{aligned} \dot{u}_1^{k+1} &= b_1 u_1^{k+1} + c_1 w_1^k + f_1, \\ \dot{w}_1^{k+1} &= b_2 w_1^{k+1} + a_1 u_1^k + f_2, \end{aligned} \tag{3.38}$$

where we used the classical transmission conditions

$$u_2^{k+1} = w_1^k, \quad w_0^{k+1} = u_1^k. \tag{3.39}$$

The corresponding initial conditions are $u_1^{k+1}(0) = v_1^0$ and $w_1^{k+1}(0) = v_2^0$. To start the WR iteration, we need to specify two initial waveforms $u_1^0(t)$ and $w_1^0(t)$ for $t \in [0, T]$, where T is the end of the transient analysis interval. The Laplace transform for $s \in \mathbb{C}$ of the homogeneous problem of (3.38) is given by

$$\begin{aligned} s\hat{u}_1^{k+1} &= b_1 \hat{u}_1^{k+1} + c_1 \hat{w}_1^k, \\ s\hat{w}_1^{k+1} &= b_2 \hat{w}_1^{k+1} + a_1 \hat{u}_1^k. \end{aligned} \tag{3.40}$$

Solving the first equation in (3.40) for $\hat{u}_1^{k+1}$, and the second one for $\hat{w}_1^{k+1}$ we find

$$\begin{aligned} \hat{u}_1^{k+1} &= \tfrac{c_1}{s-b_1} \hat{w}_1^k, \\ \hat{w}_1^{k+1} &= \tfrac{a_1}{s-b_2} \hat{u}_1^k, \end{aligned}$$

which implies, by inserting the second one at iteration k into the first one,

$$\hat{u}_1^{k+1} = \rho_{cla}(s, a_1, c_1, \boldsymbol{b}) \hat{u}_1^{k-1},$$

with the convergence factor ρ_{cla} of the classical WR algorithm given by

$$\rho_{cla}(s, a_1, c_1, \boldsymbol{b}) = \frac{a_1 c_1}{(s - b_1)(s - b_2)}. \tag{3.41}$$

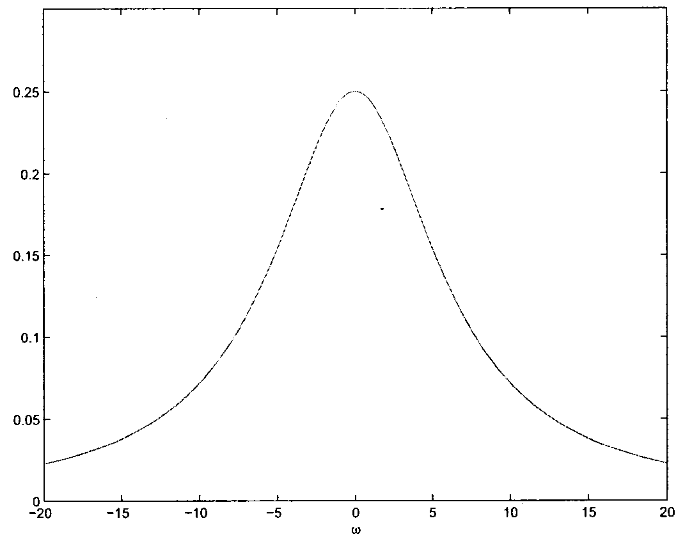

Figure 3.8: Convergence factor for the classical WR algorithm, $|\rho_{cla}(\omega)|$.

The same result holds for $\hat{w}_1^{k+1}$, and by induction we find $\hat{u}_1^{2k} = (\rho_{cla})^k \hat{u}_1^0$, and $\hat{w}_1^{2k} = (\rho_{cla})^k \hat{w}_1^0$. Note that, with the simplifying assumptions (3.7), the convergence factor ρ_{cla} given by (3.41) is the same as the one given by (3.13) for the case $j = 1$. Equation (3.41) has two poles, but they are both negative, since $b_1,\ b_2 < 0$. Therefore, by Theorem 1.4, the convergence factor ρ_{cla} is an analytic function in the right half of the complex plane, $s = \eta + i\omega,\ \eta > 0$. Furthermore, the limit of ρ_{cla} for $s := re^{i\theta}$, where $-\frac{\pi}{2} < \theta < \frac{\pi}{2}$, as $r \rightarrow \infty$ is zero, so we have one limit in all directions. Therefore, by the maximum principle for complex analytic functions, Theorem 1.5, the modulus $|\rho_{cla}|$ takes its maximum on the boundary at $\eta = 0$. Direct computation shows that $|\rho_{cla}(\omega, a_1, c_1, \boldsymbol{b})|$ has its maximum at $\omega = 0$, and that the maximum is less than one. Hence, the low frequency components in the signal, ω close to zero, will cause difficulties for the algorithm, and slow convergence. An example for the convergence factor as a function of ω is given in Figure 3.8.

3.2.2 An Optimal WR Algorithm

The new transmission conditions that are proposed by Gander and Ruehli in [31], the equivalent to (3.5) with $j = 1$, are given by

$$(u_2^{k+1} - u_1^{k+1}) + \alpha u_2^{k+1} = (w_1^k - w_0^k) + \alpha w_1^k, \quad (w_1^{k+1} - w_0^{k+1}) + \beta w_0^{k+1} = (u_2^k - u_1^k) + \beta u_1^k. \tag{3.42}$$

The new WR algorithm with the new transmission conditions for the extra small circuit is given by

$$\begin{aligned} \dot{u}_1^{k+1} &= (b_1 + \tfrac{c_1}{\alpha+1}) u_1^{k+1} + (c_1 w_1^k - \tfrac{c_1}{\alpha+1} w_0^k) + f_1, \\ \dot{w}_1^{k+1} &= (b_2 - \tfrac{a_1}{\beta-1}) w_1^{k+1} + (a_1 u_1^k + \tfrac{a_1}{\beta-1} u_2^k) + f_2, \end{aligned} \tag{3.43}$$

where we start with initial waveforms u_1^0, u_2^0, w_1^0, and w_0^0, which must satisfy the initial conditions, and for the next iterations, the values u_2^k and w_0^k are determined by the transmission conditions (3.42). Using the Laplace transform as we did in the classical case, we find from the first circuit equation, after some algebra,

$$\hat{u}_1^{k+1} = F_1(\hat{w}_1^k(\alpha + 1) - \hat{w}_0^k), \ F_1 = \frac{c_1}{(s - b_1)(\alpha + 1) - c_1}, \tag{3.44}$$

and similarly from the second circuit equation,

$$\hat{w}_1^{k+1} = F_2(\hat{u}_1^k(\beta - 1) + \hat{u}_2^k), \ F_2 = \frac{a_1}{(s - b_2)(\beta - 1) + a_1}. \tag{3.45}$$

Now, we want to obtain the convergence factor for the optimal WR algorithm in closed form, similar to the result in (3.41) for the classical WR algorithm for the extra small circuit. We need to find a relation between $\hat{u}_1^{k+1}$ and $\hat{w}_1^k$ from (3.44), and similarly a relation between $\hat{w}_1^{k+1}$ and $\hat{u}_1^k$ from (3.45). Using the transmission condition

$$(w_1^{k+1} - w_0^{k+1}) + \beta w_0^{k+1} = (u_2^k - u_1^k) + \beta u_1^k,$$

we find, together with (3.45),

$$\hat{w}_0^{k+1} = \left(\frac{1}{(\beta - 1)F_2} - \frac{1}{\beta - 1} \right) \hat{w}_1^{k+1},$$

and using this result at step k in (3.44) we find for the first sub-circuit

$$\hat{u}_1^{k+1} = F_1\left(\alpha + 1 - \frac{1}{(\beta - 1)F_2} + \frac{1}{\beta - 1}\right)\hat{w}_1^k. \tag{3.46}$$

Similarly, for the second equation we find

$$\hat{w}_1^{k+1} = F_2\left(\frac{1}{(\alpha + 1)F_1} + \frac{1}{\alpha + 1} + \beta - 1\right)\hat{u}_1^k. \tag{3.47}$$

Finally, by inserting (3.47) at iteration k into (3.46), we get a relation over two iteration steps of the optimal WR algorithm,

$$\hat{u}_1^{k+1} = \rho_{opt}(s, a_1, c_1, \boldsymbol{b}, \alpha, \beta)\hat{u}_1^{k-1},$$

where the convergence factor of the new algorithm is given by

$$\rho_{opt}(s, a_1, c_1, \boldsymbol{b}, \alpha, \beta) = \frac{(\alpha + 1)a_1 - (s - b_2)}{(\alpha + 1)(s - b_1) - c_1} \cdot \frac{(\beta - 1)c_1 + (s - b_1)}{(\beta - 1)(s - b_2) + a_1}. \tag{3.48}$$

The same result also holds for the second sub-circuit and by induction we find, as before, $\hat{u}_1^{2k} = (\rho_{opt})^k \hat{u}_1^0$, and $\hat{w}_1^{2k} = (\rho_{opt})^k \hat{w}_1^0$. Note that the convergence factor found above is the same as the one given by (3.18) with the simplifying assumptions (3.7) for the case $j = 1$. The optimal values of the parameters α and β are given in the following theorem.

Theorem 3.5 (Optimal Convergence). *The new WR algorithm (3.43) converges in two iterations, independently of the initial waveforms $\hat{u}_1^0$ and $\hat{w}_1^0$, if*

$$\alpha := \frac{s - b_2}{a_1} - 1, \quad \beta := -\frac{s - b_1}{c_1} + 1. \tag{3.49}$$

Proof. The proof is similar to the proof of Theorem 3.3. □

Now if we consider the simplifying assumptions (3.7), then the optimal choice (3.49) is the same as the one given by (3.28) for $j = 1$. We observe that the optimal choice (3.49) is a first degree polynomial in $s \in \mathbb{C}$, which corresponds to first degree time derivatives in the transmission conditions, since a multiplication with s in the frequency domain corresponds to a derivative in the time domain. Time derivatives can be implemented at a similar cost as simple voltage values in the transmission conditions, since derivatives require local information.

3.2.3 An Optimized WR Algorithm with Constant Transmission Conditions

As we have seen in Subsection 3.2.2, one can use the optimal values of the parameters α and β in (3.49) which are first degree polynomials in s to obtain optimal convergence, but one needs to implement the first order time derivatives in the transmission conditions. However, it is not the case for the larger RC circuits analyzed later, since the optimal transmission conditions there correspond to nonlocal operators in time, and we thus propose constant as well as first order approximations for the optimal choices. In this subsection, we introduce a constant approximation for the best possible transmission conditions (3.49), which leads to a very practical algorithm. The low frequency constant approximations for the optimal parameters in (3.49), are given by

$$\alpha_T = \frac{-b_2}{a_1} - 1,\ \beta_T = \frac{b_1}{c_1} + 1.$$

From Figure 3.9, we observe that the convergence factor ρ_{opt} with the Taylor constant approximation takes smaller values than the classical convergence factor ρ_{cla} for low frequencies, whereas ρ_{cla} is better for high frequencies. To find a better constant approximation, we solve an optimization problem which allows us to reduce the large $\rho_{cla}(\omega)$ of the classical WR for ω small in Figure 3.9 and make it more uniform, which will then lead to faster overall convergence of the WR algorithm. Mathematically, we want $|\rho_{opt}| \ll 1$, which leads to the min-max problem

$$\min_{\alpha,\beta}\left(\max_{\Re(s)\geq 0}|\rho_{opt}(s,a_1,\boldsymbol{b},c_1,\alpha,\beta)|\right). \tag{3.50}$$

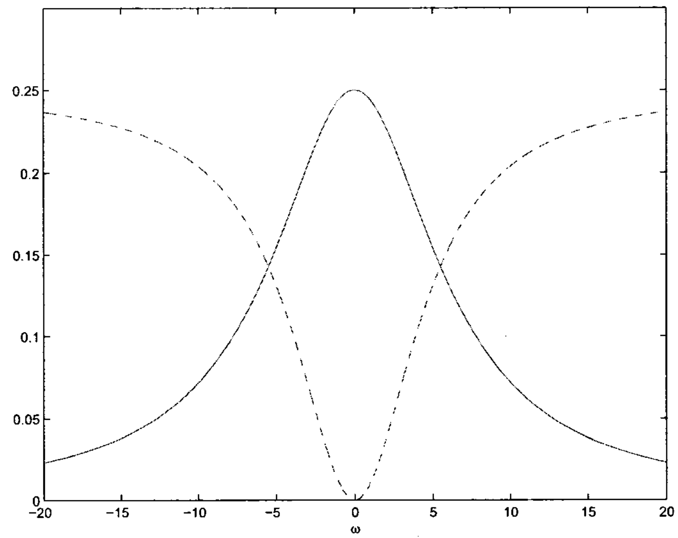

Figure 3.9: Convergence factor $|\rho_{cla}(\omega)|$ (solid line) versus $|\rho_{opt}(\omega, \alpha_T)|$ with Taylor approximation (dashed line).

If ρ_{opt} is analytic, then the maximum of its modulus is attained on the boundary, by the maximum principle, Theorem 1.5. Therefore, the first step in the optimization is to ensure that the convergence factor ρ_{opt} does not have any poles in the right half of the complex plane. The conditions for analyticity are given in the following lemma.

Lemma 3.3. *If* $b_i < 0,\ a_1,\ c_1 > 0,\ |b_1| > c_1,\ |b_2| > a_1$, *and*

$$\alpha > \frac{-c_1}{b_1} - 1 := \underline{\alpha}, \quad \beta < \frac{a_1}{b_2} + 1 := \overline{\beta}, \tag{3.51}$$

then the convergence factor ρ_{opt} *in (3.48) is an analytic function in the right half of the complex plane.*

Proof. By Theorem 1.4, we have to show that the denominators have no zeros in the right half of the complex plane. We only show the proof for the first quotient in ρ_{opt} given in (3.48) and α, since the proof for the second quotient and β is similar. The only zero of the first denominator in ρ_{opt} is given by $s = \frac{c_1}{\alpha+1} + b_1$. This pole is in the left half plane, because the condition on α in (3.51) implies that

$$(\alpha+1)b_1 + c_1 = -(\alpha+1)|b_1| + c_1 < -|b_1|(\frac{-c_1}{b_1}) + c_1 = 0.$$

$\square$

Since ρ_{opt} is analytic, we can apply again the maximum principle for complex analytic functions, Theorem 1.5. The limit of ρ_{opt} for $s := re^{i\theta}$, where $-\frac{\pi}{2} < \theta < \frac{\pi}{2}$, as $r \to \infty$ is $\left(\frac{-1}{(\alpha+1)(\beta-1)}\right)$, so we have one limit in all directions. Therefore, the maximum of ρ_{opt} for $s = \eta + i\omega$, $\eta > 0$, is attained on the boundary at $\eta = 0$. The above analysis simplifies the optimization problem to

$$\min_{\alpha>\underline{\alpha},\beta<\overline{\beta}} \left(\max_{|\omega|<\infty} |\rho_{opt}(i\omega, a_1, \boldsymbol{b}, c_1, \alpha, \beta)| \right). \tag{3.52}$$

One can see from (3.48) that the modulus of ρ_{opt} for $s = i\omega$ depends on ω^2 only, since $|((\alpha+1)a_1 + b_2) - i\omega|$ depends only on ω^2, and similarly for the other terms. Hence, it suffices to optimize for nonnegative frequencies, $\omega \geq 0$. As we have seen in Section 3.1, we assume $c_1 = a_1$, and $b_2 = b_1$, which leads to $\beta = -\alpha$ for the optimal α and β given in (3.49). In the analysis, we denote a_1 by a, and b_1 by b, and we choose $\beta = -\alpha$.

Note that with the simplifying assumptions we made, we have $\alpha_T > \underline{\alpha}$, $\beta_T < \overline{\beta}$, and $\beta_T = -\alpha_T$, for $b < 0$, $a > 0$, and $|b| > a$. In addition, α_T and β_T are the same as the values in (3.33) with $j = 1$. Now we will investigate if there exists a better choice for α such that the overall convergence factor is smaller than with the value from the low frequency approximation. The convergence factor (3.48) with the simplifying assumptions we made becomes

$$\rho_{opt0}(i\omega, a, b, \alpha) = \left(\frac{\alpha + 1 - \lambda}{(\alpha+1)\lambda - 1} \right)^2,$$

where $\lambda = \frac{s-b}{a} = \frac{-b}{a} + \frac{\omega}{a}i$, $\omega \geq 0$.

We define a new parameter γ by $\gamma = \alpha+1 > \underline{\alpha}+1 = \frac{-a}{b}$. We also define $\tilde{\omega} = \frac{\omega}{a} \geq 0$, and $\tilde{b} = \frac{-b}{a} > 1$. Hence, $\lambda = \tilde{b} + i\tilde{\omega}$. Taking the modulus of the convergence factor ρ_{opt0} we obtain

$$R_0(\tilde{\omega}, \tilde{b}, \gamma) = \frac{\tilde{b}^2 - 2\gamma\tilde{b} + \gamma^2 + \tilde{\omega}^2}{\tilde{b}^2\gamma^2 - 2\gamma\tilde{b} + 1 + \gamma^2\tilde{\omega}^2}. \tag{3.53}$$

Hence, the min-max problem (3.52) becomes

$$\min_{\gamma > \frac{1}{\tilde{b}}} \left(\max_{\tilde{\omega} \geq 0} R_0(\tilde{\omega}, \tilde{b}, \gamma) \right). \tag{3.54}$$

To solve the min-max problem (3.54), the following two lemmas are needed.

Lemma 3.4. *The function $\tilde{\omega} \mapsto R_0(\tilde{\omega}, \tilde{b}, \gamma)$ defined in (3.53) has a unique local maximum at $\tilde{\omega} = 0$ if $\gamma > \tilde{b} + \sqrt{\tilde{b}^2 - 1}$. If $1 < \gamma < \tilde{b} + \sqrt{\tilde{b}^2 - 1}$, then R_0 has a unique local minimum at $\tilde{\omega} = 0$, and if $\gamma = \tilde{b} + \sqrt{\tilde{b}^2 - 1}$, then R_0 is a constant for all $\tilde{\omega}$, and is given by*

$$R_0(\tilde{\omega}, \tilde{b}, \tilde{b} + \sqrt{\tilde{b}^2 - 1}) = \frac{1}{2\tilde{b}^2 + 2\tilde{b}\sqrt{\tilde{b}^2 - 1} - 1}.$$

Proof. A partial derivative of $R_0(\tilde{\omega}, \tilde{b}, \gamma)$ with respect to $\tilde{\omega}$ gives

$$\frac{\partial R_0}{\partial \tilde{\omega}} = \frac{2\tilde{\omega}(1 - 2\gamma\tilde{b} + 2\gamma^3\tilde{b} - \gamma^4)}{(\tilde{b}^2\gamma^2 - 2\gamma\tilde{b} + 1 + \gamma^2\tilde{\omega}^2)^2},$$

and therefore, $R_0(\tilde{\omega}, \tilde{b}, \gamma)$ has only one extremum, at $\tilde{\omega} = 0$. This extremum is a maximum if $(1 - 2\gamma\tilde{b} + 2\gamma^3\tilde{b} - \gamma^4) < 0$, and is a minimum if $(1 - 2\gamma\tilde{b} + 2\gamma^3\tilde{b} - \gamma^4) > 0$. The equation $1 - 2\gamma\tilde{b} + 2\gamma^3\tilde{b} - \gamma^4 = 0$ has the four solutions $\gamma = -1,\ 1,\ \tilde{b} \pm \sqrt{\tilde{b}^2 - 1}$. The values -1 and $\tilde{b} - \sqrt{\tilde{b}^2 - 1}$ are negative and can be neglected since $\gamma > \frac{1}{\tilde{b}} > 0$, and $\gamma = 1$ can be also neglected since $\gamma = 1$ implies $\alpha = 0$. So we have only the value $\tilde{b} + \sqrt{\tilde{b}^2 - 1}$. Since the coefficient of the highest power, γ^4, in $(1 - 2\gamma\tilde{b} + 2\gamma^3\tilde{b} - \gamma^4)$ is less than zero, we have $(1 - 2\gamma\tilde{b} + 2\gamma^3\tilde{b} - \gamma^4) < 0$, for $\gamma > \tilde{b} + \sqrt{\tilde{b}^2 - 1}$, and R_0 has a maximum at $\tilde{\omega} = 0$, and for $1 < \gamma < \tilde{b} + \sqrt{\tilde{b}^2 - 1}$, we have $(1 - 2\gamma\tilde{b} + 2\gamma^3\tilde{b} - \gamma^4) > 0$, and R_0 has a minimum at $\tilde{\omega} = 0$. At $\tilde{b} + \sqrt{\tilde{b}^2 - 1}$, we have $\frac{\partial R_0}{\partial \tilde{\omega}} = 0$, and the function $R_0(\tilde{\omega}, \tilde{b}, \tilde{b} + \sqrt{\tilde{b}^2 - 1}) = \frac{1}{2\tilde{b}^2 + 2\tilde{b}\sqrt{\tilde{b}^2 - 1} - 1}$, is a constant for all $\tilde{\omega}$. □

Lemma 3.5. *For fixed $\tilde{\omega} \geq 0$, and $\gamma > \frac{1}{\tilde{b}}$, we have $\frac{\partial R_0(\tilde{\omega},\tilde{b},\gamma)}{\partial \gamma}(\gamma - \gamma_+) \geq 0$, where $\gamma_+(\tilde{\omega}) = \frac{\tilde{b}^2+\tilde{\omega}^2+1+\sqrt{(\tilde{b}^2+\tilde{\omega}^2+1-2\tilde{b}^2)(\tilde{b}^2+\tilde{\omega}^2+1+2\tilde{b}^2)}}{2\tilde{b}}$.*

Proof. A partial derivative of R_0 with respect to γ gives

$$\frac{\partial R_0}{\partial \gamma} = -2\frac{(-\tilde{\omega}^2\tilde{b} + \tilde{b} - \tilde{b}^3)\gamma^2 + (2\tilde{\omega}^2\tilde{b}^2 - 1 + \tilde{b}^4 + \tilde{\omega}^4)\gamma - \tilde{\omega}^2\tilde{b} + \tilde{b} - \tilde{b}^3}{(1 + (\tilde{b}^2 + \tilde{\omega}^2)\gamma^2 - 2\gamma\tilde{b})^2},$$

which has two roots in γ, given by

$$\gamma_{\pm}(\tilde{\omega}) = \frac{\tilde{b}^2 + \tilde{\omega}^2 + 1 \pm \sqrt{((\tilde{b}-1)^2 + \tilde{\omega}^2)((\tilde{b}+1)^2 + \tilde{\omega}^2)}}{2\tilde{b}}.$$

Since the coefficient of γ^2 in $\frac{\partial R_0}{\partial \gamma}$ is positive for $\tilde{\omega} \geq 0$, and $\tilde{b} > 1$, the larger of the two roots is a minimum. Note that $\gamma_+ > \frac{1}{\tilde{b}}$, whereas $\gamma_- < \frac{1}{\tilde{b}}$, so γ_- can be neglected. For $\gamma > \gamma_+$, $\frac{\partial R_0}{\partial \gamma}$ is positive and hence $R_0(\tilde{\omega}, \tilde{b}, \gamma)$ increases when γ increases, whereas for $\gamma < \gamma_+$, $\frac{\partial R_0}{\partial \gamma}$ is negative and hence $R_0(\tilde{\omega}, \tilde{b}, \gamma)$ decreases when γ increases. Hence, $\frac{\partial R_0(\tilde{\omega},\tilde{b},\gamma)}{\partial \gamma}(\gamma - \gamma_+) \geq 0$. □

Theorem 3.6 (Optimized Constant Transmission Conditions). *The best performance of the optimized waveform relaxation algorithm (3.43) with constant transmission conditions is obtained for $\alpha = \alpha^*$, where $\alpha^* = \gamma^* - 1$, and γ^*, the solution of the min-max problem (3.54), is given by*

$$\gamma^* = \tilde{b} + \sqrt{\tilde{b}^2 - 1} = \frac{-b}{a} + \sqrt{\left(\frac{-b}{a}\right)^2 - 1}. \tag{3.55}$$

Proof. By Lemma 3.5, the optimal γ^* must lie in the interval $[\tilde{b}, \infty)$, since with γ outside this interval R_0 can be uniformly decreased for all $0 \leq \tilde{\omega} < \infty$ by moving γ towards the interval $[\tilde{b}, \infty)$, which is obtained using the fact that $\gamma_+(\tilde{\omega} = 0) = \tilde{b}$, and $\lim_{\tilde{\omega}\to\infty} \gamma_+(\tilde{\omega}) = \infty$. Furthermore, the partial derivative with respect to $\tilde{\omega}$ shows that R_0 has no interior maxima, Lemma 3.4. Now, for $\gamma = \tilde{b}$, we have $R_0(0, \tilde{b}, \tilde{b}) = 0$, and so increasing γ increases $R_0(0, \tilde{b}, \gamma)$ monotonically, by Lemma 3.5. On the other hand, for $\gamma = \tilde{b}$, we have $R_0(\tilde{\omega}_\infty, \tilde{b}, \tilde{b}) = \frac{1}{\tilde{b}^2} > 0$, and increasing γ decreases $R_0(\tilde{\omega}_\infty, \tilde{b}, \gamma) = \frac{1}{\gamma^2}$

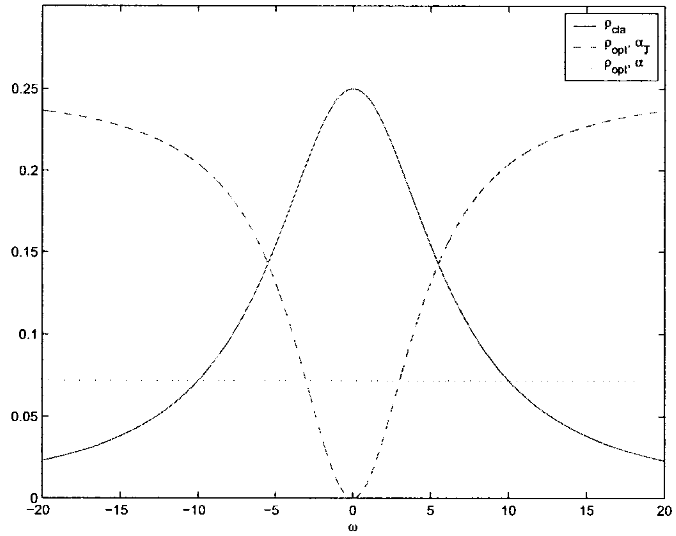

Figure 3.10: $|\rho_{cla}(\omega)|$ versus $|\rho_{opt}(\omega, \alpha^*)|$ with optimized constant, and $|\rho_{opt}(\omega, \alpha_T)|$ with Taylor approximation.

to $\lim_{\gamma\to\infty}(\frac{1}{\gamma^2}) = 0$. Therefore, by increasing γ we reach $R_0(0, \tilde{b}, \gamma) = R_0(\tilde{\omega}_\infty, \tilde{b}, \gamma)$. Solving the equation for γ implies the solution in (3.55), and other three solutions, $\gamma = -1,\ 1,\ \tilde{b} - \sqrt{\tilde{b}^2 - 1}$. Those three solutions can be discarded, since $\gamma > \frac{1}{b}$, and $\gamma = 1$ implies $\alpha = 0$. $\square$

Note that this value of γ, i.e. γ^*, is the same value that makes $\frac{\partial R_0}{\partial \tilde{\omega}} = 0$ for all $\tilde{\omega}$, and the function R_0 is equal to a constant. Figure 3.10 shows the modulus of the classical convergence factor ρ_{cla}, and the optimized convergence factor ρ_{opt} with the Taylor and optimized constant approximations, with the values of a and b from the numerical experiment in Subsection 3.2.4. One can see the better performance of the optimized constant approximation over the Taylor transmission conditions, and the classical one.

3.2.4 Numerical Experiments

We give here a numerical example to illustrate the improvements in the convergence of the optimized WR algorithm over the classical one. We use the typical values of RC circuit parameters

$$R_s = R_1 = \frac{1}{2} \text{ Ohms}, \; C_1 = C_2 = \frac{63}{100} \text{ pF},$$

for the circuit in Figure 3.7. We choose for all the numerical computations the backward Euler method, and our transient analysis time is $t \in [0, 10]$, with a time step of $\Delta t = 1/10$. We start with random initial waveforms and use an input step function with an amplitude of $I_s = 1$ and a rise time of 1 time unit. In Figure 3.11 we show the error as a function of the iterations. One can see the remarkable improvement of the optimized WR algorithm over the classical one. On the left hand side of Figure 3.11 we choose $b_2 = b_1$, which is used to compute the optimized constant $\alpha^* = 2.732$ and $\beta^* = -\alpha^*$. We also use $b_2 = b_1$ to find $\alpha_T = 1$ and $\beta_T = -1$. We can see that the optimized WR algorithm with the optimized constant approximation is better than the one with the Taylor approximation. On the right hand side of Figure 3.11 we use the circuit elements without simplifying assumptions. We use $b_2 = \frac{b_1}{2}$ to compute $\alpha_T = 0$ and $\beta_T = -1$, and to compute the numerically optimized $\alpha^* = 1.618$ and $\beta^* = -1.618$, which are used in the optimized WR algorithm, and we also use here in the WR algorithm the optimized constant $\alpha^* = 2.732$ with $\beta^* = -\alpha^*$. Note that for $b_2 = \frac{b_1}{2}$ in this circuit case, we numerically obtain optimized values for α and β that satisfy $\alpha^* = -\beta^*$, which are in general need not to be the same. One can see from the right hand side of Figure 3.11 that the best performance is obtained by using the numerically optimized constant approximation, and that the optimized approximation obtained analytically by assuming $b_2 = b_1$ is better than the Taylor approximation.

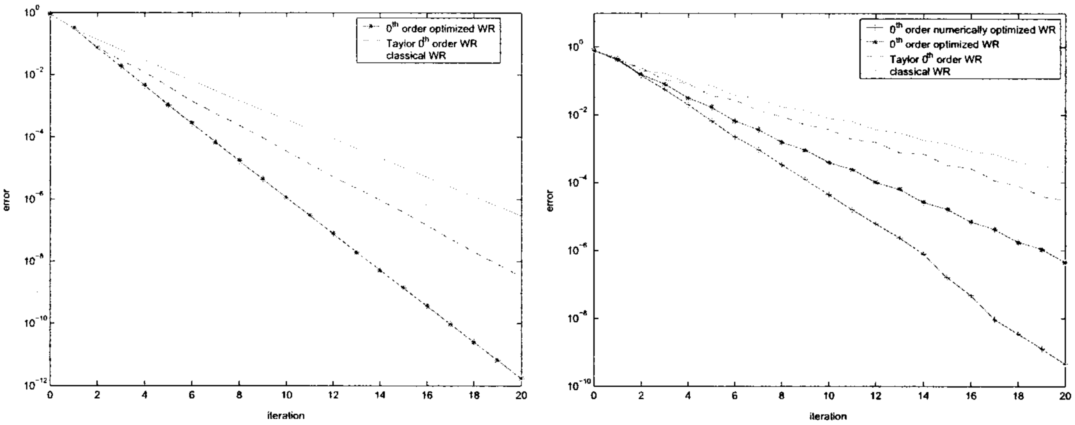

Figure 3.11: Convergence behavior of classical versus optimized WR algorithms for the extra small RC circuit.

3.3 A Small RC Type Circuit

A small RC circuit that has four nodes is given in Figure 1.1. It is twice as big as the extra small circuit in Section 3.2, and was analyzed in [31, 1]. The equations for the circuit are given in (1.5) in the introduction by the system of ODEs

$$\dot{\boldsymbol{x}} = \begin{bmatrix} b_1 & c_1 & & \\ a_1 & b_2 & c_2 & \\ & a_2 & b_3 & c_3 \\ & & a_3 & b_4 \end{bmatrix} \boldsymbol{x} + \boldsymbol{f}, \tag{3.56}$$

and the entries in the tridiagonal matrix are

$$a_i = \frac{1}{R_i C_{i+1}}, \quad b_i = \begin{cases} -(\frac{1}{R_s} + \frac{1}{R_1})\frac{1}{C_1}, & i = 1 \\ -(\frac{1}{R_{i-1}} + \frac{1}{R_i})\frac{1}{C_i}, & i = 2, 3, \\ -\frac{1}{R_{i-1}C_i}, & i = 4 \end{cases} \quad c_i = \frac{1}{R_i C_i}.$$

The source term on the right hand side is given by $\boldsymbol{f} = (I_s(t)/C_1, 0, 0, 0)^T$, for some source function $I_s(t)$, and we are also given the initial voltage values $\boldsymbol{x}(0) = (v_1^0, v_2^0, v_3^0, v_4^0)^T$ at the time $t = 0$.

3.3.1 The Classical WR Algorithm

The analysis of the classical WR algorithm for the small circuit, with the classical transmission conditions

$$u_3^{k+1} = w_1^k, \quad w_0^{k+1} = u_2^k, \tag{3.57}$$

was discussed in [31]. The classical WR algorithm applied to (3.56), with a partition into two sub-circuits, using the classical transmission conditions (3.57), is

$$\begin{aligned} \dot{\boldsymbol{u}}^{k+1} &= \begin{bmatrix} b_1 & c_1 \\ a_1 & b_2 \end{bmatrix} \boldsymbol{u}^{k+1} + \begin{pmatrix} f_1 \\ f_2 \end{pmatrix} + \begin{pmatrix} 0 \\ c_2 w_1^k \end{pmatrix}, \\ \dot{\boldsymbol{w}}^{k+1} &= \begin{bmatrix} b_3 & c_3 \\ a_3 & b_4 \end{bmatrix} \boldsymbol{w}^{k+1} + \begin{pmatrix} f_3 \\ f_4 \end{pmatrix} + \begin{pmatrix} a_2 u_2^k \\ 0 \end{pmatrix}, \end{aligned} \tag{3.58}$$

with corresponding initial conditions $\boldsymbol{u}^{k+1}(0) = (v_1^0, v_2^0)^T$ and $\boldsymbol{w}^{k+1}(0) = (v_3^0, v_4^0)^T$. To start the WR iteration, we need to specify two initial waveforms $u_2^0(t)$ and $w_1^0(t)$ for $t \in [0, T]$.

The Laplace transform was also used for the convergence study in [31, 1]. It was shown that $\hat{u}_2^{2k} = (\rho_{cla})^k \hat{u}_2^0$, and $\hat{w}_1^{2k} = (\rho_{cla})^k \hat{w}_1^0$, with the convergence factor ρ_{cla}, which is given by

$$\rho_{cla}(s, \boldsymbol{a}, \boldsymbol{b}, \boldsymbol{c}) = \frac{c_2(s - b_1)}{(s - b_1)(s - b_2) - a_1 c_1} \cdot \frac{a_2(s - b_4)}{(s - b_3)(s - b_4) - a_3 c_3}, \quad s = \eta + i\omega. \tag{3.59}$$

In [31], it is shown that the convergence factor ρ_{cla} is an analytic function in the right half of the complex plane, $s = \eta + i\omega$, $\eta > 0$. Furthermore, similar to the extra small circuit, the limit of ρ_{cla} for $s := re^{i\theta}$, where $-\frac{\pi}{2} < \theta < \frac{\pi}{2}$, as $r \to \infty$ is zero. Therefore, Theorem 1.5 implies that the modulus $|\rho_{cla}|$ takes its maximum on the boundary at $\eta = 0$. It is shown in [31] as well, that ρ_{cla} takes its maximum at $\omega = 0$. Hence, the low frequency components in the signal, ω close to zero, will cause difficulties for the algorithm, and converge slowly. An example for the convergence factor as a function of ω is given in Figure 3.12 .

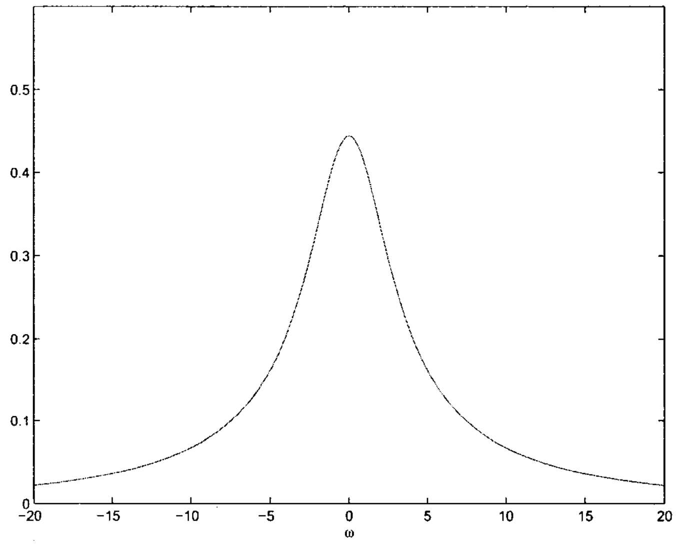

Figure 3.12: Convergence factor for the classical WR algorithm, $|\rho_{cla}(\omega)|$.

3.3.2 An Optimal WR Algorithm

The new transmission conditions which are given for this case by

$$(u_3^{k+1} - u_2^{k+1}) + \alpha u_3^{k+1} = (w_1^k - w_0^k) + \alpha w_1^k, \quad (w_1^{k+1} - w_0^{k+1}) + \beta w_0^{k+1} = (u_3^k - u_2^k) + \beta u_2^k, \tag{3.60}$$

were proposed in [31] by Gander and Ruehli. The new WR algorithm, using the new transmission conditions (3.60), is given by

$$\begin{aligned} \dot{\boldsymbol{u}}^{k+1} &= \begin{bmatrix} b_1 & c_1 \\ a_1 & b_2 + \frac{c_2}{\alpha+1} \end{bmatrix} \boldsymbol{u}^{k+1} + \begin{pmatrix} f_1 \\ f_2 \end{pmatrix} + \begin{pmatrix} 0 \\ c_2 w_1^k - \frac{c_2}{\alpha+1} w_0^k \end{pmatrix}, \\ \dot{\boldsymbol{w}}^{k+1} &= \begin{bmatrix} b_3 - \frac{a_2}{\beta-1} & c_3 \\ a_3 & b_4 \end{bmatrix} \boldsymbol{w}^{k+1} + \begin{pmatrix} f_3 \\ f_4 \end{pmatrix} + \begin{pmatrix} a_2 u_2^k + \frac{a_2}{\beta-1} u_3^k \\ 0 \end{pmatrix}, \end{aligned} \tag{3.61}$$

where the values u_3^k and w_0^k are determined by the transmission conditions (3.60). It was shown in [31], that $\hat{u}_2^{2k} = (\rho_{opt})^k \hat{u}_2^0$, and $\hat{w}_1^{2k} = (\rho_{opt})^k \hat{w}_1^0$, where the convergence factor ρ_{opt} is given by

$$\rho_{opt}(s,\boldsymbol{a},\boldsymbol{b},\boldsymbol{c},\alpha,\beta) = -\frac{c_2(s-b_1)(\beta-1)+(s-b_1)(s-b_2)-a_1c_1}{((s-b_3)(s-b_4)-a_3c_3)(\beta-1)+a_2(s-b_4)} \cdot \frac{-a_2(s-b_4)(\alpha+1)+(s-b_3)(s-b_4)-a_3c_3}{((s-b_1)(s-b_2)-a_1c_1)(\alpha+1)+c_2(b_1-s)}. \tag{3.62}$$

The best values of the parameters α and β in the transmission conditions (3.60) are

$$\alpha := \frac{-a_3c_3}{(s-b_4)a_2} + \frac{s-b_3}{a_2} - 1, \quad \beta := \frac{a_1c_1}{(s-b_1)c_2} - \frac{s-b_2}{c_2} + 1, \quad s \in \mathbb{C}, \tag{3.63}$$

where the optimal WR algorithm (3.61) converges in two iterations for this choice of parameters, independently of the guess for the initial waveforms [31].

Gander and Ruehli [31] proposed an approximation of the best possible transmission conditions (3.63). An approximation by a constant was chosen in [31], which leads to a very practical algorithm with remarkable improvement over the classical WR algorithm.

In the next subsection we will prove the optimality of the constant approximation proposed by Gander and Ruehli [31].

3.3.3 An Optimized WR Algorithm with Constant Transmission Conditions

The simplest constant approximations of the optimal parameters (3.63) in the transmission conditions are again the low frequency approximations, which are given by

$$\alpha_T = \frac{a_3c_3}{b_4a_2} - \frac{b_3}{a_2} - 1, \; \beta_T = -\frac{a_1c_1}{b_1c_2} + \frac{b_2}{c_2} + 1.$$

From Figure 3.13, we again observe that the convergence factor ρ_{opt} with the Taylor constant approximation is smaller than the classical convergence factor ρ_{cla} for low frequencies, whereas ρ_{cla} is smaller for high frequencies.

As in subsection 3.2.3, the optimization process for the WR algorithm allows us to reduce the large $\rho_{cla}(\omega)$ of the classical WR in Figure 3.13 and make it more uniform

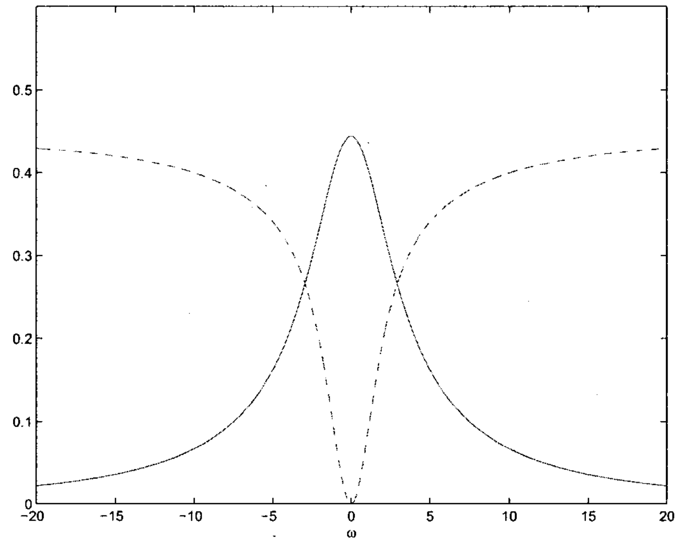

Figure 3.13: Convergence factor $|\rho_{cla}(\omega)|$ (solid line) versus $|\rho_{opt}(\omega, \alpha_T)|$ with the Taylor approximation (dashed line).

which will lead to faster convergence of the new WR algorithm. The analyticity of ρ_{opt} given in (3.62) is proved in the following lemma.

Lemma 3.6. *Let $b_i < 0$, a_i, $c_i > 0$, $b_1b_2 > a_1c_1$, $b_3b_4 > a_3c_3$ and*

$$\alpha > \frac{c_2|b_1|}{b_1b_2 - a_1c_1} - 1 =: \underline{\alpha},$$
$$\beta < -\frac{a_2|b_4|}{b_3b_4 - a_3c_3} + 1 =: \overline{\beta}.$$

Then the convergence factor ρ_{opt} in (3.62) is an analytic function in the right half of the complex plane.

Proof. See [31]. □

Therefore, the maximum of ρ_{opt} for $s = \eta + i\omega$, $\eta > 0$, is attained on the boundary. Since, the limit of ρ_{opt} for $s := re^{i\theta}$, where $-\frac{\pi}{2} < \theta < \frac{\pi}{2}$, as $r \to \infty$ is $\left(\frac{-1}{(\alpha+1)(\beta-1)}\right)$, one limit in all directions, we have that the maximum is attained at $\eta = 0$. The above analysis simplifies the optimization problem to

$$\min_{\alpha>\underline{\alpha},\beta<\overline{\beta}}\left(\max_{|\omega|<\infty}|\rho_{opt}(i\omega,\boldsymbol{a},\boldsymbol{b},\boldsymbol{c},\alpha,\beta)|\right). \tag{3.64}$$

One can see from (3.62) that the modulus of ρ_{opt} for $s=i\omega$ depends on ω^2 only, since $|c_2(i\omega-b_1)(\beta-1)+(i\omega-b_1)(i\omega-b_2)-a_1c_1|$ depends only on ω^2, and similarly for the other terms. Hence, it suffices to optimize for nonnegative frequencies, $\omega\geq 0$.

Now we will investigate if there exists a better choice for α and β such that the overall convergence with this new choice is better than the one with the low frequency approximation. We again use here the simplifying assumptions and the similarity of the subsystems, as we did in Subsection 3.2.3 for the extra small circuit case. So we choose $\beta=-\alpha$, and hence, α is the only optimization parameter left, and we also assume $c_i=a_i=a_1$, for $i=1,2,3$, and $b_i=b_1$, for $i=1,2,3,4$. We denote a_1 by a, and b_1 by b.

Note that, as in the extra small circuit case, with the simplifying assumptions we made, we have $\alpha_T>\underline{\alpha}$, $\beta_T<\overline{\beta}$, and $\beta_T=-\alpha_T$, for $b<0$, $a>0$, and $|b|>a$. In addition, α_T and β_T are the same as the values in (3.33) with $j=2$.

The convergence factor (3.62), in terms of a, b, and α becomes after simplification,

$$\rho_{opt0}(i\omega,a,b,\alpha)=\left(\frac{\alpha+1-\lambda}{(\alpha+1)\lambda-1}\right)^2, \tag{3.65}$$

where $\lambda=\frac{(s-b)^2-a^2}{a(s-b)}=\frac{-b}{a}+\frac{1}{a}\frac{s(s-b)-a^2}{s-b}$, $s=i\omega$, $\omega\geq 0$.

To further analyze the convergence factor, we use the fact that $|b|\geq 2a$ for RC type circuits, where $|b|=2a$ often holds, as we will also see in Section 3.4 for the infinitely large RC circuit. Now since $\underline{\alpha}:=\frac{a|b|}{b^2-a^2}-1$ is positive for $|b|>\frac{1+\sqrt{5}}{2}a$, and in our case we have $|b|\geq 2a>\frac{1+\sqrt{5}}{2}a$, we consider $\alpha>0$, and ρ_{opt0} is still analytic in the right half of the complex plane. In order to show that this is true, we need the following lemma.

Lemma 3.7. *Let $b < 0$, $a > 0$, and $-b \geq 2a$. If $\lambda = \frac{(s-b)^2-a^2}{a(s-b)}$, $s = \eta + i\omega$, then the modulus of λ is bigger than one in the right half of the complex plane.*

Proof. The modulus of λ is given by

$$|\lambda| = \frac{|(s-b)^2 - a^2|}{|a(s-b)|} = \frac{|(s+|b|)^2 - a^2|}{|a(s+|b|)|},$$

and using the scaling we defined in the introduction, i.e. taking $a = 1$, $b = -2c^2$, and $c \geq 1$, we have

$$|\lambda| = \sqrt{\frac{(\eta^2+1+\omega^2+4\eta c^2+2\eta+4c^2+4c^4)(\eta^2+1+\omega^2+4\eta c^2-2\eta-4c^2+4c^4)}{\eta^2+4\eta c^2+4c^4+\omega^2}}.$$

This shows that the modulus $|\lambda|$ is bigger than one, since the first factor in the numerator of the argument under the square root is bigger than the denominator, and the second factor is bigger than one for $c \geq 1$ and $\eta > 0$. Hence, $|\lambda| > 1$ in the right half of the complex plane. $\square$

Now to show that the convergence factor ρ_{opt0} is still analytic in the right half of the complex plane for $\alpha > 0$, we use the following contradiction. We take $\alpha > 0$, and we assume that ρ_{opt0} has a pole in the right half of the complex plane, then $(\alpha+1)\lambda - 1 = 0$ implies

$$\lambda = \frac{1}{\alpha+1},$$

and hence $|\lambda| = |\frac{1}{\alpha+1}| < 1$ for $\alpha > 0$, but $|\lambda| > 1$ for $s = \eta + i\omega$, $\eta > 0$, and $|b| \geq 2a$, by Lemma 3.7, which is a contradiction. So, there is no such pole, and ρ_{opt0} is analytic in the right half of the complex plane for $\alpha > 0$. In addition, the optimized value of α, as we will see later, is bigger than $\underline{\alpha}$.

We also introduce a change of variables based on the real part of $z := \frac{s(s-b)-a^2}{s-b}$, $s = i\omega$, $\omega \geq 0$, which appears in λ. We write z as

$$z := x + iy = \Re\left(\frac{s(s-b)-a^2}{s-b}\right) + \Im\left(\frac{s(s-b)-a^2}{s-b}\right)i, \tag{3.66}$$

and hence we have

$$\lambda = \frac{-b}{a} + \frac{1}{a}(x + iy). \tag{3.67}$$

The real part x is given by

$$x := X(\omega) = \frac{ba^2}{b^2 + \omega^2},$$

and the imaginary part y is given by

$$y := Y(\omega) = \frac{\omega(b^2 + \omega^2 + a^2)}{b^2 + \omega^2}.$$

The range in which x can vary can be found by taking the value of $X(\omega)$ at $\omega = 0$, and the limit as ω goes to infinity,

$$X(\omega = 0) = \frac{a^2}{b}, \qquad \lim_{\omega \to \infty} X(\omega) = 0,$$

and hence $x \in [\frac{a^2}{b}, 0)$, (note that $b < 0$).

Solving $x = X(\omega)$ for ω gives

$$\omega(x) = \pm \frac{\sqrt{-xb(xb - a^2)}}{x}.$$

Since $\omega \geq 0$, and we have $x \in [\frac{a^2}{b}, 0)$, we consider

$$\omega(x) = -\frac{\sqrt{-xb(xb - a^2)}}{x}, \tag{3.68}$$

and the other root can be discarded since it implies the same result since $|\rho_{opt}|$ depends on ω^2. Inserting the value of ω from (3.68) into $Y(\omega)$ implies after simplification

$$y = -\frac{\sqrt{-xb(xb - a^2)}(b + x)}{xb}. \tag{3.69}$$

By inserting y from equation (3.69) into (3.67), and the result into (3.65), the convergence factor (3.65) is a function of the new variable x.

The optimal value of α in (3.63) can be written in terms of λ as $\alpha = \lambda - 1$, where λ is given in (3.67). Moreover, if p is a free parameter corresponding to a constant approximation of $x+iy$ in (3.67), then a constant approximation of α is $\alpha = \frac{-b}{a} - 1 + \frac{p}{a}$.

In the new variable x, and the new parameter p for the constant approximation, the convergence factor (3.65) in modulus becomes

$$|\rho_{opt0}(x,a,b,p)| = \frac{-a^2((2b^2+2bp-a^2)x^2+(-2ba^2+b^3-bp^2)x-b^2a^2)}{((-4b^4-4b^2p^2+8b^3p+3b^2a^2+a^2p^2-4bpa^2)x^2+(2a^2p^2b+a^4b-2b^2pa^2)x+b^4a^2-2b^3pa^2+p^2b^2a^2)}.$$

Factorizing a^6 from the denominator and numerator, implies

$$|\rho_{opt0}(x,a,b,p)| := \frac{Q_1(x,a,b,p)}{Q_2(x,a,b,p)},$$

where

$$\begin{aligned} Q_1 &:= -\left(\left(2\left(\tfrac{b}{a}\right)^2+2\left(\tfrac{b}{a}\right)\left(\tfrac{p}{a}\right)-1\right)\left(\tfrac{x}{a}\right)^2+\left(-2\left(\tfrac{b}{a}\right)+\left(\tfrac{b}{a}\right)^3-\left(\tfrac{b}{a}\right)\left(\tfrac{p}{a}\right)^2\right)\left(\tfrac{x}{a}\right)-\left(\tfrac{b}{a}\right)^2\right), \\ Q_2 &:= \left(-4\left(\tfrac{b}{a}\right)^4-4\left(\tfrac{b}{a}\right)^2\left(\tfrac{p}{a}\right)^2+8\left(\tfrac{b}{a}\right)^3\left(\tfrac{p}{a}\right)+3\left(\tfrac{b}{a}\right)^2+\left(\tfrac{p}{a}\right)^2-4\left(\tfrac{b}{a}\right)\left(\tfrac{p}{a}\right)\right)\left(\tfrac{x}{a}\right)^2 \\ &\quad+\left(2\left(\tfrac{p}{a}\right)^2\left(\tfrac{b}{a}\right)+\left(\tfrac{b}{a}\right)-2\left(\tfrac{b}{a}\right)^2\left(\tfrac{p}{a}\right)\right)\left(\tfrac{x}{a}\right)+\left(\tfrac{b}{a}\right)^4-2\left(\tfrac{b}{a}\right)^3\left(\tfrac{p}{a}\right)+\left(\tfrac{p}{a}\right)^2\left(\tfrac{b}{a}\right)^2. \end{aligned}$$

We set $\tilde{p} = \frac{p}{a}$, and in addition, we set $\frac{b}{a} = -2c^2$, $c \geq 1$, since $|b| \geq 2a$, to eliminate one parameter, and assume $\tilde{x} = \frac{x}{a}$, where $\tilde{x} \in [\frac{1}{b/a}, 0) \equiv [-\frac{1}{2c^2}, 0)$.

Since we have $\alpha > 0$, the new parameter $\tilde{p}$ should satisfy $\tilde{p} > 1-2c^2$. Furthermore, the modulus of the convergence factor (3.65) is now given by

$$R_0(\tilde{x},c,\tilde{p}) = -\frac{(4c^2\tilde{p}-8c^4+1)\tilde{x}^2+(8c^6-4c^2-2c^2\tilde{p}^2)\tilde{x}+4c^4}{(64c^8-8c^2\tilde{p}-12c^4+64c^6\tilde{p}+16c^4\tilde{p}^2-\tilde{p}^2)\tilde{x}^2+(2c^2+4c^2\tilde{p}^2+8c^4\tilde{p})\tilde{x}-16c^8-16c^6\tilde{p}-4c^4\tilde{p}^2}, \tag{3.70}$$

where $\tilde{x} \in [-\frac{1}{2c^2}, 0)$, and the min-max problem (3.64) becomes

$$\min_{\tilde{p}>(1-2c^2)} \left(\max_{\frac{-1}{2c^2} \leq \tilde{x} < 0} R_0(\tilde{x},c,\tilde{p}) \right), \quad c \geq 1. \tag{3.71}$$

To analyze the min-max problem (3.71), we need the following lemmas:

Lemma 3.8. *For $\tilde{p} > 1-2c^2$, and $c \geq 1$, the polynomial L defined by*

$$L(c,\tilde{p}) := (16c^4-1)\tilde{p}^2 + 4c^2\tilde{p} - 64c^8 - 1 + 28c^4, \tag{3.72}$$

has a unique real root at

$$\tilde{p}_+ = \frac{-2c^2 + \sqrt{48c^4 + 1024c^{12} - 512c^8 - 1}}{16c^4 - 1}. \tag{3.73}$$

Moreover, $\tilde{p}_+ > 0$, *and* $L(c,\tilde{p}) > 0$ *for* $\tilde{p} > \tilde{p}_+$, *and* $L(c,\tilde{p}) < 0$ *for* $1 - 2c^2 < \tilde{p} < \tilde{p}_+$.

Proof. The polynomial L has two real roots $\tilde{p}_\pm$, which are given by

$$\tilde{p}_\pm = \frac{-2c^2 \pm \sqrt{48c^4 + 1024c^{12} - 512c^8 - 1}}{16c^4 - 1}. \tag{3.74}$$

The first root $\tilde{p}_+$ satisfies $\tilde{p}_+ > 0 > 1 - 2c^2$, since

$$\begin{aligned} \tilde{p}_+ > 0 \iff & -2c^2 + \sqrt{48c^4 + 1024c^{12} - 512c^8 - 1} > 0 \\ \iff & 48c^4 + 1024c^{12} - 512c^8 - 1 > 4c^4 \\ \iff & 44c^4 + 1024c^{12} - 512c^8 - 1 > 0, \end{aligned}$$

and the last inequality is true for $c \geq 1$, since the coefficient of the term c^{12} is the dominant one. For the second root $\tilde{p}_-$, we have $\tilde{p}_- < 1 - 2c^2$ since

$$\begin{aligned} \tilde{p}_- < 1 - 2c^2 \iff & -2c^2 - \sqrt{48c^4 + 1024c^{12} - 512c^8 - 1} < (1 - 2c^2)(16c^4 - 1) \\ \iff & 32c^6 - 16c^4 - 4c^2 + 1 < \sqrt{48c^4 + 1024c^{12} - 512c^8 - 1} \\ & \text{(both sides are positive, so square and simplify)} \\ \iff & -1024c^{10} + 192c^6 - 64c^4 - 8c^2 + 2 + 512c^8 < 0, \end{aligned}$$

and the last inequality is true for $c \geq 1$. Hence, $\tilde{p}_-$ can be discarded.

Since $L(c,\tilde{p})$ is positive for large $\tilde{p}$, because of the sign of the coefficient of $\tilde{p}^2$ which is positive, we have $L(c,\tilde{p}) > 0$ for $\tilde{p} > \tilde{p}_+$, and for $1 - 2c^2 < \tilde{p} < \tilde{p}_+$ the polynomial $L(c,\tilde{p}) < 0$. □

Lemma 3.9. *For* $\tilde{p} > 1 - 2c^2$, *and* $c \geq 1$, *the polynomial* d *given by*

$$\begin{aligned} d(c,\tilde{p}) = & \ (1 - 16c^4)\tilde{p}^4 - 4c^2\tilde{p}^3 + (128c^8 - 32c^4 + 2)\tilde{p}^2 \\ & + (80c^6 - 4c^2)\tilde{p} + 240c^8 - 32c^4 - 256c^{12} + 1, \end{aligned} \tag{3.75}$$

has only two real roots, say $\tilde{p}_1$ *and* $\tilde{p}_2$, *and* $\tilde{p}_1 < \tilde{p}_2$, *which are both bigger than zero, and has no roots in the interval* $(1 - 2c^2, 0]$. *Furthermore,* d *satisfies the following:*

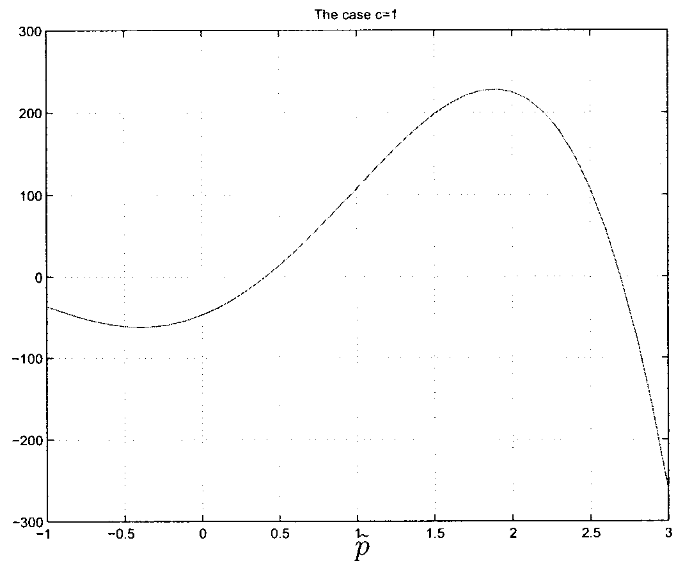

Figure 3.14: The polynomial d for the case $c = 1$.

i) $d(c, \tilde{p}) < 0$ *for* $\tilde{p} \in (1 - 2c^2, \tilde{p}_1) \bigcup (\tilde{p}_2, \infty)$,

ii) $d(c, \tilde{p}) \geq 0$ *for* $\tilde{p} \in [\tilde{p}_1, \tilde{p}_2]$.

Proof. The polynomial $d(c, \tilde{p})$ is negative for large $\tilde{p}$, because of the sign of the coefficient of $\tilde{p}^4$ which is negative. Moreover, d takes positive values, e.g. at $\tilde{p} = 2c^2$, $d(c, 2c^2) = (16c^4 - 1)^2 > 0$, hence, it must have by continuity and the Intermediate Value Theorem at least one real root $\tilde{p}_2(c) > 2c^2 > 1 - 2c^2$, $d(c, \tilde{p}_2) = 0$. An example of d with $c = 1$ and $\tilde{p} > 1 - 2c^2$ is given in Figure 3.14. To show that d has exactly two roots bigger than $1 - 2c^2$, say $\tilde{p}_1$ and $\tilde{p}_2$, and $\tilde{p}_2 > \tilde{p}_1 > 0$, we use the derivative of $d(c, \tilde{p})$ with respect to $\tilde{p}$. The derivative

$$\frac{d}{d\tilde{p}}(d(c, \tilde{p})) = 4(1 - 16c^4)\tilde{p}^3 - 12c^2\tilde{p}^2 + 2(-32c^4 + 128c^8 + 2)\tilde{p} - 4c^2 + 80c^6$$

has two real roots, say $r_1, r_2 > 1 - 2c^2$, and a third real root, say r_3, less than $1 - 2c^2$, since

$$\begin{aligned}
&\tfrac{d}{d\tilde{p}}(d(c,\tilde{p}))\,|_{\tilde{p}=-2c^2} = 4c^2(32c^4-3) > 0,\\
&\tfrac{d}{d\tilde{p}}(d(c,\tilde{p}))\,|_{\tilde{p}=1-2c^2} = -8(4c^4-2c^2-1)(4c^2-1)^2 < 0,\\
&\tfrac{d}{d\tilde{p}}(d(c,\tilde{p}))\,|_{\tilde{p}=0} = 4c^2(20c^4-1) > 0,\\
&\tfrac{d}{d\tilde{p}}(d(c,\tilde{p}))\,|_{\tilde{p}=2c^2} = -4c^2(16c^4-1) < 0.
\end{aligned}$$

Therefore, by the Intermediate Value Theorem, we have $r_3 \in (-2c^2, 1-2c^2)$, which can be discarded, $r_2 \in (1-2c^2, 0)$ which is a minimum, and $r_1 \in (0, 2c^2)$ which is a maximum.

Now, we have $d(c, 1-2c^2) = -4(4c^4-2c^2-1)(4c^2-1)^2 < 0$, and then d decreases to more negative values until d reaches its minimum at r_2, after that d starts increasing to its maximum at $r_1 \in (0, 2c^2)$, which is a positive value since $d(c, 2c^2) = (16c^4-1)^2 > 0$, and r_1, where the maximum is attained, is less than $2c^2$, so here $d(c,\tilde{p})$ has a real root which is $\tilde{p}_1 > 1-2c^2$, and more than that, we have $\tilde{p}_1 > 0$ since at $\tilde{p} = 0$, $d(c,\tilde{p})$ is negative. After d reaches its maximum at r_1, it starts decreasing again to minus infinity, so here d has its second root $\tilde{p}_2 > \tilde{p}_1 > 0$, and there are no more roots, since d decreases to minus infinity.

Therefore, $d(c,\tilde{p})$ has only two roots, $\tilde{p}_2 > \tilde{p}_1 > 0$, for $\tilde{p} > 1-2c^2$, and $c \geq 1$, and no roots in the interval $(1-2c^2, 0]$. Moreover, d falls under one of the following two cases:

i) $d(c,\tilde{p}) < 0$ for $\tilde{p} \in (1-2c^2, \tilde{p}_1) \bigcup (\tilde{p}_2, \infty)$,

ii) $d(c,\tilde{p}) \geq 0$ for $\tilde{p} \in [\tilde{p}_1, \tilde{p}_2]$.

□

Lemma 3.10. *For $c \geq 1$, the root $\tilde{p}_+$ given in (3.73) lies in the interval $[\tilde{p}_1, \tilde{p}_2]$, where $\tilde{p}_1$ and $\tilde{p}_2$ are the two real roots of d which are characterized by Lemma 3.9.*

Proof. By Lemma 3.8, we have $\tilde{p}_+ > 0$ for $c \geq 1$. Now, since $d(c,\tilde{p}_+) > 0$, $\tilde{p}_+$ must lie in the interval $[\tilde{p}_1, \tilde{p}_2]$, by Lemma 3.9. □

Lemma 3.11. *For $\tilde{p} \in [\tilde{p}_1, \tilde{p}_2]$, and $c \geq 1$, the polynomial P_2 defined by*

$$P_2(c, \tilde{p}) = (1 - 16c^4)\tilde{p}^2 - 4c^2(1 + 4c^4)\tilde{p} + 32c^8 - 28c^4 + 1,$$

is always negative.

Proof. Using the Intermediate Value Theorem, one can show that the two roots of P_2 are $r_- \in (-2c^2, 1-2c^2)$ and $r_+ \in (0, 2c^2)$. By finding the precise r_+, and substituting it into d in (3.75), we have $d(c, r_+) < 0$, and since $d(c, \tilde{p}) \geq 0$ for $\tilde{p} \in [\tilde{p}_1, \tilde{p}_2]$, Lemma 3.9, and $r_+ < 2c^2$, we have $r_- < r_+ < \tilde{p}_1$, and the two zeros $r_\pm$ are not in $[\tilde{p}_1, \tilde{p}_2]$. In addition, the coefficient of $\tilde{p}^2$ is negative, which implies that the sign of P_2 is positive only for $\tilde{p} \in (r_-, r_+)$, and is negative everywhere else. Hence, the polynomial P_2 is always negative for $\tilde{p} \in [\tilde{p}_1, \tilde{p}_2]$. □

Lemma 3.12. *For $\tilde{p} > 1 - 2c^2$, and $c \geq 1$, the polynomial P_4 defined by*

$$P_4(c, \tilde{p}) = L(c, \tilde{p})((-16c^8 + 1 - 16c^4)\tilde{p}^2 + (-4c^2 - 32c^6)\tilde{p} + 64c^{12} - 16c^8 + 1 - 28c^4),$$

where L is given in (3.72), has only two real roots, $\tilde{p}_+$ given in (3.73) and another real root, say $\hat{\tilde{p}}$, and $1 - 2c^2 < \tilde{p}_1 < \hat{\tilde{p}} < \tilde{p}_+$, where $\tilde{p}_1$ is the real root of d in Lemma 3.9. Moreover, P_4 is negative for $\tilde{p} \in (1 - 2c^2, \hat{\tilde{p}}) \bigcup (\tilde{p}_+, \infty)$, and positive for $\tilde{p} \in (\hat{\tilde{p}}, \tilde{p}_+)$.

Proof. For $\tilde{p} = \tilde{p}_+$, $\tilde{p}_-$ given in (3.74), the roots of L, we have $P_4(\tilde{p}) = 0$, which means $\tilde{p}_+ > 0$, $\tilde{p}_- < 1 - 2c^2$ are roots for $P_4(\tilde{p})$. One can also find the other two roots from $(1 - 16c^8 - 16c^4)\tilde{p}^2 - (4c^2 + 32c^6)\tilde{p} + 64c^{12} - 16c^8 + 1 - 28c^4 = 0$, which implies two roots, one is less than $1 - 2c^2$, and hence, it can be discarded, and another root $\hat{\tilde{p}} > 1 - 2c^2$, where $\hat{\tilde{p}} < \tilde{p}_+$, since $L(c, \hat{\tilde{p}}) < 0$, and $L(c, \tilde{p})$ is negative for all $\tilde{p} \in (1 - 2c^2, \tilde{p}_+)$, by Lemma 3.8.

Therefore, $P_4(\tilde{p})$ has exactly two roots bigger than $1 - 2c^2$, which are $\tilde{p}_+$ and $\hat{\tilde{p}}$. Furthermore, $d(c, \hat{\tilde{p}}) > 0$, which means $\tilde{p}_1 < \hat{\tilde{p}}$, since $1 - 2c^2 < \hat{\tilde{p}}$, and $d(c, \tilde{p})$ is positive in $(\tilde{p}_1, \tilde{p}_2)$, by Lemma 3.9. Therefore, from the sign of P_4, the polynomial P_4 is negative for $\tilde{p} \in (1 - 2c^2, \hat{\tilde{p}}) \bigcup (\tilde{p}_+, \infty)$, and positive for $\tilde{p} \in (\hat{\tilde{p}}, \tilde{p}_+)$. □

Lemma 3.13. *For $\tilde{p} > 1 - 2c^2$, and $c \geq 1$, let $x_1(c, \tilde{p})$ be given by*

$$x_1(c, \tilde{p}) = \frac{(16c^4 + 8c^2\tilde{p} + 2\sqrt{d})c^2}{L},$$

where L and d are given in (3.72) and (3.75) respectively. Then x_1 is not defined for $\tilde{p} = \tilde{p}_+$, and is complex for $\tilde{p} \in (1 - 2c^2, \tilde{p}_1) \bigcup (\tilde{p}_2, \infty)$. Furthermore, $x_1 < \frac{-1}{2c^2}$ for $[\tilde{p}_1, \tilde{p}_+)$, and $x_1 > 0$ for $(\tilde{p}_+, \tilde{p}_2]$.

Proof. By Lemma 3.8, the denominator of x_1 is zero at $\tilde{p} = \tilde{p}_+$, and by Lemma 3.9, $d(c, \tilde{p}) < 0$ for $\tilde{p} \in (1 - 2c^2, \tilde{p}_1) \bigcup (\tilde{p}_2, \infty)$. Hence, x_1 is not defined for $\tilde{p} = \tilde{p}_+$, and is complex for $\tilde{p} \in (1 - 2c^2, \tilde{p}_1) \bigcup (\tilde{p}_2, \infty)$. For $\tilde{p} \in (\tilde{p}_+, \tilde{p}_2]$, we have $x_1 > 0$, since it is a fraction of two positive quantities, Lemmas 3.8 and 3.9. Consider now the interval $[\tilde{p}_1, \tilde{p}_+)$, then

$$\begin{aligned}
x_1 < \tfrac{-1}{2c^2} &\iff \tfrac{(8\tilde{p}c^2 + 16c^4 + 2\sqrt{d})c^2}{L} < \tfrac{-1}{2c^2} \\
&\iff (8\tilde{p}c^2 + 16c^4 + 2\sqrt{d})c^2 > \tfrac{-L}{2c^2} \\
&\qquad \text{(L is negative in the interval considered)} \\
&\iff 4c^4\sqrt{d} > -L - 16\tilde{p}c^6 - 32c^8 \\
&\iff 4c^4\sqrt{d} > (1 - 16c^4)\tilde{p}^2 - 4c^2(1 + 4c^4)\tilde{p} + 32c^8 - 28c^4 + 1.
\end{aligned}$$

Now, since in the interval considered, the left hand side is positive, Lemma 3.9, and the right hand side is negative, Lemma 3.11, the last inequality is true and we have $x_1 < \frac{-1}{2c^2}$. □

Lemma 3.14. *For $\tilde{p} > 1 - 2c^2$, and $c \geq 1$, let $x_2(c, \tilde{p})$ be given by*

$$x_2(c, \tilde{p}) = \frac{(16c^4 + 8c^2\tilde{p} - 2\sqrt{d})c^2}{L},$$

where L and d are given in (3.72) and (3.75) respectively. Then x_2 is not defined for $\tilde{p} = \tilde{p}_+$, and is complex for $\tilde{p} \in (1 - 2c^2, \tilde{p}_1) \bigcup (\tilde{p}_2, \infty)$. Furthermore, $x_2 \geq \frac{-1}{2c^2}$ for $\tilde{p} \in [\hat{p}, \tilde{p}_+) \bigcup (\tilde{p}_+, \tilde{p}_2]$, and $x_2 < \frac{-1}{2c^2}$ for $[\tilde{p}_1, \hat{p})$. In addition, $x_2 < 0$ for $\tilde{p} \in [\tilde{p}_1, \tilde{p}_+) \bigcup (\tilde{p}_+, \tilde{\tilde{p}})$, and $x_2 \geq 0$ for $[\tilde{\tilde{p}}, \tilde{p}_2]$, where $\tilde{\tilde{p}} = \sqrt{4c^4 - 1}$, and $\tilde{p}_+ < \tilde{\tilde{p}} < \tilde{p}_2$.

Proof. The proof is similar to the proof of Lemma 3.13. By Lemma 3.8, the denominator of x_2 is zero at $\tilde{p} = \tilde{p}_+$, and by Lemma 3.9, $d(c, \tilde{p}) < 0$ for $\tilde{p} \in (1-2c^2, \tilde{p}_1) \bigcup (\tilde{p}_2, \infty)$. Hence, x_2 is not defined for $\tilde{p} = \tilde{p}_+$, and is complex for $\tilde{p} \in (1-2c^2, \tilde{p}_1) \bigcup (\tilde{p}_2, \infty)$. For $\tilde{p} \in [\tilde{p}_1, \tilde{p}_+)$, we have

$$\begin{aligned}
x_2 > \tfrac{-1}{2c^2} \quad &\iff \tfrac{(8\tilde{p}c^2+16c^4-2\sqrt{d})c^2}{L} > \tfrac{-1}{2c^2} \\
&\iff (8\tilde{p}c^2 + 16c^4 - 2\sqrt{d})c^2 < \tfrac{-L}{2c^2} \\
&\qquad \text{(L is negative in the interval considered)} \\
&\iff 4c^4\sqrt{d} > L + 16\tilde{p}c^6 + 32c^8 \\
&\iff 4c^4\sqrt{d} > -((1-16c^4)\tilde{p}^2 - 4c^2(1+4c^4)\tilde{p} + 32c^8 - 28c^4 + 1) \\
&\qquad \text{(R.H.S is minus the polynomial } P_2 \text{ studied in Lemma 3.11),} \\
&\qquad \text{(both sides are positive, so square and simplify)} \\
&\iff \\
&L(c,\tilde{p})((-16c^8+1-16c^4)\tilde{p}^2+(-4c^2-32c^6)\tilde{p}+64c^{12}-16c^8+1-28c^4) > 0.
\end{aligned}$$

The left hand side is the polynomial P_4 studied in Lemma 3.12. Therefore, by Lemma 3.12, we have $x_2 < \frac{-1}{2c^2}$ for $\tilde{p} \in [\tilde{p}_1, \hat{\tilde{p}})$, and for $\tilde{p} \in [\hat{\tilde{p}}, \tilde{p}_+)$, we have $x_2 \geq \frac{-1}{2c^2}$. Consider now the interval $(\tilde{p}_+, \tilde{p}_2]$, in which we have

$$\begin{aligned}
x_2 > \tfrac{-1}{2c^2} \quad &\iff \tfrac{(8\tilde{p}c^2+16c^4-2\sqrt{d})c^2}{L} > \tfrac{-1}{2c^2} \\
&\iff (8\tilde{p}c^2 + 16c^4 - 2\sqrt{d})c^2 > \tfrac{-L}{2c^2} \\
&\qquad \text{(L is positive in the interval considered)} \\
&\iff 4c^4\sqrt{d} < L + 16\tilde{p}c^6 + 32c^8 \\
&\iff 4c^4\sqrt{d} < -((1-16c^4)\tilde{p}^2 - 4c^2(1+4c^4)\tilde{p} + 32c^8 - 28c^4 + 1) \\
&\qquad \text{(has been seen earlier),} \\
&\qquad \text{(both sides are positive, so square and simplify)} \\
&\iff \\
&L(c,\tilde{p})((-16c^8+1-16c^4)\tilde{p}^2+(-4c^2-32c^6)\tilde{p}+64c^{12}-16c^8+1-28c^4) < 0.
\end{aligned}$$

The left hand side is again the polynomial P_4 studied in Lemma 3.12, and thus, $x_2 > \frac{-1}{2c^2}$ for $\tilde{p} \in (\tilde{p}_+, \tilde{p}_2]$. Therefore, $x_2 \geq \frac{-1}{2c^2}$ for $\tilde{p} \in [\hat{\tilde{p}}, \tilde{p}_+) \bigcup (\tilde{p}_+, \tilde{p}_2]$, and $x_2 < \frac{-1}{2c^2}$

for $[\tilde{p}_1, \hat{\tilde{p}})$. For $\tilde{p} \in [\tilde{p}_1, \tilde{p}_+)$, we also have

$$
\begin{aligned}
x_2 < 0 &\iff \tfrac{(8\tilde{p}c^2+16c^4-2\sqrt{d})c^2}{L} > \tfrac{-1}{2c^2} \\
&\iff 4\tilde{p}c^2 + 8c^4 - \sqrt{d} > 0 \\
&\qquad \text{(L is negative in the interval considered)} \\
&\iff (\tilde{p} - \tilde{\tilde{p}})(\tilde{p} + \tilde{\tilde{p}})(\tilde{p} - \tilde{p}_+)(\tilde{p} - \tilde{p}_-) > 0,
\end{aligned}
$$

where $\tilde{\tilde{p}} = \sqrt{4c^4 - 1}$, and $\tilde{p}_+$, $\tilde{p}_-$ are given in (3.74). Therefore, the only two roots of the left hand side in the last inequality above, which are bigger than $1 - 2c^2$, are $\tilde{p}_+$ and $\tilde{\tilde{p}}$. Moreover, since $L(c, \tilde{p})$ is positive for $\tilde{p} = \tilde{\tilde{p}} > 1 - 2c^2$, we have $\tilde{p}_+ < \tilde{\tilde{p}}$, by Lemma 3.8. Also, since $d(c, \tilde{p})$ at $\tilde{p} = \tilde{\tilde{p}}$ is positive, and $\tilde{\tilde{p}} > \tilde{p}_+$, we have $\tilde{\tilde{p}} \in (\tilde{p}_1, \tilde{p}_2)$, by Lemma 3.9. By studying the sign of the left hand side expression in the last inequality, $[(\tilde{p} - \tilde{\tilde{p}})(\tilde{p} + \tilde{\tilde{p}})(\tilde{p} - \tilde{p}_+)(\tilde{p} - \tilde{p}_-)]$, we see that $x_2 < 0$ for $\tilde{p} \in [\tilde{p}_1, \tilde{p}_+)$. Consider now the interval $(\tilde{p}_+, \tilde{p}_2]$, in which we have

$$
\begin{aligned}
x_2 < 0 &\iff \tfrac{(8\tilde{p}c^2+16c^4-2\sqrt{d})c^2}{L} > \tfrac{-1}{2c^2} \\
&\iff 4\tilde{p}c^2 + 8c^4 - \sqrt{d} < 0 \\
&\qquad \text{(L is positive in the interval considered)} \\
&\iff (\tilde{p} - \tilde{\tilde{p}})(\tilde{p} + \tilde{\tilde{p}})(\tilde{p} - \tilde{p}_+)(\tilde{p} - \tilde{p}_-) < 0,
\end{aligned}
$$

which implies that, $x_2 < 0$ for $\tilde{p} \in (\tilde{p}_+, \tilde{\tilde{p}})$, and $x_2 \geq 0$ for $\tilde{p} \in [\tilde{\tilde{p}}, \tilde{p}_2]$. Therefore, $x_2 < 0$ for $\tilde{p} \in [\tilde{p}_1, \tilde{p}_+) \bigcup (\tilde{p}_+, \tilde{\tilde{p}})$, and $x_2 \geq 0$ for $[\tilde{\tilde{p}}, \tilde{p}_2]$. □

Lemma 3.15. *The function $\tilde{x} \mapsto R_0(\tilde{x}, c, \tilde{p})$ defined in (3.70) has a unique local minimum at*

$$
\underline{\tilde{x}}(c, \tilde{p}) = \frac{(16c^4 + 8c^2\tilde{p} - 2\sqrt{d(c, \tilde{p})})c^2}{(16c^4 - 1)\tilde{p}^2 + 4c^2\tilde{p} - 64c^8 - 1 + 28c^4}, \quad d(c, \tilde{p}) \text{ given in } (3.75), \qquad (3.76)
$$

in $[\frac{-1}{2c^2}, 0)$, if $\tilde{p} \in [\hat{\tilde{p}}, \tilde{p}_+) \bigcup (\tilde{p}_+, \tilde{\tilde{p}})$ for $c \geq 1$, where $\tilde{p}_+$, $\hat{\tilde{p}}$ and $\tilde{\tilde{p}}$ are determined by Lemmas 3.8, 3.12, and 3.14 respectively. For any other value of $\tilde{p} > 1 - 2c^2$, R_0 has no extrema in $\tilde{x} \in [\frac{-1}{2c^2}, 0)$.

Proof. A partial derivative of $R_0(\tilde{x}, c, \tilde{p})$ with respect to $\tilde{x}$ shows that the roots of the polynomial

$$Q(\tilde{x}) = (\tilde{p} - 1 + 2c^2)(\tilde{p} + 1 + 2c^2)P(\tilde{x}),$$

where $P(\tilde{x})$ is given by

$$\begin{aligned} P(\tilde{x}) = \; & -2c^2(16c^4\tilde{p}^2 - \tilde{p}^2 + 4c^2\tilde{p} + 28c^4 - 64c^8 - 1)\tilde{x}^2 + 2c^2(16c^4\tilde{p} + 32c^6)\tilde{x} \\ & -2c^2(4c^4\tilde{p}^2 + 4c^4 - 16c^8), \end{aligned} \tag{3.77}$$

determine the extrema of R_0. Since $(\tilde{p} - 1 + 2c^2)(\tilde{p} + 1 + 2c^2) > 0$ for $c \geq 1$ and $\tilde{p} > 1 - 2c^2$, we have $Q(\tilde{x}) = 0 \iff P(\tilde{x}) = 0$, with the same coefficient signs. The polynomial $P(\tilde{x})$ has two roots $\bar{\tilde{x}}$ and $\underline{\tilde{x}}$ given by

$$\begin{aligned} \bar{\tilde{x}}(c, \tilde{p}) &= \tfrac{(16c^4 + 8c^2\tilde{p} + 2\sqrt{d(c,\tilde{p})})c^2}{(16c^4 - 1)\tilde{p}^2 + 4c^2\tilde{p} - 64c^8 - 1 + 28c^4}, \\ \underline{\tilde{x}}(c, \tilde{p}) &= \tfrac{(16c^4 + 8c^2\tilde{p} - 2\sqrt{d(c,\tilde{p})})c^2}{(16c^4 - 1)\tilde{p}^2 + 4c^2\tilde{p} - 64c^8 - 1 + 28c^4}, \end{aligned}$$

and $d(c, \tilde{p})$ is given in (3.75). Note that, $\bar{\tilde{x}}$ and $\underline{\tilde{x}}$ are the same x_1 and x_2 which are given in Lemmas 3.13 and 3.14, respectively. By Lemmas 3.13 and 3.14, $\bar{\tilde{x}}$ and $\underline{\tilde{x}}$ are not defined for $\tilde{p} = \tilde{p}_+$, and are complex for $\tilde{p} \in (1 - 2c^2, \tilde{p}_1) \bigcup (\tilde{p}_2, \infty)$. Therefore, we analyze for the intervals $[\tilde{p}_1, \tilde{p}_+)$ and $(\tilde{p}_+, \tilde{p}_2]$. Now, by Lemmas 3.13 and 3.14, R_0 has only one extremum in $[\frac{-1}{2c^2}, 0)$ at $\tilde{x} = \underline{\tilde{x}}$ if $\tilde{p} \in [\hat{\tilde{p}}, \tilde{p}_+) \bigcup (\tilde{p}_+, \bar{\tilde{p}})$. By studying the sign of $Q(\tilde{x})$, it is a minimum. For any other value of $\tilde{p} > 1 - 2c^2$, R_0 has no extrema in $\tilde{x}$, because either the extrema are not defined or are not in $[\frac{-1}{2c^2}, 0)$, Lemmas 3.13 and 3.14. $\square$

Note that if $\tilde{p} = \tilde{p}_+$, which is the zero of the denominator of $\bar{\tilde{x}}$ and $\underline{\tilde{x}}$ that makes them not defined, then the polynomial $P(\tilde{x})$ given in (3.77) is reduced to a polynomial of degree one, given by

$$P_r(\tilde{x}) = 2c^2(16c^4\tilde{p}_+ + 32c^6)\tilde{x} - 2c^2(4c^4\tilde{p}_+^2 + 4c^4 - 16c^8), \tag{3.78}$$

and has only one zero, given by

$$\tilde{x}_r := \frac{\tilde{p}_+^2 + 1 - 4c^4}{4\tilde{p}_+ + 8c^2} = \frac{-c^2}{16c^4 - 1},$$

and $\tilde{x}_r \in [\frac{-1}{2c^2}, 0)$. Since the reduced polynomial $P_r(\tilde{x})$ in (3.78) is just a line, and the coefficient of $\tilde{x}$ is positive, $\tilde{x}_r$ is a minimum. This case is not however of our interest, since if we take $\tilde{p} = \tilde{p}_+$, then we already have the value of the parameter $\tilde{p}$ which we want to optimize, and no more optimization process.

Lemma 3.16. *For fixed $\tilde{x} \in [-\frac{1}{2c^2}, 0)$, and $\tilde{p} > 1-2c^2$, we have $\frac{\partial R_0(\tilde{x},c,\tilde{p})}{\partial \tilde{p}}(\tilde{p}-\underline{\tilde{p}}(\tilde{x},c)) \geq 0$, where $\underline{\tilde{p}}(\tilde{x},c)$ is given by*

$$\underline{\tilde{p}}(\tilde{x},c) = \frac{6c^2\tilde{x} - 4c^4 - 16\tilde{x}c^6 - \tilde{x}^2 + 8\tilde{x}^2c^4 - \sqrt{d(\tilde{x},c)}}{2(4c^4\tilde{x} + 2c^2\tilde{x}^2)}, \tag{3.79}$$

and $d(\tilde{x},c)$ is given by

$$d(\tilde{x},c) = \left((16c^4-4c^2-1)\tilde{x}^2+(6c^2-8c^4)\tilde{x}-4c^4\right)\left((16c^4+4c^2-1)\tilde{x}^2+(8c^4+6c^2)\tilde{x}-4c^4\right). \tag{3.80}$$

Proof. A partial derivative of $R_0(\tilde{x},c,\tilde{p})$ with respect to $\tilde{p}$ shows that the roots of the polynomial

$$Q(\tilde{p}) = -\left((16c^4-1)\tilde{x}^2 + 2c^2\tilde{x} - 4c^4\right) P(\tilde{p}),$$

where $P(\tilde{p})$ is given by

$$\begin{aligned} P(\tilde{p}) = \; & -(4c^2\tilde{x}^2 + 8c^4\tilde{x})\tilde{p}^2 - (32\tilde{x}c^6 - 16\tilde{x}^2c^4 - 12c^2\tilde{x} + 8c^4 + 2\tilde{x}^2)\tilde{p} \\ & -32\tilde{x}c^8 + 48\tilde{x}^2c^6 - 16c^6 + 16c^4\tilde{x} - 8c^2\tilde{x}^2, \end{aligned} \tag{3.81}$$

determine the extrema of R_0.

For $\tilde{x} \in [-\frac{1}{2c^2}, 0)$ with $c \geq 1$, we have $-((16c^4-1)\tilde{x}^2 + 2c^2\tilde{x} - 4c^4) > 0$. Therefore, $Q(\tilde{p}) = 0 \iff P(\tilde{p}) = 0$, and they have the same coefficient signs. The polynomial $P(\tilde{p})$ has two roots $\overline{\tilde{p}}$ and $\underline{\tilde{p}}$ given by

$$\begin{aligned} \overline{\tilde{p}}(\tilde{x},c) &= \frac{6c^2\tilde{x}-4c^4-16\tilde{x}c^6-\tilde{x}^2+8\tilde{x}^2c^4+\sqrt{d(\tilde{x},c)}}{2(4c^4\tilde{x}+2c^2\tilde{x}^2)}, \\ \underline{\tilde{p}}(\tilde{x},c) &= \frac{6c^2\tilde{x}-4c^4-16\tilde{x}c^6-\tilde{x}^2+8\tilde{x}^2c^4-\sqrt{d(\tilde{x},c)}}{2(4c^4\tilde{x}+2c^2\tilde{x}^2)}, \end{aligned}$$

and $d(\tilde{x}, c)$ is given by (3.80). One can show, using the first derivative with respect to $\tilde{x}$, where $\tilde{x} \in [\frac{-1}{2c^2}, 0)$, $c \geq 1$, and finding the minimum that the two factors of d are negative for $\tilde{x} \in [\frac{-1}{2c^2}, 0)$, $c \geq 1$, i.e.

$$\begin{aligned} &(16c^4 - 4c^2 - 1)\tilde{x}^2 + (6c^2 - 8c^4)\tilde{x} - 4c^4 < 0, \\ &(16c^4 + 4c^2 - 1)\tilde{x}^2 + (6c^2 + 8c^4)\tilde{x} - 4c^4 < 0, \end{aligned} \tag{3.82}$$

and hence, $d > 0$ for $\tilde{x} \in [\frac{-1}{2c^2}, 0)$.

Now, we want to show that $\overline{\tilde{p}} < 1 - 2c^2$, and hence $\overline{\tilde{p}}$ can be discarded, and $\underline{\tilde{p}} > 1 - 2c^2$. For $\overline{\tilde{p}}$, we have

$$\begin{aligned} \overline{\tilde{p}} < 1 - 2c^2 \iff & (8c^4 - 1)\tilde{x}^2 + (6c^2 - 16c^6)\tilde{x} - 4c^4 + \sqrt{d} > 4c^2\tilde{x}(\tilde{x} + 2c^2)(1 - 2c^2) \\ & (\text{since } \tilde{x}(\tilde{x} + 2c^2) < 0) \\ \iff & \sqrt{d} > -((16c^4 - 4c^2 - 1)\tilde{x}^2 + (6c^2 - 8c^4)\tilde{x} - 4c^4) \\ & (\text{both sides are positive by (3.82), square both sides and simplify}) \\ \iff & 8c^2\tilde{x}(\tilde{x} + 2c^2)\left((16c^4 - 4c^2 - 1)\tilde{x}^2 + (6c^2 - 8c^4)\tilde{x} - 4c^4\right) > 0. \end{aligned}$$

The last inequality holds since $(16c^4 - 4c^2 - 1)\tilde{x}^2 + (6c^2 - 8c^4)\tilde{x} - 4c^4 < 0$, and $8c^2\tilde{x}(\tilde{x} + 2c^2) < 0$ for $\tilde{x} \in [\frac{-1}{2c^2}, 0)$. Hence, $\overline{\tilde{p}} < 1 - 2c^2$. For $\underline{\tilde{p}}$, we have

$$\begin{aligned} & \underline{\tilde{p}} > 1 - 2c^2, \text{ (after simplifying like before)} \\ & \iff \\ & \sqrt{d} > (16c^4 - 4c^2 - 1)\tilde{x}^2 + (6c^2 - 8c^4)\tilde{x} - 4c^4. \end{aligned}$$

The last inequality holds since the right hand side is negative, and the left hand side is positive for $\tilde{x} \in [\frac{-1}{2c^2}, 0)$. Hence, $\underline{\tilde{p}} > 1 - 2c^2$.

The coefficient of $\tilde{p}^2$ in the polynomial $P(\tilde{p})$ is positive for $\tilde{x} \in [-\frac{1}{2c^2}, 0)$ with $c \geq 1$, and hence, the larger of the two roots $\underline{\tilde{p}}$ and $\overline{\tilde{p}}$ is a minimum. Therefore, for $1 - 2c^2 < \tilde{p} < \underline{\tilde{p}}$, increasing $\tilde{p}$ decreases R_0, whereas for $\tilde{p} > \underline{\tilde{p}}$, the opposite holds, i.e. increasing $\tilde{p}$ increases R_0. $\square$

Theorem 3.7 (Optimized Constant Transmission Conditions). *The best performance of the optimized waveform relaxation algorithm (3.61) with constant transmission conditions is obtained for* $\alpha = \alpha^*$, *where*

$$\alpha^* = 2c^2 - 1 + \tilde{p}^*, \tag{3.83}$$

and $\tilde{p}^*$, *the solution of the min-max problem (3.71), is given by*

$$\tilde{p}^* = \frac{-1 + \sqrt{1 + 16c^8 - 12c^4}}{2c^2}, \tag{3.84}$$

and $c = \sqrt{\frac{-b}{2a}} \geq 1$. *Furthermore,* $\alpha^* > \frac{a|b|}{b^2 - a^2} - 1 = \underline{\alpha}$.

Proof. By Lemma 3.16, the optimal $\tilde{p}^*$ must lie in the interval $[\frac{-1}{2c^2}, \infty)$, since with $\tilde{p}$ outside this interval, R_0 can be uniformly decreased for all $\frac{-1}{2c^2} \leq \tilde{x} < 0$ by moving $\tilde{p}$ towards this interval. The left endpoint of this interval is $\underline{\tilde{p}}(\tilde{x} = \frac{-1}{2c^2})$, and the right endpoint is $\underline{\tilde{p}}(\tilde{x} = 0^-) := \lim_{\tilde{x} \to 0^-} (\underline{\tilde{p}}(\tilde{x}))$. Now, by Lemma 3.15, the maximum of the min-max problem can only be attained on the boundaries, at $\tilde{x} = \frac{-1}{2c^2}$ and at $\tilde{x} = 0^-$, since R_0 has no interior maxima. By the notation $\tilde{x} = 0^-$ we mean that $\tilde{x}$ approaches 0 from the left, since we have $\tilde{x} \in [\frac{-1}{2c^2}, 0)$, open from the right. Now, for $\tilde{p} = \underline{\tilde{p}}(\tilde{x} = \frac{-1}{2c^2}) = \frac{-1}{2c^2}$, we have $R_0(\frac{-1}{2c^2}, c, \frac{-1}{2c^2}) = 0$, and so increasing $\tilde{p}$ increases $R_0(\frac{-1}{2c^2}, c, \tilde{p})$ monotonically, by Lemma 3.16. On the other hand, for $\tilde{p} = \frac{-1}{2c^2}$, we have $R_0(0^-, c, \frac{-1}{2c^2}) = \frac{4c^2}{1+16c^8-8c^4} > 0$, $c \geq 1$, and increasing $\tilde{p}$ decreases $R_0(0^-, c, \tilde{p}) = \frac{1}{(2c^2+\tilde{p})^2}$ to $\lim_{\tilde{p} \to \infty} (\frac{1}{(2c^2+\tilde{p})^2}) = 0$. Therefore, by increasing $\tilde{p}$ we reach $R_0(\frac{-1}{2c^2}, c, \tilde{p}) = R_0(0^-, c, \tilde{p})$. Solving the equation for $\tilde{p}$ gives the solution in (3.84), and three other solutions, $\tilde{p} = 1 - 2c^2$, $-1 - 2c^2$, $\frac{-1-\sqrt{1+16c^8-12c^4}}{2c^2}$. Those three solutions can be discarded, since $\tilde{p} > 1 - 2c^2$. Therefore, we have $\alpha^* = 2c^2 - 1 + \frac{p^*}{a} = 2c^2 - 1 + \tilde{p}^*$, $c = \sqrt{\frac{-b}{2a}} \geq 1$, where $\tilde{p}^*$ is given in (3.84), and $\alpha^* > \frac{a|b|}{b^2-a^2} - 1 := \underline{\alpha}$. □

In Figure 3.15, we show the modulus of the convergence factor for the optimized WR algorithm with the optimized constant approximation, $\rho_{opt0}(\omega, \alpha^*)$, and with the

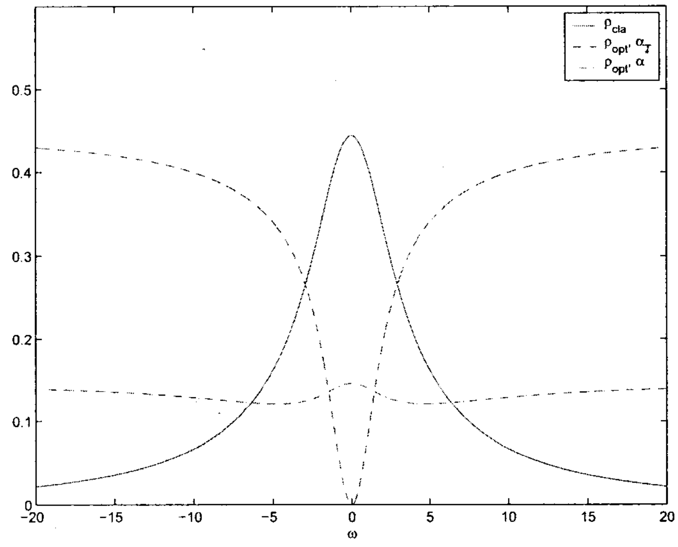

Figure 3.15: Classical convergence factor $|\rho_{cla}(\omega)|$, versus $|\rho_{opt0}(\omega, \alpha^*)|$ and $|\rho_{opt0}(\omega, \alpha_T)|$.

Taylor approximation, $\rho_{opt0}(\omega, \alpha_T)$, as well as the modulus of the classical convergence factor ρ_{cla}, for $c = 1$ from the numerical experiment in Subsection 3.3.5. One can see the remarkable improvement in magnitude and uniformity for the convergence factor with the optimized constant approximation over the classical one and the one with the Taylor approximation.

3.3.4 An Optimized WR Algorithm with First Order Transmission Conditions

We now approximate the symbols α and $\beta = -\alpha$ from (3.63) corresponding to the optimal transmission conditions by a first order polynomial in s,

$$\alpha = \alpha_0 + \alpha_1 s, \tag{3.85}$$

where we have two free parameters α_0 and α_1 that we can choose to obtain a new optimized waveform relaxation algorithm. We assume that $\alpha_1 \neq 0$, since otherwise we will get the constant approximation case. The Laplace transform of the transmission conditions in (3.60), with $\beta = -\alpha$, using the first order expansion (3.85) for α, implies

$$\begin{aligned}(\hat{u}_3^{k+1} - \hat{u}_2^{k+1}) + \alpha_0\hat{u}_3^{k+1} + \alpha_1 s\hat{u}_3^{k+1} &= (\hat{w}_1^k - \hat{w}_0^k) + \alpha_0\hat{w}_1^k + \alpha_1 s\hat{w}_1^k,\\ (\hat{w}_1^{k+1} - \hat{w}_0^{k+1}) - \alpha_0\hat{w}_0^{k+1} - \alpha_1 s\hat{w}_0^{k+1} &= (\hat{u}_3^k - \hat{u}_2^k) - \alpha_0\hat{u}_2^k - \alpha_1 s\hat{u}_2^k.\end{aligned} \tag{3.86}$$

A multiplication by s in the frequency domain corresponds to a time derivative. Now, by substituting

$$\begin{aligned}\dot{w}_1^k &= b_3 w_1^k + c_3 w_2^k + a_2 w_0^k + f_3,\\ \dot{u}_2^k &= a_1 u_1^k + b_2 u_2^k + c_2 u_3^k + f_2,\end{aligned}$$

from (3.2) for $j = 2$, into (3.86), assuming $\alpha_1 \neq 0$, we obtain

$$\begin{aligned}\dot{u}_3^{k+1} &= \tfrac{1}{\alpha_1}u_2^{k+1} - \tfrac{(1+\alpha_0)}{\alpha_1}u_3^{k+1} + \tfrac{(1+\alpha_0+\alpha_1 b_3)}{\alpha_1}w_1^k + \tfrac{(\alpha_1 a_2 - 1)}{\alpha_1}w_0^k + c_3 w_2^k + f_3,\\ \dot{w}_0^{k+1} &= \tfrac{1}{\alpha_1}w_1^{k+1} - \tfrac{(1+\alpha_0)}{\alpha_1}w_0^{k+1} + \tfrac{(1+\alpha_0+\alpha_1 b_2)}{\alpha_1}u_2^k + \tfrac{(\alpha_1 c_2 - 1)}{\alpha_1}u_3^k + a_1 u_1^k + f_2.\end{aligned} \tag{3.87}$$

These ordinary differential equations found from the transmission conditions imply the following two decoupled subsystems,

$$\begin{aligned}\begin{pmatrix}\dot{u}_1^{k+1}\\ \dot{u}_2^{k+1}\\ \dot{u}_3^{k+1}\end{pmatrix} &= \begin{bmatrix} b_1 & c_1 & \\ a_1 & b_2 & c_2\\ & \frac{1}{\alpha_1} & \frac{-(\alpha_0+1)}{\alpha_1}\end{bmatrix}\begin{pmatrix}u_1^{k+1}\\ u_2^{k+1}\\ u_3^{k+1}\end{pmatrix} + \begin{pmatrix}f_1\\ f_2\\ f_3\end{pmatrix}\\ &\quad + \begin{pmatrix}0\\ 0\\ \frac{(\alpha_1 a_2-1)}{\alpha_1}w_0^k + \frac{(1+\alpha_0+\alpha_1 b_3)}{\alpha_1}w_1^k + c_3 w_2^k\end{pmatrix},\end{aligned} \tag{3.88}$$

and

$$\begin{aligned}\begin{pmatrix}\dot{w}_0^{k+1}\\ \dot{w}_1^{k+1}\\ \dot{w}_2^{k+1}\end{pmatrix} &= \begin{bmatrix} \frac{-(\alpha_0+1)}{\alpha_1} & \frac{1}{\alpha_1} & \\ a_2 & b_3 & c_3\\ & a_3 & b_4\end{bmatrix}\begin{pmatrix}w_0^{k+1}\\ w_1^{k+1}\\ w_2^{k+1}\end{pmatrix} + \begin{pmatrix}f_2\\ f_3\\ f_4\end{pmatrix}\\ &\quad + \begin{pmatrix}a_1 u_1^k + \frac{(1+\alpha_0+\alpha_1 b_2)}{\alpha_1}u_2^k + \frac{(\alpha_1 c_2-1)}{\alpha_1}u_3^k\\ 0\\ 0\end{pmatrix},\end{aligned} \tag{3.89}$$

with the initial conditions $\boldsymbol{u}^{k+1}(0) = (v_1^0, v_2^0, v_3^0)^T$ and $\boldsymbol{w}^{k+1}(0) = (v_2^0, v_3^0, v_4^0)^T$, where now the transmission conditions are already implemented in the algorithm. To start the WR iteration, some initial waveforms $\boldsymbol{u}^0(t)$ and $\boldsymbol{w}^0(t)$ are used. The subsystems are now bigger than those we obtained using the constant approximation in Subsection 3.3.3. However, the first order approximation leads to better convergence as we will see.

The Laplace transform of (3.88) and (3.89) yields in the $s \in \mathbb{C}$ domain

$$
\begin{aligned}
s\hat{\boldsymbol{u}}^{k+1} &= \begin{bmatrix} b_1 & c_1 & \\ a_1 & b_2 & c_2 \\ & \frac{1}{\alpha_1} & \frac{-(\alpha_0+1)}{\alpha_1} \end{bmatrix} \hat{\boldsymbol{u}}^{k+1} + \begin{pmatrix} 0 \\ 0 \\ \frac{(\alpha_1 a_2 - 1)}{\alpha_1}\hat{w}_0^k + \frac{(1+\alpha_0+\alpha_1 b_3)}{\alpha_1}\hat{w}_1^k + c_3\hat{w}_2^k \end{pmatrix}, \\
s\hat{\boldsymbol{w}}^{k+1} &= \begin{bmatrix} \frac{-(\alpha_0+1)}{\alpha_1} & \frac{1}{\alpha_1} & \\ a_2 & b_3 & c_3 \\ & a_3 & b_4 \end{bmatrix} \hat{\boldsymbol{w}}^{k+1} + \begin{pmatrix} a_1\hat{u}_1^k + \frac{(1+\alpha_0+\alpha_1 b_2)}{\alpha_1}\hat{u}_2^k + \frac{(\alpha_1 c_2 - 1)}{\alpha_1}\hat{u}_3^k \\ 0 \\ 0 \end{pmatrix}.
\end{aligned}
\tag{3.90}
$$

A straightforward computation for the first subsystem in (3.90) implies

$$
\hat{u}_2^{k+1} = \frac{c_2(s-b_1)}{(s-b_1)(s-b_2) - a_1 c_1}\hat{u}_3^{k+1}. \tag{3.91}
$$

From the first equation in (3.86) we obtain

$$
\hat{u}_3^{k+1} = \frac{1}{(\alpha_0 + \alpha_1 s + 1)}(\hat{u}_2^{k+1} + \hat{w}_1^k - \hat{w}_0^k + (\alpha_0 + \alpha_1 s)\hat{w}_1^k). \tag{3.92}
$$

Substituting (3.92) into (3.91), we get after some algebra,

$$
\hat{u}_2^{k+1} = F_1(\hat{w}_1^k - \hat{w}_0^k + (\alpha_0 + \alpha_1 s)\hat{w}_1^k), \tag{3.93}
$$

where F_1 is given by

$$
F_1 = \frac{c_2(s-b_1)}{(\alpha_0 + \alpha_1 s + 1)((s-b_1)(s-b_2) - a_1 c_1) - c_2(s-b_1)}.
$$

Similarly, from the second subsystem, we obtain

$$
\hat{w}_1^{k+1} = F_2(\hat{u}_3^k - \hat{u}_2^k - (\alpha_0 + \alpha_1 s)\hat{u}_2^k), \tag{3.94}
$$

where F_2 is given by

$$F_2 = \frac{a_2(s-b_4)}{-(\alpha_0+\alpha_1 s+1)((s-b_3)(s-b_4)-a_3c_3)+a_2(s-b_4)}.$$

As before, we need to find a relation between $\hat{u}_2^{k+1}$ and $\hat{w}_1^k$, and similarly a relation between $\hat{w}_1^{k+1}$ and $\hat{u}_2^k$. Using the second transmission condition in (3.86), we find, together with (3.94),

$$\hat{w}_0^{k+1} = \left(\frac{1}{\alpha_0+\alpha_1 s+1} - \frac{1}{(\alpha_0+\alpha_1 s+1)F_2}\right)\hat{w}_1^{k+1},$$

and using this result at step k in (3.93), we find for the first sub-circuit

$$\hat{u}_2^{k+1} = F_1\left(\alpha_0+\alpha_1 s+1 - \frac{1}{\alpha_0+\alpha_1 s+1} + \frac{1}{(\alpha_0+\alpha_1 s+1)F_2}\right)\hat{w}_1^k. \tag{3.95}$$

With a similar manipulation for the second subsystem, we find

$$\hat{w}_1^{k+1} = F_2\left(\frac{1}{(\alpha_0+\alpha_1 s+1)F_1} + \frac{1}{\alpha_0+\alpha_1 s+1} - (\alpha_0+\alpha_1 s+1)\right)\hat{u}_2^k. \tag{3.96}$$

Finally, by inserting (3.96) at iteration k into (3.95), we get a relation over two iteration steps of the optimized WR algorithm,

$$\hat{u}_2^{k+1} = \rho_{opt1}(s,\boldsymbol{a},\boldsymbol{c},\boldsymbol{b},\alpha_0,\alpha_1)\hat{u}_2^{k-1},$$

where the convergence factor of the new algorithm is given by

$$\begin{aligned}\rho_{opt1}(s,\boldsymbol{a},\boldsymbol{b},\boldsymbol{c},\alpha_0,\alpha_1) &= \frac{c_2(s-b_1)(\alpha_0+\alpha_1 s+1)-((s-b_1)(s-b_2)-a_1c_1)}{((s-b_3)(s-b_4)-a_3c_3)(\alpha_0+\alpha_1 s+1)-a_2(s-b_4)}\\ &\quad\cdot\frac{a_2(s-b_4)(\alpha_0+\alpha_1 s+1)-((s-b_3)(s-b_4)-a_3c_3)}{((s-b_1)(s-b_2)-a_1c_1)(\alpha_0+\alpha_1+1)-c_2(s-b_1)}.\end{aligned}$$

Using the simplifying assumptions as in Subsection 3.3.3, i.e. $c_i = a_i = a_1 = a$, for $i = 1,2,3$, and $b_i = b_1 = b$, for $i = 1,2,3,4$, we obtain

$$\rho_{opt1}(s,a,b,\alpha_0,\alpha_1) = \left(\frac{a(s-b)(\alpha_0+\alpha_1 s+1)-((s-b)^2-a^2)}{((s-b)^2-a^2)(\alpha_0+\alpha_1 s+1)-a(s-b)}\right)^2. \tag{3.97}$$

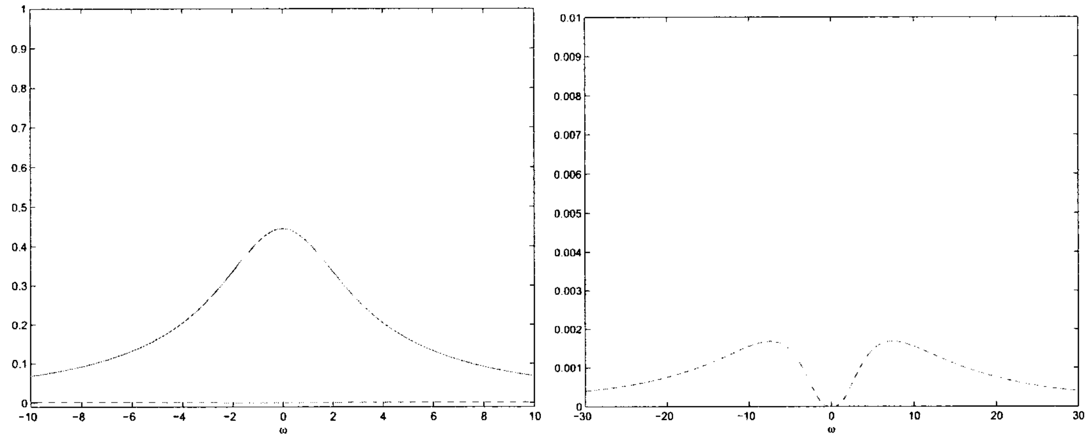

Figure 3.16: Left: optimized convergence factor with the Taylor approximation $|\rho_{opt1}(\omega, \alpha_{0T}, \alpha_{1T})|$ (dashed line) versus classical convergence factor $|\rho_{cla}(\omega)|$ (solid line). Right: zoom of $|\rho_{opt1}(\omega, \alpha_{0T}, \alpha_{1T})|$.

The same result also holds for the second sub-circuit and by induction we find, as before, $\hat{u}_2^{2k} = (\rho_{opt1})^k \hat{u}_2^0$ and $\hat{w}_1^{2k} = (\rho_{opt1})^k \hat{w}_1^0$. The convergence factor ρ_{opt1} in (3.97) can be expressed in terms of λ,

$$\rho_{opt1}(s, a, b, \alpha_0, \alpha_1) = \left(\frac{(\alpha_0 + \alpha_1 s) + 1 - \lambda}{((\alpha_0 + \alpha_1 s) + 1)\lambda - 1} \right)^2, \tag{3.98}$$

where $\lambda = \frac{(s-b)^2 - a^2}{a(s-b)} = \frac{-b}{a} + \frac{1}{a} \frac{s(s-b) - a^2}{s-b}$.

The simplest first order approximation of the optimal α is the low frequency approximation by using a Taylor expansion about $s = 0$, which is given by

$$\alpha_{0T} = \frac{-b}{a} - 1 + \frac{a}{b} > 0, \ \alpha_{1T} = \frac{b^2 + a^2}{ab^2} > 0.$$

In Figure 3.16 on the left, we compare the classical convergence factor with the optimized convergence factor with the Taylor approximation, and we observe the better convergence of the optimized convergence factor with the Taylor approximation over the classical one.

Similar to the optimized WR algorithm with constant transmission conditions in

Subsection 3.3.3, we use an optimization process to get the best performance of the new WR algorithm. We again want $|\rho_{opt1}| \ll 1$.

Lemma 3.17. *If the circuit parameters satisfy the inequalities*

$$\begin{aligned} a > 0,\ b < 0,\ |b| \geq 2a, \\ \alpha_0 \geq 0,\ \alpha_1 > 0, \end{aligned} \tag{3.99}$$

then the convergence factor ρ_{opt1} in (3.98) is an analytic function in the right half of the complex plane, $s = \eta + i\omega$, $\eta > 0$.

Proof. By Theorem 1.4, we need to show that the denominator does not have zeros in the right half of the complex plane. We show this by contradiction: Assume there is a zero, $\lambda(1 + \alpha_0 + \alpha_1 s) - 1 = 0$, then we have $\lambda = \frac{1}{1+\alpha_0+\alpha_1 s}$, which implies $|\lambda| = \frac{1}{(1+\alpha_0+\alpha_1\eta)^2+\omega^2\alpha_1^2} < 1$, with the condition (3.99) on α_0 and α_1. On the other hand, we have, $|\lambda| = \frac{|(s-b)^2-a^2|}{|a(s-b)|}$, and by Lemma 3.7 the modulus $|\lambda|$ is bigger than one in the right half of the complex plane, and thus we have a contradiction. Hence, poles are excluded and the denominator has no zeros in the right half of the complex plane. □

Since ρ_{opt1} is analytic, we can apply the maximum principle, Theorem 1.5, and therefore, the maximum of $|\rho_{opt1}|$ is attained on the boundary. Now, since for $s = re^{i\theta}$, $-\frac{\pi}{2} < \theta < \frac{\pi}{2}$, the limit of ρ_{opt1} is zero as r goes to infinity, i.e. the same limit in all directions, the maximum of $|\rho_{opt1}|$ is attained at $\eta = 0$. As in Subsection 3.3.3, the modulus of ρ_{opt1} for $s = i\omega$ depends on ω^2 only, and it suffices to optimize for nonnegative frequencies, $\omega \geq 0$. Therefore, we need to solve the min-max problem

$$\min_{\alpha_0\geq 0, \alpha_1 > 0}\left(\max_{\omega\geq 0}|\rho_{opt1}(i\omega, a, b, \alpha_0, \alpha_1)|\right). \tag{3.100}$$

The optimal value of α is given by $\alpha = \lambda - 1$, and a first order approximation is

$$\alpha = \alpha_0 + \alpha_1 s = \frac{-b}{a} - 1 + \frac{p}{a} + \frac{q}{a}s,$$

where $p,\ q$ are new parameters. Considering this first order approximation, and using in addition the change of variables (3.66) for the convergence factor, the modulus of the convergence factor ρ_{opt1} in (3.98), after factorizing a^7 from the denominator and numerator to eliminate one parameter, is given by

$$|\rho_{opt1}(x,a,b,p,q)| := \frac{Q_1(x,a,b,p,q)}{Q_2(x,a,b,p,q)},$$

where

$$\begin{aligned}
Q_1 := &\left(2\tfrac{b}{a}\tfrac{p}{a} - 2q\left(\tfrac{b}{a}\right)^2 + 2\left(\tfrac{b}{a}\right)^2 - 1\right)\left(\tfrac{x}{a}\right)^3 \\
&+ \left(-\tfrac{b}{a}\left(\tfrac{p}{a}\right)^2 - 2q\left(\tfrac{b}{a}\right)^3 + 2q\tfrac{b}{a} + \left(\tfrac{b}{a}\right)^3 + \left(\tfrac{b}{a}\right)^3 q^2 - 2\tfrac{b}{a}\right)\left(\tfrac{x}{a}\right)^2 \\
&+ \left(2q\left(\tfrac{b}{a}\right)^2 - \left(\tfrac{b}{a}\right)^2 q^2 - \left(\tfrac{b}{a}\right)^2\right)\tfrac{x}{a}, \\
Q_2 := &\left(\left(\tfrac{b}{a}\right)^2 q^2 + 4\tfrac{b}{a}\tfrac{p}{a} + 4\left(\tfrac{b}{a}\right)^2\left(\tfrac{p}{a}\right)^2 + 2q\left(\tfrac{b}{a}\right)^2 - 4\left(\tfrac{b}{a}\right)^4 q^2 - 8\left(\tfrac{b}{a}\right)^3\tfrac{p}{a}\right. \\
&\left. - \left(\tfrac{p}{a}\right)^2 - 3\left(\tfrac{b}{a}\right)^2 + 4\left(\tfrac{b}{a}\right)^4\right)\left(\tfrac{x}{a}\right)^3 \\
&+ \left(-\tfrac{b}{a}q^2 - 2q\tfrac{b}{a} + 2\left(\tfrac{b}{a}\right)^2\tfrac{p}{a} - \tfrac{b}{a} - 2\left(\tfrac{p}{a}\right)^2\tfrac{b}{a} + 2q\left(\tfrac{b}{a}\right)^3 + 6\left(\tfrac{b}{a}\right)^3 q^2\right)\left(\tfrac{x}{a}\right)^2 \\
&+ \left(-\left(\tfrac{b}{a}\right)^4 - 2q\left(\tfrac{b}{a}\right)^2 + \left(\tfrac{b}{a}\right)^4 q^2 - 2\left(\tfrac{b}{a}\right)^2 q^2 - \left(\tfrac{p}{a}\right)^2\left(\tfrac{b}{a}\right)^2 + 2\left(\tfrac{b}{a}\right)^3\tfrac{p}{a}\right)\tfrac{x}{a} \\
&- \left(\tfrac{b}{a}\right)^3 q^2.
\end{aligned}$$

Letting $\tilde{p} = \frac{p}{a}$, $\frac{b}{a} = -2c^2$, where $c \geq 1$, and $\tilde{x} = \frac{x}{a}$, as for the constant approximation in Subsection 3.3.3, the modulus of the convergence factor ρ_{opt1} in (3.98) becomes

$$R_1(\tilde{x},c,\tilde{p},q) := \frac{P_1(\tilde{x},c,\tilde{p},q)}{P_2(\tilde{x},c,\tilde{p},q)}, \tag{3.101}$$

where

$$\begin{aligned}
P_1 := &-(((8qc^4 - 8c^4 + 1 + 4c^2\tilde{p})\tilde{x}^2 + (-16qc^6 - 2c^2\tilde{p}^2 - 4c^2 + 4qc^2 + 8c^6 + 8c^6q^2)\tilde{x} \\
&+4c^4 - 8qc^4 + 4c^4q^2)\tilde{x}), \\
P_2 := &(4c^4q^2 - 8c^2\tilde{p} + 16c^4\tilde{p}^2 + 8qc^4 - 64c^8q^2 + 64c^6\tilde{p} - \tilde{p}^2 - 12c^4 + 64c^8)\tilde{x}^3 \\
&+(2c^2q^2 + 4qc^2 + 8c^4\tilde{p} + 2c^2 + 4c^2\tilde{p}^2 - 16qc^6 - 48c^6q^2)\tilde{x}^2 \\
&+(-16c^8 - 8qc^4 + 16c^8q^2 - 8c^4q^2 - 4c^4\tilde{p}^2 - 16c^6\tilde{p})\tilde{x} + 8c^6q^2.
\end{aligned}$$

The optimized parameters are given by $\alpha_0 = \frac{-b}{a} - 1 + \frac{p}{a} = 2c^2 - 1 + \tilde{p}$, and $\alpha_1 = \frac{q}{a}$, and since for analyticity in the right half of the complex plane we need $\alpha_0 \geq 0$, and $\alpha_1 > 0$, we require $\tilde{p} \geq 1 - 2c^2$, and $q > 0$. The min-max problem (3.100) then becomes

$$\min_{\tilde{p} \geq 1-2c^2, q>0} \left(\max_{\frac{-1}{2c^2} \leq \tilde{x} < 0} R_1(\tilde{x}, c, p, q) \right) = \max_{\frac{-1}{2c^2} \leq \tilde{x} < 0} R_1(\tilde{x}, c, p^*, q^*), \; c \geq 1. \tag{3.102}$$

Since it is hard to solve the optimization problem (3.102) we use asymptotics, and since for RC type circuits or diffusion type equations $|b| = 2a$, which corresponds to c going to 1, often holds, we take $c = \sqrt{1+\epsilon}$, and for ϵ small we have the following result.

Theorem 3.8 (Optimized First Order Transmission Conditions). *If in the optimized WR algorithm with first order transmission conditions (3.88), (3.89) the free parameters are chosen to be $\alpha_0 = \alpha_0^* = 2c^2 - 1 + \tilde{p}^*$, and $\alpha_1 = \alpha_1^* = \frac{q^*}{a}$, where $c = \sqrt{\frac{-b}{2a}} = \sqrt{1+\epsilon} \geq 1$ and a, b are the entries of the matrices in (3.88), (3.89), and $\tilde{p}^*$ and q^* are defined by the system of equations*

$$R_1(\tilde{x}_0, c, \tilde{p}^*, q^*) = R_1(\bar{\tilde{x}}, c, \tilde{p}^*, q^*), \qquad \frac{\partial}{\partial q} R_1(\bar{\tilde{x}}, c, \tilde{p}^*, q^*) = 0, \tag{3.103}$$

where $\tilde{x}_0 = \frac{-1}{2c^2}$, $R_1(\tilde{x}, c, \tilde{p}, q)$ is given in (3.101), and $\bar{\tilde{x}}$ is given by the root of the polynomial $P(\tilde{x})$ given in (A.1) in Appendix A, giving the maximum of R_1, then for ϵ small, $R_1(\tilde{x}, c, \tilde{p}^*, q^*) \leq R_1(\tilde{x}_0, c, \tilde{p}^*, q^*) := \bar{R}_{O1}$ for all $\tilde{x} \in [\tilde{x}_0, 0)$. Moreover, we have the asymptotic result

$$\tilde{p}^* \approx -0.4655, \; q^* \approx 1.1378, \; \bar{R}_{O1} \approx 0.0007.$$

Proof. A partial derivative of R_1 with respect to $\tilde{x}$ shows that the roots of the polynomial $P(\tilde{x})$ given in (A.1) determine the extrema of R_1. First, to see that there is indeed a solution as stated in (3.103) for ϵ small, we substitute $c = \sqrt{1+\epsilon}$, and we use the ansatz $\tilde{p} = C_p \epsilon^{\gamma_1}$, $q = C_q \epsilon^{\gamma_2}$, and $\bar{\tilde{x}} = C_1 \epsilon^{\delta}$, and determine the leading asymptotic terms as ϵ goes to zero of the root of the polynomial $P(\tilde{x})$, and the equations (3.103). Note that the second equation in (3.103) holds if and only if $Q(\bar{\tilde{x}}, c, \tilde{p}^*, q^*) = 0$ holds, where the polynomial $Q(\tilde{x}, c, \tilde{p}, q)$ is given in (A.2) in Appendix A. The leading asymptotic terms as ϵ goes to zero are

$$\begin{aligned} P(\bar{\tilde{x}}) &= P_{Expan}, \\ Q(\bar{\tilde{x}}) &= Q_{Expan}, \\ R_1(\tilde{x}_0) &= R_{1\tilde{x}_0 Expan}, \\ R_1(\bar{\tilde{x}}) &= R_{1\bar{\tilde{x}} Expan}, \end{aligned} \tag{3.104}$$

which are given in Appendix A. Equating the exponents in these three equations leads to $\gamma_1 = \gamma_2 = \delta = 0$, which implies the same equations as for the case $c = 1$. Since the constants need to match as well, we obtain $C_p = -0.4655$, $C_q = 1.1378$, and $C_1 = -0.2617$, by solving the resulting equations. Since $c = \sqrt{\frac{-b}{2a}} = \sqrt{1+\epsilon}$, we have $\epsilon = \frac{-b}{2a} - 1$, and using these results we get

$$\begin{aligned} \tilde{p}^* &:= C_p(\tfrac{-b}{2a} - 1)^{\gamma_1} = C_p = -0.4655, \\ q^* &:= C_q(\tfrac{-b}{2a} - 1)^{\gamma_2} = C_q = 1.1378. \end{aligned} \tag{3.105}$$

Now, to see that there is indeed only one interior maximum, which we denote by $\bar{\tilde{x}}$, we take $c = \sqrt{1+\epsilon}$, and we substitute $\tilde{p}^*$, q^* from (3.105) into $P(\tilde{x})$. The leading terms of the polynomial $P(\tilde{x})$ as ϵ goes to zero are

$$P(\tilde{x}) = 7.1756762\tilde{x}^4 - 2.0577882\tilde{x}^3 - 10.88760728\tilde{x}^2 - 5.58470978\tilde{x} - 0.78638698 + O(\epsilon),$$

which is a polynomial of degree 4 in $\tilde{x}$ plus higher order terms. As ϵ goes to 0, finding the roots of this 4^{th} degree polynomial implies the four roots -0.5737, -0.4610, -0.2617, and 1.5832. Only two roots lie in the interval $[-\frac{1}{2}, 0)$, which are one maximum given by $\bar{\tilde{x}} = -0.2617$ and one minimum. Therefore, as ϵ goes to zero, $R_1(\tilde{x}, \tilde{p}^*, q^*)$ has only one interior maximum at $\bar{\tilde{x}}$, where $\tilde{p}^*$ and q^* are given in (3.105). Since R_1 has only one interior maximum for $\tilde{x} \in [\frac{-1}{2c^2}, 0)$, $c = \sqrt{1+\epsilon}$, and ϵ small, and no other interior maximum as we have shown above, and since in addition, $R_1 \longrightarrow 0$ as $\tilde{x} \longrightarrow 0$, the maximum of R_1 can be attained either on the boundary at $\tilde{x} = \tilde{x}_0$ or at the maximum $\bar{\tilde{x}}$. Balancing the value of R_1 at the two locations as stated in (3.103) guarantees then that R_1 is uniformly bounded by R_1 at $\tilde{x}_0$ for ϵ small. Now, expanding $\bar{R}_{O1}$ for ϵ small, we get

$$\bar{R}_{O1} \approx \frac{1 + 4C_p + 4C_p^2}{24C_p + 9C_p^2 + 16},$$

and substituting from (3.105) we obtain the asymptotic result

$$\bar{R}_{O1} \approx 0.0007.$$

Finally, α_0^* and α_1^* are given by

$$\alpha_0^* = 2c^2 - 1 + \frac{p^*}{a} = 2c^2 - 1 + \tilde{p}^*, \; \alpha_1^* = \frac{q^*}{a}, \; c = \sqrt{\frac{-b}{2a}} \geq 1,$$

and $\tilde{p}^*$, q^* are given in (3.105). □

In Figure 3.17 on the left, we observe the better convergence we get by using the first order approximation over the classical convergence and the convergence using the optimized constant approximation. We show in Figure 3.17 on the right the result of the optimization with respect to α_0 and α_1 using the circuit elements from the numerical experiment in Subsection 3.3.5. The solution of the min-max problem occurs when the convergence factor at $\omega = 0$ and at $\omega = \overline{\omega}$ are balanced, where $\overline{\omega} > 0$ is the interior maximum of the modulus of the convergence factor. We also show in Figure 3.17 on the right the better convergence we obtain using the optimized values α_0^* and α_1^* over the one using the low frequency first order approximation α_{0T} and α_{1T}.

3.3.5 Numerical Experiments

We give now a numerical example to illustrate the improvements in the convergence of the optimized WR algorithm over the classical one as we did for the extra small

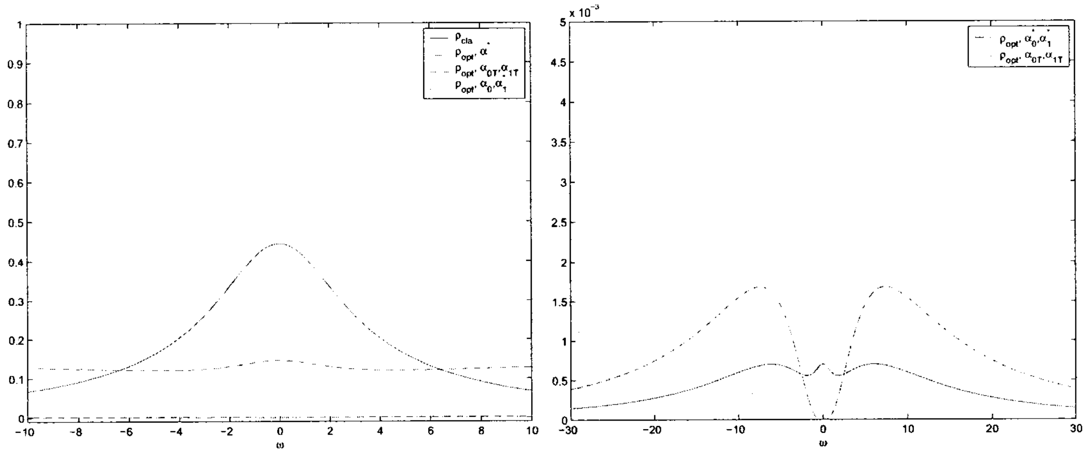

Figure 3.17: On the left: classical convergence factor $|\rho_{cla}(\omega)|$ versus $|\rho_{opt0}(\omega, \alpha^*)|$, $|\rho_{opt1}(\omega, \alpha_{0T}, \alpha_{1T})|$, and $|\rho_{opt1}(\omega, \alpha_0^*, \alpha_1^*)|$. On the right: convergence factor with the optimized first order approximation $|\rho_{opt1}(\omega, \alpha_0^*, \alpha_1^*)|$ versus $|\rho_{opt1}(\omega, \alpha_{0T}, \alpha_{1T})|$.

circuit case. We use again typical values of the RC circuit parameters,

$$R_s = R_1 = R_2 = R_3 = \frac{1}{2} \text{ Ohms}, \; C_1 = C_2 = C_3 = C_4 = \frac{63}{100} \text{ pF},$$

for the circuit in Figure 1.1. We choose also the backward Euler method to integrate in time, and the transient analysis time is $t \in [0, 10]$, with a time step of $\Delta t = 1/10$. We start with random initial waveforms and use an input step function with an amplitude of $I_s = 1$ and a rise time of 1 time unit. In Figure 3.18 we show the error as a function of the iterations. One can see the remarkable improvement of the optimized WR algorithm over the classical one. Furthermore, the optimized WR algorithm with first order transmission conditions converges faster than the one with constant transmission conditions. We use $b_4 = b_1$, which is a simplifying assumption we used to compute the optimized constant and first order approximations with $\beta = -\alpha$, and show the result on the left hand side of Figure 3.18. We use the optimized value $\alpha^* = 1.618$ as well as the Taylor approximation $\alpha_T = 0.5$ in the optimized WR algorithm with constant transmission conditions. The optimized values $\alpha_0^* = 0.5345$,

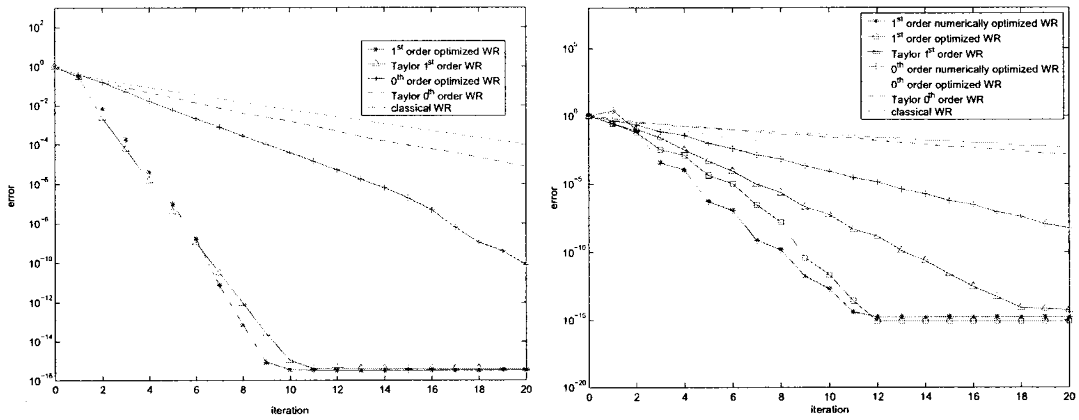

Figure 3.18: Convergence behavior of classical versus optimized WR algorithms for the small circuit.

$\alpha_1^* = 0.3585$, and the Taylor approximations $\alpha_{0T} = 0.5$, $\alpha_{1T} = 0.3937$ are also used in the optimized WR algorithm with first order transmission conditions. On the right hand side of Figure 3.18, we use $b_4 = \frac{b_1}{2}$, and we find the Taylor approximation $\alpha_T = 0$ and $\beta = -0.5$, and the numerically optimized constant approximation $\alpha^* = 2.3002$ and $\beta^* = -0.6953$, which we use in the constant optimized WR algorithm. The optimized constant approximation $\alpha^* = 1.618$ with $\beta^* = -\alpha^*$ computed using the simplifying assumptions is also used in the constant optimized WR algorithm. We also use $b_4 = \frac{b_1}{2}$ to compute the first order Taylor approximation $\alpha_{0T} = 0$, $\alpha_{1T} = 0.63$, and the numerically optimized first order approximation $\alpha_0^* = 0.5031$, $\alpha_1^* = 0.390$, and we choose $\beta^* = -\alpha^*$. The optimized first order approximation used here for this case is again $\alpha_0^* = 0.5345$, $\alpha_1^* = 0.3585$ with $\beta^* = -\alpha^*$.

3.4 An Infinitely Large RC type Circuit

We analyze in this section an infinitely large RC circuit and its infinite size system of equations, as is indicated in Figure 3.19. The equations for the infinitely large circuit

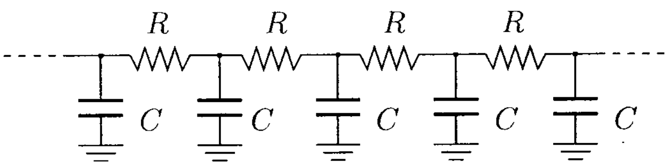

Figure 3.19: An infinitely large RC circuit chain.

are

$$\dot{\boldsymbol{x}} = \begin{bmatrix} \ddots & \ddots & \ddots & & \\ & a & b & c & \\ & & a & b & c \\ & & & \ddots & \ddots & \ddots \end{bmatrix} \boldsymbol{x} + \boldsymbol{f}. \tag{3.106}$$

The entries in the tridiagonal matrix are given by

$$a = \frac{1}{RC}; \quad b = -\left(\frac{2}{R}\right)\frac{1}{C}; \quad c = \frac{1}{RC} = a,$$

where the circuit elements R and C are assumed to be strictly positive and constant. The source term on the right hand side is given by the vector of functions $\boldsymbol{f}(t) = (\ldots, f_{-1}(t), f_0(t), f_1(t), \ldots)^T$, and we need an initial condition $\boldsymbol{x}(0) = (\ldots, v^0_{-1}, v^0_0, v^0_1, \ldots)^T$. Since the circuit is infinitely large, we have to assume that all voltage values stay bounded as we move toward the infinite ends of the circuit to have a well posed problem.

3.4.1 The Classical WR Algorithm

The Classical WR algorithm was discussed in [31, 1]. Therefore, I will briefly summarize the results. The algorithm is given by

$$\dot{\boldsymbol{u}}^{k+1} = \begin{bmatrix} \ddots & \ddots & \ddots \\ & a & b & a \\ & & a & b \end{bmatrix} \boldsymbol{u}^{k+1} + \begin{pmatrix} \vdots \\ f_{-1} \\ f_0 \end{pmatrix} + \begin{pmatrix} \vdots \\ 0 \\ a w_1^k \end{pmatrix},$$

$$\dot{\boldsymbol{w}}^{k+1} = \begin{bmatrix} b & a & & \\ a & b & a & \\ & \ddots & \ddots & \ddots \end{bmatrix} \boldsymbol{w}^{k+1} + \begin{pmatrix} f_1 \\ f_2 \\ \vdots \end{pmatrix} + \begin{pmatrix} au_0^k \\ 0 \\ \vdots \end{pmatrix}, \tag{3.107}$$

with the initial conditions $\boldsymbol{u}^{k+1}(0) = (\ldots, v_{-1}^0, v_0^0)^T$ and $\boldsymbol{w}^{k+1}(0) = (v_1^0, v_2^0, \ldots)^T$. To start the classical WR iteration, we use some initial waveforms $\boldsymbol{u}^0(t)$ and $\boldsymbol{w}^0(t)$ for $t \in [0, T]$.

Similar to the analysis for the finite size RC circuits, the Laplace transform is used for the convergence study, and the homogeneous problem is sufficient. It was shown in [31] that

$$\hat{u}_0^{2k} = (\rho_{claL})^k \hat{u}_0^0, \quad \hat{w}_1^{2k} = (\rho_{claL})^k \hat{w}_1^0,$$

where the convergence factor ρ_{claL} is given by

$$\rho_{claL}(s, a, b) = \frac{a^2}{(a\lambda_+^{-1} + b - s)(a\lambda_- + b - s)} = \left(\frac{1}{\lambda_+}\right)^2, \tag{3.108}$$

and λ_+ is given by

$$\lambda_+ = \frac{s - b + \sqrt{(s-b)^2 - 4a^2}}{2a}. \tag{3.109}$$

Furthermore, $|\lambda_+| > 1$, for $s := \eta + i\omega$, $\eta > 0$, and $|b| \geq 2a$, see [31]. Note that this λ_+ is the same as the limit for λ_j given in (3.13) for the finite size RC circuit of size $n = 2j$, and thus $\rho_{cla(j)}$ converges to ρ_{claL} as j goes to infinity.

The convergence factor, as before, depends on $s \in \mathbb{C}$, the parameter in the Laplace transform. The classical WR, as is evident from (3.108), always converges for a large number of iterations since $|\lambda_+| > 1$, but convergence might be very slow. Also, the convergence factor is analytic for $s = \eta + i\omega$, $\eta > 0$, under the condition $|b| \geq 2a$, and in addition, if we let $s = re^{i\theta}$, $-\frac{\pi}{2} < \theta < \frac{\pi}{2}$, then the limit as r goes to infinity is zero, and therefore, using the maximum principle for analytic functions, Theorem 1.5, the maximum of ρ_{claL} is attained on the boundary of the right half of the complex plane,

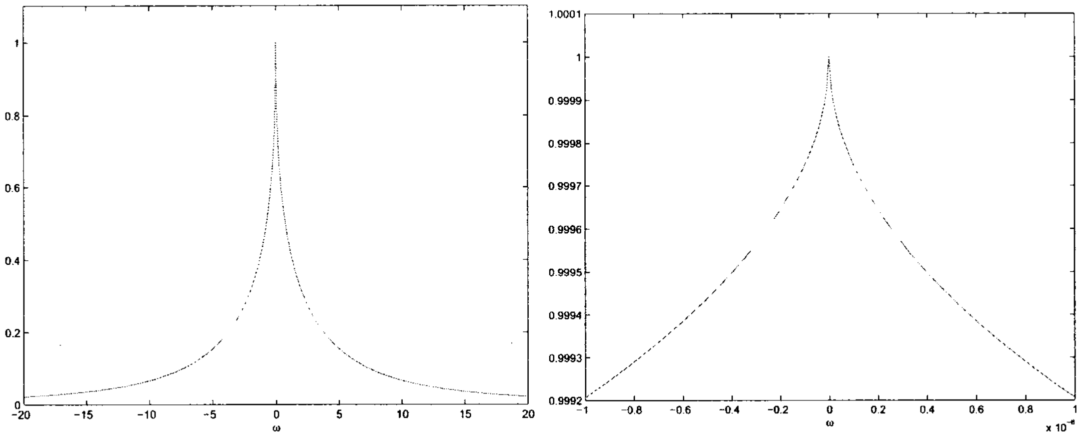

Figure 3.20: Convergence factor for the classical WR algorithm, $|\rho_{claL}(\omega)|$ on the left, and zoom on the right showing $|\rho_{claL}(\omega)|$ for ω around zero.

at $\eta = 0$. Taking the limit on the boundary as ω goes to zero implies

$$\lim_{\omega \to 0} |\rho_{claL}(i\omega, a, b)| = \frac{|b| - \sqrt{b^2 - 4a^2}}{|b| + \sqrt{b^2 - 4a^2}} \begin{array}{l} = 1, \text{ if } |b| = 2a, \\ < 1, \text{ if } |b| > 2a, \end{array}$$

where $|b| = 2a$ is often the case for RC type circuits, or diffusion type problems. Therefore, the convergence will be very slow for low frequencies ω and the mode $\omega = 0$ will not converge. Usually in a realistic transient analysis, estimates for the maximum and minimum frequencies are considered [31]. The estimate for the lowest frequency occurring in the transient analysis depends on the length of the time interval $[0, T]$. As in [31], we expand the signal in a sine series $sin(\frac{k\pi t}{T})$, for $k = 1, 2, \ldots$. This leads to the estimate $\omega_{min} = \frac{\pi}{T}$ for the lowest relevant frequency. The maximum frequency ω_{max} depends on the time discretization and we use $\omega_{max} = \frac{\pi}{\Delta t}$, which is the highest possible oscillation on a grid with spacing Δt. An example for the convergence factor as a function of ω is given in Figure 3.20, which shows a similar convergence to the one for the extra small, and small systems, i.e. low frequencies converge slowly, whereas high frequencies converge vary fast, but now $\omega = 0$ does not converge.

3.4.2 An Optimal WR Algorithm

The analysis of the optimal WR algorithm was discussed in [31, 1] as well, but in the following subsections we will extend the analysis and prove new results. In [31], new transmission conditions were introduced, which are given by

$$\begin{aligned}(u_1^{k+1}-u_0^{k+1})+\alpha u_1^{k+1}&=(w_1^k-w_0^k)+\alpha w_1^k,\\(w_1^{k+1}-w_0^{k+1})+\beta w_0^{k+1}&=(u_1^k-u_0^k)+\beta u_0^k,\end{aligned}\tag{3.110}$$

and the new WR algorithm is

$$\begin{aligned}\dot{\boldsymbol{u}}^{k+1}&=\begin{bmatrix}\ddots&\ddots&\ddots&\\&a&b&a\\&&a&b+\frac{a}{\alpha+1}\end{bmatrix}\boldsymbol{u}^{k+1}+\begin{pmatrix}\vdots\\f_{-1}\\f_0\end{pmatrix}+\begin{pmatrix}\vdots\\0\\aw_1^k-\frac{a}{\alpha+1}w_0^k\end{pmatrix},\\\dot{\boldsymbol{w}}^{k+1}&=\begin{bmatrix}b-\frac{a}{\beta-1}&a&&\\a&b&a&\\&\ddots&\ddots&\ddots\end{bmatrix}\boldsymbol{w}^{k+1}+\begin{pmatrix}f_1\\f_2\\\vdots\end{pmatrix}+\begin{pmatrix}au_0^k+\frac{a}{\beta-1}u_1^k\\0\\\vdots\end{pmatrix},\end{aligned}\tag{3.111}$$

together with the transmission conditions (3.110), which define the values u_1^k and w_0^k. It was shown in [31] that

$$\hat{u}_0^{2k}=(\rho_{optL})^k\,\hat{u}_0^0,\quad \hat{w}_1^{2k}=(\rho_{optL})^k\,\hat{w}_1^0,$$

where the convergence factor ρ_{optL} is given by

$$\rho_{optL}(s,a,b,\alpha,\beta)=\frac{(\alpha+1)-\lambda_+}{(\alpha+1)\lambda_+-1}\cdot\frac{(\beta-1)+\lambda_+}{(\beta-1)\lambda_++1}.\tag{3.112}$$

The new WR algorithm (3.111) converges in two iterations for the choice of parameters

$$\alpha:=\lambda_+-1,\quad \beta:=1-\lambda_+,\tag{3.113}$$

independently of the guess for the initial waveforms, which is proved in [31]. In the next subsections, the optimal parameters in (3.113) will be approximated by constant and first order approximations in a similar way to the small RC circuits in Subsections 3.2.3, 3.3.3, and 3.3.4.

3.4.3 An Optimized WR Algorithm with Constant Transmission Conditions

In this subsection, we assume that the parameters are just constants. By using a Taylor expansion about $s = 0$, we get a simple constant approximation of the optimal parameters α and β given in (3.113). The low frequency constant approximation is given by

$$\alpha_T = \frac{-b + \sqrt{b^2 - 4a^2}}{2a} - 1, \quad \beta_T = 1 - \frac{-b + \sqrt{b^2 - 4a^2}}{2a}.$$

Therefore, for the case $-b = 2a$, there is no low frequency constant approximation since with $-b = 2a$, we have $\alpha_T = \beta_T = 0$, but for the case $-b > 2a$, we have $\alpha_T > 0$ and $\beta_T < 0$ as a low frequency constant approximation, and $\beta_T = -\alpha_T$.

A better approximation is obtained, as before, by solving a min-max problem. The analyticity of ρ_{optL} in the right half of the complex plane was shown in [31] for $a > 0$, $b < 0$, $|b| \geq 2a$, and $\alpha > 0$, $\beta < 0$. By Theorem 1.5, the maximum of ρ_{optL} for $s = \eta + i\omega$, $\eta > 0$, is attained on the boundary. As for the extra small and small circuits, the limit of ρ_{optL} for $s = re^{i\theta}$, $-\frac{\pi}{2} < \theta < \frac{\pi}{2}$, as r goes to infinity is one limit in all directions, which is equal to $\left(\frac{-1}{(\alpha+1)(\beta-1)}\right)$, and therefore, the maximum of ρ_{optL} is attained at $\eta = 0$.

We again use the similarity of the subsystems, which are behaving identically on both sides of the partition, so we take $\beta = -\alpha$, and hence the convergence factor ρ_{optL} in (3.112) with constant approximation is

$$\rho_{optL0}(i\omega, a, b, \alpha) = \left(\frac{\alpha + 1 - \lambda_+}{(\alpha+1)\lambda_+ - 1}\right)^2. \tag{3.114}$$

Let us now consider λ_+ in (3.109) with $s = i\omega$, $\omega \neq 0$, and assume that $\lambda_+ := x + iy = \Re(\lambda_+) + i\Im(\lambda_+)$. Then the real part x is given by

$$x := X(\omega) = \frac{-b}{2a} + \psi(\omega),$$

where

$$\psi(\omega) = \frac{\sqrt{2\sqrt{\omega^4 + 2\omega^2 b^2 + 8\omega^2 a^2 + b^4 - 8b^2 a^2 + 16a^4} - 2\omega^2 + 2b^2 - 8a^2}}{4a},$$

and the imaginary part y is given by

$$y := Y(\omega) = \frac{\omega}{2a} - \frac{2\omega b}{|2b\omega|}\varphi(\omega),$$

where

$$\varphi(\omega) = \frac{\sqrt{2\sqrt{\omega^4 + 2\omega^2 b^2 + 8\omega^2 a^2 + b^4 - 8b^2 a^2 + 16a^4} + 2\omega^2 - 2b^2 + 8a^2}}{4a}.$$

For any $\omega > 0$, we have $Y(\omega) = \frac{\omega}{2a} + \varphi(\omega)$, and for $\omega < 0$, we have $Y(\omega) = -\frac{|\omega|}{2a} - \varphi(\omega) = -(\frac{|\omega|}{2a} + \varphi(\omega))$ since $b < 0$, and hence, $(Y(|\omega|))^2 = (Y(-|\omega|))^2$, since $\varphi(\omega)$ depends only on ω^2.

To summarize, the modulus $|\rho_{optL0}(\omega)|$ satisfies $|\rho_{optL0}(|\omega|)| = |\rho_{optL0}(-|\omega|)|$, since the real part $x := X(\omega)$ depends only on ω^2, and the imaginary part $y := Y(\omega)$, using the fact that $b < 0$, satisfies $(Y(|\omega|))^2 = (Y(-|\omega|))^2$. Therefore, it suffices to optimize for positive frequencies, $\omega > 0$. Furthermore, for any $\omega \neq 0$, we have $x > 1$, since $|b| \geq 2a$, and $\frac{-b}{2a}$ is added to a positive quantity, and hence $|\lambda_+| > 1$. Now if $\omega = 0$, then we get $\lambda_+ = x = \frac{-b}{2a} + \frac{\sqrt{b^2 - 4a^2}}{2a}$, so $|\lambda_+| > 1$ for the case when $-b > 2a$, and $\lambda_+ = 1$ if and only if $-b = 2a$.

Note also that the modulus of ρ_{optL0} in (3.114) satisfies

$$\begin{aligned}
&|\rho_{optL0}| \leq 1 \iff |\alpha + 1 - \lambda_+| \leq |(\alpha+1)\lambda_+ - 1| \iff \\
&|\alpha + 1 - x - iy| \leq |(\alpha+1)x - 1 + i(\alpha+1)y| \iff \\
&(\alpha + 1 - x)^2 + y^2 \leq ((\alpha+1)x - 1)^2 + (\alpha+1)^2 y^2 \iff \\
&(\alpha+1)^2 + x^2 + y^2 \leq (\alpha+1)^2 x^2 + 1 + (\alpha+1)^2 y^2 \iff \\
&(\alpha+1)^2 - 1 \leq ((\alpha+1)^2 - 1)x^2 + ((\alpha+1)^2 - 1)y^2 \iff \\
&1 \leq x^2 + y^2 \iff 1 \leq |\lambda_+|.
\end{aligned}$$

The above analysis simplifies the optimization process to

$$\min_{\alpha>0}\left(\max_{0<\omega_{min}\leq\omega<\infty}|\rho_{optL0}(i\omega,a,b,\alpha)|\right),\ -b\geq 2a, \tag{3.115}$$

where we truncated the frequency range by a minimal frequency relevant for our problem.

For finding a better constant approximation α, a change of variables based on the real part of λ_+ was introduced in [1], and a time scaling (introduced in the introduction) was used as well, where a and b were scaled to $\tilde{a}=1$ and $\tilde{b}=\frac{b}{a}=-2c^2$, where $c=\sqrt{\frac{-b}{2a}}\geq 1$, and then everywhere in the analysis, a was replaced by 1, and b by $-2c^2$. As shown in [1], the real part x of λ_+ is now given by

$$x:=X(\omega,c)=c^2+\frac{1}{4}\sqrt{2\sqrt{\omega^4+8\omega^2c^4+8\omega^2+16c^8-32c^4+16}-2\omega^2+8c^4-8}, \tag{3.116}$$

and $x\in[x_{min},x_\infty)$, where

$$\begin{aligned}
x_{min}&=c^2+\tfrac{\sqrt{2}}{4}\sqrt{\sqrt{\chi}-\tilde{\omega}_{min}^2+4c^4-4}>x_0=\lim_{\omega\to 0}X(\omega,c)=c^2+\sqrt{c^4-1},\\
\chi&=\tilde{\omega}_{min}^4+8\tilde{\omega}_{min}^2c^4+8\tilde{\omega}_{min}^2+16c^8-32c^4+16,\\
x_\infty&=\lim_{\omega\to\infty}X(\omega,c)=2c^2,
\end{aligned} \tag{3.117}$$

and $\tilde{\omega}_{min}=\frac{\omega_{min}}{a}$, where ω_{min} is the truncation threshold of the low frequencies. The modulus of ρ_{optL0} is given by

$$R_0(x,c,\alpha)=|\rho_{optL0}|=\frac{2(\alpha+1)^2c^2-(\alpha+1)^2x-4(\alpha+1)xc^2+2(\alpha+1)x^2+x}{-4(\alpha+1)xc^2+2(\alpha+1)x^2+2c^2-x+(\alpha+1)^2x}, \tag{3.118}$$

where $\alpha>0$ and $c\geq 1$. Again, the limit of R_0 as x goes to x_∞ is equal to $\left(\frac{1}{\alpha+1}\right)^2$.

Theorem 3.9 (Optimized Constant Transmission Conditions). *The best performance of the optimized WR algorithm (3.111) with constant transmission conditions is obtained for $\alpha=\alpha^*$, where α^* is the solution of the equation*

$$R_0(x_{min},c,\alpha^*)=R_0(x_{max},c,\alpha^*),$$

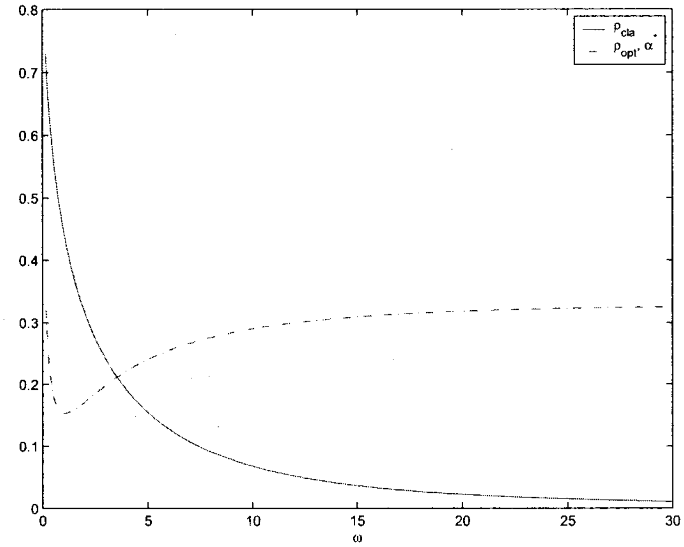

Figure 3.21: Convergence factor for the optimized WR algorithm $|\rho_{optL0}(\omega, \alpha^*)|$ versus the classical convergence factor $|\rho_{claL}(\omega)|$.

and is given, for $x_{max} \longrightarrow x_\infty$, by

$$\alpha^* = x_{min} + \sqrt{x_{min}^2 - 1} - 1,$$

where x_{min} and x_∞ are given in (3.117), R_0 is given in (3.118), and $c = \sqrt{\frac{-b}{2a}} \geq 1$.

Proof. See [1]. □

In Figure 3.21 we show the convergence factor of the optimized WR algorithm with the constant approximation α^* and compare it to the classical one.

3.4.4 An Optimized WR Algorithm with First Order Transmission Conditions

In this subsection, we introduce a first order approximation for the optimal parameter α given in (3.113), as for the small circuits, where we take again $\beta = -\alpha$. Therefore,

α will be approximated by

$$\alpha := \alpha_0 + \alpha_1 s, \; s := \eta + i\omega \in \mathbb{C},$$

for some constants α_0 and $\alpha_1 \neq 0$, since otherwise we get the constant approximation. The optimized WR algorithm with the first order transmission conditions as given in [1], is

$$\begin{pmatrix} \vdots \\ \dot{u}_{-1}^{k+1} \\ \dot{u}_0^{k+1} \\ \dot{u}_1^{k+1} \end{pmatrix} = \begin{bmatrix} \ddots & \ddots & \ddots & & \\ & a & b & a & \\ & & a & b & a \\ & & & \frac{1}{\alpha_1} & \frac{-(\alpha_0+1)}{\alpha_1} \end{bmatrix} \begin{pmatrix} \vdots \\ u_{-1}^{k+1} \\ u_0^{k+1} \\ u_1^{k+1} \end{pmatrix} + \begin{pmatrix} \vdots \\ f_{-1} \\ f_0 \\ f_1 \end{pmatrix} + \begin{pmatrix} 0 \\ \vdots \\ 0 \\ \frac{(\alpha_1 a-1)}{\alpha_1} w_0^k + \frac{(1+\alpha_0+\alpha_1 b)}{\alpha_1} w_1^k + a w_2^k \end{pmatrix}, \tag{3.119}$$

and

$$\begin{pmatrix} \dot{w}_0^{k+1} \\ \dot{w}_1^{k+1} \\ \dot{w}_2^{k+1} \\ \vdots \end{pmatrix} = \begin{bmatrix} \frac{-(\alpha_0+1)}{\alpha_1} & \frac{1}{\alpha_1} & & & \\ a & b & a & & \\ & a & b & a & \\ & & \ddots & \ddots & \ddots \end{bmatrix} \begin{pmatrix} w_0^{k+1} \\ w_1^{k+1} \\ w_2^{k+1} \\ \vdots \end{pmatrix} + \begin{pmatrix} f_0 \\ f_1 \\ f_2 \\ \vdots \end{pmatrix} + \begin{pmatrix} a u_{-1}^k + \frac{(1+\alpha_0+\alpha_1 b)}{\alpha_1} u_0^k + \frac{(\alpha_1 a-1)}{\alpha_1} u_1^k \\ 0 \\ \vdots \\ 0 \end{pmatrix}; \tag{3.120}$$

with the initial conditions $\boldsymbol{u}^{k+1}(0) = (\ldots, v_{-1}^0, v_0^0, v_1^0)^T$ and $\boldsymbol{w}^{k+1}(0) = (v_0^0, v_1^0, v_2^0, \ldots)^T$, respectively, where now the transmission conditions are already implemented in the algorithm. To start the WR iteration, some initial waveforms $\boldsymbol{u}^0(t)$ and $\boldsymbol{w}^0(t)$ are used.

The analysis of the optimized WR algorithm with first order transmission conditions is discussed in [1]. The convergence factor ρ_{optL1} is given by

$$\rho_{optL1}(s,a,b,\alpha_0,\alpha_1) = \left(\frac{(\alpha_0+\alpha_1 s+1)-\lambda_+}{\lambda_+(\alpha_0+\alpha_1 s+1)-1} \right)^2, \tag{3.121}$$

where λ_+ is given in (3.109).

As shown in [1], the convergence factor ρ_{optL1} is an analytic function in the right half of the complex plane, $s = \eta + i\omega$, $\eta > 0$, under the conditions $b < 0$, $a > 0$, $|b| \geq 2a$, $\alpha_0 \geq 0$, and $\alpha_1 > 0$. Therefore, using the maximum principle, Theorem 1.5, the maximum of $|\rho_{optL1}|$ is attained on the boundary. Now, since for $s = re^{i\theta}$, $-\frac{\pi}{2} < \theta < \frac{\pi}{2}$, the limit of ρ_{optL1} equals zero as r goes to infinity, the maximum of $|\rho_{optL1}|$ is attained at $\eta = 0$.

The simplest first order approximation is again the low frequency approximation which is given by

$$\alpha_{0T} = \frac{-b+\sqrt{b^2-4a^2}}{2a} - 1, \ \alpha_{1T} = \frac{1+\frac{-b}{\sqrt{b^2-4a^2}}}{2a}.$$

Therefore, for the case $-b = 2a$, there is no low frequency first order approximation, since with $-b = 2a$, we have $\alpha_{0T} = 0$, but α_{1T} is not defined, because of the $\sqrt{b^2-2a}$ term in the denominator. For the case $-b > 2a$, we have $\alpha_{0T} > 0$, and $\alpha_{1T} > 0$ as a low frequency first order approximation.

We will again look for a better choice of the first order approximation of α. As in Subsection 3.4.3, it suffices to optimize for positive frequencies, $\omega > 0$, since $|\rho_{optL1}|$ depends only on ω^2, because we have the same λ_+ as in (3.109). This yields the optimization problem

$$\min_{\alpha_0 \geq 0, \alpha_1 > 0} \left(\max_{\omega_{\min} \leq \omega < \infty} |\rho_{optL1}(i\omega,a,b,\alpha_0,\alpha_1)| \right), \ |b| \geq 2a. \tag{3.122}$$

We solve here a min-max problem similar to the one in Subsection 3.4.3 but now with two parameters, $\alpha_0 \geq 0$ and $\alpha_1 > 0$.

To further analyze the convergence factor, we introduce a new change of variables, different from the one that is used in Subsection 3.4.3 and was first introduced in [1]. This new change of variables simplifies the computations for finding the solution of the min-max problem (3.122), and it is based on the real part of

$$z := s + \sqrt{(s-b)^2 - 4a^2} = x + iy,\ s = i\omega,\ \omega \geq \omega_{min} > 0,$$

which appears in λ_+, where we have now

$$\lambda_+ = \frac{-b}{2a} + \frac{z}{2a}. \tag{3.123}$$

The real part x of z is given by

$$x := X(\omega) = \frac{1}{2}\sqrt{2\sqrt{\omega^4 + 2b^2\omega^2 + 8a^2\omega^2 + b^4 - 8b^2a^2 + 16a^4} - 2\omega^2 + 2b^2 - 8a^2},$$

and the imaginary part y is given by

$$y := Y(\omega) = \omega + \frac{1}{2}\sqrt{2\sqrt{\omega^4 + 2b^2\omega^2 + 8a^2\omega^2 + b^4 - 8b^2a^2 + 16a^4} + 2\omega^2 - 2b^2 + 8a^2}.$$

The range in which x can vary can again be found by taking the value of $X(\omega)$ at $\omega = \omega_{min} > 0$, and the limit as ω goes to infinity,

$$\begin{aligned} x_{min} &= \tfrac{\sqrt{2}}{2}\sqrt{\sqrt{\chi} - \omega_{min}^2 + b^2 - 4a^2} > x_0 = \lim_{\omega \to 0} X(\omega) = \sqrt{b^2 - 4a^2}, |b| \geq 2a, \\ \chi &= \omega_{min}^4 + 2b^2\omega_{min}^2 + 8a^2\omega_{min}^2 + b^4 - 8b^2a^2 + 16a^4, \\ x_\infty &= \lim_{\omega \to \infty} X(\omega) = \sqrt{b^2} = |b|, \end{aligned} \tag{3.124}$$

and hence, $x \in [x_{min}, |b|)$. Solving $x = X(\omega)$ for ω leads to

$$\omega(x) = \pm\frac{\sqrt{(b^2 - x^2)(x^2 - b^2 + 4a^2)x}}{b^2 - x^2},$$

and inserting this into $Y(\omega)$ implies after simplifications,

$$y = \sqrt{\frac{x^2 - b^2 + 4a^2}{b^2 - x^2}}(x - b). \tag{3.125}$$

By inserting y from equation (3.125) into (3.123), and then inserting the result into (3.121), the convergence factor (3.121) is a function of the new variable x.

The optimal parameter α in (3.113) is given by $\alpha := \lambda_+ - 1$, and hence a first order approximation is

$$\alpha = \alpha_0 + \alpha_1 s = \frac{-b}{2a} - 1 + \frac{p}{2a} + \frac{q}{2a}s, \tag{3.126}$$

where p and q are new parameters.

In the new variable x, and using the first order approximation (3.126), the convergence factor ρ_{optL1} in modulus becomes, after factorizing a^5 from the denominator and numerator to eliminate one parameter,

$$|\rho_{optL1}(x, a, b, p, q)| := \frac{Q_1(x, a, b, p, q)}{Q_2(x, a, b, p, q)},$$

where

$$\begin{aligned}
Q_1(x, a, b, p, q) = {} & ((-2q + q^2)\left(\tfrac{x}{a}\right)^4 + \left(2\tfrac{p}{a} - 2\tfrac{b}{a} + 2\tfrac{b}{a}q\right)\left(\tfrac{x}{a}\right)^3 \\
& + \left(-\left(\tfrac{b}{a}\right)^2 q^2 + 2q\left(\tfrac{b}{a}\right)^2 - 8q + 4q^2 + \left(\tfrac{b}{a}\right)^2 - \left(\tfrac{p}{a}\right)^2 + 4\right)\left(\tfrac{x}{a}\right)^2 \\
& + \left(-8\tfrac{b}{a} + 2\left(\tfrac{b}{a}\right)^3 - 2\left(\tfrac{b}{a}\right)^3 q + 8\tfrac{b}{a}q - 2\left(\tfrac{b}{a}\right)^2\tfrac{p}{a}\right)\tfrac{x}{a} \\
& + \left(\tfrac{b}{a}\right)^2\left(\tfrac{p}{a}\right)^2 - \left(\tfrac{b}{a}\right)^4 + 4\left(\tfrac{b}{a}\right)^2)\left(\tfrac{b}{a} + \tfrac{x}{a}\right), \\
Q_2(x, a, b, p, q) = {} & (2q - q^2)\left(\tfrac{x}{a}\right)^5 + \left(q^2\tfrac{b}{a} + 2\tfrac{p}{a} - 2\tfrac{b}{a}\right)\left(\tfrac{x}{a}\right)^4 \\
& + \left(-2\tfrac{b}{a}\tfrac{p}{a} - 4 + 8q + \left(\tfrac{b}{a}\right)^2 + \left(\tfrac{b}{a}\right)^2 q^2 - 4q^2 - 4q\left(\tfrac{b}{a}\right)^2 + \left(\tfrac{p}{a}\right)^2\right)\left(\tfrac{x}{a}\right)^3 \\
& + \left(-\tfrac{b}{a}\left(\tfrac{p}{a}\right)^2 - 2\left(\tfrac{b}{a}\right)^2\tfrac{p}{a} - \left(\tfrac{b}{a}\right)^3 q^2 + 3\left(\tfrac{b}{a}\right)^3 - 4\tfrac{b}{a} + 4\tfrac{b}{a}q^2\right)\left(\tfrac{x}{a}\right)^2 \\
& + \left(-\left(\tfrac{b}{a}\right)^4 + 2\left(\tfrac{b}{a}\right)^3\tfrac{p}{a} + 2q\left(\tfrac{b}{a}\right)^4 - 8q\left(\tfrac{b}{a}\right)^2 - \left(\tfrac{b}{a}\right)^2\left(\tfrac{p}{a}\right)^2 + 4\left(\tfrac{b}{a}\right)^2\right)\tfrac{x}{a} \\
& + \left(\tfrac{p}{a}\right)^2\left(\tfrac{b}{a}\right)^3 - \left(\tfrac{b}{a}\right)^5 + 4\left(\tfrac{b}{a}\right)^3.
\end{aligned}$$

By setting $\tilde{p} = \frac{p}{a}$, and as before, $\frac{b}{a} = -2c^2,\ c \geq 1$, and $\tilde{x} = \frac{x}{a}$, the modulus of the convergence factor ρ_{optL1} is

$$R_1(\tilde{x}, c, \tilde{p}, q) := \frac{P_1(\tilde{x}, c, \tilde{p}, q)}{P_2(\tilde{x}, c, \tilde{p}, q)}, \tag{3.127}$$

where

$$
\begin{aligned}
P_1(\tilde{x}, c, \tilde{p}, q) = &((-2q + q^2)\tilde{x}^4 + (2\tilde{p} + 4c^2 - 4c^2 q)\tilde{x}^3 \\
&+(-4q^2c^4 + 8qc^4 - 8q + 4q^2 + 4c^4 - \tilde{p}^2 + 4)\tilde{x}^2 \\
&+(16c^2 - 16c^6 + 16c^6 q - 16c^2 q - 8\tilde{p}c^4)\tilde{x} + 4c^4\tilde{p}^2 - 16c^8 + 16c^4)(\tilde{x} - 2c^2), \\
P_2(\tilde{x}, c, \tilde{p}, q) = &((2q - q^2)\tilde{x}^5 + (4c^2 - 2q^2c^2 + 2\tilde{p})\tilde{x}^4 \\
&+(4c^2\tilde{p} - 4 + 8q + 4c^4 + 4q^2c^4 - 4q^2 - 16qc^4 + \tilde{p}^2)\tilde{x}^3 \\
&+(8c^2 - 8\tilde{p}c^4 + 2c^2\tilde{p}^2 + 8q^2c^6 - 24c^6 - 8q^2c^2)\tilde{x}^2 \\
&+(-16c^8 - 16c^6\tilde{p} + 32qc^8 - 32qc^4 - 4c^4\tilde{p}^2 + 16c^4)\tilde{x} \\
&-8\tilde{p}^2c^6 + 32c^{10} - 32c^6),
\end{aligned}
$$

and $\tilde{x} \in [\tilde{x}_{min}, 2c^2)$, where $\tilde{x}_{min} = \frac{x_{min}}{a}$ in (3.124) is given in terms of $\tilde{\omega}_{min} = \frac{\omega_{min}}{a}$ and c, and goes to $\tilde{x}_0 = \frac{x_0}{a} = 2\sqrt{c^4 - 1}$, as $\tilde{\omega}_{min}$ goes to zero.

The optimized parameters are given by $\alpha_0 = \frac{-b}{2a} - 1 + \frac{p}{2a} = c^2 - 1 + \frac{\tilde{p}}{2}$, and $\alpha_1 = \frac{q}{2a}$, where $\tilde{p}$ and q will be determined using R_1 in (3.127). Since for analyticity in the right half of the complex plane, we need $\alpha_0 \geq 0$, and $\alpha_1 > 0$, we require $\tilde{p} \geq 2(1 - c^2)$, and $q > 0$.

The new min-max problem which we need to solve is in the new variables given by

$$
\min_{\tilde{p} \geq 2(1-c^2), q>0} \left(\max_{\tilde{x}_{min} \leq \tilde{x} < 2c^2} R_1(\tilde{x}, c, \tilde{p}, q) \right) = \max_{\tilde{x}_{min} \leq \tilde{x} < 2c^2} R_1(\tilde{x}, c, \tilde{p}^*, q^*), \; c \geq 1. \tag{3.128}
$$

Theorem 3.10 (Optimized First Order Transmission Conditions). *If in the optimized WR algorithm with first order transmission conditions (3.119), (3.120) the free parameters are chosen to be*

$$
\alpha_0 = \alpha_0^* = c^2 - 1 + \frac{\tilde{p}^*}{2} \textit{ and } \alpha_1 = \alpha_1^* = \frac{q^*}{2a},
$$

where $c = \sqrt{\frac{-b}{2a}} \geq 1$, *and* a, b *are the entries of the matrices in (3.119), (3.120), and* $\tilde{p}^*$ *and* q^* *are defined by the systems of nonlinear equations*

$$
R_1(\tilde{x}_{min}, c, \tilde{p}^*, q^*) = R_1(\bar{\tilde{x}}_1, c, \tilde{p}^*, q^*) = R_1(\bar{\tilde{x}}_2, c, \tilde{p}^*, q^*), \; \textit{if } c = 1 \textit{ and } \tilde{\omega}_{min} > 0, \tag{3.129}
$$

and

$$R_1(\tilde{x}_0, c, \tilde{p}^*, q^*) = R_1(\bar{\bar{x}}_1, c, \tilde{p}^*, q^*) = R_1(\bar{\bar{x}}_2, c, \tilde{p}^*, q^*), \text{ if } c > 1 \text{ and } \tilde{\omega}_{min} = 0, \quad (3.130)$$

where $R_1(\tilde{x}, c, \tilde{p}, q)$ *is given in (3.127), and* $\bar{\bar{x}}_1$, $\bar{\bar{x}}_2$ *are given by the positive roots of the polynomial* $P(\tilde{x})$ *given in (A.3) in Appendix A, giving the maxima of* R_1*, then for the case* $c = 1$ *and* $\tilde{\omega}_{min} > 0$, $R_1(\tilde{x}, c, \tilde{p}^*, q^*) \leq R_1(\tilde{x}_{min}, c, \tilde{p}^*, q^*) =: \bar{R}_{O1}$*, for all* $\tilde{x} \in [\tilde{x}_{min}, 2c^2)$*, and for the case* $c > 1$ *and* $\tilde{\omega}_{min} = 0$, $R_1(\tilde{x}, c, \tilde{p}^*, q^*) \leq R_1(\tilde{x}_0, c, \tilde{p}^*, q^*) =: \bar{\bar{R}}_{O1}$*, for all* $\tilde{x} \in [\tilde{x}_0, 2c^2)$*. For* $c = 1$, $\tilde{\omega}_{min} = \epsilon_\omega > 0$, ϵ_ω *small, we have the asymptotic result*

$$\tilde{p}^* = 2^{\frac{2}{5}}(\tilde{\omega}_{min})^{\frac{4}{10}}, \qquad q^* = 2^{\frac{4}{5}}(\tilde{\omega}_{min})^{\frac{-2}{10}}, \qquad \bar{R}_{O1} \approx 1 - 4(2^{\frac{1}{10}})(\tilde{\omega}_{min})^{\frac{1}{10}}, \qquad (3.131)$$

and for $\tilde{\omega}_{min} = 0$, $c = \sqrt{1 + \epsilon_c}$, ϵ_c *small, we have the asymptotic result*

$$\tilde{p}^* = 2(2^{\frac{1}{5}})(c^2 - 1)^{\frac{4}{10}}, \qquad q^* = 2^{\frac{2}{5}}(c^2 - 1)^{\frac{-2}{10}}, \qquad \bar{\bar{R}}_{O1} \approx 1 - 4(2^{\frac{3}{10}})(c^2 - 1)^{\frac{1}{10}}. \qquad (3.132)$$

Proof. A partial derivative of R_1 with respect to $\tilde{x}$ shows that the roots of $P(\tilde{x})$ given in (A.3) determine the extrema of R_1. Since $P(\tilde{x})$ is a bi-quartic in $\tilde{x}$ with real coefficients, it has at most four real positive roots, and hence, for $\tilde{x}_{min} \leq \tilde{x} < 2c^2$ with $c = 1$, $\tilde{\omega}_{min} > 0$, and for $\tilde{x}_0 \leq \tilde{x} < 2c^2$ with $c > 1$, $\tilde{\omega}_{min} = 0$, R_1 can have at most two interior maxima. Since R_1 goes to zero as $\tilde{x}$ goes to $2c^2$, which is the limit as $\omega \longrightarrow \infty$, the maximum in the min-max problem (3.128) can be attained either on the boundary, for the case $c = 1$ and $\tilde{\omega}_{min} > 0$ at $\tilde{x} = \tilde{x}_{min}$ and for the case $c > 1$ and $\tilde{\omega}_{min} = 0$ at $\tilde{x} = \tilde{x}_0$, or at either of the two maxima, which we denote by $\bar{\bar{x}}_1$ and $\bar{\bar{x}}_2$. Balancing the value of R_1 at all these three locations as stated in (3.129) for the first case and in (3.130) for the second one, guarantees then that R_1 is uniformly bounded by R_1 at $\tilde{x}_{min}$ for the case $c = 1$ and $\tilde{\omega}_{min} > 0$, and at $\tilde{x}_0$ for the case $c > 1$ and $\tilde{\omega}_{min} = 0$. To see that there is indeed such a solution for (3.129) where we have

$c = 1$, for $\tilde{\omega}_{min} = \epsilon_\omega$ small, we use the ansatz $\tilde{p} = C_p \epsilon_\omega^{\gamma_1}$, $q = C_q \epsilon_\omega^{\gamma_2}$, $\bar{\tilde{x}}_1 = C_1 \epsilon_\omega^{\delta_1}$, and $\bar{\tilde{x}}_2 = C_2 \epsilon_\omega^{\delta_2}$, and determine the leading asymptotic terms as ϵ_ω goes to zero of the two roots of the polynomial $P(\tilde{x})$, which leads to

$$\begin{aligned} P(\bar{\tilde{x}}_1) &= 512 C_1^2 C_p \epsilon_\omega^{\gamma_1 + 2\delta_1} - 256 C_1^4 C_q \epsilon_\omega^{\gamma_2 + 4\delta_1} + \dots, \\ P(\bar{\tilde{x}}_2) &= 32 C_2^6 C_q^3 \epsilon_\omega^{3\gamma_2 + 6\delta_2} - 4 C_2^8 C_q^4 \epsilon_\omega^{4\gamma_2 + 8\delta_2} + \dots. \end{aligned}$$

Similarly, expanding the equations (3.129) for ϵ_ω small, we find the leading terms

$$\begin{aligned} 1 - &\tfrac{4\sqrt{2}}{C_p} \epsilon_\omega^{\frac{1}{2} - \gamma_1} + \dots \\ &= 1 - \tfrac{2C_p}{C_1} \epsilon_\omega^{\gamma_1 - \delta_1} - C_1 C_q \epsilon_\omega^{\gamma_2 + \delta_1} + \dots \\ &\quad = 1 - \tfrac{8}{C_q C_2} \epsilon_\omega^{-(\gamma_2 + \delta_2)} - C_2 \epsilon_\omega^{\delta_2} + \dots. \end{aligned}$$

Equating the exponents in these four equations leads to $\gamma_1 = \frac{4}{10}$, $\gamma_2 = -\frac{2}{10}$, $\delta_1 = \frac{3}{10}$, and $\delta_2 = \frac{1}{10}$, and since the constants need to match as well, we obtain

$$C_p = 2^{\frac{2}{5}}, \qquad C_q = 2^{\frac{4}{5}}, \qquad C_1 = 2^{\frac{3}{10}}, \qquad C_2 = 2(2^{\frac{1}{10}}).$$

Now using these results in R_1 and expanding $\bar{R}_{O1} = R_1(\tilde{x}_{min}, c, \tilde{p}^*, q^*)$ for $\tilde{\omega}_{min} = \epsilon_\omega$ small, we find the asymptotic results (3.131).

Similarly for the second case, to see that there is a solution for (3.130) where we now have $\tilde{\omega}_{min} = 0$, for $c = \sqrt{1 + \epsilon_c}$, ϵ_c small, we use the ansatz $\tilde{p} = C_p \epsilon_c^{\gamma_1}$, $q = C_q \epsilon_c^{\gamma_2}$, $\bar{\tilde{x}}_1 = C_1 \epsilon_c^{\delta_1}$, and $\bar{\tilde{x}}_2 = C_2 \epsilon_c^{\delta_2}$, and determine the leading asymptotic terms as ϵ_c goes to zero of the two roots of the polynomial $P(\tilde{x})$, which leads to

$$\begin{aligned} P(\bar{\tilde{x}}_1) &= 512 C_1^2 C_p \epsilon_c^{\gamma_1 + 2\delta_1} - 256 C_1^4 C_q \epsilon_c^{\gamma_2 + 4\delta_1} + \dots, \\ P(\bar{\tilde{x}}_2) &= 32 C_2^6 C_q^3 \epsilon_c^{3\gamma_2 + 6\delta_2} - 4 C_2^8 C_q^4 \epsilon_c^{4\gamma_2 + 8\delta_2} + \dots. \end{aligned}$$

The leading terms we find by expanding the equations (3.130) for ϵ_c small are

$$\begin{aligned} 1 - &\tfrac{8\sqrt{2}}{C_p} \epsilon_c^{\frac{1}{2} - \gamma_1} + \dots \\ &= 1 - \tfrac{2C_p}{C_1} \epsilon_c^{\gamma_1 - \delta_1} - C_1 C_q \epsilon_c^{\gamma_2 + \delta_1} + \dots \\ &\quad = 1 - \tfrac{8}{C_q C_2} \epsilon_c^{-(\gamma_2 + \delta_2)} - C_2 \epsilon_c^{\delta_2} + \dots. \end{aligned}$$

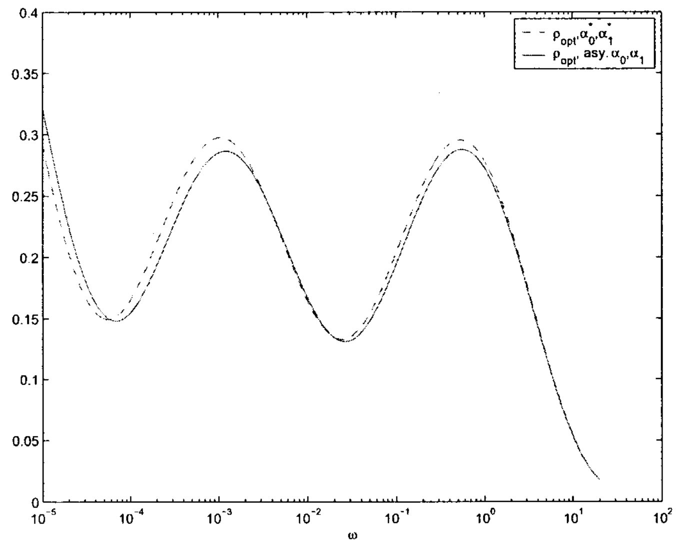

Figure 3.22: Convergence factor of the optimized WR algorithm with the optimized first order approximation $|\rho_{optL1}(\omega, \alpha_0^*, \alpha_1^*)|$ versus the one with the asymptotically optimized values.

Equating the exponents in these four equations leads to $\gamma_1 = \frac{4}{10}$, $\gamma_2 = -\frac{2}{10}$, $\delta_1 = \frac{3}{10}$, and $\delta_2 = \frac{1}{10}$, and since the constants need to match as well, we obtain

$$C_p = 2(2^{\frac{1}{5}}), \qquad C_q = 2^{\frac{2}{5}}, \qquad C_1 = 2^{\frac{9}{10}}, \qquad C_2 = 2(2^{\frac{3}{10}}).$$

Now using these results in R_1 and expanding $\overline{\overline{R}}_{O1} = R_1(\tilde{x}_0, c, \tilde{p}^*, q^*)$ for ϵ_c small, we find the asymptotic results (3.132). Note that the expansions we obtain for the two cases have the same exponents, they are only different by a constant.

Since $\alpha_0 = c^2 - 1 + \frac{\tilde{p}}{2}$, and $\alpha_1 = \frac{q}{2a}$, we have

$$\alpha_0^* = c^2 - 1 + \frac{\tilde{p}^*}{2}, \qquad \alpha_1^* = \frac{q^*}{2a}.$$

□

We show in Figure 3.22 the result of the optimization with respect to α_0 and α_1 with values of a and b from the numerical experiment in Subsection 3.4.5, and we use

$\omega_{min} = 0.00001$. The solution of the min-max problem occurs when the convergence factor at $\omega = \omega_{min}$, $\omega = \bar{\omega}_1$, and $\omega = \bar{\omega}_2$ are balanced, where $\bar{\omega}_1$, $\bar{\omega}_2 > 0$ are the interior maxima of the modulus of the convergence factor. We observe that the convergence factor with the optimized values α_0^* and α_1^* is close to the one with the asymptotically optimized values.

We use now $\omega_{min} = \frac{\pi}{20}$ to compute the numerically and the asymptotically optimized α_0^* and α_1^* as well as the optimized constant α^*, using the circuit parameters in Subsection 3.4.5, and we show the convergence factors as a function of ω in Figure 3.23. On the left of Figure 3.23, we observe the better convergence factor we get by using the first order approximation over the constant approximation, and compared to the classical convergence factor. On the right, we show the convergence factor of the optimized WR algorithm with the first order approximation using the numerically optimized α_0^* and α_1^*, and using the asymptotically optimized values. Note that the minimal frequency we choose, $\omega_{min} = \frac{\pi}{20}$, is not small enough to be smaller than the two maxima which we assure their existence for small ω_{min}, and thus we have only one maximum for ρ_{optL1} using the numerically optimized values, which is bigger than ω_{min} and the other one is smaller, and for the one with the asymptotically optimized values there are no interior maxima in this case. Note also that ρ_{optL1} with the asymptotically optimized values is better than ρ_{optL1} with the numerically optimized values for high frequencies.

Table 3.1 gives a comparison of the optimized α_0^* and α_1^* from (3.129) with the asymptotic approximation (3.131) using the circuit parameters in Subsection 3.4.5, and a comparison of the optimized α_0^* and α_1^* from (3.130) with the asymptotic approximation (3.132). One can see from the first part that the asymptotic result for α_0^* and α_1^* is close to the optimized α_0^* and α_1^* for small ω_{min}, and from the second, one can see that the values are close for c close to one. Furthermore, for larger values of ω_{min} and c, the asymptotic approximation can be used as a good initial guess for the

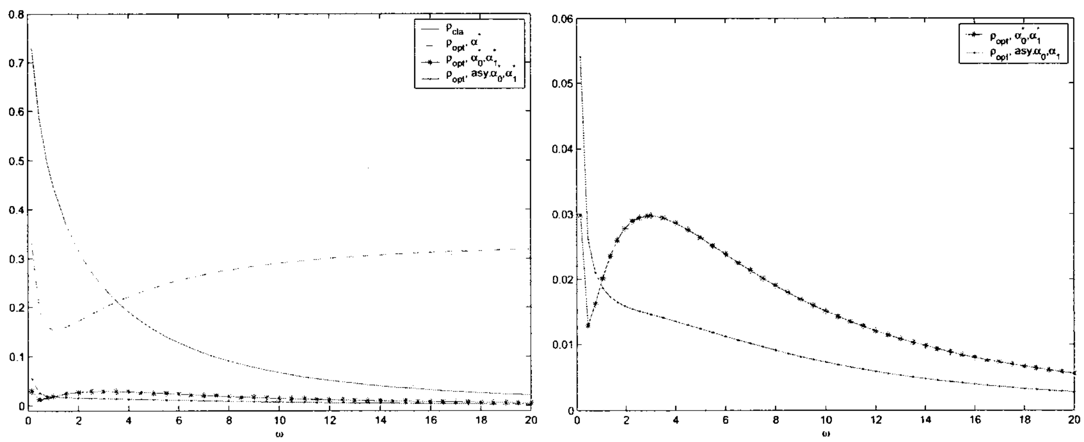

Figure 3.23: On the left: classical convergence factor $|\rho_{claL}(\omega)|$ versus convergence factor of the optimized WR algorithm with the optimized constant approximation $|\rho_{optL0}(\omega, \alpha^*)|$, and the one with the first order approximation $|\rho_{optL1}(\omega, \alpha_0^*, \alpha_1^*)|$ using the numerically and asymptotically optimized values. On the right: $|\rho_{optL1}(\omega, \alpha_0^*, \alpha_1^*)|$ using the numerically optimized values versus the one using the asymptotically optimized values.

Table 3.1: Comparison of the optimized α_0^*, α_1^* from Theorem 3.10 and their asymptotic approximation.

ω_{min}	0.01	0.001	0.0001	0.00001	0.000001
opt.α_0^*, α_1^*	0.049,1.095	0.021,1.558	0.009,2.338	0.0038,3.600	0.0016,5.6134
asy.α_0^*, α_1^*	0.066,0.868	0.026,1.375	0.010,2.180	0.0042,3.455	0.0017,5.4757
c^2	1.01	1.001	1.0001	1.00001	1.000001
opt.α_0^*, α_1^*	0.209,0.549	0.076,0.841	0.0294,1.319	0.0116,2.083	0.0046,3.297
asy.α_0^*, α_1^*	0.192,0.522	0.074,0.827	0.0290,1.311	0.0115,2.078	0.0046,3.294

nonlinear equation solver to find the optimized α_0^* and α_1^* from (3.129) and (3.130) respectively.

3.4.5 Numerical Experiments

We solve here a model RC circuit with 100 nodes with the same typical parameters we used for the extra small and small circuits,

$$R_s = R_i = \frac{1}{2} \text{ Ohms}, \; i = 1, \ldots, 99, \; C_i = \frac{63}{100} \text{ pF}, \; i = 1, \ldots, 100.$$

We again use the backward Euler method, and our transient analysis time now is $t \in [0, 20]$, with a time step of $\Delta t = 1/20$. We start with random initial waveforms and use an input step function with an amplitude of $I_s = 1$ and a rise time of 1 time unit. We consider $\omega_{min} = \frac{\pi}{20}$, and we use the optimized value $\alpha^* = 0.7346$ in the optimized WR algorithm with constant transmission conditions, and the numerically optimized values $\alpha_0^* = 0.1756$, $\alpha_1^* = 0.6556$, as well as the asymptotic values $\alpha_0^* = 0.1982$, $\alpha_1^* = 0.5003$ in the optimized WR algorithm with first order transmission conditions. In Figure 3.24 we show the error as a function of the WR iterations. One can see the remarkable improvement of the optimized WR algorithm over the classical one. Furthermore, the optimized WR algorithm with first order transmission conditions

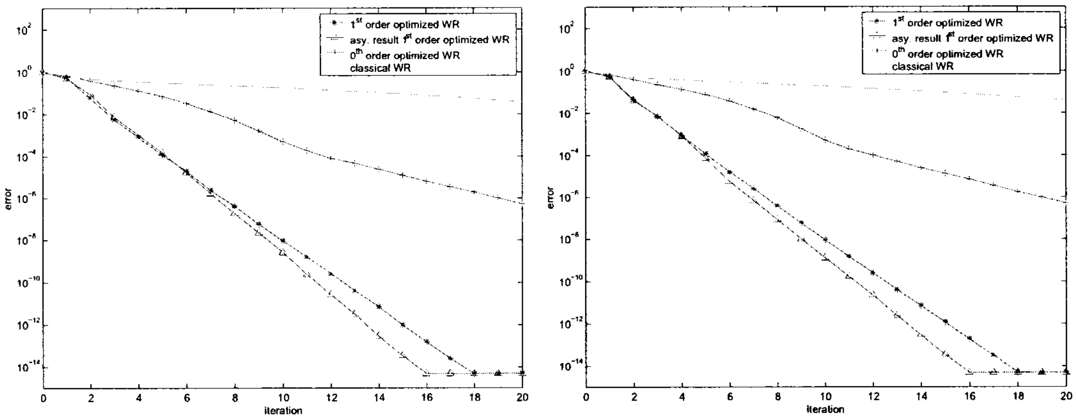

Figure 3.24: Convergence behavior of classical versus optimized WR algorithms for large RC circuit.

converges faster than the one with constant transmission conditions. Note that the optimized WR algorithm with the asymptotic values α_0^* and α_1^* from Theorem 3.10 converges even a bit faster than the one with the numerically optimized values α_0^* and α_1^* for $\omega_{min} = \frac{\pi}{20}$. In fact, we have already seen on the right hand side of Figure 3.23 that the convergence factor with the asymptotic values is better than the one with the numerically optimized values for high frequencies which is the case here. On the left hand side of Figure 3.24, we use $b_{100} = b_1$, and on the right hand side, we choose $b_{100} = \frac{b_1}{2}$, and show the results.

Chapter 4

Transmission Line Type Circuits

In this chapter we analyze the classical, an optimal, and optimized WR algorithms for transmission line type circuits. As for the RC type circuits in Chapter 3, the results we obtain for the transmission line circuits we are analyzing here will be of great interest in decomposing a general circuit which has transmission line circuits connecting its parts which might include nonlinear components. So we also look here for transmission line circuits in the general circuit and we partition there since we know how to do the partitioning for the transmission line circuit with an excellent performance using the results from this chapter. Note that we consider here a single transmission line and we analyze a longitudinal decoupling of this transmission line, a problem which does not converge for a reasonable number of iterations using classical WR algorithms. See [38] for solving multiple coupled transmission lines using WR methods. We start with finite size transmission line type circuits, and then we study an infinitely large transmission line circuit for which we investigate and analyze the convergence of the WR algorithms. We are analyzing a Jacobi type iteration here, but the Gauss-Seidel case is similar.

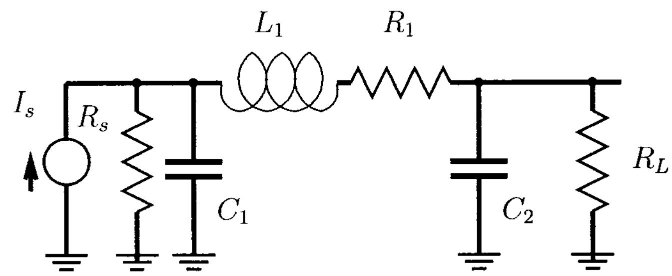

Figure 4.1: A very small transmission line circuit.

4.1 A Very Small Transmission Line Type Circuit

We start with the simple transmission line circuit given in Figure 4.1. The circuit equations are of the form

$$\dot{\boldsymbol{x}} = \begin{bmatrix} b_1 & c_1 & \\ a_1 & b_2 & c_2 \\ & a_2 & b_3 \end{bmatrix} \boldsymbol{x} + \boldsymbol{f}, \tag{4.1}$$

with vector of unknown waveforms $\boldsymbol{x} = (v_1, i_1, v_2)^T$, which consists of two nodal capacitive voltages alternating with an inductance current in the transmission line circuit. The entries in the tridiagonal matrix are given by

$$a_i = \begin{cases} \frac{1}{L_{(i+1)/2}}, & i = 1 \\ \frac{1}{C_{(i/2)+1}}, & i = 2 \end{cases}, \quad c_i = \begin{cases} -\frac{1}{C_{(i+1)/2}}, & i = 1 \\ -\frac{1}{L_{i/2}}, & i = 2 \end{cases}, \quad b_i = \begin{cases} -\frac{1}{R_s C_1}, & i = 1 \\ -\frac{R_{i/2}}{L_{i/2}}, & i = 2 \\ -\frac{1}{R_L C_2}, & i = 3 \end{cases}, \tag{4.2}$$

where the resistor values R_s, R_1, and R_L, the inductor L_1, and the capacitors C_1 and C_2 are strictly positive constants. The source term on the right hand side is given by $\boldsymbol{f}(t) = (I_s(t)/C_1, 0, 0)^T$, for some source function $I_s(t)$, and we are also given the initial values $\boldsymbol{x}(0) = (v_1^0, i_1^0, v_2^0)^T$ at the time $t = 0$. We use three different ways here to decompose the system into two subsystems. In the first one, we partition the system at an even row without overlap, which corresponds to a cut at the inductance current in the system, and in the second one, we partition at an odd row without overlap as well, which corresponds to a cut at a nodal capacitive voltage, and we obtain two subsystems of different size. In the third way, we partition the system in the middle, where we use an overlap to get two subsystems of the same size.

4.1.1 Analysis of the Classical WR Algorithm Without Overlap

We partition the system first at an even row into two subsystems or sub-circuits, and we call the values in subsystem one $\boldsymbol{u}(t)$ and in subsystem two $w_1(t)$. The classical WR algorithm applied to (4.1) with two sub-circuits is given by

$$\begin{aligned} \dot{\boldsymbol{u}}^{k+1} &= \begin{bmatrix} b_1 & c_1 \\ a_1 & b_2 \end{bmatrix} \boldsymbol{u}^{k+1} + \begin{pmatrix} f_1 \\ f_2 \end{pmatrix} + \begin{pmatrix} 0 \\ c_2 w_1^k \end{pmatrix}, \\ \dot{w}_1^{k+1} &= b_3 w_1^{k+1} + f_3 + a_2 u_2^k, \end{aligned} \tag{4.3}$$

where we used the classical transmission conditions

$$u_3^{k+1} = w_1^k, \quad w_0^{k+1} = u_2^k. \tag{4.4}$$

The corresponding initial conditions are $\boldsymbol{u}^{k+1}(0) = (v_1^0, i_1^0)^T$ and $w_1^{k+1}(0) = v_2^0$. To start the WR iteration, we need to specify initial waveforms $\boldsymbol{u}^0(t) = (u_1^0(t), u_2^0(t))^T$ and $w_1^0(t)$ for $t \in [0, T]$.

Similar to the analysis in the previous chapter, we use the Laplace transform and we consider the homogeneous problem. The Laplace transform with Laplace parameter $s \in \mathbb{C}$ of (4.3) is given by

$$s\hat{\boldsymbol{u}}^{k+1} = \begin{bmatrix} b_1 & c_1 \\ a_1 & b_2 \end{bmatrix} \hat{\boldsymbol{u}}^{k+1} + \begin{pmatrix} 0 \\ c_2 \hat{w}_1^k \end{pmatrix}, \quad s\hat{w}_1^{k+1} = b_3 \hat{w}_1^{k+1} + a_2 \hat{u}_2^k \ . \tag{4.5}$$

Solving the first equation in (4.5) for $\hat{u}_2^{k+1}$, we find

$$\hat{u}_2^{k+1} = \frac{c_2(s-b_1)}{(s-b_1)(s-b_2)-a_1c_1}\hat{w}_1^k, \tag{4.6}$$

and similarly solving the second equation in (4.5) for $\hat{w}_1^{k+1}$, we get

$$\hat{w}_1^{k+1} = \frac{a_2}{s-b_3}\hat{u}_2^k. \tag{4.7}$$

Inserting (4.7) at iteration k into (4.6), we find a relation over two iteration steps of the WR algorithm,

$$\hat{u}_2^{k+1} = \rho_{cla}(s,\boldsymbol{a},\boldsymbol{b},\boldsymbol{c})\hat{u}_2^{k-1},$$

where the convergence factor ρ_{cla} of the classical WR algorithm is given by

$$\rho_{cla}(s,\boldsymbol{a},\boldsymbol{b},\boldsymbol{c}) = \frac{a_2c_2(s-b_1)}{(s-b_3)((s-b_1)(s-b_2)-a_1c_1)}. \tag{4.8}$$

The same result holds for $\hat{w}_1^{k+1}$, and by induction we obtain $\hat{u}_2^{2k} = (\rho_{cla})^k\,\hat{u}_2^0$ and $\hat{w}_1^{2k} = (\rho_{cla})^k\,\hat{w}_1^0$.

We consider now the classical WR algorithm applied to (4.1) with a partition at an odd row,

$$\begin{aligned}\dot{u}_1^{k+1} &= b_1u_1^{k+1} + f_1 + c_1w_1^k,\\ \dot{\boldsymbol{w}}^{k+1} &= \begin{bmatrix} b_2 & c_2\\ a_2 & b_3\end{bmatrix}\boldsymbol{w}^{k+1} + \begin{pmatrix} f_2\\ f_3\end{pmatrix} + \begin{pmatrix} a_1u_1^k\\ 0\end{pmatrix},\end{aligned} \tag{4.9}$$

with corresponding initial conditions $u_1^{k+1}(0) = v_1^0$ and $\boldsymbol{w}^{k+1}(0) = (i_1^0, v_2^0)^T$. The Laplace transform of (4.9) is given by

$$s\hat{u}_1^{k+1} = b_1\hat{u}_1^{k+1} + c_1\hat{w}_1^k, \quad s\hat{\boldsymbol{w}}^{k+1} = \begin{bmatrix} b_2 & c_2\\ a_2 & b_3\end{bmatrix}\hat{\boldsymbol{w}}^{k+1} + \begin{pmatrix} a_1\hat{u}_1^k\\ 0\end{pmatrix}. \tag{4.10}$$

In a way similar to the one used for the cut at an even row, we obtain the convergence factor ρ_{cla} of the classical WR algorithm with a cut at an odd row,

$$\rho_{cla}(s,\boldsymbol{a},\boldsymbol{b},\boldsymbol{c}) = \frac{a_1c_1(s-b_3)}{(s-b_1)((s-b_3)(s-b_2)-a_2c_2)}. \tag{4.11}$$

The same result holds for $\hat{w}_1^{k+1}$, and by induction we obtain $\hat{u}_1^{2k} = (\rho_{cla})^k \hat{u}_1^0$ and $\hat{w}_1^{2k} = (\rho_{cla})^k \hat{w}_1^0$. One can see that the convergence factor ρ_{cla} with a partition at an even row is the same as the convergence factor ρ_{cla} with a partition at an odd row whenever the elements of the vectors $\boldsymbol{a}$, $\boldsymbol{b}$, and $\boldsymbol{c}$ satisfy the relations $c_2 = -a_1$, $c_1 = -a_2$, and $b_3 = b_1$, which is the case we consider for the infinitely large circuit system, as we will see later. Therefore, we will only study the convergence factor in (4.11). The two convergence factors are also the same when $a_1 = a_2$, $c_1 = c_2$, and $b_1 = b_3$. However, this is not the case for the transmission line circuits as one can see from the circuit parameters given in (4.2).

Note that we can only analyze for the classical WR algorithm if the convergence test $|\rho_{cla}| < 1$ is satisfied, since ρ_{cla} is a fixed function of the circuit parameters in the classical WR algorithm, as is evident from (4.11).

Now, for $\Re(s) > 0$ the denominator in (4.11) does not vanish, because $a_i > 0$, $c_i < 0$, and $b_i < 0$ for the circuit we consider. Hence, by Theorem 1.4, the convergence factor is an analytic function in the right half of the complex plane. The limit of ρ_{cla} for $s = re^{i\theta}$, $-\pi/2 < \theta < \pi/2$, as $r \to \infty$ is zero, therefore, by the maximum principle for complex analytic functions, Theorem 1.5, the modulus $|\rho_{cla}|$ takes its maximum on the boundary at $\eta = 0$. The modulus of ρ_{cla} for $s = i\omega$, with the simplifying assumptions $c_1 = -a_2$, $c_2 = -a_1$, and $b_3 = b_1$ is given by

$$|\rho_{cla}(i\omega, a_1, a_2, b_1, b_2)| = \frac{a_2 a_1}{\sqrt{\omega^4 + (-2a_2a_1 + b_2^2 + b_1^2)\omega^2 + a_2^2a_1^2 + b_1^2b_2^2 + 2b_1b_2a_2a_1}}. \tag{4.12}$$

The modulus of the classical convergence factor depends on ω^2 only as one can see from (4.12). Furthermore, $|\rho_{cla}|$ might take values bigger than one as we show in the following lemma.

Lemma 4.1. *Let a_1, $a_2 > 0$, b_1, $b_2 < 0$. If $A := \frac{a_1 a_2}{b_2^2} > 0$, and $b := \frac{b_1}{b_2} > 0$ are in the* *region* $\Omega := \{(A,b) : A \geq A_{h+},\ b > 0\}$, *where*

$$A_{h+} = \frac{1+b+2\sqrt{b}}{2}(1+b),$$

then there exists $\omega > 0$ *such that* $|\rho_{cla}(\omega)| \geq 1$.

Proof. The modulus of the classical convergence factor squared is

$$|\rho_{cla}(i\omega, a_1, a_2, b_1, b_2)|^2 = \frac{P_1}{P_2} = \frac{a_2^2 a_1^2}{\omega^4 + (-2a_2a_1 + b_2^2 + b_1^2)\omega^2 + a_2^2a_1^2 + b_1^2b_2^2 + 2b_1b_2a_2a_1},$$

where $P_1, P_2 > 0$. The polynomial $p(\omega, a_1, a_2, b_1, b_2) = P_1 - P_2$ is

$$p(\omega, a_1, a_2, b_1, b_2) = -\omega^4 + (-b_2^2 - b_1^2 + 2a_2a_1)\omega^2 - b_1^2b_2^2 - 2b_1b_2a_2a_1.$$

Factorizing out b_2^4 and letting $A = \frac{a_1a_2}{b_2^2}$, $b = \frac{b_1}{b_2}$, and $x = \frac{\omega^2}{b_2^2}$, the polynomial p becomes

$$\tilde{p}(x, A, b, b_2) = b_2^4\left(-x^2 + (2A - (b^2+1))x - (b^2 + 2bA)\right),$$

and we consider the function f which is given by

$$f(x, A, b) = \left(-x^2 + (2A - (b^2+1))x - (b^2 + 2bA)\right), \tag{4.13}$$

where $A > 0$, $b > 0$, and $x \geq 0$. For $x \geq 0$, the sign of f will indicate where $P_1 > P_2$ and where $P_1 < P_2$.

The maximum value of f is attained at $x^\star = \frac{2A-(b^2+1)}{2}$. We treat two cases:

1. If $x^\star \geq 0$, i.e. $A \geq \frac{b^2+1}{2}$, then we consider the function

$$f(x = x^\star, A, b) = A^2 - (b+1)^2A + \frac{1}{4}(b^2-1)^2.$$

2. If $x^\star < 0$, then the maximum is attained at $x = 0$, and we consider the function

$$f(x = 0, A, b) = -(b^2 + 2bA).$$

For the first case, if we let $h(A,b) := A^2 - (b+1)^2 A + \frac{1}{4}(b^2-1)^2$, then the equation $h(A,b) = 0$ has two roots in terms of b,

$$A_{h\pm} = \frac{1+b \pm 2\sqrt{b}}{2}(1+b).$$

Now, since $A_{h+} > \frac{1+b^2}{2}$, and $A_{h-} < \frac{1+b^2}{2}$, and using the sign of h, we get $h(A,b) < 0$ for $\frac{1+b^2}{2} \le A < A_{h+}$, and $h(A,b) \ge 0$ for $A \ge A_{h+}$. For the second case, we have $-(2bA + b^2) < 0$ on the entire region, where $0 < A < \frac{1+b^2}{2}$, $b > 0$.

Hence, the function f given in (4.13) is less than zero for $0 < A < A_{h+}$, $b > 0$, and thus $|\rho_{cla}| < 1$, whereas $f(x, A, b)$ takes values greater than or equal zero in the region $\Omega = \{(A,b) : A \ge A_{h+},\ b > 0\}$, and since $A_{h+} > \frac{1+b^2}{2}$, and $x = \frac{\omega^2}{b_2^2}$, there exists $\omega > 0$ at which $|\rho_{cla}|$ takes values greater than or equal one. □

4.1.2 Analysis of the Classical WR Algorithm With Overlap

In this subsection we study the classical WR algorithm with overlap, which leads to two subsystems of the same size. A partition of the system in (4.1) with overlap is given by

$$\begin{aligned} \dot{\boldsymbol{u}} &= \begin{bmatrix} b_1 & c_1 \\ a_1 & b_2 \end{bmatrix} \boldsymbol{u} + \begin{pmatrix} f_1 \\ f_2 \end{pmatrix} + \begin{pmatrix} 0 \\ c_2 u_3 \end{pmatrix}, \\ \dot{\boldsymbol{w}} &= \begin{bmatrix} b_2 & c_2 \\ a_2 & b_3 \end{bmatrix} \boldsymbol{w} + \begin{pmatrix} f_2 \\ f_3 \end{pmatrix} + \begin{pmatrix} a_1 w_0 \\ 0 \end{pmatrix}. \end{aligned} \tag{4.14}$$

Now, using the classical transmission conditions

$$u_3^{k+1} = w_2^k, \quad w_0^{k+1} = u_1^k, \tag{4.15}$$

the classical WR algorithm is

$$\begin{aligned} \dot{\boldsymbol{u}}^{k+1} &= \begin{bmatrix} b_1 & c_1 \\ a_1 & b_2 \end{bmatrix} \boldsymbol{u}^{k+1} + \begin{pmatrix} f_1 \\ f_2 \end{pmatrix} + \begin{pmatrix} 0 \\ c_2 w_2^k \end{pmatrix}, \\ \dot{\boldsymbol{w}}^{k+1} &= \begin{bmatrix} b_2 & c_2 \\ a_2 & b_3 \end{bmatrix} \boldsymbol{w}^{k+1} + \begin{pmatrix} f_2 \\ f_3 \end{pmatrix} + \begin{pmatrix} a_1 u_1^k \\ 0 \end{pmatrix}, \end{aligned} \tag{4.16}$$

with corresponding initial conditions $\boldsymbol{u}^{k+1}(0) = (v_1^0, i_1^0)T$ and $\boldsymbol{w}^{k+1}(0) = (i_1^0, v_2^0)^T$. To start the WR iteration, we need to specify initial waveforms $\boldsymbol{u}^0(t) = (u_1^0(t), u_2^0(t))^T$ and $\boldsymbol{w}^0(t) = (w_1^0(t), w_2^0(t))^T$ for $t \in [0, T]$.

The Laplace transform applied to the homogeneous problem of (4.16) implies

$$\begin{aligned} s\hat{\boldsymbol{u}}^{k+1} &= \begin{bmatrix} b_1 & c_1 \\ a_1 & b_2 \end{bmatrix} \hat{\boldsymbol{u}}^{k+1} + \begin{pmatrix} 0 \\ c_2 \hat{w}_2^k \end{pmatrix}, \\ s\hat{\boldsymbol{w}}^{k+1} &= \begin{bmatrix} b_2 & c_2 \\ a_2 & b_3 \end{bmatrix} \hat{\boldsymbol{w}}^{k+1} + \begin{pmatrix} a_1 \hat{u}_1^k \\ 0 \end{pmatrix}. \end{aligned} \tag{4.17}$$

Solving the first system of equations in (4.17) for $\hat{u}_2^{k+1}$, and using $\hat{w}_2^k = \frac{a_2}{s-b_3}\hat{w}_1^k$ from the second subsystem of equations, we find

$$\hat{u}_2^{k+1} = \frac{c_2(s-b_1)}{(s-b_1)(s-b_2)-a_1c_1}\hat{w}_2^k = \frac{c_2(s-b_1)}{(s-b_1)(s-b_2)-a_1c_1} \cdot \frac{a_2}{s-b_3}\hat{w}_1^k. \tag{4.18}$$

Similarly, solving the second equation in (4.17) for $\hat{w}_1^{k+1}$, and using $\hat{u}_1^k = \frac{c_1}{s-b_1}\hat{u}_2^k$ from the first subsystem of equations, we get

$$\hat{w}_1^{k+1} = \frac{a_1(s-b_3)}{(s-b_3)(s-b_2)-a_2c_2}\hat{u}_1^k = \frac{a_1(s-b_3)}{(s-b_3)(s-b_2)-a_2c_2} \cdot \frac{c_1}{s-b_1}\hat{u}_2^k. \tag{4.19}$$

Inserting (4.19) at iteration k into (4.18), we find a relation over two iteration steps of the classical WR algorithm,

$$\hat{u}_2^{k+1} = \rho_{cla}(s, \boldsymbol{a}, \boldsymbol{b}, \boldsymbol{c})\hat{u}_2^{k-1},$$

where the convergence factor ρ_{cla} of the classical WR algorithm with overlap is given by

$$\rho_{cla}(s, \boldsymbol{a}, \boldsymbol{b}, \boldsymbol{c}) = \frac{a_1c_1}{(s-b_1)(s-b_2)-a_1c_1} \cdot \frac{a_2c_2}{(s-b_3)(s-b_2)-a_2c_2}. \tag{4.20}$$

The same result holds for $\hat{w}_1^{k+1}$, and by induction we obtain $\hat{u}_2^{2k} = (\rho_{cla})^k \hat{u}_2^0$ and $\hat{w}_1^{2k} = (\rho_{cla})^k \hat{w}_1^0$.

By Theorem 1.4, the convergence factor ρ_{cla} in (4.20) is an analytic function of $s = \eta + i\omega$ in the right half of the complex plane, $\eta > 0$, since the denominator in (4.20) does not vanish, because $a_i > 0$, $c_i < 0$, and $b_i < 0$ for the circuit we consider. In addition, the limit of ρ_{cla} for $s = re^{i\theta}$, $-\pi/2 < \theta < \pi/2$, as $r \to \infty$ is zero. Therefore, by Theorem 1.5, the maximum of $|\rho_{cla}|$ is attained on the boundary at $\eta = 0$. With the simplifying assumptions $c_1 = -a_2$, $c_2 = -a_1$, and $b_3 = b_1$, the classical convergence factor ρ_{cla} in (4.20) with overlap is given by

$$\rho_{cla}(s, \boldsymbol{a}, \boldsymbol{b}) = \left(\frac{a_1 a_2}{(s-b_1)(s-b_2)+a_1 a_2}\right)^2,$$

and it is equal to ρ_{cla} in (4.11) without overlap squared. Note that $(s - b_3)$ in the numerator is cancelled with $(s - b_1)$ in the denominator in ρ_{cla} in (4.11) after the simplifying assumptions. Therefore, Lemma 4.1 holds for ρ_{cla} with overlap, and hence, the classical WR algorithm with overlap still might not converge. An example of the convergence factor as a function of ω for a typical set of transmission line circuit parameters is given in Figure 4.2 on the left hand side, where $R_s = 0.05$. On the right hand side of Figure 4.2 we give another example, where we now take $R_s = 0.5$, and we keep the other circuit elements the same as before. From the graph on the left, we see that the low frequency components in the signal, ω close to zero, will cause difficulties for the algorithm, and slow convergence. On the right, there are even values greater than one, and the classical WR algorithm is not convergent.

4.1.3 An Optimal WR Algorithm without Overlap

Recall that the classical transmission conditions with a cut at an even row were

$$u_3^{k+1} = w_1^k, \quad w_0^{k+1} = u_2^k.$$

From this we see that in the first sub-circuit the voltage u_3 is directly replaced in (4.3) by a voltage source, whereas in the second sub-circuit the current w_0 is directly replaced by a current source. Hence, sub-circuit one passes only current information to sub-circuit two, while sub-circuit two passes only voltage information to sub-circuit

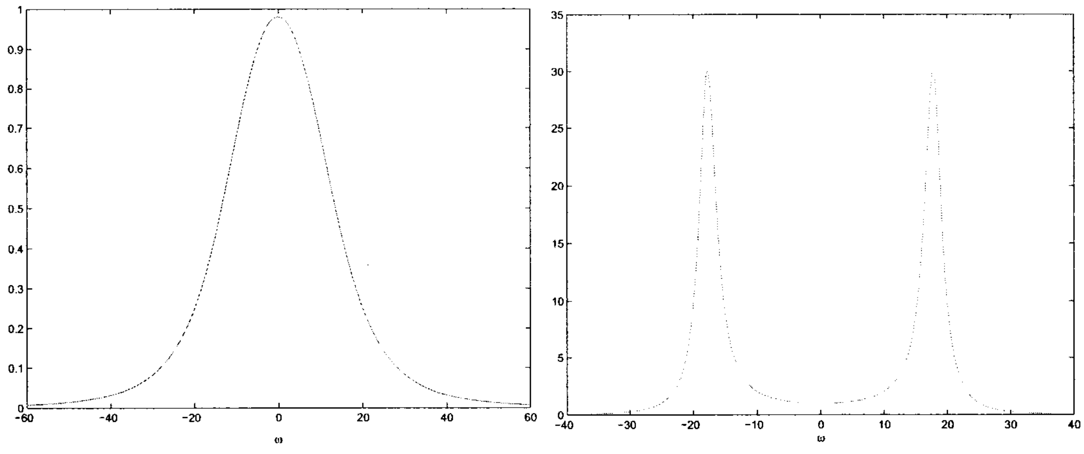

Figure 4.2: Convergence factor for the classical WR algorithm, $|\rho_{cla}(\omega)|$.

one. At convergence we obtain with the classical transmission conditions

$$u_3^\infty = w_1^\infty, \quad w_0^\infty = u_2^\infty. \tag{4.21}$$

Under these conditions, the nodes at the subsystem boundaries assume the converged voltage and current respectively, as expected. For the optimal WR algorithm, with a partition at an even row, we propose transmission conditions which exchange both current and voltage information in both directions,

$$u_3^{k+1} + \alpha u_2^{k+1} = w_1^k + \alpha w_0^k, \quad w_1^{k+1} + \beta w_0^{k+1} = u_3^k + \beta u_2^k. \tag{4.22}$$

By comparing (4.4) with the new transmission conditions (4.22), we now exchange a combination of voltage and current in both directions, and we introduced weighting factors α and β which can be used to optimize the performance of the new WR algorithm. Note that the new transmission conditions lead to the correct solution of the underlying TEM circuit equations if the new WR algorithm converges and if $\alpha \neq \beta$, because then at convergence we have from (4.22)

$$\begin{aligned} (u_3^\infty - w_1^\infty) \;+\; \alpha\;(u_2^\infty - w_0^\infty) \;&=\; 0, \\ (u_3^\infty - w_1^\infty) \;+\; \beta\;(u_2^\infty - w_0^\infty) \;&=\; 0, \end{aligned}$$

and the determinant of this system is different from zero if $\alpha \neq \beta$, and hence the old transmission conditions (4.4) are implied by the new ones. The new WR algorithm is

$$\begin{aligned} \dot{\boldsymbol{u}}^{k+1} &= \begin{bmatrix} b_1 & c_1 \\ a_1 & b_2 - c_2\alpha \end{bmatrix} \boldsymbol{u}^{k+1} + \begin{pmatrix} f_1 \\ f_2 \end{pmatrix} + \begin{pmatrix} 0 \\ c_2(w_1^k + \alpha w_0^k) \end{pmatrix}, \\ \dot{w}_1^{k+1} &= (b_3 - \tfrac{a_2}{\beta}) w_1^{k+1} + f_3 + \tfrac{a_2}{\beta}(\beta u_2^k + u_3^k), \end{aligned} \tag{4.23}$$

where the values u_3^k and w_0^k are determined by the transmission conditions (4.22). Taking the Laplace transform as we did before, we find from the circuit equation for the first subsystem after some algebra,

$$\hat{u}_2^{k+1} = F_1(w_1^k + \alpha w_0^k), \quad F_1 = \frac{c_2(s - b_1)}{(s - b_1)(s - b_2 + c_2\alpha) - a_1 c_1}, \tag{4.24}$$

and similarly from the circuit equation for the second subsystem

$$\hat{w}_1^{k+1} = F_2(u_3^k + \beta u_2^k), \quad F_2 = \frac{a_2}{\beta(s - b_3) + a_2}. \tag{4.25}$$

Using the transmission condition

$$\hat{w}_1^{k+1} + \beta \hat{w}_0^{k+1} = \hat{u}_3^k + \beta \hat{u}_2^k,$$

together with (4.25), we find

$$\hat{w}_0^{k+1} = \left(\frac{1}{\beta F_2} - \frac{1}{\beta}\right) \hat{w}_1^{k+1},$$

and using this result at step k in (4.24), we find for the first subsystem

$$\hat{u}_2^{k+1} = F_1 \left(1 + \alpha \left(\frac{1}{\beta F_2} - \frac{1}{\beta}\right)\right) \hat{w}_1^k. \tag{4.26}$$

Similarly we find for the second subsystem

$$\hat{w}_1^{k+1} = F_2 \left(\frac{1}{F_1} - \alpha + \beta\right) \hat{u}_2^k. \tag{4.27}$$

Finally, by inserting (4.27) at iteration k into (4.26), we get a relation over two iteration steps of the new WR algorithm,

$$\hat{u}_2^{k+1} = \rho_{opt}(s, \boldsymbol{a}, \boldsymbol{b}, \boldsymbol{c}, \alpha, \beta)\hat{u}_2^{k-1},$$

where the convergence factor of the new WR algorithm is given by

$$\rho_{opt}(s, \boldsymbol{a}, \boldsymbol{b}, \boldsymbol{c}, \alpha, \beta) = F_1 F_2 \left(\tfrac{1}{F_1} - \alpha + \beta\right)\left(1 + \tfrac{\alpha}{\beta F_2} - \tfrac{\alpha}{\beta}\right) = \tfrac{L_1\alpha + C_1}{L_2\alpha + C_2} \cdot \tfrac{L_2\beta + C_2}{L_1\beta + C_1}, \quad (4.28)$$

and we introduced the functions

$$\begin{aligned} L_1 &:= s - b_3, \\ C_1 &:= a_2, \\ L_2 &:= c_2(s - b_1), \\ C_2 &:= s^2 - (b_1 + b_2)s - a_1 c_1 + b_1 b_2, \end{aligned}$$

in order to better show the structure of the convergence factor. The same result also holds for subsystem two, and by induction we obtain as before $\hat{u}_2^{2k} = (\rho_{opt})^k \hat{u}_2^0$ and $\hat{w}_1^{2k} = (\rho_{opt})^k \hat{w}_1^0$. From the convergence factor (4.28), the optimal values of the parameters α and β can be derived.

Theorem 4.1 (Optimal Convergence). *The new WR algorithm (4.23) converges in two iterations, independently of the initial waveforms $\hat{\boldsymbol{u}}^0$ and $\hat{\boldsymbol{w}}^0$, if*

$$\begin{aligned} \hat{\alpha}_{even} = \alpha(s) &= -\tfrac{a_2}{s - b_3}, \\ \hat{\beta}_{even} = \beta(s) &= -\tfrac{s^2 - (b_1 + b_2)s + b_1 b_2 - a_1 c_1}{c_2(s - b_1)}. \end{aligned} \quad (4.29)$$

Proof. The convergence factor vanishes if we insert (4.29) into ρ_{opt} given by (4.28). Hence, $\hat{u}_2^2$ and $\hat{w}_1^2$ are identically zero, independently of $\hat{u}_2^0$ and $\hat{w}_1^0$. □

For the case with a partition at an odd row, similar results hold. However in this case, sub-circuit one passes only voltage information to sub-circuit two, while sub-circuit two passes only current information to sub-circuit one. The new transmission conditions which exchange both current and voltage information in both directions are

$$u_2^{k+1} + \alpha u_1^{k+1} = w_1^k + \alpha w_0^k, \quad w_1^{k+1} + \beta w_0^{k+1} = u_2^k + \beta u_1^k, \tag{4.30}$$

and the new WR algorithm is

$$\begin{aligned} \dot{u}_1^{k+1} &= (b_1 - c_1\alpha)u_1^{k+1} + f_1 + c_1(w_1^k + \alpha w_0^k), \\ \dot{\boldsymbol{w}}^{k+1} &= \begin{bmatrix} b_2 - \frac{a_1}{\beta} & c_2 \\ a_2 & b_3 \end{bmatrix} \boldsymbol{w}^{k+1} + \begin{pmatrix} f_2 \\ f_3 \end{pmatrix} + \begin{pmatrix} \frac{a_1}{\beta}(\beta u_1^k + u_2^k) \\ 0 \end{pmatrix}, \end{aligned} \tag{4.31}$$

where the values u_2^k and w_0^k are determined by the transmission conditions (4.30). Using similar computations as those used with the cut at an even row, the convergence factor of the new WR algorithm is given by

$$\rho_{opt}(s, \boldsymbol{a}, \boldsymbol{b}, \boldsymbol{c}, \alpha, \beta) = F_1F_2\left(\frac{1}{F_1} - \alpha + \beta\right)\left(1 + \frac{\alpha}{\beta F_2} - \frac{\alpha}{\beta}\right) = \frac{L_1\beta + C_1}{L_2\beta + C_2} \cdot \frac{L_2\alpha + C_2}{L_1\alpha + C_1}, \tag{4.32}$$

where

$$\begin{aligned} L_1 &:= c_1, \\ C_1 &:= s - b_1, \\ L_2 &:= s^2 - (b_3 + b_2)s + b_2b_3 - c_2a_2, \\ C_2 &:= a_1(s - b_3). \end{aligned}$$

The optimal values of α and β are given in the following theorem.

Theorem 4.2 (Optimal Convergence). *The new WR algorithm (4.31) converges in two iterations, independently of the initial waveforms $\hat{\mathbf{u}}^0$ and $\hat{\mathbf{w}}^0$, if*

$$\begin{aligned} \hat{\alpha}_{odd} = \alpha(s) &= -\frac{a_1(s-b_3)}{s^2-(b_3+b_2)s+b_2b_3-c_2a_2}, \\ \hat{\beta}_{odd} = \beta(s) &= -\frac{s-b_1}{c_1}. \end{aligned} \tag{4.33}$$

Proof. The proof is similar to the proof of Theorem 4.1. □

Remark 4.1. *Theorems 4.1 and 4.2 imply a relation between the optimal parameters obtained with a cut at an even row and those obtained with a cut at an odd row. Assuming that the elements in the vectors* $\boldsymbol{a}$, $\boldsymbol{b}$, *and* $\boldsymbol{c}$ *satisfy the simplifying assumptions* $c_2 = -a_1$, $c_1 = -a_2$, *and* $b_3 = b_1$, *the optimal parameters satisfy*

$$\hat{\alpha}_{even} = \frac{-1}{\hat{\beta}_{odd}}, \quad \hat{\beta}_{even} = \frac{-1}{\hat{\alpha}_{odd}}.$$

4.1.4 An Optimal WR algorithm with Overlap

We now analyze an optimal WR algorithm with overlap at the second row. Using the new transmission conditions

$$u_3^{k+1} + \alpha u_2^{k+1} = w_2^k + \alpha w_1^k, \quad w_1^{k+1} + \beta w_0^{k+1} = u_2^k + \beta u_1^k, \tag{4.34}$$

the new WR algorithm with overlap is

$$\begin{aligned} \dot{\boldsymbol{u}}^{k+1} &= \begin{bmatrix} b_1 & c_1 \\ a_1 & b_2 - c_2\alpha \end{bmatrix} \boldsymbol{u}^{k+1} + \begin{pmatrix} f_1 \\ f_2 \end{pmatrix} + \begin{pmatrix} 0 \\ c_2(w_2^k + \alpha w_1^k) \end{pmatrix}, \\ \dot{\boldsymbol{w}}^{k+1} &= \begin{bmatrix} b_2 - \frac{a_1}{\beta} & c_2 \\ a_2 & b_3 \end{bmatrix} \boldsymbol{w}^{k+1} + \begin{pmatrix} f_2 \\ f_3 \end{pmatrix} + \begin{pmatrix} \frac{a_1}{\beta}(u_2^k + \beta u_1^k) \\ 0 \end{pmatrix}; \end{aligned} \tag{4.35}$$

where the values u_3^k and w_0^k are determined by the transmission conditions (4.34). The Laplace transform applied to the homogeneous problem of (4.35) implies

$$\begin{aligned} s\hat{\boldsymbol{u}}^{k+1} &= \begin{bmatrix} b_1 & c_1 \\ a_1 & b_2 - c_2\alpha \end{bmatrix} \hat{\boldsymbol{u}}^{k+1} + \begin{pmatrix} 0 \\ c_2(\hat{w}_2^k + \alpha \hat{w}_1^k) \end{pmatrix}, \\ s\hat{\boldsymbol{w}}^{k+1} &= \begin{bmatrix} b_2 - \frac{a_1}{\beta} & c_2 \\ a_2 & b_3 \end{bmatrix} \hat{\boldsymbol{w}}^{k+1} + \begin{pmatrix} \frac{a_1}{\beta}(\hat{u}_2^k + \beta \hat{u}_1^k) \\ 0 \end{pmatrix}. \end{aligned} \tag{4.36}$$

From the circuit equation for the first subsystem, after some algebra, we find

$$\hat{u}_2^{k+1} = F_1(\hat{w}_2^k + \alpha \hat{w}_1^k), \quad F_1 = \frac{c_2(s - b_1)}{(s - b_1)(s - b_2 + c_2\alpha) - a_1 c_1}, \tag{4.37}$$

and similarly from the circuit equation for the second subsystem, we have

$$\hat{w}_1^{k+1} = F_2(\hat{u}_2^k + \beta\hat{u}_1^k), \quad F_2 = \frac{a_1(s-b_3)}{\beta((s-b_2)(s-b_3) - a_2c_2) + a_1(s-b_3)}. \tag{4.38}$$

Using the second transmission condition in (4.34), together with (4.38), we find

$$\hat{w}_0^{k+1} = \left(\frac{1}{\beta F_2} - \frac{1}{\beta}\right)\hat{w}_1^{k+1}.$$

Furthermore, using the equation at the interface in the second subsystem in (4.14) at step k, we get $\hat{w}_2^k$ in terms of $\hat{w}_1^k$ and $\hat{w}_0^k$, which is given by

$$\hat{w}_2^k = \frac{1}{c_2}((s-b_2)\hat{w}_1^k - a_1\hat{w}_0^k).$$

Now substituting at step k from above into (4.37), we find for the first subsystem

$$\hat{u}_2^{k+1} = F_1\left(\frac{s-b_2}{c_2} - \frac{a_1}{c_2}\left(\frac{1}{\beta F_2} - \frac{1}{\beta}\right) + \alpha\right)\hat{w}_1^k. \tag{4.39}$$

Similarly we find for the second subsystem

$$\hat{w}_1^{k+1} = F_2\left(1 + \frac{\beta}{a_1}(s-b_2) - \frac{\beta c_2}{a_1}\left(\frac{1}{F_1} - \alpha\right)\right)\hat{u}_2^k. \tag{4.40}$$

Finally, by inserting (4.40) at iteration k into (4.39), we get a relation over two iteration steps of the new WR algorithm,

$$\hat{u}_2^{k+1} = \rho_{opt}(s, \boldsymbol{a}, \boldsymbol{b}, \boldsymbol{c}, \alpha, \beta)\hat{u}_2^{k-1},$$

where the convergence factor is given by

$$\begin{aligned} &\rho_{opt}(s, \boldsymbol{a}, \boldsymbol{b}, \boldsymbol{c}, \alpha, \beta) \\ &= F_1F_2\left(\tfrac{s-b_2}{c_2} - \tfrac{a_1}{c_2}\left(\tfrac{1}{\beta F_2} - \tfrac{1}{\beta}\right) + \alpha\right)\left(1 + \tfrac{\beta}{a_1}(s-b_2) - \tfrac{\beta c_2}{a_1}\left(\tfrac{1}{F_1} - \alpha\right)\right) \\ &= \tfrac{a_1a_2 + \alpha a_1(s-b_3)}{(s-b_1)(s-b_2+\alpha c_2) - a_1c_1} \cdot \tfrac{\beta c_1c_2 + c_2(s-b_1)}{(s-b_3)(\beta(s-b_2)+a_1) - \beta a_2c_2}. \end{aligned} \tag{4.41}$$

Alternatively, one can just substitute $\hat{w}_2^k = \frac{a_2}{s-b_3}\hat{w}_1^k$ from the second equation in the second subsystem in (4.36) into (4.37), and $\hat{u}_1^k = \frac{c_1}{s-b_1}\hat{u}_2^k$ from the first equation in the first subsystem in (4.36) into (4.38), to obtain

$$\hat{u}_2^{k+1} = F_1(\frac{a_2}{s-b_3} + \alpha)\hat{w}_1^k, \quad \hat{w}_1^{k+1} = F_2(\frac{c_1\beta}{s-b_1} + 1)\hat{u}_2^k,$$

and then by substituting the second equation into the first one above at step k, we get

$$\hat{u}_2^{k+1} = \rho_{opt}(s, \boldsymbol{a}, \boldsymbol{b}, \boldsymbol{c}, \alpha, \beta)\hat{u}_2^{k-1},$$

where the convergence factor is given by

$$\rho_{opt}(s, \boldsymbol{a}, \boldsymbol{b}, \boldsymbol{c}, \alpha, \beta) = F_1 F_2 \left(\frac{a_2}{s - b_3} + \alpha\right)\left(\frac{c_1\beta}{s - b_1} + 1\right),$$

and after simplifying we get the same convergence factor as in (4.41).

Theorem 4.3 (Optimal Convergence). *The new WR algorithm (4.35) converges in two iterations, independently of the initial waveforms $\hat{\boldsymbol{u}}^0$ and $\hat{\boldsymbol{w}}^0$, if*

$$\begin{aligned} \hat{\alpha} = \alpha(s) &= -\tfrac{a_2}{s-b_3}, \\ \hat{\beta} = \beta(s) &= -\tfrac{s-b_1}{c_1}. \end{aligned} \tag{4.42}$$

Proof. The proof is similar to the proof of Theorem 4.1. □

In the next subsection, we will choose the approximation by a constant for the optimal transmission conditions from Theorem 4.3 in order to obtain a practical WR algorithm.

4.1.5 An Optimized WR algorithm with Overlap and Constant Approximation

We approximate the optimal parameters (4.42) in the transmission conditions by constants. The low frequency constant approximation using a Taylor expansion about $s = 0$ is given by

$$\alpha_T = \frac{a_2}{b_3}, \quad \beta_T = \frac{b_1}{c_1}.$$

Next, we show that ρ_{opt} in (4.41) is analytic in the right half of the complex plane, and thus the maximum of its modulus is attained on the boundary, by the maximum principle, Theorem 1.5. We will need

Theorem 4.4 (Vieta's formulas). *Let the n^{th} degree polynomial $P(x)$ be given by*

$$P(x) = x^n + a_1 x^{n-1} + \ldots + a_k x^{n-k} + \ldots + a_n.$$

Assuming $P(x)$ has n roots c_1, $c_2, \ldots,$ c_n, where we allow the possibility of multiple roots, we obtain the following expressions for the coefficients a_i in terms of the roots c_i:

$$\begin{aligned} a_1 &= -(c_1 + c_2 + \ldots + c_n), \\ a_k &= (-1)^k \sum_{i_1 < i_2 < \ldots < i_k} c_{i_1} c_{i_2} \ldots c_{i_k}, \\ a_n &= (-1)^n c_1 c_2 \ldots c_n. \end{aligned}$$

If the leading coefficient is $a_0 \neq 1$, then the same formulas give expressions for the ratios $\frac{a_i}{a_0}$.

Proof. See [39]. □

Now we give the conditions for analyticity of ρ_{opt} in the following lemma.

Lemma 4.2. *If $a_i > 0$, $c_i < 0$, and $b_i < 0$, and*

$$\alpha < 0, \quad \beta > 0, \tag{4.43}$$

then the convergence factor ρ_{opt} in (4.41) is an analytic function in the right half of the complex plane, $s = \eta + i\omega$, $\eta > 0$.

Proof. By Theorem 1.4, we need to show that the denominators have no zeros in the right half of the complex plane. We show the proof only for one quotient, the proof for the other one is similar. We consider the quotient with β in (4.41), whose denominator is

$$\beta s^2 + ((-b_3 - b_2)\beta + a_1)s + (b_2 b_3 - c_2 a_2)\beta - a_1 b_3.$$

By Vieta's formulas, Theorem 4.4, the product of the zeros satisfies $s_1 s_2 = b_2 b_3 - c_2 a_2 - a_1 b_3/\beta > 0$, and the sum satisfies $s_1 + s_2 = b_3 + b_2 - a_1/\beta < 0$, if $\beta > 0$. Hence,

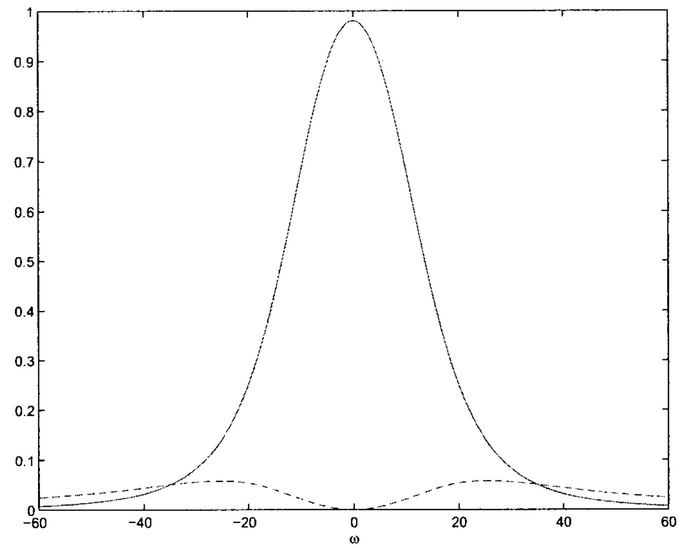

Figure 4.3: Convergence factor $|\rho_{cla}(\omega)|$ (solid line) versus optimized convergence factor $|\rho_{opt}(\omega, \alpha_T)|$ (dashed line).

if both zeros are real, then they must be negative. If they are complex conjugate, then their real part is identical and hence must be negative as well by the inequality on their sum. Thus there is no pole in the right half of the complex plane. $\square$

Note that with the simplifying assumptions $c_1 = -a_2$, $c_2 = -a_1$, and $b_3 = b_1$, we obtain $\beta_T = -\frac{1}{\alpha_T}$, and for b_i, $c_i < 0$, and $a_i > 0$, we get $\alpha_T < 0$, and $\beta_T > 0$.

In Figure 4.3 we show the modulus of the convergence factor of the classical WR algorithm and the modulus of the optimized convergence factor using the Taylor approximation. We observe the better convergence we obtain from the optimized convergence factor with the Taylor approximation over the classical one.

Taking $s = re^{i\theta}$, $-\pi/2 < \theta < \pi/2$, the limit of ρ_{opt} in all directions, as $r \to \infty$ is zero. Since ρ_{opt} is analytic in the right half of the complex plane, we can apply the maximum principle for analytic functions, Theorem 1.5, and since we have the same limit at infinity in all directions, the maximum of $|\rho_{opt}(s)|$ for $s = \eta + i\omega$, $\eta > 0$, is attained on the boundary at $\eta = 0$. Furthermore, the modulus of the convergence factor (4.41) for $s = i\omega$ depends on ω^2 only, since from the first quotient we have that $|a_1a_2+\alpha a_1(s-b_3)|$ and $|(s-b_1)((s-b_2)+\alpha c_2)-a_1c_1|$ both depend on ω^2 only, and the same holds for the second quotient. Therefore, it suffices to optimize for nonnegative frequencies, $\omega \geq 0$.

From the optimal choice (4.42) with overlap, and the simplifying assumptions $c_1 = -a_2$, $c_2 = -a_1$, and $b_3 = b_1$, we have $\beta_{opt} = -\frac{1}{\alpha_{opt}}$, which motivates us to assume $\beta = -\frac{1}{\alpha}$ in order to simplify the optimization process. Note that the optimal choices (4.29) and (4.33) which are obtained using the partitioning without overlap do not imply such a simple relation, even with the same simplifying assumptions. They imply relations which are operators in s.

Remark 4.2. *With the simplifying assumptions $c_1 = -a_2$, $c_2 = -a_1$, and $b_3 = b_1$, the optimal convergence factor without overlap with a cut at an even row (4.28) and with the choice of parameters $\beta = -\alpha + \frac{s-b_2}{a_1}$, which is motivated by the fact that the optimal values (4.29) satisfy this relation, is equal to the optimal convergence factor with overlap (4.41), where the overlap is at an even row, and with the choice of parameters $\beta = -\frac{1}{\alpha}$.*

We now introduce an optimization process for the new WR algorithm with overlap (4.35) to get a better constant approximation, which will lead to much faster overall convergence. Moreover, it allows us to convert a divergent WR algorithm into a convergent one. For the rest of this subsection, we will look for a solution to the min-max problem

$$\min_{\alpha<0,\beta>0} \left(\max_{\omega\geq 0} |\rho_{opt}(\omega, \boldsymbol{a}, \boldsymbol{b}, \boldsymbol{c}, \alpha, \beta)| \right). \tag{4.44}$$

To further analyze the convergence factor (4.41), we assume $c_1 = -a_2$, $c_2 = -a_1$, and $b_3 = b_1$, and we choose $\beta = -\frac{1}{\alpha}$. This will simplify the optimization process.

Now, we investigate the best choice for α. With the simplifying assumptions, the

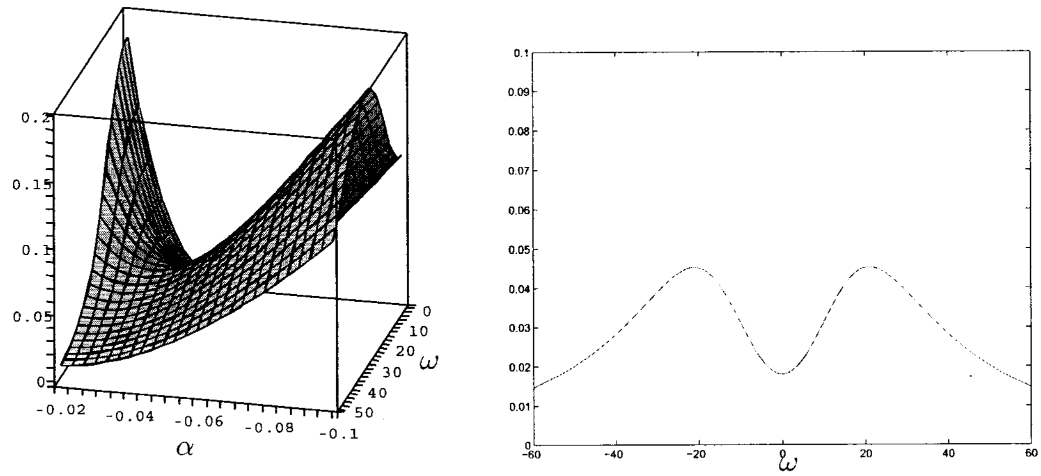

Figure 4.4: Left: convergence factor $|\rho_{opt}(\omega, \alpha)|$. Right: optimized convergence factor $|\rho_{opt}(\omega, \alpha^*)|$.

convergence factor (4.41) becomes

$$\rho_{opt}(s, a_1, a_2, b_1, b_2, \alpha) = \left(\frac{a_1(a_2 + \alpha(s - b_1))}{(s - b_1)(s - b_2 - \alpha a_1) + a_1 a_2} \right)^2. \tag{4.45}$$

We show on the left hand side of Figure 4.4 the function $|\rho_{opt}(\omega, \alpha)|$ for the numerical example in Subsection 4.1.6. One can observe the solution of the optimization problem, which is the minimum with respect to α of the maximum with respect to ω of $|\rho_{opt}|$. In this example, the numerically optimized α is equal to $\alpha^* = -0.0381$, and this leads to the convergence factor shown on the right hand side of Figure 4.4.

To obtain an explicit formula for the constant approximation of the optimal parameter we use asymptotics: we notice that a_1 is much bigger than b_1, which is in turn much bigger than a_2 and b_2 in a typical transmission line circuit. The typical transmission line circuit parameters per unit length are: $L = 4.95e - 3$ μH/cm, $C = 0.63$ pF/cm, and $R = 0.5e - 3$ kOhms/cm. In addition, we have $R_s = R_L = 0.05$ kOhms. The total resistance for resistors connected in series is obtained by adding their values, and the same holds for inductors connected in series. For capacitors it is different, where now the total capacitance of capacitors connected in parallel is obtained by adding their values. Therefore, assuming we have n sections in a 1 cm transmission line circuit, each section has $\frac{4.95e-3}{n}$ μH of inductance, $\frac{0.5e-3}{n}$ kOhms of resistance, and $\frac{0.63}{n}$ pF of capacitance, and thus we have

$$a_1 = n\frac{1}{4.95e-3},\ b_1 = -n\frac{1}{0.0315},\ a_2 = n\frac{1}{0.63},\ b_2 = -\frac{0.5e-3}{4.95e-3}. \tag{4.46}$$

Note that n is a small number for the finite size circuit case we are analyzing and can not be very large. We therefore use a two scale expansion, for ϵ small

$$a_1 = O\left(\frac{1}{\epsilon}\right),\ b_1 = O\left(\frac{1}{\sqrt{\epsilon}}\right),\ a_2 = O(1),\ b_2 = O(1). \tag{4.47}$$

The modulus of the convergence factor ρ_{opt} in (4.45) is given by

$$R_0(\omega, a_1, a_2, b_1, b_2, \alpha) = \frac{P_1(\omega, a_1, a_2, b_1, b_2, \alpha)}{P_2(\omega, a_1, a_2, b_1, b_2, \alpha)},$$

where

$$\begin{aligned} P_1 &:= a_1^2(a_2^2 - 2a_2\alpha b_1 + \alpha^2 b_1^2 + \alpha^2\omega^2), \\ P_2 &:= \omega^4 - 2\omega^2 a_1 a_2 + a_1^2\alpha^2 b_1^2 + 2a_1^2 a_2\alpha b_1 + 2\alpha a_1 b_1^2 b_2 + a_1^2 a_2^2 \\ &\quad + 2a_1 a_2 b_2 b_1 + b_2^2 b_1^2 + \omega^2 b_1^2 + a_1^2\alpha^2\omega^2 + 2\omega^2\alpha a_1 b_2 + b_2^2\omega^2. \end{aligned}$$

Now, we assume $a_1 = n\tilde{a}_1$, $a_2 = n\tilde{a}_2$, $b_1 = n\tilde{b}_1$, $b_2 = n\tilde{b}_2$, and $\omega = n\tilde{\omega}$, where from the typical values in (4.46) we have the typical values

$$\tilde{a}_1 = \frac{1}{4.95e-3},\ \tilde{a}_2 = \frac{1}{0.63},\ \tilde{b}_1 = -\frac{1}{0.0315},\ \tilde{b}_2 = -\frac{0.5e-3}{4.95e-3}\cdot\frac{1}{n}. \tag{4.48}$$

Note that n which appears in $\tilde{b}_2$ is again the number of sections which is assumed to be a fixed number and does not depend on ϵ. Moreover, $\tilde{\omega} \geq 0$ is a new variable. Then, after factorizing n^4 from the numerator and denominator of R_0, the modulus of the convergence factor R_0 becomes

$$\tilde{R}_0(\tilde{\omega}, \tilde{a}_1, \tilde{a}_2, \tilde{b}_1, \tilde{b}_2, \alpha) = \frac{\tilde{P}_1(\tilde{\omega}, \tilde{a}_1, \tilde{a}_2, \tilde{b}_1, \tilde{b}_2, \alpha)}{\tilde{P}_2(\tilde{\omega}, \tilde{a}_1, \tilde{a}_2, \tilde{b}_1, \tilde{b}_2, \alpha)}, \tag{4.49}$$

where

$$\tilde{P}_1 := \tilde{a}_1^2(\tilde{a}_2^2 - 2\tilde{a}_2\alpha\tilde{b}_1 + \alpha^2\tilde{b}_1^2 + \alpha^2\tilde{\omega}^2),$$
$$\tilde{P}_2 := \tilde{\omega}^4 - 2\tilde{\omega}^2\tilde{a}_1\tilde{a}_2 + \tilde{a}_1^2\alpha^2\tilde{b}_1^2 + 2\tilde{a}_1^2\tilde{a}_2\alpha\tilde{b}_1 + 2\alpha\tilde{a}_1\tilde{b}_1^2\tilde{b}_2 + \tilde{a}_1^2\tilde{a}_2^2$$
$$+2\tilde{a}_1\tilde{a}_2\tilde{b}_2\tilde{b}_1 + \tilde{b}_2^2\tilde{b}_1^2 + \tilde{\omega}^2\tilde{b}_1^2 + \tilde{a}_1^2\alpha^2\tilde{\omega}^2 + 2\tilde{\omega}^2\alpha\tilde{a}_1\tilde{b}_2 + \tilde{b}_2^2\tilde{\omega}^2.$$

Numerical experiments show that the solution of the min-max problem (4.44) with the choice $\beta = -\frac{1}{\alpha}$, is characterized by the system of equations

$$\nabla_{\alpha,\tilde{\omega}}\tilde{R}_0(\tilde{\omega},\tilde{a}_1,\tilde{a}_2,\tilde{b}_1,\tilde{b}_2,\alpha) = 0 \Leftrightarrow \begin{cases} \frac{\partial \tilde{R}_0}{\partial \tilde{\omega}}(\bar{\tilde{\omega}},\tilde{a}_1,\tilde{a}_2,\tilde{b}_1,\tilde{b}_2,\alpha^*) = 0, \\ \frac{\partial \tilde{R}_0}{\partial \alpha}(\bar{\tilde{\omega}},\tilde{a}_1,\tilde{a}_2,\tilde{b}_1,\tilde{b}_2,\alpha^*) = 0, \end{cases} \tag{4.50}$$

where $\tilde{R}_0$ is given in (4.49), and $\bar{\tilde{\omega}}$ is the interior maximum of $\tilde{R}_0$. Note that by assuming $\bar{\tilde{\omega}}$ to be an interior maximum of $\tilde{R}_0$, where $\frac{\partial \tilde{R}_0}{\partial \tilde{\omega}}(\bar{\tilde{\omega}},\tilde{a}_1,\tilde{a}_2,\tilde{b}_1,\tilde{b}_2,\alpha) = 0$, the min-max problem becomes

$$\min_{\alpha<0}\left(\tilde{R}_0(\bar{\tilde{\omega}}(\alpha),\tilde{a}_1,\tilde{a}_2,\tilde{b}_1,\tilde{b}_2,\alpha)\right),$$

and thus

$$\frac{\partial \tilde{R}_0}{\partial \alpha}(\bar{\tilde{\omega}},\tilde{a}_1,\tilde{a}_2,\tilde{b}_1,\tilde{b}_2,\alpha) + \frac{\partial \tilde{R}_0}{\partial \tilde{\omega}}(\bar{\tilde{\omega}},\tilde{a}_1,\tilde{a}_2,\tilde{b}_1,\tilde{b}_2,\alpha)\frac{\partial \bar{\tilde{\omega}}}{\partial \alpha} = 0$$

implies

$$\frac{\partial \tilde{R}_0}{\partial \alpha}(\bar{\tilde{\omega}},\tilde{a}_1,\tilde{a}_2,\tilde{b}_1,\tilde{b}_2,\alpha) = 0,$$

which gives the extrema of $\tilde{R}_0(\bar{\tilde{\omega}},\tilde{a}_1,\tilde{a}_2,\tilde{b}_1,\tilde{b}_2,\alpha)$ in α.

A partial derivative of $\tilde{R}_0$ with respect to $\tilde{\omega}$ shows that the roots of the polynomial

$$\begin{aligned} P(\tilde{\omega},\alpha) = \; & \tilde{\omega}(-2\tilde{a}_1^2\alpha^2\tilde{\omega}^4 + 2\tilde{a}_1^2(4\tilde{a}_2\alpha\tilde{b}_1 - 2\alpha^2\tilde{b}_1^2 - 2\tilde{a}_2^2)\tilde{\omega}^2 \\ & +2\tilde{a}_1^2(2\tilde{a}_2\alpha\tilde{b}_1^3 + 4\alpha^3\tilde{a}_1^2\tilde{a}_2\tilde{b}_1 - 2\tilde{a}_2^2\alpha\tilde{a}_1\tilde{b}_2 - \tilde{a}_2^2\tilde{b}_2^2 - 4\tilde{a}_2^2\alpha\tilde{b}_1\tilde{a}_1 + 2\tilde{a}_2\alpha\tilde{b}_1\tilde{b}_2^2 \\ & +2\alpha^2\tilde{b}_1^2\tilde{a}_1\tilde{a}_2 - \alpha^2\tilde{b}_1^4 + 2\tilde{a}_2^3\tilde{a}_1 - \tilde{a}_2^2\tilde{b}_1^2 + 6\alpha^2\tilde{a}_1\tilde{a}_2\tilde{b}_2\tilde{b}_1) \end{aligned} \tag{4.51}$$

give the extrema of $\tilde{R}_0$ in $\tilde{\omega}$. Since $P(\tilde{\omega},\alpha)$ is a product of $\tilde{\omega}$ and a bi-quadratic polynomial in $\tilde{\omega}$ with real coefficients, it has at most two positive roots, in addition to the root $\tilde{\omega} = 0$. Hence, for $\tilde{\omega} > 0$, $\tilde{R}_0$ can have at most one interior maximum which is denoted by $\overline{\tilde{\omega}}$. A partial derivative of $\tilde{R}_0$ with respect to α shows that the roots of the polynomial

$$\begin{aligned} Q(\alpha,\tilde{\omega}) = \; & -2\tilde{a}_1^2(-2\tilde{a}_2\tilde{b}_1^3\tilde{a}_1^2 - 2\tilde{a}_2\tilde{b}_1\tilde{a}_1^2\tilde{\omega}^2 - \tilde{b}_1^4\tilde{a}_1\tilde{b}_2 - \tilde{\omega}^4\tilde{a}_1\tilde{b}_2 - 2\tilde{b}_1^2\tilde{\omega}^2\tilde{a}_1\tilde{b}_2)\alpha^2 \\ & -2\tilde{a}_1^2(-\tilde{b}_1^4\tilde{b}_2^2 - \tilde{b}_1^4\tilde{\omega}^2 - \tilde{\omega}^4\tilde{b}_2^2 - \tilde{\omega}^6 - 2\tilde{a}_2\tilde{b}_1^3\tilde{a}_1\tilde{b}_2 - 2\tilde{b}_1^2\tilde{b}_2^2\tilde{\omega}^2 - 2\tilde{a}_2\tilde{b}_1\tilde{\omega}^2\tilde{a}_1\tilde{b}_2 \\ & -2\tilde{b}_1^2\tilde{\omega}^4 + 2\tilde{b}_1^2\tilde{\omega}^2\tilde{a}_1\tilde{a}_2 + 2\tilde{\omega}^4\tilde{a}_1\tilde{a}_2)\alpha \\ & -2\tilde{a}_1^2(\tilde{a}_2\tilde{b}_1\tilde{\omega}^4 - 2\tilde{a}_2^2\tilde{b}_1\tilde{\omega}^2\tilde{a}_1 + \tilde{a}_2\tilde{b}_1\tilde{b}_2^2\tilde{\omega}^2 + 3\tilde{a}_2^2\tilde{b}_1^2\tilde{a}_1\tilde{b}_2 + 2\tilde{a}_2^3\tilde{b}_1\tilde{a}_1^2 \\ & +\tilde{a}_2\tilde{b}_1^3\tilde{b}_2^2 + \tilde{a}_2\tilde{b}_1^3\tilde{\omega}^2 + \tilde{a}_1\tilde{a}_2^2\tilde{\omega}^2\tilde{b}_2) \end{aligned} \tag{4.52}$$

give the extrema of $\tilde{R}_0$ in α. To see that there is indeed a solution for the system in (4.50) for ϵ small, we use the ansatz $\alpha = C_\alpha\epsilon^{\gamma_1}$, and $\overline{\tilde{\omega}} = C_{\tilde{\omega}}\epsilon^{\gamma_2}$. Then, we substitute $\tilde{a}_1$ by $\frac{1}{\epsilon}$ and $\tilde{b}_1$ by $\frac{\tilde{C}}{\sqrt{\epsilon}}$ in $\tilde{R}_0$, and determine the leading asymptotic terms as ϵ goes to zero of the equations in (4.50). This leads to

$$\begin{aligned} P(\overline{\tilde{\omega}},\alpha^*) = \; & -\tfrac{2C_{\tilde{\omega}}}{\epsilon^{9/2}}(C_\alpha^2C_{\tilde{\omega}}^4\epsilon^{2\gamma_1+5\gamma_2+5/2} + 2C_{\tilde{\omega}}^2\tilde{a}_2^2\epsilon^{3\gamma_2+5/2} - 4C_{\tilde{\omega}}^2\tilde{a}_2C_\alpha\tilde{C}\epsilon^{3\gamma_2+2+\gamma_1} \\ & -2\tilde{a}_2^3\epsilon^{\gamma_2+3/2} + 4\tilde{a}_2^2C_\alpha\tilde{C}\epsilon^{\gamma_1+\gamma_2+1} - 2\tilde{a}_2C_\alpha\tilde{C}^3\epsilon^{\gamma_1+\gamma_2+1} \\ & +\tilde{a}_2^2\tilde{C}^2\epsilon^{\gamma_2+3/2} + C_\alpha^2\tilde{C}^4\epsilon^{\gamma_2+2\gamma_1+1/2} - 2C_\alpha^2\tilde{C}^2\tilde{a}_2\epsilon^{\gamma_2+2\gamma_1+1/2} \\ & -4C_\alpha^3\tilde{a}_2\tilde{C}\epsilon^{\gamma_2+3\gamma_1} + 2C_{\tilde{\omega}}^2C_\alpha^2\tilde{C}^2\epsilon^{3\gamma_2+3/2+2\gamma_1}) + \ldots, \\ Q(\alpha^*,\overline{\tilde{\omega}}) = \; & -\tfrac{2}{\epsilon^{11/2}}(2\tilde{a}_2^3\tilde{C}\epsilon - 2\tilde{a}_2\tilde{C}^3C_\alpha^2\epsilon^{2\gamma_1} - C_{\tilde{\omega}}^6C_\alpha\epsilon^{6\gamma_2+\gamma_1+7/2} + \tilde{a}_2\tilde{C}^3C_{\tilde{\omega}}^2\epsilon^{2\gamma_2+2} \\ & +2C_\alpha\tilde{a}_2\tilde{C}^2C_{\tilde{\omega}}^2\epsilon^{2\gamma_2+\gamma_1+3/2} - C_\alpha\tilde{C}^4C_{\tilde{\omega}}^2\epsilon^{2\gamma_2+\gamma_1+3/2} + \tilde{a}_2\tilde{C}C_{\tilde{\omega}}^4\epsilon^{4\gamma_2+3} \\ & -2\tilde{a}_2^2\tilde{C}C_{\tilde{\omega}}^2\epsilon^{2\gamma_2+2} + 2C_{\tilde{\omega}}^4C_\alpha\tilde{a}_2\epsilon^{\gamma_1+4\gamma_2+5/2} - 2\tilde{a}_2\tilde{C}C_\alpha^2C_{\tilde{\omega}}^2\epsilon^{2\gamma_1+2\gamma_2+1} \\ & -2C_\alpha\tilde{C}^2C_{\tilde{\omega}}^4\epsilon^{\gamma_1+4\gamma_2+5/2}) + \ldots. \end{aligned}$$

Equating the exponents in these two equations leads to $\gamma_1 = \frac{1}{2}$ and $\gamma_2 = -\frac{1}{2}$. The constants need to mach as well, and thus we obtain C_α and $C_{\tilde{\omega}}$ by solving the resulting equations, and they will both depend on $\tilde{C}$, which is given by $\tilde{C} := \frac{\tilde{b}_1}{\sqrt{\tilde{a}_1}}$. The resulting leading terms in $Q(\alpha^*,\overline{\tilde{\omega}})$ form a polynomial of degree two in C_α, so by solving

$Q(\alpha^*, \bar{\tilde{\omega}}) = 0$ for C_α, we have C_α in terms of $\tilde{a}_2$, $\tilde{C}$, and $C_{\tilde{\omega}}$,

$$\begin{aligned}
C_\alpha^{\pm} &:= \tfrac{X \pm \sqrt{Y}}{2(2\tilde{a}_2\tilde{C}C_{\tilde{\omega}}^2 + 2\tilde{a}_2\tilde{C}^3)},\\
X &:= 2C_{\tilde{\omega}}^4\tilde{a}_2 - \tilde{C}^4C_{\tilde{\omega}}^2 - C_{\tilde{\omega}}^6 + 2\tilde{C}^2C_{\tilde{\omega}}^2\tilde{a}_2 - 2\tilde{C}^2C_{\tilde{\omega}}^4,\\
Y &:= 16\tilde{a}_2^4\tilde{C}^4 - 12\tilde{C}^4C_{\tilde{\omega}}^6\tilde{a}_2 - 4\tilde{C}^6C_{\tilde{\omega}}^4\tilde{a}_2 - 12C_{\tilde{\omega}}^8\tilde{C}^2\tilde{a}_2 + C_{\tilde{\omega}}^{12} + \tilde{C}^8C_{\tilde{\omega}}^4 + 6\tilde{C}^4C_{\tilde{\omega}}^8\\
&\quad +4C_{\tilde{\omega}}^{10}\tilde{C}^2 + 4C_{\tilde{\omega}}^8\tilde{a}_2^2 + 16C_{\tilde{\omega}}^6\tilde{a}_2^2\tilde{C}^2 + 20\tilde{C}^4C_{\tilde{\omega}}^4\tilde{a}_2^2 + 16\tilde{a}_2^4\tilde{C}^2C_{\tilde{\omega}}^2 - 16\tilde{a}_2^3\tilde{C}^2C_{\tilde{\omega}}^4\\
&\quad +8\tilde{a}_2^2\tilde{C}^6C_{\tilde{\omega}}^2 - 16\tilde{a}_2^3\tilde{C}^4C_{\tilde{\omega}}^2 + 4\tilde{C}^6C_{\tilde{\omega}}^6 - 4C_{\tilde{\omega}}^{10}\tilde{a}_2,
\end{aligned} \tag{4.53}$$

Now substituting C_α^+ into the leading terms in $P(\bar{\tilde{\omega}}, \alpha^*)$ and solving the resulting equation for $C_{\tilde{\omega}}$, the desired solution for $C_{\tilde{\omega}}$ is given by the square root of the zero of a polynomial of degree four which depends on $\tilde{a}_2$ and $\tilde{C}$, and is given by

$$P_4(Z) = 3Z^4 + (4\tilde{C}^2 - 4\tilde{a}_2)Z^3 + (-2\tilde{a}_2\tilde{C}^2 + \tilde{C}^4)Z^2 - 6\tilde{a}_2^2\tilde{C}^2 Z + 2\tilde{a}_2^3\tilde{C}^2 - 2\tilde{C}^4\tilde{a}_2^2.$$

Assuming that $Z(\tilde{a}_2, \tilde{C})$ is a zero of the polynomial P_4 above, we approximate the zero by a Taylor expansion about the point (x_0, y_0), where x_0 and y_0 are the typical values of $\tilde{a}_2$ and $\tilde{C}$ from (4.48) respectively, and thus we obtain

$$Z(\tilde{a}_2, \tilde{C}) = Z(x_0, y_0) + \frac{\partial Z}{\partial \tilde{a}_2}(x_0, y_0)(\tilde{a}_2 - x_0) + \frac{\partial Z}{\partial \tilde{C}}(x_0, y_0)(\tilde{C} - y_0) + \ldots.$$

Now, $P_4(Z(\tilde{a}_2, \tilde{C}), \tilde{a}_2, \tilde{C}) = 0$ implies

$$\begin{aligned}
\tfrac{\partial P_4}{\partial Z} \cdot \tfrac{\partial Z}{\partial \tilde{a}_2} + \tfrac{\partial P_4}{\partial \tilde{a}_2} &= 0,\\
\tfrac{\partial P_4}{\partial Z} \cdot \tfrac{\partial Z}{\partial \tilde{C}} + \tfrac{\partial P_4}{\partial \tilde{C}} &= 0.
\end{aligned}$$

Hence, $\frac{\partial Z}{\partial \tilde{a}_2} = -\frac{\left(\frac{\partial P_4}{\partial \tilde{a}_2}\right)}{\left(\frac{\partial P_4}{\partial Z}\right)}$ and $\frac{\partial Z}{\partial \tilde{C}} = -\frac{\left(\frac{\partial P_4}{\partial \tilde{C}}\right)}{\left(\frac{\partial P_4}{\partial Z}\right)}$. Using the values of x_0 and y_0 from the typical transmission line circuit, and in addition using $Z_0 := Z(x_0, y_0)$, which is the numerical solution of $P_4(Z) = 0$ after substituting x_0 and y_0 into P_4 and is given by $Z_0 = 2.1736$, we find $\frac{\partial Z}{\partial \tilde{a}_2}(x_0, y_0)$ and $\frac{\partial Z}{\partial \tilde{C}}(x_0, y_0)$. Thus the Taylor approximation of the zero is

$$Z(\tilde{a}_2, \tilde{C}) = -0.0343 + 1.3478\tilde{a}_2 - 0.0307\tilde{C},$$

and hence, we find

$$C_{\tilde{\omega}} := \sqrt{-0.0343 + 1.3478\tilde{a}_2 - 0.0307\tilde{C}}.$$

Substituting the approximated $C_{\tilde{\omega}}$ into C_α^+ in (4.53), we obtain C_α^+ in terms of $\tilde{a}_2$ and $\tilde{C}$ only. Finally, we find a Taylor approximation of C_α^+ about the point $(\tilde{a}_2, \tilde{C}) = (x_0, y_0)$ from the typical transmission line circuit, to get the simple result

$$C_\alpha = C_\alpha^+ = -0.4503 - 0.2837\tilde{a}_2 - 0.1604\tilde{C},$$

which is used together with $\alpha = C_\alpha \epsilon^{\gamma_1}$ to obtain α^*,

$$\alpha^* = (-0.4503 - 0.2837\tilde{a}_2 - 0.1604\frac{\tilde{b}_1}{\sqrt{\tilde{a}_1}})\frac{1}{\sqrt{\tilde{a}_1}}. \tag{4.54}$$

Note that $\tilde{b}_2$ does not appear in the asymptotic result for α^*, $\tilde{b}_2$ only appears in higher order terms in the asymptotic expansion.

We choose $R_s = 0.05$ kOhms and $R = 0.5e - 3$ kOhms from the typical transmission line circuit elements, and we vary the circuit elements L_1 and C_1 to plot the optimized α^* from (4.50) and the asymptotic result (4.54) on the left hand side of Figure 4.5. In addition, on the right hand side of Figure 4.5, we plot the maximum of the convergence factor as a function of the circuit elements L_1 and C_1 using the optimized α^* from (4.50) and the asymptotic result (4.54). One can see that the two surfaces of the convergence factors are close.

An example of the convergence factor as a function of the frequency ω is given in Figure 4.6 using the typical transmission line circuit elements from Subsection 4.1.6. On the left hand side of Figure 4.6, we compare the optimized convergence factor with the classical one. On the right hand side, we plot the optimized convergence factor with the numerically optimized value $\alpha^* = -0.0381$, the asymptotic value $\alpha^*_{asy} = -0.0382$ from the result in (4.54), and the low frequency approximation $\alpha_T = -0.05$. All are much better than the classical convergence factor, and one can see that the numerically optimized and asymptotic results are very close.

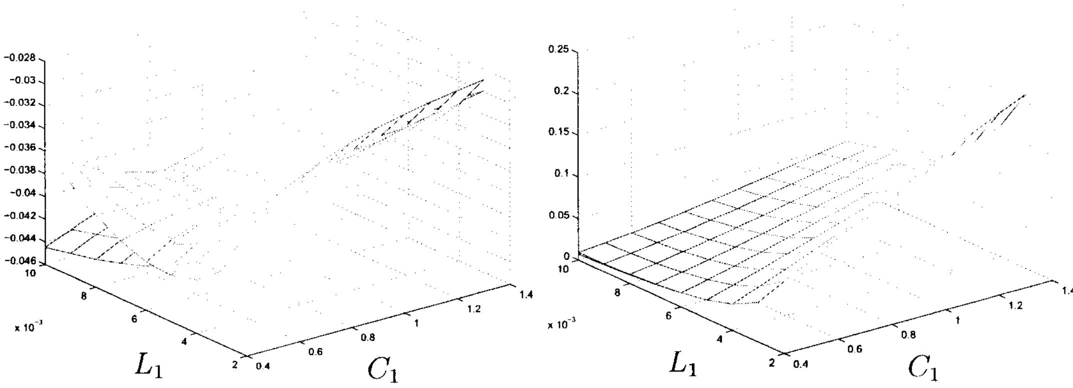

Figure 4.5: Left: optimized α^* from (4.50) versus asymptotic result (4.54). Right: maximum of $|\rho_{opt}(\overline{\omega}, \alpha^*)|$ versus maximum of $|\rho_{opt}(\overline{\omega}, \alpha^*_{asy})|$ as functions of the circuit elements L_1 and C_1.

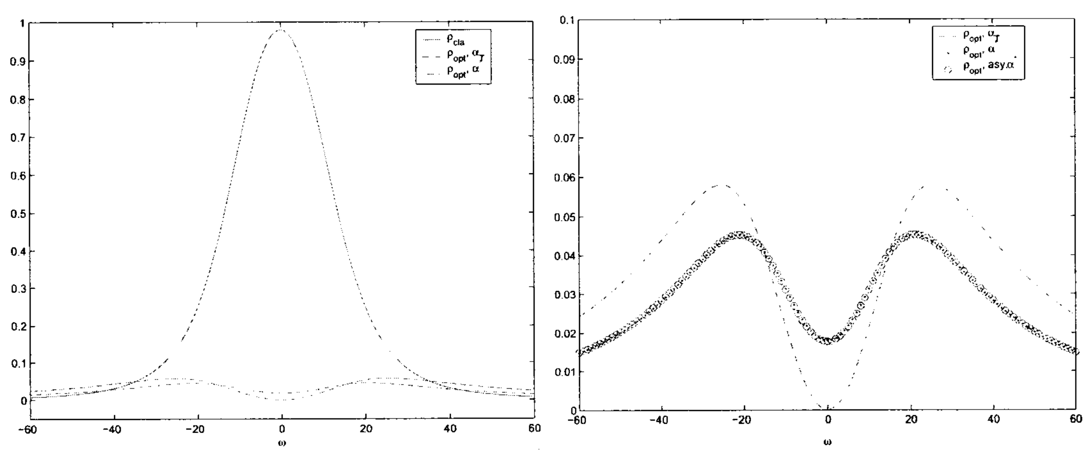

Figure 4.6: Optimized convergence factor versus the classical one on the left. On the right, convergence factor for the optimized WR algorithm applied to the extra small circuit.

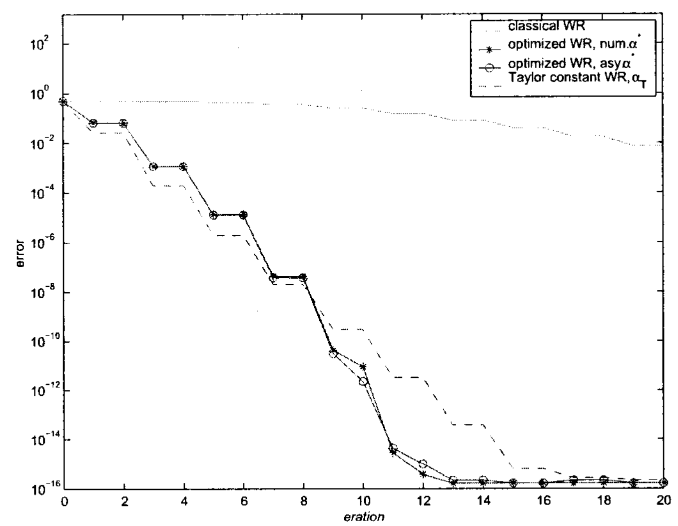

Figure 4.7: Convergence behavior of the classical versus the optimized WR algorithms for extra small transmission line circuit.

4.1.6 Numerical Experiments

We give now a numerical experiment for the extra small transmission line circuit given in Figure 4.1. We use the typical transmission line circuit elements $R_s = R_L = 0.05$ kOhms, $R_1 = 0.5e-3$ kOhms, $C_1 = C_2 = 0.63$ pF, and $L_1 = 4.95e-3$ μH, with source $I_s = 10t$ for $0 < t < 0.1$ and $I_s = 1$ mA for $t \geq 0.1$, and the analysis time interval is $[0, T]$, with $T = 1$ ns. The solution is computed using the backward Euler method, with $\Delta t = \frac{1}{10}$, and zero initial waveforms. The parameters we use are the numerically optimized value $\alpha^* = -0.0381$, the asymptotic value $\alpha^*_{asy} = -0.0382$ from the result in (4.54), and the Taylor approximation $\alpha_T = -0.05$. We also choose $\beta^* = -\frac{1}{\alpha^*}$. In Figure 4.7, we show the error as a function of the iterations. One can see the remarkable improvement of the optimized WR algorithm over the classical one.

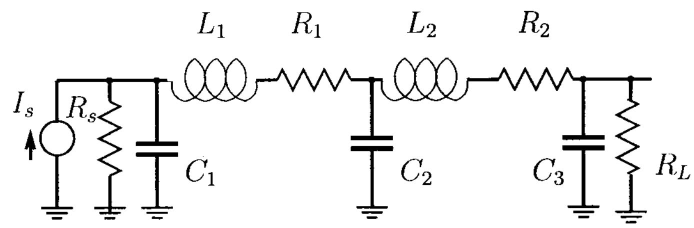

Figure 4.8: A small transmission line with transport behavior.

4.2 A Small Transmission Line Circuit

In this section we analyze the classical, an optimal, and optimized WR algorithms for the small TEM mode lumped circuit in Figure 4.8. The circuit equations are given by

$$\dot{\boldsymbol{x}} = \begin{bmatrix} b_1 & c_1 & & & \\ a_1 & b_2 & c_2 & & \\ & a_2 & b_3 & c_3 & \\ & & a_3 & b_4 & c_4 \\ & & & a_4 & b_5 \end{bmatrix} \boldsymbol{x} + \boldsymbol{f}, \tag{4.55}$$

with the vector of unknown waveforms $\boldsymbol{x} = (v_1, i_1, v_2, i_2, v_3)^T$, which consists of nodal capacitive voltages alternating with inductance currents in the transmission line circuit. The entries of the matrix are given by

$$a_i = \begin{cases} \frac{1}{L_{(i+1)/2}}, & i \text{ odd} \\ \frac{1}{C_{(i/2)+1}}, & i \text{ even} \end{cases}, \quad c_i = \begin{cases} -\frac{1}{C_{(i+1)/2}}, & i \text{ odd} \\ -\frac{1}{L_{i/2}}, & i \text{ even} \end{cases}, \quad b_i = \begin{cases} -\frac{1}{R_s C_1}, & i = 1 \\ -\frac{R_{i/2}}{L_{i/2}}, & i \text{ even} \\ 0, & i > 1 \text{ odd} \\ -\frac{1}{R_L C_3}, & i = 5 \end{cases},$$

and the source on the right hand side is given by $\boldsymbol{f}(t) = (I_s(t)/C_1, 0, 0, 0, 0)^T$. We also need the initial values $\boldsymbol{x}(0) = (v_1^0, i_1^0, v_2^0, i_2^0, v_3^0)^T$ to start the transient simulation.

4.2.1 Analysis of the Classical WR Algorithm without Overlap

We partition the circuit at an even and at an odd row into two sub-circuits or subsystems as we have done for the extra small transmission line circuit case, and obtain the classical WR algorithms

$$\begin{aligned}
\dot{\boldsymbol{u}}^{k+1} &= \begin{bmatrix} b_1 & c_1 \\ a_1 & b_2 \end{bmatrix} \boldsymbol{u}^{k+1} + \begin{pmatrix} f_1 \\ f_2 \end{pmatrix} + \begin{pmatrix} 0 \\ c_2 w_1^k \end{pmatrix}, \\
\dot{\boldsymbol{w}}^{k+1} &= \begin{bmatrix} b_3 & c_3 & \\ a_3 & b_4 & c_4 \\ & a_4 & b_5 \end{bmatrix} \boldsymbol{w}^{k+1} + \begin{pmatrix} f_3 \\ f_4 \\ f_5 \end{pmatrix} + \begin{pmatrix} a_2 u_2^k \\ 0 \\ 0 \end{pmatrix},
\end{aligned} \tag{4.56}$$

and

$$\begin{aligned}
\dot{\boldsymbol{u}}^{k+1} &= \begin{bmatrix} b_1 & c_1 & \\ a_1 & b_2 & c_2 \\ & a_2 & b_3 \end{bmatrix} \boldsymbol{u}^{k+1} + \begin{pmatrix} f_1 \\ f_2 \\ f_3 \end{pmatrix} + \begin{pmatrix} 0 \\ 0 \\ c_3 w_1^k \end{pmatrix}, \\
\dot{\boldsymbol{w}}^{k+1} &= \begin{bmatrix} b_4 & c_4 \\ a_4 & b_5 \end{bmatrix} \boldsymbol{w}^{k+1} + \begin{pmatrix} f_4 \\ f_5 \end{pmatrix} + \begin{pmatrix} a_3 u_3^k \\ 0 \end{pmatrix}.
\end{aligned} \tag{4.57}$$

Similar computations to those for the extra small transmission line circuit show that the convergence factor of the classical WR algorithm with a cut at an even row is given by

$$\rho_{cla}(s, \boldsymbol{a}, \boldsymbol{b}, \boldsymbol{c}) = \frac{a_2(s-b_4)(s-b_5) - a_2 a_4 c_4}{(s-b_3)(s-b_4)(s-b_5) - a_4 c_4 (s-b_3) - a_3 c_3 (s-b_5)} \cdot \frac{c_2(s-b_1)}{(s-b_1)(s-b_2) - a_1 c_1}, \tag{4.58}$$

and the convergence factor with a cut at an odd row is given by

$$\rho_{cla}(s, \boldsymbol{a}, \boldsymbol{b}, \boldsymbol{c}) = \frac{c_3(s-b_1)(s-b_2) - a_1 c_1 c_3}{(s-b_1)(s-b_2)(s-b_3) - a_1 c_1 (s-b_3) - a_2 c_2 (s-b_1)} \cdot \frac{a_3(s-b_5)}{(s-b_4)(s-b_5) - a_4 c_4}. \tag{4.59}$$

Note also that the convergence factor ρ_{cla} with a partition at an even row is the same as the convergence factor ρ_{cla} with a partition at an odd row, assuming that the elements of the vectors $\boldsymbol{a}$, $\boldsymbol{b}$, and $\boldsymbol{c}$ satisfy the simplifying assumptions $a_3 = -c_2 = -c_4 = a_1$, $a_4 = -c_1 = -c_3 = a_2$, $b_5 = b_1$, $b_3 = 0$, and $b_4 = b_2$. Now for $\Re(s) > 0$ the denominator in (4.59) does not vanish, because $a_i > 0$, $c_i < 0$ and $b_i \leq 0$ for the TEM circuit we consider. Hence the convergence factor is an analytic function of $s = \eta + i\omega$ whenever $\eta > 0$. The limit of ρ_{cla} for $s = re^{i\theta}$, $-\pi/2 < \theta < \pi/2$, as $r \to \infty$ is zero, therefore, by the maximum principle for complex analytic functions, Theorem 1.5, the modulus $|\rho_{cla}|$ takes its maximum on the boundary at $\eta = 0$. The modulus of ρ_{cla} for $s = i\omega$ is given by

$$|\rho_{cla}(i\omega, a_1, a_2, b_1, b_2)| = \frac{\sqrt{a_1^2 a_2^2 (b_1^2+\omega^2)}}{\sqrt{\omega^6+(-4a_1a_2+b_1^2+b_2^2)\omega^4+(4a_1^2a_2^2+b_1^2b_2^2+2a_1a_2b_1b_2-2a_1a_2b_1^2)\omega^2+a_1^2a_2^2b_1^2}}, \tag{4.60}$$

where we assume the elements of the vectors $\boldsymbol{a}$, $\boldsymbol{b}$, and $\boldsymbol{c}$ to satisfy the simplifying assumptions $a_3 = -c_2 = -c_4 = a_1$, $a_4 = -c_1 = -c_3 = a_2$, $b_3 = 0$, $b_5 = b_1$, and $b_4 = b_2$. The modulus of the classical convergence factor $|\rho_{cla}|$ depends on ω^2 only, as one can see from (4.60). Furthermore, $|\rho_{cla}|$ might take values bigger than one as is evident from the following Lemma. Note first that, for $\omega = 0$, we have $|\rho_{cla}(0, a_1, a_2, b_1, b_2)| = 1$, and hence the classical WR algorithm is not convergent for $\omega = 0$.

Lemma 4.3. *Let a_1, $a_2 > 0$, b_1, $b_2 < 0$. If $A := \frac{a_1 a_2}{b_2^2} > 0$, and $b := \frac{b_1}{b_2} > 0$ are in the region Ω_+ defined by*

$$\begin{aligned}\Omega_+ := \;& \{(A,b) : A_{h+} \leq A, 0 < b \leq 3\} \bigcup \{(A,b) : \tfrac{b^2+1}{4} < A \leq A_{h-}, c \leq b < 3\} \\ & \bigcup \{(A,b) : \tfrac{b^2+1}{4} < A, 3 < b\},\end{aligned}$$

where c is the only real root of the polynomial $l(b) = 5b^4 - 8b^3 - 14b^2 - 8b - 3$ in the interval $(0,3]$ as is given in Figure 4.9, and

$$A_{h\pm} = \tfrac{2 \pm \sqrt{4-(b-1)^2}}{2}(b+1),$$

then there exists $\omega > 0$ such that $|\rho_{cla}|$ given in (4.60) takes values greater than or equal one.

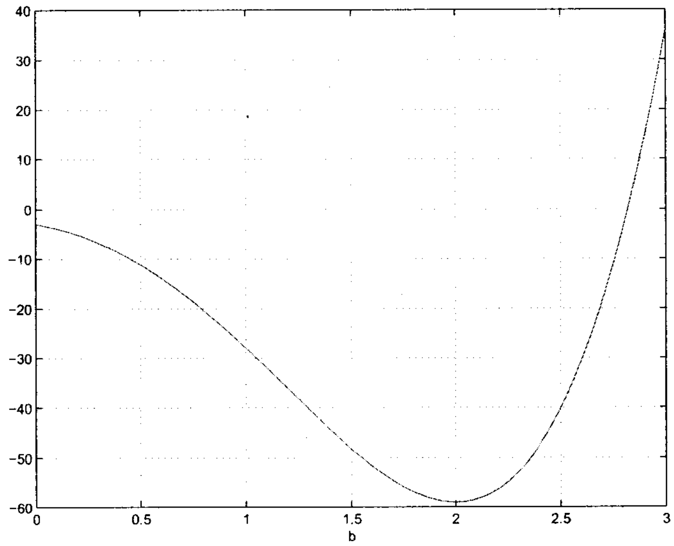

Figure 4.9: The zero of the polynomial $l(b)$ in the interval $(0, 3]$.

Proof. The modulus of the classical convergence factor squared is

$$|\rho_{cla}(i\omega, a_1, a_2, b_1, b_2)|^2 = \frac{P_1(i\omega, a_1, a_2, b_1, b_2)}{P_2(i\omega, a_1, a_2, b_1, b_2)},$$

where

$$\begin{aligned} P_1 &:= a_1^2 a_2^2 (b_1^2 + \omega^2), \\ P_2 &:= \omega^6 + (-4a_1a_2 + b_1^2 + b_2^2)\omega^4 + (4a_1^2a_2^2 + b_1^2b_2^2 + 2a_1a_2b_1b_2 - 2a_1a_2b_1^2)\omega^2 \\ &\quad + a_1^2a_2^2b_1^2, \end{aligned}$$

and $P_1, P_2 > 0$. The polynomial $p(\omega, a_1, a_2, b_1, b_2) = P_1 - P_2$ is

$$p(\omega, a_1, a_2, b_1, b_2) = -\omega^6 + (4a_1a_2 - b_1^2 - b_2^2)\omega^4 + (2a_1a_2b_1^2 - 3a_1^2a_2^2 - b_1^2b_2^2 - 2a_1a_2b_1b_2)\omega^2.$$

Factorizing out b_2^6 and letting $A = \frac{a_1a_2}{b_2^2}$, $b = \frac{b_1}{b_2}$, and $x = \frac{\omega^2}{b_2^2} > 0$, the polynomial p becomes

$$\begin{aligned} \tilde{p}(x, A, b, b_2) &= b_2^6 \left(-x^3 + (4A - (b^2+1))x^2 + (2Ab^2 - 3A^2 - b^2 - 2Ab)x\right) \\ &= b_2^6 x \left(-x^2 + (4A - (b^2+1))x + (2Ab^2 - 3A^2 - b^2 - 2Ab)\right), \end{aligned}$$

where $A > 0$, $b > 0$, and $x > 0$. We now define the function f by

$$f(x, A, b) = -x^2 + (4A - (b^2 + 1))x + (2Ab^2 - 3A^2 - b^2 - 2Ab), \tag{4.61}$$

with $x > 0$. Since $x > 0$, the sign of f indicates where the polynomial $\tilde{p}$ is negative and where it is positive, which will show where $P_1 > P_2$ and where $P_1 < P_2$. The maximum value of f is attained at $x^\star = \frac{4A-(b^2+1)}{2}$. We treat two cases:

1. If $x^\star > 0$, i.e. $A > \frac{b^2+1}{4}$, then we consider the function

$$f(x = x^\star, A, b) = A^2 - 2(b+1)A + \frac{1}{4}(b^2 - 1)^2.$$

2. If $x^\star \leq 0$, then the maximum is attained at $x = 0$, which implies $\omega = 0$, and hence, $|\rho_{cla}|$ is equal to one as noted earlier.

Therefore, we will study the first case only. Now, if $h(A, b) = A^2 - 2(b+1)A + \frac{1}{4}(b^2-1)^2$, then the equation $h(A, b) = 0$ has two roots in terms of b,

$$A_{h\pm} = \frac{2 \pm \sqrt{4 - (b-1)^2}}{2}(b+1), \tag{4.62}$$

where we assume $4 - (b-1)^2 \geq 0$, which implies $-1 \leq b \leq 3$, but we know $b > 0$, so we get $0 < b \leq 3$. Note that, for $b > 3$, the polynomial $h(A, b)$ is positive everywhere and there are no roots. Since $h(A, b)$ is a quadratic polynomial in A, and the sign of the coefficient of A^2 is positive, $h(A, b) < 0$ for $A \in (A_{h-}, A_{h+})$, and $h(A, b) \geq 0$ otherwise. The root $A_{h+}(b) > \frac{b^2+1}{4}$, since

$$\begin{aligned}
\tfrac{2+\sqrt{4-(b-1)^2}}{2}(b+1) > \tfrac{b^2+1}{4} \quad &\Leftrightarrow 2(2 + \sqrt{4 - (b-1)^2})(b+1) > b^2 + 1 \\
&\Leftrightarrow 4(b+1) + 2(b+1)\sqrt{4 - (b-1)^2} > b^2 + 1 \\
&\Leftrightarrow 4b - b^2 + 3 > -2(b+1)\sqrt{4 - (b-1)^2}.
\end{aligned}$$

The last inequality is true, because for $0 < b \leq 3$, we have $4b - b^2 + 3 > 2b - b^2 + 3 \geq 0 \geq -2(b+1)\sqrt{4 - (b-1)^2}$. Now we will look for solutions of the equation $A_{h-} = \frac{b^2+1}{4}$

for $0 < b \leq 3$:

$$\begin{aligned}\tfrac{2-\sqrt{4-(b-1)^2}}{2}(b+1) = \tfrac{b^2+1}{4} &\Leftrightarrow 2(2-\sqrt{4-(b-1)^2})(b+1) = b^2+1\\ &\Leftrightarrow 4(b+1) - 2(b+1)\sqrt{4-(b-1)^2} = b^2+1\\ &\Leftrightarrow 4b - b^2 + 3 = 2(b+1)\sqrt{4-(b-1)^2}.\end{aligned}$$

Since both sides are positive for $0 < b \leq 3$, we square both sides, and obtain after simplifications the equation

$$l(b) := 5b^4 - 8b^3 - 14b^2 - 8b - 3 = 0, \tag{4.63}$$

where $l(b)$ is shown in Figure 4.9. Since l is a polynomial of b, it is continuous, and differentiable everywhere. As is evident in Figure 4.9, equation (4.63) has only one root, say c, in the interval $(0, 3]$. Therefore, $A_{h-} < \frac{b^2+1}{4}$ in the interval $(0, c)$, and $A_{h-} \geq \frac{b^2+1}{4}$ in the interval $[c, 3]$, where c is the solution of equation (4.63), $c \approx 2.821$.

To summarize, we have $h(A, b) < 0$ in the region $\Omega_- = \{(A, b) : \frac{b^2+1}{4} < A < A_{h+}, 0 < b \leq c\} \bigcup \{(A, b) : A_{h-} < A < A_{h+}, c < b \leq 3\}$, and $h(A, b) \geq 0$ in the region $\Omega_+ = \{(A, b) : A_{h+} \leq A, 0 < b \leq 3\} \bigcup \{(A, b) : \frac{b^2+1}{4} < A \leq A_{h-}, c \leq b < 3\} \bigcup \{(A, b) : \frac{b^2+1}{4} < A, 3 < b\}$. The regions are shown in Figure 4.10. Therefore, the function f given in (4.61) satisfies $f(x, A, b) < 0$ in Ω_-, and $f(x, A, b)$ takes values greater than or equal zero in Ω_+. The function f equals zero on the boundary of Ω_+, where the maximum value of f is zero. Hence, for a_1, a_2, b_1, and b_2 in the region Ω_+, there exists $\omega > 0$ such that the modulus of the classical convergence factor satisfies $|\rho_{cla}| \geq 1$. □

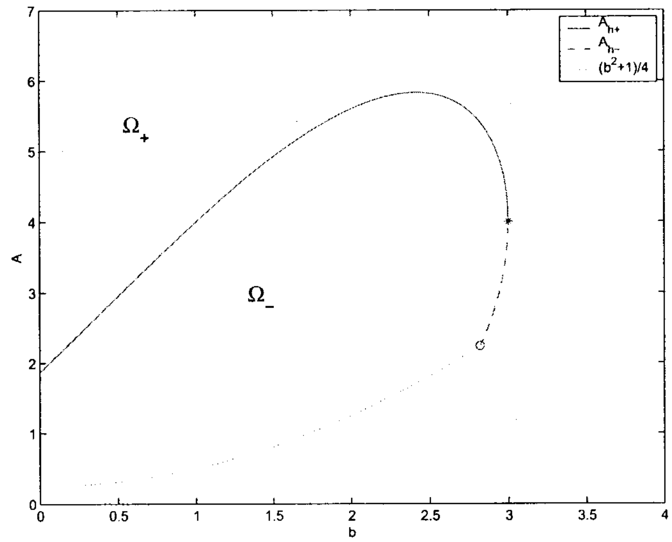

Figure 4.10: Regions where $|\rho_{cla}| < 1$ and $|\rho_{cla}| \geq 1$.

4.2.2 Analysis of the Classical WR Algorithm with Overlap

We now analyze the classical WR algorithm with overlap at the odd row in the middle, which leads to two subsystems of the same size,

$$\begin{aligned}
\dot{\boldsymbol{u}}^{k+1} &= \begin{bmatrix} b_1 & c_1 & \\ a_1 & b_2 & c_2 \\ & a_2 & b_3 \end{bmatrix} \boldsymbol{u}^{k+1} + \begin{pmatrix} f_1 \\ f_2 \\ f_3 \end{pmatrix} + \begin{pmatrix} 0 \\ 0 \\ c_3 w_2^k \end{pmatrix}, \\
\dot{\boldsymbol{w}}^{k+1} &= \begin{bmatrix} b_3 & c_3 & \\ a_3 & b_4 & c_4 \\ & a_4 & b_5 \end{bmatrix} \boldsymbol{w}^{k+1} + \begin{pmatrix} f_3 \\ f_4 \\ f_5 \end{pmatrix} + \begin{pmatrix} a_2 u_2^k \\ 0 \\ 0 \end{pmatrix}.
\end{aligned} \tag{4.64}$$

Using a similar analysis to the one introduced in Subsection 4.1.2, we find the convergence factor of the classical WR algorithm with overlap,

$$\rho_{cla}(s, \boldsymbol{a}, \boldsymbol{b}, \boldsymbol{c}) = \frac{a_2 c_2 (s-b_1)}{(s-b_3)((s-b_1)(s-b_2)-a_1 c_1)-a_2 c_2 (s-b_1)} \cdot \frac{a_3 c_3 (s-b_5)}{(s-b_3)((s-b_4)(s-b_5)-a_4 c_4)-a_3 c_3 (s-b_5)}. \tag{4.65}$$

By Theorem 1.4, the convergence factor ρ_{cla} in (4.65) is an analytic function of s in the right half of the complex plane, since the denominator in (4.65) does not vanish, because $a_i > 0$, $c_i < 0$, and $b_i \leq 0$ for the circuit we consider. Furthermore, the limit of ρ_{cla} for $s = re^{i\theta}$, $-\pi/2 < \theta < \pi/2$, as $r \longrightarrow \infty$ is zero, therefore, by Theorem 1.5, the maximum of $|\rho_{cla}|$ is attained on the boundary at $\eta = 0$. Note also that, with the simplifying assumptions $c_1 = c_3 = -a_4 = -a_2$, $c_2 = c_4 = -a_3 = -a_1$, $b_3 = 0$, $b_4 = b_2$, and $b_5 = b_1$, the classical convergence factor ρ_{cla} in (4.65) with overlap is given by

$$\rho_{cla}(s, \boldsymbol{a}, \boldsymbol{b}) = \left(\frac{a_1 a_2 (s - b_1)}{s((s - b_1)(s - b_2) + a_1 a_2) + a_1 a_2 (s - b_1)}\right)^2,$$

and it is equal to ρ_{cla} in (4.59) without overlap squared. Therefore, Lemma 4.3 holds for ρ_{cla} with overlap, and hence, the classical WR algorithm with overlap still might not converge. An example for the convergence factor as a function of ω is given in Figure 4.11 for a typical set of TEM circuit parameters. One can see why TEM type circuits are hard to solve with classical waveform relaxation: only high frequency components in the signal converge, a large band of frequencies around $\omega = 0$, in the example $\omega \in [-27, 27]$, has a convergence factor bigger than one and hence will cause difficulties for the algorithm.

4.2.3 An Optimal WR Algorithm without Overlap

The new WR algorithm without overlap and with a cut at an even row is given by

$$\begin{aligned} \dot{\boldsymbol{u}}^{k+1} &= \begin{bmatrix} b_1 & c_1 \\ a_1 & b_2 - c_2\alpha \end{bmatrix} \boldsymbol{u}^{k+1} + \begin{pmatrix} f_1 \\ f_2 \end{pmatrix} + \begin{pmatrix} 0 \\ c_2(w_1^k + \alpha w_0^k) \end{pmatrix}, \\ \dot{\boldsymbol{w}}^{k+1} &= \begin{bmatrix} b_3 - \frac{a_2}{\beta} & c_3 & \\ a_3 & b_4 & c_4 \\ & a_4 & b_5 \end{bmatrix} \boldsymbol{w}^{k+1} + \begin{pmatrix} f_3 \\ f_4 \\ f_5 \end{pmatrix} + \begin{pmatrix} \frac{a_2}{\beta}(\beta u_2^k + u_3^k) \\ 0 \\ 0 \end{pmatrix}, \end{aligned} \tag{4.66}$$

where we used the new transmission conditions

$$u_3^{k+1} + \alpha u_2^{k+1} = w_1^k + \alpha w_0^k, \quad w_1^{k+1} + \beta w_0^{k+1} = u_3^k + \beta u_2^k. \tag{4.67}$$

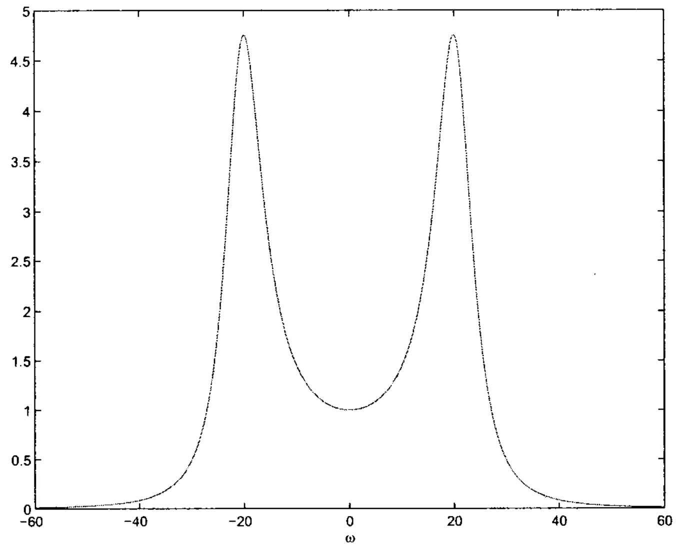

Figure 4.11: Convergence factor as a function of the frequency parameter ω for the classical WR algorithm applied to the small TEM circuit.

Similar to the very small circuit, Subsection 4.1.3, the key improvement in the new WR algorithms is better transmission conditions than the ones used for the classical WR algorithm. Similar calculations to those in Subsection 4.1.3 with a cut at an even row lead to the convergence factor

$$\rho_{opt}(s, \boldsymbol{a}, \boldsymbol{b}, \boldsymbol{c}, \alpha, \beta) = F_1 F_2 \left(\tfrac{1}{F_1} - \alpha + \beta\right)\left(1 + \tfrac{\alpha}{\beta F_2} - \tfrac{\alpha}{\beta}\right) = \tfrac{L_1\beta + C_1}{L_2\beta + C_2} \cdot \tfrac{L_2\alpha + C_2}{L_1\alpha + C_1}, \quad (4.68)$$

where

$$\begin{aligned}
L_1 &:= c_2 s - c_2 b_1, \\
C_1 &:= s^2 - (b_1 + b_2)s + b_1 b_2 - a_1 c_1, \\
L_2 &:= s^3 - (b_3 + b_4 + b_5)s^2 + (b_3 b_5 + b_3 b_4 + b_4 b_5 - a_4 c_4 - a_3 c_3)s \\
&\quad -b_3 b_4 b_5 + a_3 c_3 b_5 + a_4 c_4 b_3, \\
C_2 &:= a_2 s^2 - (a_2 b_5 + a_2 b_4)s + b_4 b_5 a_2 - a_2 a_4 c_4.
\end{aligned}$$

We also obtain $\hat{u}_2^{2k} = (\rho_{opt})^k \, \hat{u}_2^0$ and $\hat{w}_1^{2k} = (\rho_{opt})^k \, \hat{w}_1^0$.

Theorem 4.5 (Optimal Convergence). *The new WR algorithm (4.66) converges in two iterations, independently of the initial waveforms $\hat{\boldsymbol{u}}^0$ and $\hat{\boldsymbol{w}}^0$, if*

$$\begin{aligned}
\hat{\alpha}_{even} = \alpha(s) &= -\frac{a_2s^2-(a_2b_5+a_2b_4)s+b_4b_5a_2-a_2a_4c_4}{s^3-(b_3+b_4+b_5)s^2+(b_3b_5+b_3b_4+b_4b_5-a_4c_4-a_3c_3)s-b_3b_4b_5+a_3c_3b_5+a_4c_4b_3},\\
\hat{\beta}_{even} = \beta(s) &= -\frac{s^2-(b_1+b_2)s+b_1b_2-a_1c_1}{c_2s-c_2b_1}.
\end{aligned} \tag{4.69}$$

Proof. The proof is similar to the proof of Theorem 4.1. □

Now for the cut at an odd row, the new WR algorithm using the new transmission conditions

$$u_4^{k+1} + \alpha u_3^{k+1} = w_1^k + \alpha w_0^k, \quad w_1^{k+1} + \beta w_0^{k+1} = u_4^k + \beta u_3^k, \tag{4.70}$$

is given by

$$\begin{aligned}
\dot{\boldsymbol{u}}^{k+1} &= \begin{bmatrix} b_1 & c_1 & \\ a_1 & b_2 & c_2 \\ & a_2 & b_3 - c_3\alpha \end{bmatrix} \boldsymbol{u}^{k+1} + \begin{pmatrix} f_1 \\ f_2 \\ f_3 \end{pmatrix} + \begin{pmatrix} 0 \\ 0 \\ c_3(w_1^k + \alpha w_0^k) \end{pmatrix},\\
\dot{\boldsymbol{w}}^{k+1} &= \begin{bmatrix} b_4 - \frac{a_3}{\beta} & c_4 \\ a_4 & b_5 \end{bmatrix} \boldsymbol{w}^{k+1} + \begin{pmatrix} f_4 \\ f_5 \end{pmatrix} + \begin{pmatrix} \frac{a_3}{\beta}(\beta u_3^k + u_4^k) \\ 0 \end{pmatrix}.
\end{aligned} \tag{4.71}$$

The convergence factor of the new WR algorithm with a cut at an odd row is

$$\rho_{opt}(s, \boldsymbol{a}, \boldsymbol{b}, \boldsymbol{c}, \alpha, \beta) = F_1F_2\left(\frac{1}{F_1} - \alpha + \beta\right)\left(1 + \frac{\alpha}{\beta F_2} - \frac{\alpha}{\beta}\right) = \frac{L_1\beta+C_1}{L_2\beta+C_2} \cdot \frac{L_2\alpha+C_2}{L_1\alpha+C_1}, \tag{4.72}$$

where

$$\begin{aligned}
L_1 &:= c_3s^2 - (b_2c_3 + b_1c_3)s + b_1b_2c_3 - a_1c_1c_3,\\
C_1 &:= s^3 - (b_3 + b_2 + b_1)s^2 + (b_2b_3 + b_1b_3 + b_1b_2 - a_1c_1 - a_2c_2)s\\
&\quad -b_1b_2b_3 + a_1c_1b_3 + a_2c_2b_1,\\
L_2 &:= s^2 - (b_5 + b_4)s + b_4b_5 - c_4a_4,\\
C_2 &:= a_3s - a_3b_5.
\end{aligned}$$

We also obtain as before $\hat{u}_3^{2k} = (\rho_{opt})^k\, \hat{u}_3^0$ and $\hat{w}_1^{2k} = (\rho_{opt})^k\, \hat{w}_1^0$.

Theorem 4.6 (Optimal Convergence). *The new WR algorithm (4.71) converges in two iterations, independently of the initial waveforms $\hat{\boldsymbol{u}}^0$ and $\hat{\boldsymbol{w}}^0$, if*

$$\begin{aligned}\hat{\alpha}_{odd} = \alpha(s) &= -\frac{a_3 s - a_3 b_5}{s^2-(b_5+b_4)s+b_4b_5-c_4a_4},\\ \hat{\beta}_{odd} = \beta(s) &= -\frac{s^3-(b_3+b_2+b_1)s^2+(b_2b_3+b_1b_3+b_1b_2-a_1c_1-a_2c_2)s-b_1b_2b_3+a_1c_1b_3+a_2c_2b_1}{c_3s^2-(b_2c_3+b_1c_3)s+b_1b_2c_3-a_1c_1c_3}.\end{aligned} \tag{4.73}$$

Proof. The proof is similar to the proof of Theorem 4.1. □

Remark 4.3. *Theorems 4.5 and 4.6 imply a relation between the optimal parameters obtained with a cut at an even row and those obtained with a cut at an odd row. Assuming that the elements in the vectors $\boldsymbol{a}$, $\boldsymbol{b}$, and $\boldsymbol{c}$ satisfy the simplifying assumptions $a_3 = -c_2 = -c_4 = a_1$, $a_4 = -c_1 = -c_3 = a_2$, $b_5 = b_1$, and $b_4 = b_2$, the optimal parameters satisfy*

$$\hat{\alpha}_{even} = \frac{-1}{\hat{\beta}_{odd}}; \quad \hat{\beta}_{even} = \frac{-1}{\hat{\alpha}_{odd}}.$$

4.2.4 An Optimal WR Algorithm with Overlap

We now analyze an optimal WR algorithm with overlap at the third row. Using the new transmission conditions

$$u_4^{k+1} + \alpha u_3^{k+1} = w_2^k + \alpha w_1^k, \quad w_1^{k+1} + \beta w_0^{k+1} = u_3^k + \beta u_2^k, \tag{4.74}$$

the new WR algorithm is

$$\begin{aligned}\dot{\boldsymbol{u}}^{k+1} &= \begin{bmatrix} b_1 & c_1 & \\ a_1 & b_2 & c_2 \\ & a_2 & b_3 - c_3\alpha \end{bmatrix} \boldsymbol{u}^{k+1} + \begin{pmatrix} f_1 \\ f_2 \\ f_3 \end{pmatrix} + \begin{pmatrix} 0 \\ 0 \\ c_3(w_2^k + \alpha w_1^k) \end{pmatrix},\\ \dot{\boldsymbol{w}}^{k+1} &= \begin{bmatrix} b_3 - \frac{a_2}{\beta} & c_3 & \\ a_3 & b_4 & c_4 \\ & a_4 & b_5 \end{bmatrix} \boldsymbol{w}^{k+1} + \begin{pmatrix} f_3 \\ f_4 \\ f_5 \end{pmatrix} + \begin{pmatrix} \frac{a_2}{\beta}(u_3^k + \beta u_2^k) \\ 0 \\ 0 \end{pmatrix}.\end{aligned} \tag{4.75}$$

The analysis is similar to the one used before, where we use the Laplace transform, and we consider the homogeneous system. The convergence factor of the new WR algorithm with overlap, obtained after some computations, is

$$\begin{aligned}
&\rho_{opt}(s, \boldsymbol{a}, \boldsymbol{b}, \boldsymbol{c}, \alpha, \beta) \\
&= F_1 F_2 \left(\tfrac{s-b_3}{c_3} - \tfrac{a_2}{c_3}\left(\tfrac{1}{\beta F_2} - \tfrac{1}{\beta}\right) + \alpha\right)\left(1 + \tfrac{\beta}{a_2}(s-b_3) - \tfrac{\beta c_3}{a_2}\left(\tfrac{1}{F_1} - \alpha\right)\right) \\
&= \tfrac{a_2 a_3 (s-b_5) + \alpha a_2((s-b_4)(s-b_5) - a_4 c_4)}{(s-b_3+c_3\alpha)((s-b_1)(s-b_2)-a_1c_1) - a_2 c_2 (s-b_1)} \cdot \tfrac{\beta c_2 c_3 (s-b_1) + c_3((s-b_1)(s-b_2) - a_1 c_1)}{(\beta(s-b_3)+a_2)((s-b_4)(s-b_5)-a_4c_4) - \beta a_3 c_3 (s-b_5)}.
\end{aligned} \tag{4.76}$$

In addition, we have as before $\hat{u}_3^{2k} = (\rho_{opt})^k \hat{u}_3^0$ and $\hat{w}_1^{2k} = (\rho_{opt})^k \hat{w}_1^0$.

Theorem 4.7 (Optimal Convergence). *The new WR algorithm (4.75) converges in two iterations, independently of the initial waveforms $\hat{\boldsymbol{u}}^0$ and $\hat{\boldsymbol{w}}^0$, if*

$$\begin{aligned}
\hat{\alpha} = \alpha(s) &= -\tfrac{a_3(s-b_5)}{(s-b_4)(s-b_5)-a_4c_4}, \\
\hat{\beta} = \beta(s) &= -\tfrac{(s-b_1)(s-b_2)-a_1c_1}{c_2(s-b_1)}.
\end{aligned} \tag{4.77}$$

Proof. The proof is similar to the proof of Theorem 4.1. □

Similar to the extra small transmission line circuit case, we choose an approximation by a constant of the optimal parameters in the next subsection.

4.2.5 An Optimized WR Algorithm with Overlap and Constant approximation

The low frequency approximation of the optimal parameters (4.77) in the transmission conditions is

$$\alpha_T = \frac{a_3 b_5}{b_4 b_5 - c_4 a_4}, \quad \beta_T = \frac{b_1 b_2 - a_1 c_1}{c_2 b_1}.$$

The conditions for analyticity with the corresponding parameters range are given in the following lemma.

Lemma 4.4. *If $b_i \le 0$, $a_i > 0$, and $c_i < 0$, and*

$$\alpha < 0, \quad \beta > 0, \tag{4.78}$$

then the convergence factor ρ_{opt} in (4.76) is an analytic function in the right half of the complex plane, $s = \eta + i\omega$, $\eta > 0$.

Proof. By Theorem 1.4, we have to show that the denominators have no zeros in the right half of the complex plane. We will show the proof for one quotient, and the proof for the other one is similar. The denominator of the first factor of the convergence factor (4.76) is

$$s^3 + (c_3\alpha - b_1 - b_3 - b_2)s^2 + (b_1b_2 + b_2b_3 + b_1b_3 - a_1c_1 - a_2c_2 + (-b_2c_3 - b_1c_3)\alpha)s$$
$$+(-a_1c_1c_3 + b_1b_2c_3)\alpha + a_2c_2b_1 - b_1b_2b_3 + a_1c_1b_3.$$

Now, by Vieta's formulas, Theorem 4.4, the product of the roots satisfies $s_1s_2s_3 = -((-a_1c_1c_3 + b_1b_2c_3)\alpha + a_2c_2b_1 - b_1b_2b_3 + a_1c_1b_3) < 0$, and the sum $s_1 + s_2 + s_3 = b_1 + b_3 + b_2 - c_3\alpha < 0$ with $\alpha < 0$. Furthermore, the pairwise products summed satisfy $s_1s_2 + s_1s_3 + s_2s_3 = -a_1c_1 + b_1b_2 + b_2b_3 + b_1b_3 - a_2c_2 + (-b_2c_3 - b_1c_3)\alpha > 0$, with $\alpha < 0$. Hence, if one zero is real and the other two are complex conjugate, say $s_1 \in \mathbb{R}$, $s_2 = x + iy$ and $s_3 = x - iy$, then we have $s_1s_2 + s_1s_3 + s_2s_3 = 2s_1x + x^2 + y^2$, $s_1 + s_2 + s_3 = s_1 + 2x$, and $s_1s_2s_3 = s_1(x^2 + y^2)$. So, if $s_1 > 0$ and $x > 0$, then we get a contradiction with the inequality on their product and their sum. If $s_1 > 0$ and $x < 0$, then we get a contradiction with the inequality on their product. If $s_1 < 0$ and $x > 0$, then we have, using the equality on the sum, $s_1 = b_1 + b_3 + b_2 - c_3\alpha - 2x$, and using the equality on the pairwise products summed, $2s_1x + x^2 + y^2 = -a_1c_1 + b_1b_2 + b_2b_3 + b_1b_3 - a_2c_2 + (-b_2c_3 - b_1c_3)\alpha$. Multiplying the second equality by s_1, we get

$$2s_1^2x = (b_1+b_3+b_2-c_3\alpha-2x)(-a_1c_1+b_1b_2+b_2b_3+b_1b_3-a_2c_2+(-b_2c_3-b_1c_3)\alpha)-s_1(x^2+y^2).$$

Using the equality on the product, we have $s_1(x^2 + y^2) = -((-a_1c_1c_3 + b_1b_2c_3)\alpha +$

$a_2c_2b_1 - b_1b_2b_3 + a_1c_1b_3)$. After some simplifications, this implies

$$\begin{aligned} 2s_1^2x = \ & (2b_1c_3\alpha+2b_2c_3\alpha+2a_1c_1-2b_3b_2-2b_1b_3+2a_2c_2 - 2b_1b_2)x+b_1b_3^2+b_1^2b_2+b_1^2b_3 \\ & +b_1b_2^2+b_3b_2^2+b_2b_3^2+c_3a_2c_2\alpha-2b_1b_2c_3\alpha-2b_3b_2c_3\alpha-2b_3b_1c_3\alpha+c_3^2b_2\alpha^2 \\ & +c_3^2b_1\alpha^2-b_1^2c_3\alpha-b_2^2c_3\alpha-b_2a_1c_1-b_2a_2c_2-b_1a_1c_1+2b_1b_2b_3-b_3a_2c_2, \end{aligned}$$

and hence, $2s_1^2x < 0$ for b_1, b_2, b_3, c_1, c_2, c_3 and α negative, and a_1 and a_2 positive, which contradicts the fact that $2s_1^2x > 0$ for $x > 0$, which means s_1 and x must be negative. Now if the three zeros are real, they must be negative, since if the three are positive, then we have a contradiction with the inequality on the sum, if any two are negative and the third is positive, then we have a contradiction with the inequality on the product. The last possible case is the case when one zero is negative and the other two are positive, say $s_1 > 0, s_2 > 0$ and $s_3 < 0$. Then we have, using the inequality on the pairwise products summed, $s_1s_2 - |s_3|(s_1+s_2) > 0$, which implies $|s_3| < \frac{s_1s_2}{s_1+s_2}$. However, $s_1 + s_2 - |s_3| > s_1 + s_2 - \frac{s_1s_2}{s_1+s_2} = \frac{s_1^2+s_1s_2+s_2^2}{s_1+s_2} > 0$, which contradicts the inequality on the sum. Thus there is no pole in the right half of the complex plane from the second factor. □

As in the extra small case, if we take $a_3 = -c_2 = -c_4 = a_1$, $a_4 = -c_1 = -c_3 = a_2$, $b_3 = 0$, $b_5 = b_1$, and $b_4 = b_2$, we obtain $\beta_T = -\frac{1}{\alpha_T}$. For $b_i < 0$, $c_i < 0$, and $a_i > 0$, we have $\alpha_T < 0$ and $\beta_T > 0$.

We show in Figure 4.12 the classical convergence factor and the optimized one with the Taylor approximation. We observe the remarkable improvement of the optimized convergence over the classical one.

Taking $s = re^{i\theta}$, $-\pi/2 < \theta < \pi/2$, the limit of ρ_{opt} as r goes to infinity is zero. Since ρ_{opt} is analytic in the right half of the complex plane, we can apply the maximum principle for analytic functions, Theorem 1.5, and since we have the same limit at infinity in all directions, the maximum of $|\rho_{opt}(s)|$ for $s = \eta + i\omega$, $\eta > 0$, is attained on the boundary at $\eta = 0$. For $s = i\omega$, from the first quotient of the convergence

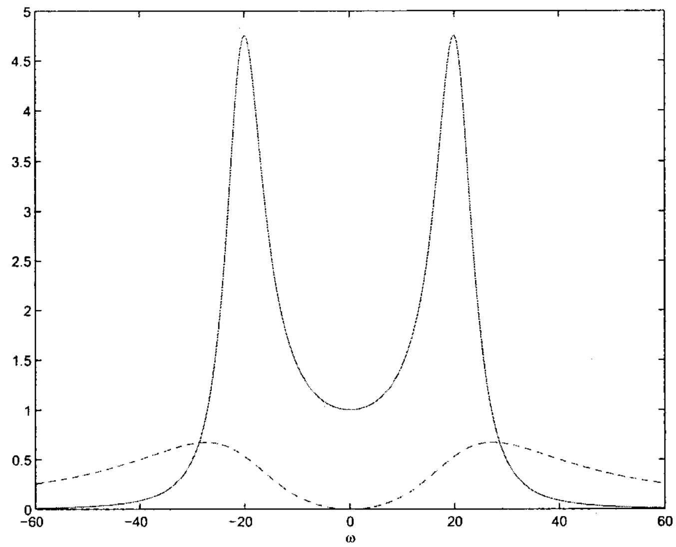

Figure 4.12: Classical convergence factor (solid line) versus the optimized convergence factor with the Taylor approximation (dashed line).

factor ρ_{opt} in (4.76), we have

$$a_2a_3(s-b_5)+\alpha a_2((s-b_4)(s-b_5)-a_4c_4) = \\ a_2(\alpha(b_4b_5-a_4c_4)-a_3b_5-\alpha\omega^2+i(a_3-\alpha(b_4+b_5))\omega),$$

and

$$(s-b_3+c_3\alpha)((s-b_1)(s-b_2)-a_1c_1)-a_2c_2(s-b_1) = \\ \alpha c_3(b_1b_2-a_1c_1)-b_1b_2b_3+a_1c_1b_3+a_2c_2b_1+(b_1+b_2+b_3-\alpha c_3)\omega^2 \\ -i((b_1+b_2)\alpha c_3-b_1b_2-b_1b_3-b_2b_3+a_1c_1+a_2c_2+\omega^2)\omega,$$

which implies that $|a_2a_3(s-b_5)+\alpha a_2((s-b_4)(s-b_5)-a_4c_4)|$, and $|(s-b_3+c_3\alpha)((s-b_1)(s-b_2)-a_1c_1)-a_2c_2(s-b_1)|$ both depend on ω^2 only. The same holds for the second quotient. Therefore, the modulus of ρ_{opt} for $s=i\omega$ depends on ω^2 only, and hence, it suffices to optimize for nonnegative frequencies, $\omega \geq 0$. We consider here again the WR algorithm with one overlap at an odd row, for the same reasons as in Subsection 4.1.5 for the extra small circuit case. From the optimal choice (4.77) with overlap, and the simplifying assumptions $c_1 = c_3 = -a_4 = -a_2$, $c_2 = c_4 = -a_3 = -a_1$, $b_3 = 0$, $b_5 = b_1$, and $b_4 = b_2$, we have $\beta_{opt} = -\frac{1}{\alpha_{opt}}$. The other optimal choices without overlap lead to relations which are operators in s.

Remark 4.4. *With the simplifying assumptions $c_1 = c_3 = -a_4 = -a_2$, $c_2 = c_4 = -a_3 = -a_1$, $b_3 = 0$, $b_5 = b_1$, and $b_4 = b_2$, the optimal convergence factor without overlap, with a cut at an odd row (4.72), and with the choice of parameters $\beta = -\alpha + \frac{s}{a_2}$, motivated by the optimal choice, is equal to the optimal convergence factor with overlap (4.76), where the overlap is at an odd row, and with the choice of parameters $\beta = -\frac{1}{\alpha}$.*

To further analyze the convergence factor (4.76), we assume $c_2 = c_4 = -a_3 = -a_1$, $c_1 = c_3 = -a_4 = -a_2$, $b_3 = 0$, $b_5 = b_1$, and $b_4 = b_2$, and we choose $\beta = -\frac{1}{\alpha}$. This will simplify the optimization process.

Now we look for a better choice for α such that the overall convergence is faster. With the simplifying assumptions, the convergence factor becomes

$$\rho_{opt}(s, a_1, a_2, b_1, b_2, \alpha) = \left(\frac{a_2(a_1(s-b_1) + \alpha((s-b_1)(s-b_2) + a_1a_2)}{(s - a_2\alpha)((s-b_1)(s-b_2) + a_1a_2) + a_1a_2(s-b_1)} \right)^2, \tag{4.79}$$

and we look for solutions of the min-max problem

$$\min_{\alpha<0} \left(\max_{\omega \geq 0} |\rho_{opt}(i\omega, a_1, a_2, b_1, b_2, \alpha)| \right). \tag{4.80}$$

On the left hand side of Figure 4.13, we show the function $|\rho_{opt}(\omega, \alpha)|$ for the numerical example in Subsection 4.2.6. In this example, we find the numerically optimized α, which is $\alpha^* = -12.9733$, and leads to the convergence factor shown on the right hand side of Figure 4.13. To solve the min-max problem (4.80) approximately we again use the two scale expansion introduced in Subsection 4.1.5, where we have

$$\begin{aligned} a_1 &= \tfrac{n}{4.95e-3} = O\left(\tfrac{1}{\epsilon}\right), \; b_1 = -\tfrac{n}{0.0315} = O\left(\tfrac{1}{\sqrt{\epsilon}}\right), \\ a_2 &= \tfrac{n}{0.63} = O(1), \; b_2 = -\tfrac{0.5e-3}{4.95e-3} = O(1), \end{aligned} \tag{4.81}$$

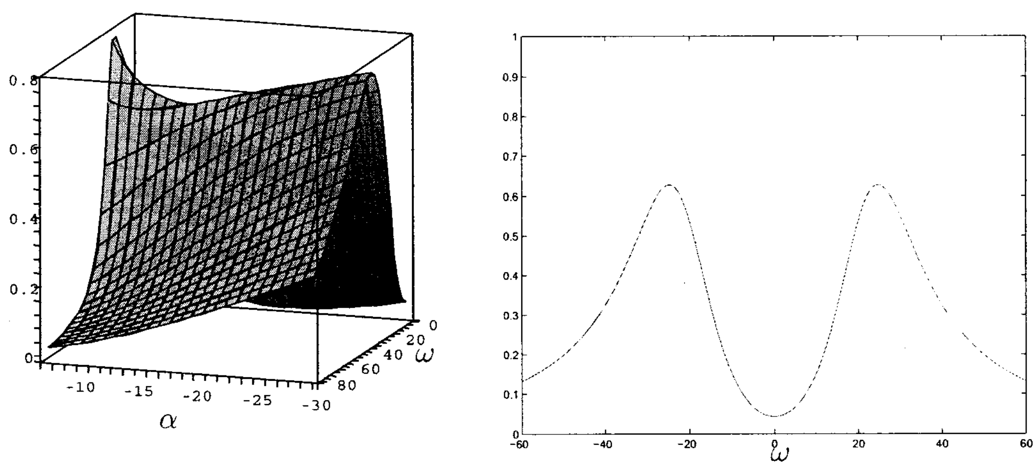

Figure 4.13: Left: convergence factor $|\rho_{opt}(\omega,\alpha)|$. Right: optimized convergence factor $|\rho_{opt}(\omega,\alpha^*)|$.

and n is again the number of sections in 1 cm of circuit length. The modulus of the convergence factor ρ_{opt} in (4.79) is given by

$$R_0(\omega,a_1,a_2,b_1,b_2,\alpha)=\frac{P_1(\omega,a_1,a_2,b_1,b_2,\alpha)}{P_2(\omega,a_1,a_2,b_1,b_2,\alpha)},$$

where

$$\begin{aligned}
P_1 :=\ & a_2^2(a_1^2b_1^2-2b_1^2b_2\alpha a_1-2a_1^2a_2\alpha b_1+b_1^2b_2^2\alpha^2+2b_1b_2\alpha^2a_1a_2+a_1^2a_2^2\alpha^2+a_1^2\omega^2\\
&-2\omega^2b_2\alpha a_1+\omega^2b_2^2\alpha^2+\omega^2b_1^2\alpha^2-2\omega^2\alpha^2a_1a_2+\omega^4\alpha^2),\\
P_2 :=\ & a_2^2\omega^4\alpha^2+4a_2^2a_1^2\omega^2+a_2^2a_1^2b_1^2+2a_2^2b_1^2b_2\alpha a_1+2a_2^3b_1b_2\alpha^2a_1+2a_2^2\omega^2b_2\alpha a_1\\
&+a_2^4a_1^2\alpha^2+a_2^2\omega^2b_2^2\alpha^2-4\omega^4a_1a_2+b_1^2b_2^2\omega^2+a_2^2\omega^2b_1^2\alpha^2+a_2^2b_1^2b_2^2\alpha^2+2a_2^3a_1^2\alpha b_1\\
&-2a_2^3\omega^2\alpha^2a_1-2\omega^2b_1^2a_2a_1+\omega^4b_2^2+\omega^6+2\omega^2b_2a_2a_1b_1+\omega^4b_1^2.
\end{aligned}$$

Again, assuming $a_1=n\tilde{a}_1$, $a_2=n\tilde{a}_2$, $b_1=n\tilde{b}_1$, $b_2=n\tilde{b}_2$, and $\omega=n\tilde{\omega}$, where from the typical values in (4.81) we have the typical values

$$\tilde{a}_1=\frac{1}{4.95e-3},\quad \tilde{a}_2=\frac{1}{0.63},\quad \tilde{b}_1=-\frac{1}{0.0315},\quad \tilde{b}_2=-\frac{0.5e-3}{4.95e-3}\cdot\frac{1}{n},\tag{4.82}$$

and $\tilde{\omega} \geq 0$ is a new variable, and factorizing n^6 from the numerator and denominator of R_0, the modulus of the convergence factor R_0 becomes

$$\tilde{R}_0(\tilde{\omega}, \tilde{a}_1, \tilde{a}_2, \tilde{b}_1, \tilde{b}_2, \alpha) = \frac{\tilde{P}_1(\tilde{\omega}, \tilde{a}_1, \tilde{a}_2, \tilde{b}_1, \tilde{b}_2, \alpha)}{\tilde{P}_2(\tilde{\omega}, \tilde{a}_1, \tilde{a}_2, \tilde{b}_1, \tilde{b}_2, \alpha)}, \tag{4.83}$$

where

$$\begin{aligned}
\tilde{P}_1 :=\ & \tilde{a}_2^2(\tilde{a}_1^2\tilde{b}_1^2 - 2\tilde{b}_1^2\tilde{b}_2\alpha\tilde{a}_1 - 2\tilde{a}_1^2\tilde{a}_2\alpha\tilde{b}_1 + \tilde{b}_1^2\tilde{b}_2^2\alpha^2 + 2\tilde{b}_1\tilde{b}_2\alpha^2\tilde{a}_1\tilde{a}_2 + \tilde{a}_1^2\tilde{a}_2^2\alpha^2 + \tilde{a}_1^2\tilde{\omega}^2 \\
& -2\tilde{\omega}^2\tilde{b}_2\alpha\tilde{a}_1 + \tilde{\omega}^2\tilde{b}_2^2\alpha^2 + \tilde{\omega}^2\tilde{b}_1^2\alpha^2 - 2\tilde{\omega}^2\alpha^2\tilde{a}_1\tilde{a}_2 + \tilde{\omega}^4\alpha^2), \\
\tilde{P}_2 :=\ & \tilde{a}_2^2\tilde{\omega}^4\alpha^2 + 4\tilde{a}_2^2\tilde{a}_1^2\tilde{\omega}^2 + \tilde{a}_2^2\tilde{a}_1^2\tilde{b}_1^2 + 2\tilde{a}_2^2\tilde{b}_1^2\tilde{b}_2\alpha\tilde{a}_1 + 2\tilde{a}_2^3\tilde{b}_1\tilde{b}_2\alpha^2\tilde{a}_1 + 2\tilde{a}_2^2\tilde{\omega}^2\tilde{b}_2\alpha\tilde{a}_1 \\
& +\tilde{a}_2^4\tilde{a}_1^2\alpha^2 + \tilde{a}_2^2\tilde{\omega}^2\tilde{b}_2^2\alpha^2 - 4\tilde{\omega}^4\tilde{a}_1\tilde{a}_2 + \tilde{b}_1^2\tilde{b}_2^2\tilde{\omega}^2 + \tilde{a}_2^2\tilde{\omega}^2\tilde{b}_1^2\alpha^2 + \tilde{a}_2^2\tilde{b}_1^2\tilde{b}_2^2\alpha^2 + 2\tilde{a}_2^3\tilde{a}_1^2\alpha\tilde{b}_1 \\
& -2\tilde{a}_2^3\tilde{\omega}^2\alpha^2\tilde{a}_1 - 2\tilde{\omega}^2\tilde{b}_1^2\tilde{a}_2\tilde{a}_1 + \tilde{\omega}^4\tilde{b}_2^2 + \tilde{\omega}^6 + 2\tilde{\omega}^2\tilde{b}_2\tilde{a}_2\tilde{a}_1\tilde{b}_1 + \tilde{\omega}^4\tilde{b}_1^2.
\end{aligned}$$

Numerical experiments show again that the solution of the min-max problem (4.80) with the choice $\beta = -\frac{1}{\alpha}$ is characterized by the system of equations

$$\nabla_{\alpha,\tilde{\omega}}\tilde{R}_0(\tilde{\omega}, \tilde{a}_1, \tilde{a}_2, \tilde{b}_1, \tilde{b}_2, \alpha) = 0 \Leftrightarrow \begin{cases} \frac{\partial \tilde{R}_0}{\partial \tilde{\omega}}(\bar{\tilde{\omega}}, \tilde{a}_1, \tilde{a}_2, \tilde{b}_1, \tilde{b}_2, \alpha^*) = 0, \\ \frac{\partial \tilde{R}_0}{\partial \alpha}(\bar{\tilde{\omega}}, \tilde{a}_1, \tilde{a}_2, \tilde{b}_1, \tilde{b}_2, \alpha^*) = 0, \end{cases} \tag{4.84}$$

where $\tilde{R}_0$ is given in (4.83), and $\bar{\tilde{\omega}}$ is the interior maximum of $\tilde{R}_0$.

To see that there is indeed a solution for the system in (4.84) for ϵ small, we use the ansatz $\alpha = C_\alpha\epsilon^{\gamma_1}$, and $\bar{\tilde{\omega}} = C_{\tilde{\omega}}\epsilon^{\gamma_2}$. Then, we substitute $\tilde{a}_1$ by $\frac{1}{\epsilon}$, and $\tilde{b}_1$ by $\frac{\tilde{C}}{\sqrt{\epsilon}}$ in $\tilde{R}_0$, and determine the leading asymptotic terms as ϵ goes to zero of the equations in (4.84). The analysis and the ideas are the same here. However, the polynomials are more complicated, because we have a more complicated convergence factor. The polynomial $P(\tilde{\omega}, \alpha)$, the equivalent to $P(\tilde{\omega}, \alpha)$ in (4.51), will now be a product of $\tilde{\omega}$ and a bi-quartic polynomial of $\tilde{\omega}$ with real coefficients. The polynomial $Q(\alpha, \tilde{\omega})$, the equivalent to $Q(\alpha, \tilde{\omega})$ in (4.52), is still a quadratic polynomial in α, but is more complicated. The leading asymptotic terms as ϵ goes to zero are given by

$$
\begin{aligned}
P(\overline{\tilde{\omega}}, \alpha^*) = \tfrac{2\tilde{a}_2^2 C_{\tilde{\omega}}}{\epsilon^{11/2}} \big(& -C_{\tilde{\omega}}^4 \tilde{C}^4 C_\alpha^2 \epsilon^{5\gamma_2+7/2+2\gamma_1} + 2C_\alpha^2 \tilde{a}_2^3 \tilde{C}^2 \epsilon^{\gamma_2+2\gamma_1+3/2} - C_\alpha^2 C_{\tilde{\omega}}^8 \epsilon^{2\gamma_1+9\gamma_2+11/2} \\
& +6C_{\tilde{\omega}}^4 \tilde{a}_2 C_\alpha \tilde{C} \epsilon^{5\gamma_2+3+\gamma_1} + 8C_{\tilde{\omega}}^2 C_\alpha^3 \tilde{a}_2^3 \tilde{C} \epsilon^{3\gamma_2+3+3\gamma_1} + 10\tilde{a}_2^3 C_\alpha \tilde{C} \epsilon^{\gamma_1+\gamma_2+1} \\
& +8C_{\tilde{\omega}}^2 C_\alpha^2 \tilde{a}_2^3 \epsilon^{3\gamma_2+5/2+2\gamma_1} - 2C_{\tilde{\omega}}^6 \tilde{C}^2 C_\alpha^2 \epsilon^{7\gamma_2+9/2+2\gamma_1} - 8C_{\tilde{\omega}}^4 \tilde{a}_2^2 C_\alpha^2 \epsilon^{5\gamma_2+7/2+2\gamma_1} \\
& +4C_{\tilde{\omega}}^6 C_\alpha^2 \tilde{a}_2 \epsilon^{7\gamma_2+9/2+2\gamma_1} - 3\tilde{a}_2^2 \tilde{C}^2 \epsilon^{\gamma_2+1/2} - 4C_{\tilde{\omega}}^4 \tilde{C}^2 \epsilon^{5\gamma_2+5/2} + 2\tilde{C}^4 \tilde{a}_2 \epsilon^{\gamma_2+1/2} \\
& -2C_{\tilde{\omega}}^2 \tilde{a}_2^2 \tilde{C}^2 C_\alpha^2 \epsilon^{3\gamma_2+5/2+2\gamma_1} + 4C_{\tilde{\omega}}^4 \tilde{C}^2 C_\alpha^2 \tilde{a}_2 \epsilon^{5\gamma_2+7/2+2\gamma_1} - 16C_{\tilde{\omega}}^2 \tilde{a}_2^2 C_\alpha \tilde{C} \epsilon^{3\gamma_2+2+\alpha} \\
& -2C_{\tilde{\omega}}^2 \tilde{C}^4 \epsilon^{3\gamma_2+3/2} + 4C_{\tilde{\omega}}^2 \tilde{a}_2 C_\alpha \tilde{C}^3 \epsilon^{3\gamma_2+2+\gamma_1} - 8C_\alpha^3 \tilde{a}_2^4 \tilde{C} \epsilon^{\gamma_2+3\gamma_1+2} + 8C_{\tilde{\omega}}^2 \tilde{C}^2 \tilde{a}_2 \epsilon^{3\gamma_2+3/2} \\
& +4\tilde{C}^3 C_\alpha^3 \tilde{a}_2^3 \epsilon^{\gamma_2+3\gamma_1+2} - 2C_{\tilde{\omega}}^6 \epsilon^{7\gamma_2+7/2} - 4\tilde{a}_2^2 C_\alpha \tilde{C}^3 \epsilon^{\gamma_2+\gamma_1+1} \\
& +4C_{\tilde{\omega}}^4 \tilde{a}_2 \epsilon^{5\gamma_2+5/2} - 3\tilde{a}_2^4 C_\alpha^2 \epsilon^{\gamma_2+2\gamma_1+3/2} \big) + \ldots, \\
Q(\alpha^*, \overline{\tilde{\omega}}) = -\tfrac{2\tilde{a}_2^2}{\epsilon^{11/2}} \big(& \tilde{a}_2 \tilde{C}^3 C_{\tilde{\omega}}^4 \epsilon^{4\gamma_2+2} - C_\alpha \tilde{C}^4 C_{\tilde{\omega}}^6 \epsilon^{6\gamma_2+\gamma_1+7/2} + 2\tilde{a}_2^3 \tilde{C}^3 - 3\tilde{a}_2^4 C_\alpha C_{\tilde{\omega}}^2 \epsilon^{\gamma_1+2\gamma_2+3/2} \\
& -12\tilde{a}_2^2 C_\alpha C_{\tilde{\omega}}^6 \epsilon^{6\gamma_2+\gamma_1+7/2} - 4\tilde{a}_2^2 \tilde{C} C_{\tilde{\omega}}^4 \epsilon^{4\gamma_2+2} - 2\tilde{a}_2^2 \tilde{C}^3 C_{\tilde{\omega}}^2 \epsilon^{2\gamma_2+1} - 2\tilde{a}_2^5 \tilde{C} C_\alpha^2 \epsilon^{2\gamma_1+1} \\
& +10\tilde{a}_2^3 C_\alpha C_{\tilde{\omega}}^4 \epsilon^{\gamma_1+4\gamma_2+5/2} + 5\tilde{a}_2^3 \tilde{C} C_{\tilde{\omega}}^2 \epsilon^{2\gamma_2+1} - 2C_\alpha \tilde{C}^2 C_{\tilde{\omega}}^8 \epsilon^{8\gamma_2+\gamma_1+9/2} + \tilde{a}_2 \tilde{C} C_{\tilde{\omega}}^6 \epsilon^{6\gamma_2+3} \\
& +2C_\alpha \tilde{C}^4 C_{\tilde{\omega}}^4 \tilde{a}_2 \epsilon^{\gamma_1+4\gamma_2+5/2} + 4\tilde{a}_2^4 \tilde{C} C_{\tilde{\omega}}^2 C_\alpha^2 \epsilon^{2\gamma_2+2\gamma_1+2} - 2\tilde{a}_2^3 \tilde{C}^3 C_{\tilde{\omega}}^2 C_\alpha^2 \epsilon^{2\gamma_2+2\gamma_1+2} \\
& -2\tilde{a}_2^3 \tilde{C} C_{\tilde{\omega}}^4 C_\alpha^2 \epsilon^{4\gamma_2+2\gamma_1+3} + 8C_\alpha \tilde{C}^2 C_{\tilde{\omega}}^6 \tilde{a}_2 \epsilon^{6\gamma_2+\gamma_1+7/2} - 8\tilde{a}_2^2 C_\alpha C_{\tilde{\omega}}^4 \tilde{C}^2 \epsilon^{\gamma_1+4\gamma_2+5/2} \\
& +6C_{\tilde{\omega}}^8 C_\alpha \tilde{a}_2 \epsilon^{8\gamma_2+\gamma_1+9/2} - C_\alpha C_{\tilde{\omega}}^{10} \epsilon^{\gamma_1+10\gamma_2+11/2} + 2\tilde{a}_2^3 C_\alpha C_{\tilde{\omega}}^2 \tilde{C}^2 \epsilon^{\gamma_1+2\gamma_2+3/2} \big) + \ldots .
\end{aligned}
$$

Equating the exponents in these two equations leads to $\gamma_1 = \gamma_2 = -\frac{1}{2}$. The constants need to mach as well, and thus, we obtain C_α and $C_{\tilde{\omega}}$ by solving the resulting equations, and they will both depend on $\tilde{C}$, which again is given by $\tilde{C} := \frac{\tilde{b}_1}{\sqrt{\tilde{a}_1}}$. The resulting leading terms in $Q(\alpha^*, \overline{\tilde{\omega}})$ form a polynomial of degree two in C_α, so by solving $Q(\alpha^*, \overline{\tilde{\omega}}) = 0$ for C_α, we have C_α in terms of $\tilde{a}_2$, $\tilde{C}$, and $C_{\tilde{\omega}}$,

$$
\begin{aligned}
C_\alpha^\pm &:= \tfrac{X \pm \sqrt{Y}}{2(2\tilde{a}_2^3 \tilde{C}^3 C_{\tilde{\omega}}^2 + 2\tilde{a}_2^3 \tilde{C} C_{\tilde{\omega}}^4 + 2\tilde{a}_2^5 \tilde{C} - 4\tilde{a}_2^4 \tilde{C} C_{\tilde{\omega}}^2)}, \\
X &:= -2\tilde{C}^2 C_{\tilde{\omega}}^8 - 12\tilde{a}_2^2 C_{\tilde{\omega}}^6 + 8\tilde{C}^2 C_{\tilde{\omega}}^6 \tilde{a}_2 - \tilde{C} C_{\tilde{\omega}}^6 - 8\tilde{a}_2^2 C_{\tilde{\omega}}^4 \tilde{C}^2 - C_{\tilde{\omega}}^{10} + 2\tilde{a}_2^3 C_{\tilde{\omega}}^2 \tilde{C}^2 + 6C_{\tilde{\omega}}^8 \tilde{a}_2 \\
&\quad +2\tilde{C}^4 C_{\tilde{\omega}}^4 \tilde{a}_2 - 3\tilde{a}_2^4 C_{\tilde{\omega}}^2 + 10\tilde{a}_2^3 C_{\tilde{\omega}}^4, \\
Y &:= 160\tilde{C}^2 C_{\tilde{\omega}}^{14} \tilde{a}_2^2 - 48\tilde{C}^4 C_{\tilde{\omega}}^{14} \tilde{a}_2 + 144\tilde{C}^4 C_{\tilde{\omega}}^{12} \tilde{a}_2^2 - 204\tilde{C}^4 C_{\tilde{\omega}}^{10} \tilde{a}_2^3 - 40\tilde{C}^2 C_{\tilde{\omega}}^{16} \tilde{a}_2 \\
&\quad +396\tilde{C}^2 C_{\tilde{\omega}}^{10} \tilde{a}_2^4 - 332\tilde{C}^2 C_{\tilde{\omega}}^{12} \tilde{a}_2^3 - 304\tilde{a}_2^5 C_{\tilde{\omega}}^8 \tilde{C}^2 + 158\tilde{C}^4 C_{\tilde{\omega}}^8 \tilde{a}_2^4 + 48\tilde{C}^6 C_{\tilde{\omega}}^{10} \tilde{a}_2^2 \\
&\quad -4\tilde{C}^8 C_{\tilde{\omega}}^{10} \tilde{a}_2 - 108\tilde{a}_2^5 C_{\tilde{\omega}}^6 \tilde{C}^4 + 200\tilde{a}_2^6 C_{\tilde{\omega}}^6 \tilde{C}^2 - 124\tilde{a}_2^7 C_{\tilde{\omega}}^4 \tilde{C}^2 + 4\tilde{C}^8 C_{\tilde{\omega}}^8 \tilde{a}_2^2 \\
&\quad +16\tilde{a}_2^6 \tilde{C}^6 C_{\tilde{\omega}}^2 - 48\tilde{a}_2^7 \tilde{C}^4 C_{\tilde{\omega}}^2 + 40\tilde{a}_2^8 \tilde{C}^2 C_{\tilde{\omega}}^2 + 9\tilde{a}_2^8 C_{\tilde{\omega}}^4 - 60\tilde{a}_2^7 C_{\tilde{\omega}}^6 + 16\tilde{a}_2^8 \tilde{C}^4 + C_{\tilde{\omega}}^{20}
\end{aligned}
$$

$$
\begin{aligned}
&+4\tilde{C}^2C_{\tilde{\omega}}^{18}+270\tilde{a}_2^4C_{\tilde{\omega}}^{12}+60\tilde{a}_2^2C_{\tilde{\omega}}^{16}-164\tilde{a}_2^3C_{\tilde{\omega}}^{14}+172\tilde{a}_2^6C_{\tilde{\omega}}^{8}-276\tilde{a}_2^5C_{\tilde{\omega}}^{10}\\
&-12C_{\tilde{\omega}}^{18}\tilde{a}_2+6\tilde{C}^4C_{\tilde{\omega}}^{16}+100\tilde{a}_2^6C_{\tilde{\omega}}^4\tilde{C}^4+16\tilde{a}_2^4C_{\tilde{\omega}}^6\tilde{C}^6-36\tilde{C}^6C_{\tilde{\omega}}^8\tilde{a}_2^3\\
&-24\tilde{C}^6C_{\tilde{\omega}}^{12}\tilde{a}_2-16\tilde{a}_2^5\tilde{C}^6C_{\tilde{\omega}}^4+4\tilde{C}^6C_{\tilde{\omega}}^{14}+\tilde{C}^8C_{\tilde{\omega}}^{12}.
\end{aligned}
\tag{4.85}
$$

Now substituting again C_α^+ into the leading terms in $P(\overline{\tilde{\omega}},\alpha^*)$ and solving the resulting equation for $C_{\tilde{\omega}}$, the desired solution for $C_{\tilde{\omega}}$ is given by the square root of the zero of a polynomial of degree eight which depends on $\tilde{a}_2$ and $\tilde{C}$, and is given by

$$
\begin{aligned}
P_8(Z)=&5Z^8+(18\tilde{C}^2-34\tilde{a}_2)Z^7+(24\tilde{C}^4-103\tilde{C}^2\tilde{a}_2+89\tilde{a}_2^2)Z^6+(216\tilde{a}_2^2\tilde{C}^2+14\tilde{C}^6\\
&-116\tilde{a}_2^3-106\tilde{C}^4\tilde{a}_2)Z^5+(79\tilde{a}_2^4-206\tilde{a}_2^3\tilde{C}^2+3\tilde{C}^8-41\tilde{a}_2\tilde{C}^6+151\tilde{a}_2^2\tilde{C}^4)Z^4\\
&+(-76\tilde{a}_2^3\tilde{C}^4+28\tilde{a}_2^2\tilde{C}^6-26\tilde{a}_2^5+56\tilde{a}_2^4\tilde{C}^2-4\tilde{a}_2\tilde{C}^8)Z^3+(3\tilde{a}_2^6+53\tilde{a}_2^5\tilde{C}^2\\
&-2\tilde{a}_2^3\tilde{C}^6-19\tilde{a}_2^4\tilde{C}^4)Z^2+(30\tilde{a}_2^5\tilde{C}^4-6\tilde{a}_2^4\tilde{C}^6-30\tilde{a}_2^6\tilde{C}^2)Z\\
&-6\tilde{a}_2^6\tilde{C}^4+2\tilde{a}_2^5\tilde{C}^6+4\tilde{a}_2^7\tilde{C}^2.
\end{aligned}
$$

A Taylor expansion about the point $(\tilde{a}_2,\tilde{C})=(x_0,y_0)$ from the typical transmission line circuit elements in (4.82) is also used here in a similar way to the one in Subsection 4.1.5 to approximate the zero of the polynomial P_8, and we find

$$C_\omega := \sqrt{0.6638+2.3321\tilde{a}_2+0.5944\tilde{C}}.$$

Then substituting the approximated $C_{\tilde{\omega}}$ into C_α^+ in (4.85), we obtain C_α^+ in terms of $\tilde{a}_2$ and $\tilde{C}$. Again, we find a Taylor approximation of C_α^+ about the point $(\tilde{a}_2,\tilde{C})=(x_0,y_0)$ to get the simple result

$$C_\alpha = C_\alpha^+ = -1.2500+0.3769\tilde{a}_2+0.1220\tilde{C},$$

which is used together with $\alpha = C_\alpha\epsilon^{\gamma_1}$ to obtain α^*,

$$\alpha^* = (-1.2500+0.3769\tilde{a}_2+0.1220\frac{\tilde{b}_1}{\sqrt{\tilde{a}_1}})\sqrt{\tilde{a}_1}. \tag{4.86}$$

Note that here also $\tilde{b}_2$ does not appear in the asymptotic result for α^*, $\tilde{b}_2$ only appears in higher order terms in the asymptotic expansion. However, α^* given in (4.86) for the

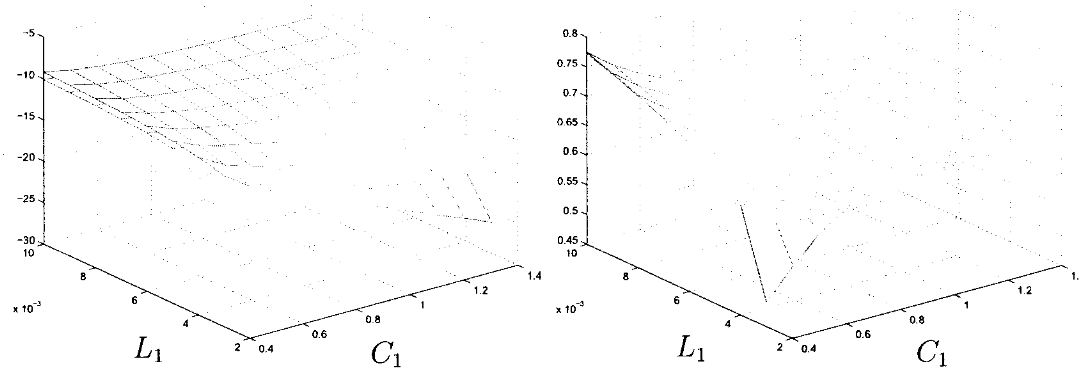

Figure 4.14: Left: optimized α^* from (4.84) versus asymptotic result (4.86). Right: maximum of $|\rho_{opt}(\overline{\omega}, \alpha^*)|$ versus maximum of $|\rho_{opt}(\overline{\omega}, \alpha^*_{asy})|$ as functions of the circuit elements L_1 and C_1.

small circuit case, where we have the overlap at an odd row, is completely different from α^* given in (4.54) for the extra small circuit case, where we have the overlap at an even row.

In Figure 4.14, we choose $R_s = R_L = 0.05$ kOhms and $R_1 = R_2 = 0.5e - 3$ kOhms from Subsection 4.2.6, and we vary the circuit elements L_1 and C_1 to plot the optimized α^* from (4.84) and the asymptotic result (4.86) on the left hand side. In addition, on the right hand side of Figure 4.14, we plot the maximum of the convergence factor as a function of the circuit elements L_1 and C_1 using the optimized α^* from (4.84) and the asymptotic result (4.86). One can see that the two surfaces of the convergence factors are close.

An example for the optimized convergence factor as a function of the frequency ω is given in Figure 4.15, using the typical transmission line circuit elements from Subsection 4.2.6. On the left hand side of Figure 4.15, we compare the classical convergence factor with the optimized one, where we observe the better behavior of the optimized convergence factor over the classical one. On the right hand side of Figure

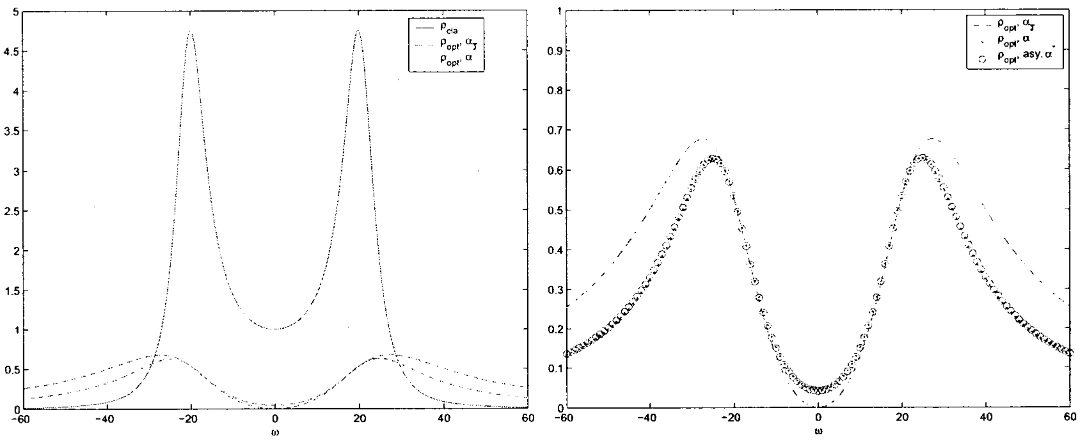

Figure 4.15: Left: convergence factor $|\rho_{cla}(\omega)|$ versus $|\rho_{opt}(\omega, \alpha_T)|$ and $|\rho_{opt}(\omega, \alpha^*)|$. Right: optimized convergence factors $|\rho_{opt}(\omega, \alpha_T)|$ with the Taylor approximation, $|\rho_{opt}(\omega, \alpha^*)|$ with the numerically optimized value, and $|\rho_{opt}(\omega, \alpha^*_{asy})|$ with the asymptotically optimized value.

4.15, we plot the optimized convergence factor with the numerically optimized value $\alpha^* = -12.9733$, the asymptotic value $\alpha^*_{asy} = -13.1346$, and the Taylor approximation $\alpha_T = -19.8020$, and one can see again that the numerically optimized and asymptotic results are very close. In addition, one can observe that the Taylor approximation works well. Note that for the case when the overlap is at an even row which was the case for the very small circuit, we have a small value for α^*, and it is given by $\alpha^* = -0.0381$, whereas for the overlap at an odd row which is the case here for the small circuit, α^* is a bigger value, and is given by $\alpha^* = -12.9733$. Moreover, from Figures 4.6 and 4.15 we observe that the modulus of the convergence factor for the small transmission line circuit case takes bigger values than those for the extra small circuit case, and thus as we increase the size of the circuit the convergence factor becomes bigger and bigger.

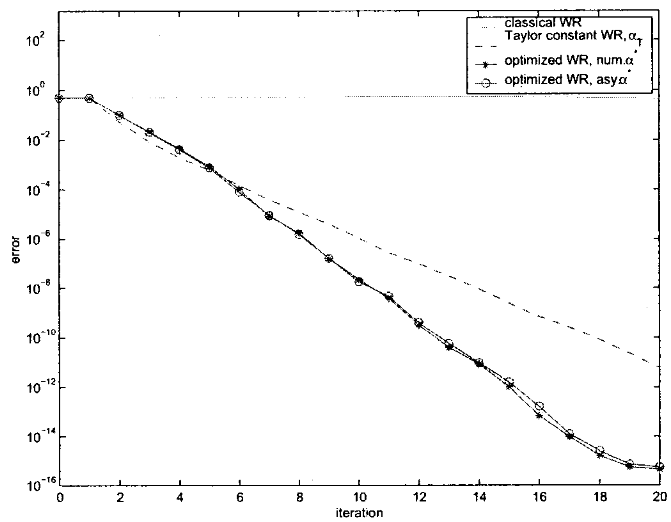

Figure 4.16: Convergence behavior of the classical versus the optimized WR algorithms for a small transmission line circuit.

4.2.6 Numerical Experiments

We give here a numerical experiment for the small transmission line given in Figure 4.8. We use the typical transmission line circuit elements $R_s = R_L = 0.05$ kOhms, $R_1 = R_2 = 0.5e - 3$ kOhms, $C_1 = C_2 = C_3 = 0.63$ pF, and $L_1 = L_2 = 4.95e - 3$ μH, with source $I_s = 10t$ for $0 < t < 0.1$ and $I_s = 1$ mA for $t \geq 0.1$, and the analysis time interval is $[0, T]$, with $T = 1$ ns. The solution is computed using the backward Euler method, with $\Delta t = \frac{1}{10}$, and zero initial waveforms. The parameters we use are the numerically optimized value $\alpha^* = -12.9733$, the asymptotic value $\alpha^*_{asy} = -13.1346$ from the result in (4.86), and the Taylor approximation $\alpha_T = -19.8020$. We also choose $\beta^* = -\frac{1}{\alpha^*}$. In Figure 4.16 we show the error as a function of the iterations. One can see how much the convergence has improved by using the optimized WR algorithm over the classical one. One can also compare the error decay for the small circuit case with the one for the extra small circuit case in Figure 4.7, which shows the similar behavior of convergence for the WR algorithms.

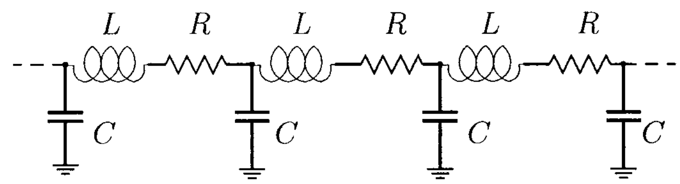

Figure 4.17: An infinitely long transmission line circuit.

4.3 An Infinitely Large Transmission Line Circuit

In the previous sections we analyzed relatively small circuits. In this section we present an analysis for the infinitely large circuit shown in Figure 4.17, to investigate the impact of the circuit size on the performance of the optimized WR algorithm. The equations of the large circuit are

$$\dot{\boldsymbol{x}} = \left(\begin{array}{cccccccc} \ddots & \ddots & \ddots & & & & & \\ & a & b & -a & & & & \\ & & -c & 0 & c & & & \\ & & & a & b & -a & & \\ & & & & -c & 0 & c & \\ & & & & & \ddots & \ddots & \ddots \end{array}\right) \boldsymbol{x} + \boldsymbol{f}, \tag{4.87}$$

where the vector of unknown waveforms is

$$\boldsymbol{x} = (\dots, x_{-2}, x_{-1}, x_0, x_1, x_2, x_3, \dots)^T = (\dots, i_{-1}, v_{-1}, i_0, v_0, i_1, v_1, \dots)^T.$$

The odd indices represent the nodal voltages, and the even indices represent the inductance currents in the transmission line circuit. The entries of the matrix are given by

$$a = \frac{1}{L}, \quad c = -\frac{1}{C}, \quad b = -\frac{R}{L}. \tag{4.88}$$

The source term on the right hand side, and an initial condition are given by

$$\boldsymbol{f}(t) = (\dots, f_{-1}(t), f_0(t), f_1(t), \dots)^T, \; \boldsymbol{x}(0) = (\dots, i^0_{-1}, v^0_{-1}, i^0_0, v^0_0, i^0_1, v^0_1, \dots)^T.$$

Since the circuit is infinitely large, we assume that all voltages and currents values stay bounded as we approach the infinite ends of the circuit to have a well posed problem.

4.3.1 Analysis of the Classical WR Algorithm without Overlap

We partition the circuit at an even row into two sub-circuits or subsystems, and we call the unknown values in the first subsystem $\boldsymbol{u}(t)$ and in the second subsystem $\boldsymbol{w}(t)$. The classical WR algorithm applied to (4.87) with two semi-infinite sub-circuits is given by

$$\begin{aligned}
\dot{\boldsymbol{u}}^{k+1} &= \begin{bmatrix} \ddots & \ddots & \ddots & \\ & -c & 0 & c \\ & & a & b \end{bmatrix} \boldsymbol{u}^{k+1} + \begin{pmatrix} \vdots \\ f_{-1} \\ f_0 \end{pmatrix} + \begin{pmatrix} \vdots \\ 0 \\ -aw_1^k \end{pmatrix}, \\
\dot{\boldsymbol{w}}^{k+1} &= \begin{bmatrix} 0 & c & & \\ a & b & -a & \\ & \ddots & \ddots & \ddots \end{bmatrix} \boldsymbol{w}^{k+1} + \begin{pmatrix} f_1 \\ f_2 \\ \vdots \end{pmatrix} + \begin{pmatrix} -cu_0^k \\ 0 \\ \vdots \end{pmatrix};
\end{aligned} \tag{4.89}$$

with corresponding initial conditions $\boldsymbol{u}^{k+1}(0) = (\dots, i_{-1}^0, v_{-1}^0, i_0^0)^T$ and $\boldsymbol{w}^{k+1}(0) = (v_0^0, i_1^0, v_1^0, \dots)^T$, and some initial waveforms $\boldsymbol{u}^0(t)$ and $\boldsymbol{w}^0(t)$. The Laplace transform of the homogeneous problem yields in the $s \in \mathbb{C}$ domain

$$\begin{aligned}
s\hat{\boldsymbol{u}}^{k+1} &= \begin{bmatrix} \ddots & \ddots & \ddots & \\ & -c & 0 & c \\ & & a & b \end{bmatrix} \hat{\boldsymbol{u}}^{k+1} + \begin{pmatrix} \vdots \\ 0 \\ -a\hat{w}_1^k \end{pmatrix}, \\
s\hat{\boldsymbol{w}}^{k+1} &= \begin{bmatrix} 0 & c & & \\ a & b & -a & \\ & \ddots & \ddots & \ddots \end{bmatrix} \hat{\boldsymbol{w}}^{k+1} + \begin{pmatrix} -c\hat{u}_0^k \\ 0 \\ \vdots \end{pmatrix}.
\end{aligned} \tag{4.90}$$

Solving the first system of equations for $\hat{u}_j^{k+1}$ corresponds to solving the recurrence relations

$$\begin{aligned} a\hat{u}_{j-1}^{k+1} + (b-s)\hat{u}_j^{k+1} - a\hat{u}_{j+1}^{k+1} &= 0, \quad j = 0, -2, -4 \ldots, \\ -c\hat{u}_{j-1}^{k+1} + (0-s)\hat{u}_j^{k+1} + c\hat{u}_{j+1}^{k+1} &= 0, \quad j = -1, -3, -5, \ldots, \end{aligned}$$

or

$$\begin{aligned} a\hat{u}_{2j-1}^{k+1} + (b-s)\hat{u}_{2j}^{k+1} - a\hat{u}_{2j+1}^{k+1} &= 0, \\ -c\hat{u}_{2j-2}^{k+1} - s\hat{u}_{2j-1}^{k+1} + c\hat{u}_{2j}^{k+1} &= 0, \quad j = 0, -1, -2, \ldots. \end{aligned} \tag{4.91}$$

Solving the second equation in (4.91) for the odd indices, with $s = \eta + i\omega$, $\eta > 0$, we get $\hat{u}_{2j-1}^{k+1} = \frac{c}{s}(\hat{u}_{2j}^{k+1} - \hat{u}_{2j-2}^{k+1})$, and substituting this result into the other equation, we find the recurrence relation

$$-\frac{ac}{s}\hat{u}_{2j-2}^{k+1} + (\frac{2ac}{s} + (b-s))\hat{u}_{2j}^{k+1} - \frac{ac}{s}\hat{u}_{2j+2}^{k+1} = 0, \quad j = 0, -1, -2, \ldots,$$

and using the fact that $a > 0$, $b < 0$, and $c < 0$ from (4.88), we get

$$\frac{a|c|}{s}\hat{u}_{2j-2}^{k+1} - (\frac{2a|c|}{s} + (|b| + s))\hat{u}_{2j}^{k+1} + \frac{a|c|}{s}\hat{u}_{2j+2}^{k+1} = 0, \quad j = 0, -1, -2, \ldots. \tag{4.92}$$

The general solution of (4.92) is

$$\hat{u}_{2j}^{k+1} = A^{k+1}\lambda_+^{2j} + B^{k+1}\lambda_-^{2j}, \tag{4.93}$$

where $\lambda_\pm^2$ are the roots of the characteristic polynomial of the recurrence relation,

$$\lambda_\pm^2 = \frac{2a|c| + s(|b| + s) \pm \sqrt{(2a|c| + s(|b| + s))^2 - 4a^2|c|^2}}{2a|c|}, \tag{4.94}$$

and A^{k+1}, B^{k+1} are some constants. We now study $\lambda_\pm^2$ in (4.94) in more detail.

Lemma 4.5. *The roots $\lambda_\pm^2$ given in equation (4.94) satisfy for $s = \eta + i\omega$, $\eta \geq 0$,*

- $|\lambda_+^2| > 1$ *for* $\{(\eta, \omega) : -\sqrt{2a|c| + |b|\eta + \eta^2} < \omega \leq \sqrt{2a|c| + |b|\eta + \eta^2},\ \eta \geq 0\} \setminus \{(0, 0)\}$,

- $|\lambda_-^2| > 1$ *for* $\{(\eta, \omega) : \omega \leq -\sqrt{2a|c| + |b|\eta + \eta^2}$, *or* $\omega > \sqrt{2a|c| + |b|\eta + \eta^2}$, $\eta \geq 0\}$,
- $|\lambda_+^2| = |\lambda_-^2| = 1 \iff \lambda_+^2 = \lambda_-^2 = 1 \iff \omega = \eta = 0$.

Proof. Let $\tilde{c} = a|c|$ to eliminate one parameter, and $z = 2 + C_1 s + C_2 s^2$, where $s = \eta + i\omega$, $C_1 = \frac{|b|}{\tilde{c}}$, and $C_2 = \frac{1}{\tilde{c}}$. Then $\lambda_\pm^2$ is given by

$$\lambda_\pm^2 = \frac{z \pm \sqrt{z^2 - 4}}{2}, \tag{4.95}$$

where $z = x + iy$ with

$$x = 2 + C_1\eta + C_2(\eta^2 - \omega^2), \quad y = \omega(C_1 + 2C_2\eta). \tag{4.96}$$

The real parts of λ_+^2 and λ_-^2 are given by

$$\Re(\lambda_+^2) = \tfrac{1}{2}x + \tfrac{1}{4}\sqrt{2\sqrt{x^4 + 2x^2y^2 - 8x^2 + y^4 + 8y^2 + 16} + 2x^2 - 2y^2 - 8},$$
$$\Re(\lambda_-^2) = \tfrac{1}{2}x - \tfrac{1}{4}\sqrt{2\sqrt{x^4 + 2x^2y^2 - 8x^2 + y^4 + 8y^2 + 16} + 2x^2 - 2y^2 - 8}.$$

Now, we will treat several cases separately.

1. We start by assuming that $y \neq 0$ and $x \neq 0$. In this case, the imaginary parts of λ_+^2 and λ_-^2 are given by

$$\Im(\lambda_+^2) = \tfrac{1}{2}y + \tfrac{1}{4}\tfrac{2xy}{|2xy|}\sqrt{2\sqrt{x^4 + 2x^2y^2 - 8x^2 + y^4 + 8y^2 + 16} - 2x^2 + 2y^2 + 8},$$
$$\Im(\lambda_-^2) = \tfrac{1}{2}y - \tfrac{1}{4}\tfrac{2xy}{|2xy|}\sqrt{2\sqrt{x^4 + 2x^2y^2 - 8x^2 + y^4 + 8y^2 + 16} - 2x^2 + 2y^2 + 8}.$$

By the definition (4.96) of x, and with the assumption $x > 0$, we obtain

$$x = 2 + C_1\eta + C_2(\eta^2 - \omega^2) > 0,$$

which implies

$$-\sqrt{\frac{2 + C_1\eta + C_2\eta^2}{C_2}} < \omega < \sqrt{\frac{2 + C_1\eta + C_2\eta^2}{C_2}}.$$

For $x > 0$ and any $y \neq 0$, we have

$$(\Im(\lambda_+^2))^2 = \left(\tfrac{1}{2}|y| + \tfrac{1}{4}\sqrt{2\sqrt{x^4 + 2x^2y^2 - 8x^2 + y^4 + 8y^2 + 16} - 2x^2 + 2y^2 + 8}\right)^2,$$
$$(\Im(\lambda_-^2))^2 = \left(\tfrac{1}{2}|y| - \tfrac{1}{4}\sqrt{2\sqrt{x^4 + 2x^2y^2 - 8x^2 + y^4 + 8y^2 + 16} - 2x^2 + 2y^2 + 8}\right)^2.$$

Since $(\Re(\lambda_+^2))^2 > (\Re(\lambda_-^2))^2$ and $(\Im(\lambda_+^2))^2 > (\Im(\lambda_-^2))^2$, we have

$$|\lambda_+^2|^2 = (\Re(\lambda_+^2))^2 + (\Im(\lambda_+^2))^2 > (\Re(\lambda_-^2))^2 + (\Im(\lambda_-^2))^2 = |\lambda_-^2|^2,$$

and by Vieta's formulas, Theorem 4.4, we have $|\lambda_+^2||\lambda_-^2| = 1$, and hence, we get $|\lambda_+^2| > 1$ and $|\lambda_-^2| < 1$. Now $x < 0$ implies

$$\omega < -\sqrt{\frac{2 + C_1\eta + C_2\eta^2}{C_2}} \quad \text{or} \quad \omega > \sqrt{\frac{2 + C_1\eta + C_2\eta^2}{C_2}},$$

and for any $y \neq 0$, we have

$$(\Re(\lambda_+^2))^2 = \left(\tfrac{1}{2}|x| - \tfrac{1}{4}\sqrt{2\sqrt{x^4 + 2x^2y^2 - 8x^2 + y^4 + 8y^2 + 16} + 2x^2 - 2y^2 - 8}\right)^2,$$
$$(\Re(\lambda_-^2))^2 = \left(\tfrac{1}{2}|x| + \tfrac{1}{4}\sqrt{2\sqrt{x^4 + 2x^2y^2 - 8x^2 + y^4 + 8y^2 + 16} + 2x^2 - 2y^2 - 8}\right)^2,$$

and

$$(\Im(\lambda_+^2))^2 = \left(\tfrac{1}{2}|y| - \tfrac{1}{4}\sqrt{2\sqrt{x^4 + 2x^2y^2 - 8x^2 + y^4 + 8y^2 + 16} - 2x^2 + 2y^2 + 8}\right)^2,$$
$$(\Im(\lambda_-^2))^2 = \left(\tfrac{1}{2}|y| + \tfrac{1}{4}\sqrt{2\sqrt{x^4 + 2x^2y^2 - 8x^2 + y^4 + 8y^2 + 16} - 2x^2 + 2y^2 + 8}\right)^2.$$

Since now $(\Re(\lambda_+^2))^2 < (\Re(\lambda_-^2))^2$ and $(\Im(\lambda_+^2))^2 < (\Im(\lambda_-^2))^2$, we have

$$|\lambda_+^2|^2 = (\Re(\lambda_+^2))^2 + (\Im(\lambda_+^2))^2 < (\Re(\lambda_-^2))^2 + (\Im(\lambda_-^2))^2 = |\lambda_-^2|^2.$$

Therefore, $|\lambda_+^2| < 1$ and $|\lambda_-^2| > 1$.

2. If $x = 0$, then $\omega = \pm\sqrt{\frac{2+C_1\eta+C_2\eta^2}{C_2}}$, $y = \pm\sqrt{\frac{2+C_1\eta+C_2\eta^2}{C_2}}(C_1 + 2C_2\eta)$, and $z = iy$, where y can not be zero, since C_1 and C_2 are positive, and $\eta \geq 0$. In this case, $\lambda_\pm^2$ can be simplified to

$$\lambda_\pm^2 = \frac{1}{2}(y \pm \sqrt{y^2 + 4})i.$$

Hence, $|\lambda_+^2|^2 = \frac{y^2}{2} + \frac{y}{2}\sqrt{y^2+4} + 1$ and $|\lambda_-^2|^2 = \frac{y^2}{2} - \frac{y}{2}\sqrt{y^2+4} + 1$. So if $y < 0$, then $|\lambda_+^2| < |\lambda_-^2|$, which implies $|\lambda_+^2| < 1$ and $|\lambda_-^2| > 1$. If $y > 0$, then $|\lambda_+^2| > |\lambda_-^2|$, which gives $|\lambda_+^2| > 1$ and $|\lambda_-^2| < 1$.

3. In this case we consider $y = 0$. We have $y = 0$ if and only if $\omega = 0$ since C_1 and C_2 are positive, and $\eta \geq 0$, which also implies that $x \neq 0$. The roots $\lambda_\pm^2$ are now given by

$$\lambda_\pm^2 = \frac{2 + C_1\eta + C_2\eta^2 \pm \sqrt{(2 + C_1\eta + C_2\eta^2)^2 - 4}}{2}.$$

For $\eta = 0$, we get $\lambda_+^2 = \lambda_-^2 = 1$. The only other solution for $\lambda_+^2 = \lambda_-^2 = 1$ is when $\eta = -\frac{C_1}{C_2}$, which is excluded since $\eta \geq 0$. For $\eta > 0$, we have $\lambda_+^2 > \lambda_-^2$, which implies $|\lambda_+^2| > |\lambda_-^2|$, and hence $|\lambda_+^2| > 1$ and $|\lambda_-^2| < 1$.

4. For the last part of the proof, we consider $\lambda_\pm^2$ in (4.95), and for λ_-^2 we have

$$\begin{aligned} \lambda_-^2 = \tfrac{z-\sqrt{z^2-4}}{2} = 1 \; &\Leftrightarrow z - 2 = \sqrt{z^2-4} \\ &\Leftrightarrow (z-2)^2 = z^2 - 4 \\ &\Leftrightarrow z = 2, \end{aligned}$$

and therefore, $z = 2 + C_1 s + C_2 s^2 = 2$ if and only if $s = 0$, or $s = -\frac{C_1}{C_2}$. The two roots are real, which means $\omega = 0$, and they both satisfy the equation $\frac{z-\sqrt{z^2-4}}{2} = 1$, so we did not add roots by squaring both sides of the equation. The root $\eta = -\frac{C_1}{C_2}$ is less than zero, so it can be discarded.

A similar argument follows for λ_+^2. Hence we have only one root that satisfies the equation $\frac{z\pm\sqrt{z^2-4}}{2} = 1$, which is $s = 0$, or equivalently $\eta = 0$ and $\omega = 0$.

We have shown that for $\eta \geq 0$ and $-\sqrt{\frac{2+C_1\eta+C_2\eta^2}{C_2}} < \omega \leq \sqrt{\frac{2+C_1\eta+C_2\eta^2}{C_2}}$, except at the point $(\eta, \omega) = (0, 0)$, we have $|\lambda_+^2| > 1$ and $|\lambda_-^2| < 1$, and for $\eta \geq 0$ and $\omega \leq -\sqrt{\frac{2+C_1\eta+C_2\eta^2}{C_2}}$ or $\omega > \sqrt{\frac{2+C_1\eta+C_2\eta^2}{C_2}}$, we have $|\lambda_-^2| > 1$ and $|\lambda_+^2| < 1$. Substituting back C_1 and C_2 into the original parameters a, b, and c we get the required results. Finally, for $\eta = 0$ and $\omega = 0$, $\lambda_+^2 = \lambda_-^2 = 1$ and thus $|\lambda_+^2| = |\lambda_-^2| = 1$. □

To determine the constants A^{k+1} and B^{k+1} for the general solution (4.93), we need to use the transmission conditions at the subsystems interface and the boundedness condition at infinity. Let us consider first the case when $|\lambda_+^2| > 1$, and since $|\lambda_+^2||\lambda_-^2| = 1$, we have $|\lambda_-^2| < 1$, and by the boundedness assumption on the solution, we obtain $B^{k+1} = 0$. Hence, $\hat{u}_{2j}^{k+1} = A^{k+1}\lambda_+^{2j}$ and $\hat{u}_{2j-1}^{k+1} = \frac{c}{s}A^{k+1}\lambda_+^{2j-2}(\lambda_+^2 - 1)$. To determine A^{k+1}, we use the last equation of the first subsystem at the interface

$$a\hat{u}_{-1}^{k+1} + (b-s)\hat{u}_0^{k+1} = A^{k+1}(\frac{ac}{s}(1-\lambda_+^{-2}) + b - s) = a\hat{w}_1^k,$$

which leads to

$$A^{k+1} = \frac{as\hat{w}_1^k}{ac(1-\lambda_+^{-2}) + s(b-s)},$$

and by Vieta's formulas, Theorem 4.4, $\lambda_+^2 + \lambda_-^2 = \frac{s(b-s)}{ac} + 2$, and thus we can simplify A^{k+1} to

$$A^{k+1} = \frac{s\hat{w}_1^k}{c(\lambda_+^2 - 1)}.$$

Hence the general solutions for $\hat{u}_{2j}^{k+1}$ and $\hat{u}_{2j-1}^{k+1}$ are given by

$$\begin{aligned} \hat{u}_{2j}^{k+1} &= \tfrac{s\hat{w}_1^k}{c(\lambda_+^2-1)}\lambda_+^{2j}, \\ \hat{u}_{2j-1}^{k+1} &= \hat{w}_1^k\lambda_+^{2j-2}, \quad j = 0, -1, -2, \ldots. \end{aligned} \tag{4.97}$$

Similarly, solving the second subsystem for $\hat{w}_{2j}^{k+1}$ and $\hat{w}_{2j-1}^{k+1}$, we obtain

$$\begin{aligned} \hat{w}_{2j}^{k+1} &= B^{k+1}\lambda_-^{2j}, \\ \hat{w}_{2j-1}^{k+1} &= \tfrac{c}{s}B^{k+1}\lambda_-^{2j-2}(\lambda_-^2 - 1), \quad j = 1, 2, 3, \ldots. \end{aligned}$$

To Determine B^{k+1}, we now use the first equation of the second subsystem at the interface

$$-s\hat{w}_1^{k+1} + c\hat{w}_2^{k+1} = -s\frac{c}{s}B^{k+1}(\lambda_-^2 - 1) + cB^{k+1}\lambda_-^2 = c\hat{u}_0^k,$$

and we find

$$B^{k+1} = \hat{u}_0^k,$$

and hence the general solutions for $\hat{w}_{2j}^{k+1}$ and $\hat{w}_{2j-1}^{k+1}$ are given by

$$\begin{aligned} \hat{w}_{2j}^{k+1} &= \hat{u}_0^k \lambda_-^{2j}, \\ \hat{w}_{2j-1}^{k+1} &= \tfrac{c(\lambda_-^2-1)\hat{u}_0^k}{s} \lambda_-^{2j-2}, \quad j = 1, 2, 3, \ldots. \end{aligned} \tag{4.98}$$

Inserting this result at iteration k into (4.97), we find over two iteration steps of the WR algorithm the mapping

$$\hat{u}_0^{k+1} = \rho_{cla}(s, a, b, c)\hat{u}_0^{k-1},$$

where the convergence factor ρ_{cla} is given by

$$\rho_{cla}(s, a, b, c) = \frac{\lambda_-^2 - 1}{\lambda_+^2 - 1} = -\lambda_-^2, \tag{4.99}$$

where we used $\lambda_+^2 \lambda_-^2 = 1$ to obtain the last equality on the right. The second case is when $|\lambda_-^2| > 1$, and for this case, we obtain with a similar calculations

$$\rho_{cla}(s, a, b, c) = \frac{\lambda_+^2 - 1}{\lambda_-^2 - 1} = -\lambda_+^2. \tag{4.100}$$

The case where $\lambda_\pm^2 = 1$, implies that $s = 0$, i.e. $\eta = \omega = 0$. Note that the limit of ρ_{cla} as $s \to 0$ is one and the algorithm is not convergent. To summarize, we have for $\eta > 0$

$$\rho_{cla}(s, a, b, c) = \begin{cases} -\lambda_-^2, & |\lambda_+^2| > 1, \\ -\lambda_+^2, & |\lambda_+^2| < 1. \end{cases} \tag{4.101}$$

The same convergence factor ρ_{cla} is also found if we partition the circuit at an odd row. To see this, we consider the classical WR algorithm applied to (4.87), partitioned at an odd row with two sub-circuits,

$$\begin{aligned} \dot{\boldsymbol{u}}^{k+1} &= \begin{bmatrix} \ddots & \ddots & \ddots & \\ & a & b & -a \\ & & -c & 0 \end{bmatrix} \boldsymbol{u}^{k+1} + \begin{pmatrix} \vdots \\ f_{-2} \\ f_{-1} \end{pmatrix} + \begin{pmatrix} \vdots \\ 0 \\ c w_0^k \end{pmatrix}, \\ \dot{\boldsymbol{w}}^{k+1} &= \begin{bmatrix} b & -a & & \\ -c & 0 & c & \\ & \ddots & \ddots & \ddots \end{bmatrix} \boldsymbol{w}^{k+1} + \begin{pmatrix} f_0 \\ f_1 \\ \vdots \end{pmatrix} + \begin{pmatrix} a u_{-1}^k \\ 0 \\ \vdots \end{pmatrix}, \end{aligned} \tag{4.102}$$

with corresponding initial conditions $\boldsymbol{u}^{k+1}(0) = (\ldots, i^0_{-2}, v^0_{-2}, i^0_{-1})^T$ and $\boldsymbol{w}^{k+1}(0) = (v^0_{-1}, i^0_0, v^0_0, \ldots)^T$. The Laplace transform of the homogeneous problem yields in the $s \in \mathbb{C}$ domain

$$
\begin{aligned}
s\hat{\boldsymbol{u}}^{k+1} &= \begin{bmatrix} \ddots & \ddots & \ddots & \\ & a & b & -a \\ & & -c & 0 \end{bmatrix} \hat{\boldsymbol{u}}^{k+1} + \begin{pmatrix} \vdots \\ 0 \\ c\hat{w}^k_0 \end{pmatrix}, \\
s\hat{\boldsymbol{w}}^{k+1} &= \begin{bmatrix} b & -a & & \\ -c & 0 & c & \\ & \ddots & \ddots & \ddots \end{bmatrix} \hat{\boldsymbol{w}}^{k+1} + \begin{pmatrix} a\hat{u}^k_{-1} \\ 0 \\ \vdots \end{pmatrix}.
\end{aligned}
\tag{4.103}
$$

The same type solution is found since we have the same recurrence relations and the boundedness condition. Again, we consider the case when $|\lambda^2_+| > 1$, and from the last equation of the first subsystem at the interface

$$c\hat{u}^{k+1}_{-2} + s\hat{u}^{k+1}_{-1} = cA^{k+1}\lambda_+^{-2}(1 + \lambda^2_+ - 1) = c\hat{w}^k_0,$$

we get

$$A^{k+1} = \hat{w}^k_0.$$

Hence, the general solutions are

$$
\begin{aligned}
\hat{u}^{k+1}_{2j} &= \hat{w}^k_0 \lambda^{2j}_+, \\
\hat{u}^{k+1}_{2j+1} &= \tfrac{c}{s}\hat{w}^k_0 \lambda^{2j}_+ (\lambda^2_+ - 1), \quad j = -1, -2, \ldots.
\end{aligned}
\tag{4.104}
$$

Similarly for the second subsystem, the first equation at the interface is

$$(s - b)\hat{w}^{k+1}_0 + a\hat{w}^{k+1}_1 = B^{k+1}(\frac{ac}{s}(\lambda^2_- - 1) + s - b) = a\hat{u}^k_{-1},$$

which leads to

$$B^{k+1} = \frac{as}{ac(\lambda^2_- - 1) + s(s - b)}\hat{u}^k_{-1} = \frac{s}{c(1 - \lambda^2_+)}\hat{u}^k_{-1}.$$

Hence the general solutions for $\hat{w}_{2j}^{k+1}$ and $\hat{w}_{2j+1}^{k+1}$ are given by

$$\begin{aligned}\hat{w}_{2j}^{k+1} &= \tfrac{s\lambda_-^{2j}}{c(1-\lambda_+^2)}\hat{u}_{-1}^k,\\ \hat{w}_{2j+1}^{k+1} &= \lambda_-^{2j+2}\hat{u}_{-1}^k, \quad j=0,1,2,\ldots.\end{aligned} \tag{4.105}$$

Inserting this result at iteration k into (4.104) we find

$$\hat{u}_{-1}^{k+1} = \rho_{cla}(s,a,b,c)\hat{u}_{-1}^{k-1},$$

where the convergence factor ρ_{cla} is given by

$$\rho_{cla}(s,a,b,c) = -\lambda_-^2.$$

For the case when $|\lambda_-^2| > 1$, we similarly find

$$\rho_{cla}(s,a,b,c) = -\lambda_+^2.$$

Therefore, we get the same convergence factor ρ_{cla} whether we cut at an even row or at an odd row. This will be different for the new WR algorithm as we will see later. Since the same result holds for $\hat{w}_1^{k+1}$, we find by induction $\hat{u}_0^{2k} = (\rho_{cla})^k\hat{u}_0^0$ and $\hat{w}_1^{2k} = (\rho_{cla})^k\hat{w}_1^0$.

Next, we will show that the convergence factor (4.101) is an analytic function for $\eta > 0$, which allows us then to apply the maximum principle for complex analytic functions. We will need

Theorem 4.8. *Let D_1 and D_2 be two disjoint connected open regions, whose boundaries share a common contour Γ. Let $f(z)$ be analytic in D_1 and continuous in $D_1 \bigcup \Gamma$ and $g(z)$ be analytic in D_2 and continuous in $D_2 \bigcup \Gamma$, and let $f(z) = g(z)$ on Γ. Then the function*

$$H(z) = \begin{cases} f(z), & z \in D_1,\\ f(z) = g(z), & z \in \Gamma,\\ g(z), & z \in D_2,\end{cases}$$

is analytic in $D = D_1 \bigcup \Gamma \bigcup D_2$. We say that $g(z)$ is the ***analytic continuation*** *of $f(z)$.*

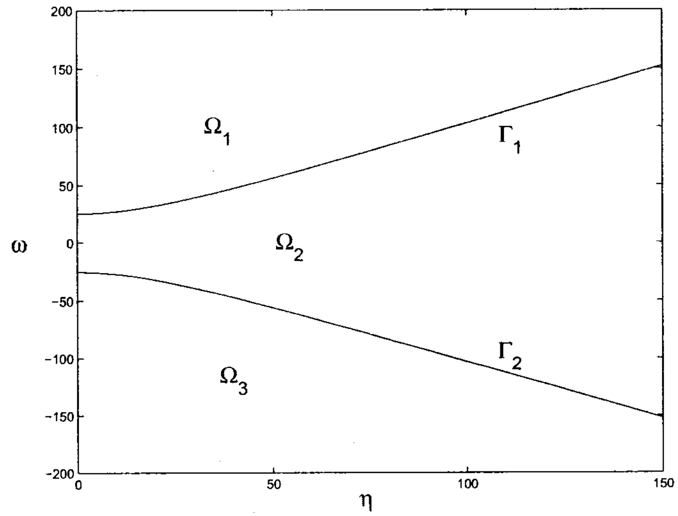

Figure 4.18: Regions in (4.106).

Proof. See [40]. □

Lemma 4.6. *If $f_\pm(z) = \pm\sqrt{z}$, then for $z = -x + iy$, $x > 0$, we have*

$$\lim_{y\downarrow 0} f_+(z) = \lim_{y\uparrow 0} f_-(z).$$

Proof. Since $f_\pm = \pm\sqrt{-x+iy} = \pm(\frac{\sqrt{-x+\sqrt{x^2+y^2}}}{\sqrt{2}} + i\frac{y}{|y|}\frac{\sqrt{x+\sqrt{x^2+y^2}}}{\sqrt{2}})$, we obtain

$$\lim_{y\downarrow 0} f_+(z) = +(0 + i\sqrt{x}) = i\sqrt{x},$$

and

$$\lim_{y\uparrow 0} f_-(z) = -(0 - i\sqrt{x}) = i\sqrt{x}.$$

Therefore, $\lim_{y\downarrow 0} f_+(z) = \lim_{y\uparrow 0} f_-(z)$. □

We now define the following subregions of the complex plane, as shown in Figure 4.18,

$$\begin{aligned}
\Omega_1 &= \{s \in \mathbb{C} : \omega > \omega^*, \eta > 0\}, \\
\Omega_2 &= \{s \in \mathbb{C} : -\omega^* < \omega < \omega^*, \eta > 0\}, \\
\Omega_3 &= \{s \in \mathbb{C} : \omega < -\omega^*, \eta > 0\}, \\
\Gamma_1 &= \{s \in \mathbb{C} : \omega = \omega^*, \eta > 0\}, \\
\Gamma_2 &= \{s \in \mathbb{C} : \omega = -\omega^*, \eta > 0\},
\end{aligned} \tag{4.106}$$

where $\omega^* = \sqrt{2a|c| + |b|\eta + \eta^2}$. Further, we define the functions g_1, g_2, and g_3 by

$$\begin{aligned}
g_1(s,a,b,c) &= \begin{cases} -\lambda_+^2, & s \in \Omega_1, \\ \lim\limits_{\omega \downarrow \omega^*}(-\lambda_+^2), & s \in \Gamma_1, \end{cases} \\
g_2(s,a,b,c) &= \begin{cases} -\lambda_-^2, & s \in \Omega_2 \bigcup \Gamma_1, \\ \lim\limits_{\omega \downarrow -\omega^*}(-\lambda_-^2), & s \in \Gamma_2, \end{cases} \\
g_3(s,a,b,c) &= \ -\lambda_+^2, \quad s \in \Omega_3 \bigcup \Gamma_2.
\end{aligned}$$

The convergence factor for the classical WR algorithm ρ_{cla} in (4.101) is now given by

$$\rho_{cla}(s,a,b,c) \quad = \quad \begin{cases} g_1(s,a,b,c), & s \in \Omega_1, \\ g_2(s,a,b,c), & s \in \Gamma_1, \\ g_2(s,a,b,c), & s \in \Omega_2, \\ g_3(s,a,b,c), & s \in \Gamma_2, \\ g_3(s,a,b,c), & s \in \Omega_3. \end{cases} \tag{4.107}$$

Theorem 4.9. *If $a > 0$, $b < 0$, and $c < 0$, then the convergence factor ρ_{cla} of the classical WR in (4.107) is an analytic function of s in the right half of the complex plane.*

Proof. The $\lambda_\pm^2$ given in (4.95) are analytic functions in Ω_1, Ω_2, and Ω_3 separately, since the argument under the square root avoids the negative real axis under the condition $\omega \neq \pm\omega^*$, since only for $\omega = \pm\omega^*$, we have $\Im(z^2-4) = 0$ and $\Re(z^2-4) < 0$, which is the branch cut that we may take, and the values $\omega = \pm\omega^*$ are excluded in Ω_1, Ω_2, and Ω_3. By Lemma 4.6, $\lim\limits_{\omega\uparrow\omega^*} \lambda_-^2 = \lim\limits_{\omega\downarrow\omega^*} \lambda_+^2$, and similarly $\lim\limits_{\omega\uparrow-\omega^*} \lambda_-^2 = \lim\limits_{\omega\downarrow-\omega^*} \lambda_+^2$.

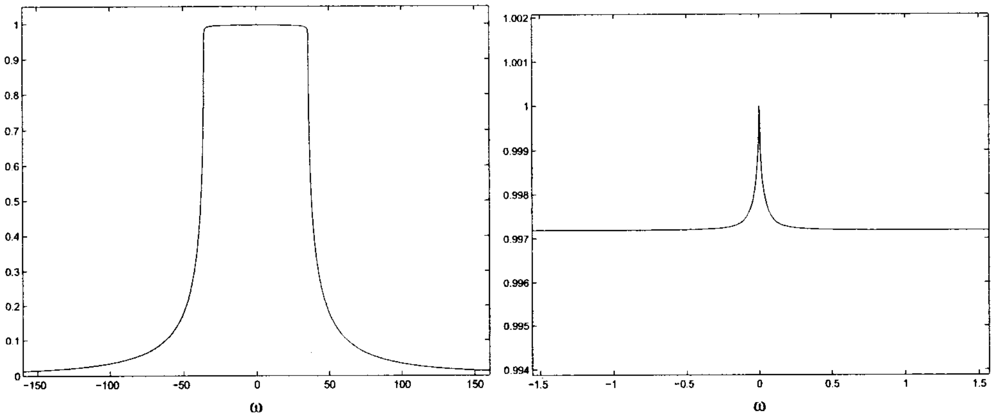

Figure 4.19: Convergence factor $|\rho_{cla}(\omega)|$ as a function of the frequency parameter ω on the left, and zoom on the right showing $|\rho_{cla}|$ for ω around zero.

Hence, for $s \in \Gamma_1$, we have $g_1(s,a,b,c) = g_2(s,a,b,c)$, and for $s \in \Gamma_2$, we have $g_2(s,a,b,c) = g_3(s,a,b,c)$. Now, g_1 is analytic in Ω_1 and continuous in $\Omega_1 \bigcup \Gamma_1$, g_2 is analytic in Ω_2 and continuous in $\Gamma_1 \bigcup \Omega_2 \bigcup \Gamma_2$, and g_3 is analytic in Ω_3 and continuous in $\Omega_3 \bigcup \Gamma_2$. Therefore by Theorem 4.8, ρ_{cla} is analytic in $D = \Omega_1 \bigcup \Gamma_1 \bigcup \Omega_2 \bigcup \Gamma_2 \bigcup \Omega_3$, which is the right half of the complex plane, $s = \eta + i\omega$, $\eta > 0$. $\square$

We again use the maximum principle for analytic functions, Theorem 1.5, to find the maximum of $|\rho_{cla}|$ to be on the boundary of the right half of the complex plane, and since for $s = re^{i\theta}$, $-\pi/2 < \theta < \pi/2$, we have $\lim_{r\to\infty} \rho_{cla} = 0$, for both cases $|\lambda_+^2| > 1$ and $|\lambda_+^2| < 1$, the maximum will be at $\eta = 0$. However, taking the limit on the boundary as ω goes to zero, we find as noted earlier that $|\rho_{cla}| = 1$. This implies that convergence will be very slow for low frequencies, ω close to zero and the mode $\omega = 0$ will not converge. An example for the convergence factor as a function of ω is given in Figure 4.19. We observe that the low frequencies converge slowly and the high frequencies converge very fast.

4.3.2 Analysis of the Classical WR Algorithm with Overlap

In this subsection we analyze the classical WR algorithm with overlap at an odd row. The classical WR algorithm is now given by

$$\begin{aligned}
\dot{\boldsymbol{u}}^{k+1} &= \begin{bmatrix} \ddots & \ddots & \ddots & \\ & a & b & -a \\ & & -c & 0 \end{bmatrix} \boldsymbol{u}^{k+1} + \begin{pmatrix} \vdots \\ f_{-2} \\ f_{-1} \end{pmatrix} + \begin{pmatrix} \vdots \\ 0 \\ c w_0^k \end{pmatrix}, \\
\dot{\boldsymbol{w}}^{k+1} &= \begin{bmatrix} 0 & c & & \\ a & b & -a & \\ & \ddots & \ddots & \ddots \end{bmatrix} \boldsymbol{w}^{k+1} + \begin{pmatrix} f_{-1} \\ f_0 \\ \vdots \end{pmatrix} + \begin{pmatrix} -c u_{-2}^k \\ 0 \\ \vdots \end{pmatrix},
\end{aligned} \tag{4.108}$$

with corresponding initial conditions $\boldsymbol{u}^{k+1}(0) = (\ldots, v_{-2}^0, i_{-1}^0, v_{-1}^0)^T$ and $\boldsymbol{w}^{k+1}(0) = (v_{-1}^0, i_0^0, v_0^0, \ldots)^T$. The same type solution as for the classical WR algorithm without overlap is found, since we have the same recurrence relations and the boundedness condition. With similar computations to those with the classical WR algorithm without overlap, we obtain the convergence factor ρ_{cla} for the WR algorithm with overlap, which is given by

$$\rho_{cla}(s, a, b, c) = \begin{cases} (\lambda_-^2)^2, & |\lambda_+^2| > 1, \\ (\lambda_+^2)^2, & |\lambda_+^2| < 1. \end{cases} \tag{4.109}$$

For an overlap at an even row the same convergence factor as in (4.109) is found. Note also that the classical convergence factor found here with overlap is the same as the classical one without overlap squared, which was also the case for the extra small and small circuits as shown before. Therefore, ρ_{cla} in (4.109) is analytic in the right half of the complex plane by Theorem 4.9, and satisfies the other results in Subsection 4.3.1.

4.3.3 An Optimal WR Algorithm without Overlap

To obtain an optimal WR algorithm, we replace the classical transmission conditions with a partition at an even row,

$$u_1^{k+1} = w_1^k, \quad w_0^{k+1} = u_0^k,$$

by the new transmission conditions

$$u_1^{k+1} + \alpha u_0^{k+1} = w_1^k + \alpha w_0^k, \quad w_1^{k+1} + \beta w_0^{k+1} = u_1^k + \beta u_0^k. \tag{4.110}$$

Analogous to the extra small and small circuit cases, these new transmission conditions exchange a combination of voltage and current in both directions, and they imply the old ones at convergence if $\alpha \neq \beta$. The partitioned infinite system with the parameters α and β for the new WR algorithm is given by

$$\begin{aligned}
\dot{\boldsymbol{u}}^{k+1} &= \begin{bmatrix} \ddots & \ddots & \ddots & \\ & -c & 0 & c \\ & & a & b+\alpha a \end{bmatrix} \boldsymbol{u}^{k+1} + \begin{pmatrix} \vdots \\ f_{-1} \\ f_0 \end{pmatrix} + \begin{pmatrix} \vdots \\ 0 \\ -a(w_1^k + \alpha w_0^k) \end{pmatrix}, \\
\dot{\boldsymbol{w}}^{k+1} &= \begin{bmatrix} \frac{c}{\beta} & c & & \\ a & b & -a & \\ & \ddots & \ddots & \ddots \end{bmatrix} \boldsymbol{w}^{k+1} + \begin{pmatrix} f_1 \\ f_2 \\ \vdots \end{pmatrix} + \begin{pmatrix} -\frac{c}{\beta}(u_1^k + \beta u_0^k) \\ 0 \\ \vdots \end{pmatrix},
\end{aligned} \tag{4.111}$$

together with the transmission conditions (4.110), which define the values u_1^k and w_0^k. Taking the Laplace transform for $s \in \mathbb{C}$ as before and assuming that the solutions stay bounded, we find the same type of solution for the recurrence relation as in the classical WR algorithm. Again for $s = \eta + i\omega$, $\eta > 0$, and considering the case where $|\lambda_+^2| > 1$, we get

$$\begin{aligned}
\hat{u}_{2j-2}^{k+1} &= A^{k+1}\lambda_+^{2j-2}, \quad \hat{u}_{2j-1}^{k+1} = \tfrac{c}{s}A^{k+1}\lambda_+^{2j-2}(\lambda_+^2 - 1), \quad j = 1, 0, -1, -2, \ldots, \\
\hat{w}_{2j}^{k+1} &= B^{k+1}\lambda_-^{2j}, \quad \hat{w}_{2j+1}^{k+1} = \tfrac{c}{s}B^{k+1}\lambda_-^{2j}(\lambda_-^2 - 1), \quad j = 0, 1, 2, 3, \ldots.
\end{aligned}$$

where the constants A^{k+1} and B^{k+1} are now different due to the new transmission conditions. Using (4.110), we find

$$A^{k+1} = \frac{c(\lambda_-^2 - 1) + \alpha s}{c(\lambda_+^2 - 1) + \alpha s} B^k, \quad B^{k+1} = \frac{c(\lambda_+^2 - 1) + \beta s}{c(\lambda_-^2 - 1) + \beta s} A^k.$$

Applying the second relation at step k to the first one, we obtain

$$\hat{u}_0^{k+1} = \rho_{opt}(s, a, b, c, \alpha, \beta)\hat{u}_0^{k-1},$$

where the convergence factor ρ_{opt} is given by

$$\rho_{opt}(s, a, b, c, \alpha, \beta) = \frac{c(\lambda_-^2 - 1) + \alpha s}{c(\lambda_+^2 - 1) + \alpha s} \cdot \frac{c(\lambda_+^2 - 1) + \beta s}{c(\lambda_-^2 - 1) + \beta s}. \tag{4.112}$$

Similarly for the case where $|\lambda_-^2| > 1$, we find

$$\rho_{opt}(s, a, b, c, \alpha, \beta) = \frac{c(\lambda_+^2 - 1) + \alpha s}{c(\lambda_-^2 - 1) + \alpha s} \cdot \frac{c(\lambda_-^2 - 1) + \beta s}{c(\lambda_+^2 - 1) + \beta s}. \tag{4.113}$$

The same relation also holds for the other subsystem, and by induction we find $\hat{u}_0^{2k} = (\rho_{opt})^k \hat{u}_0^0$ and $\hat{w}_1^{2k} = (\rho_{opt})^k \hat{w}_1^0$. To summarize, we have for $\eta > 0$

$$\rho_{opt}(s, a, b, c, \alpha, \beta) = \begin{cases} \frac{c(\lambda_-^2-1)+\alpha s}{c(\lambda_+^2-1)+\alpha s} \cdot \frac{c(\lambda_+^2-1)+\beta s}{c(\lambda_-^2-1)+\beta s}, & |\lambda_+^2| > 1, \\ \frac{c(\lambda_+^2-1)+\alpha s}{c(\lambda_-^2-1)+\alpha s} \cdot \frac{c(\lambda_-^2-1)+\beta s}{c(\lambda_+^2-1)+\beta s}, & |\lambda_+^2| < 1. \end{cases} \tag{4.114}$$

The optimal values of the parameters α and β can be found from the convergence factor (4.114).

Theorem 4.10 (Optimal Convergence). *The new WR algorithm (4.111) converges in two iterations for the choice of parameters*

$$\hat{\alpha}_{even} := \frac{-c(\lambda_-^2 - 1)}{s}, \quad \hat{\beta}_{even} := \frac{-c(\lambda_+^2 - 1)}{s}, \quad \textit{for} \quad |\lambda_+^2| > 1, \tag{4.115}$$

$$\hat{\alpha}_{even} := \frac{-c(\lambda_+^2 - 1)}{s}, \quad \hat{\beta}_{even} := \frac{-c(\lambda_-^2 - 1)}{s}, \quad \textit{for} \quad |\lambda_+^2| < 1, \tag{4.116}$$

independently of the guess for the initial waveforms $\hat{\boldsymbol{u}}^0$ *and* $\hat{\boldsymbol{w}}^0$.

Proof. The convergence factor vanishes if we insert (4.115) and (4.116) into ρ_{opt} given by (4.114) for $|\lambda_+^2| > 1$ and $|\lambda_+^2| < 1$ respectively. Hence, $\hat{u}_0^2$ and $\hat{w}_1^2$ are identically zero, independently of the initial waveforms $\hat{u}_0^0$ and $\hat{w}_1^0$. □

Note that, similar to the classical WR algorithm, the limit of ρ_{opt} as s goes to zero is one, which is the value that implies $\lambda_+^2 = \lambda_-^2 = 1$, and thus the parameters α and β can not be used to optimize the performance of the new WR algorithm at $\omega = 0$.

The new transmission conditions with a partition at an odd row are given by

$$u_0^{k+1} + \alpha u_{-1}^{k+1} = w_0^k + \alpha w_{-1}^k, \quad w_0^{k+1} + \beta w_{-1}^{k+1} = u_0^k + \beta u_{-1}^k. \tag{4.117}$$

The partitioned infinite system with the parameters α and β for the new WR algorithm is now given by

$$\begin{aligned}
\dot{\boldsymbol{u}}^{k+1} &= \begin{bmatrix} \ddots & \ddots & \ddots & \\ & a & b & -a \\ & & -c & -\alpha c \end{bmatrix} \boldsymbol{u}^{k+1} + \begin{pmatrix} \vdots \\ f_{-2} \\ f_{-1} \end{pmatrix} + \begin{pmatrix} \vdots \\ 0 \\ c(w_0^k + \alpha w_{-1}^k) \end{pmatrix}, \\
\dot{\boldsymbol{w}}^{k+1} &= \begin{bmatrix} b - \frac{a}{\beta} & -a & & \\ -c & 0 & c & \\ & \ddots & \ddots & \ddots \end{bmatrix} \boldsymbol{w}^{k+1} + \begin{pmatrix} f_0 \\ f_1 \\ \vdots \end{pmatrix} + \begin{pmatrix} \frac{a}{\beta}(u_0^k + \beta u_{-1}^k) \\ 0 \\ \vdots \end{pmatrix}.
\end{aligned} \tag{4.118}$$

With similar computations to those for the partition at an even row, we obtain the convergence factor ρ_{opt} for $|\lambda_+^2| > 1$, which is now given by

$$\rho_{opt}(s, a, b, c, \alpha, \beta) = \frac{\alpha c(1 - \lambda_+^2) + s}{\alpha c(1 - \lambda_-^2) + s} \cdot \frac{\beta c(1 - \lambda_-^2) + s}{\beta c(1 - \lambda_+^2) + s}. \tag{4.119}$$

For the case when $|\lambda_-^2| > 1$, we get

$$\rho_{opt}(s, a, b, c, \alpha, \beta) = \frac{\alpha c(1 - \lambda_-^2) + s}{\alpha c(1 - \lambda_+^2) + s} \cdot \frac{\beta c(1 - \lambda_+^2) + s}{\beta c(1 - \lambda_-^2) + s}. \tag{4.120}$$

Thus,

$$\rho_{opt}(s,a,b,c,\alpha,\beta) = \begin{cases} \frac{\alpha c(1-\lambda_+^2)+s}{\alpha c(1-\lambda_-^2)+s}\cdot\frac{\beta c(1-\lambda_-^2)+s}{\beta c(1-\lambda_+^2)+s}, & |\lambda_+^2|>1, \\ \frac{\alpha c(1-\lambda_-^2)+s}{\alpha c(1-\lambda_+^2)+s}\cdot\frac{\beta c(1-\lambda_+^2)+s}{\beta c(1-\lambda_-^2)+s}, & |\lambda_+^2|<1. \end{cases} \tag{4.121}$$

The optimal values of α and β are given in the following theorem.

Theorem 4.11 (Optimal Convergence). *The new WR algorithm (4.118) converges in two iterations for the choice of parameters*

$$\hat{\alpha}_{odd} := \frac{-s}{c(1-\lambda_+^2)}, \quad \hat{\beta}_{odd} := \frac{-s}{c(1-\lambda_-^2)}, \quad for \quad |\lambda_+^2|>1, \tag{4.122}$$

$$\hat{\alpha}_{odd} := \frac{-s}{c(1-\lambda_-^2)}, \quad \hat{\beta}_{odd} := \frac{-s}{c(1-\lambda_+^2)}, \quad for \quad |\lambda_+^2|<1, \tag{4.123}$$

independently of the guess for the initial waveforms $\hat{\boldsymbol{u}}^0$ *and* $\hat{\boldsymbol{w}}^0$.

Proof. The proof is analogous to the proof of Theorem 4.10. □

Remark 4.5. *Theorems 4.10 and 4.11 imply a relation between the best parameters obtained with a cut at an even row and a cut at an odd row. They imply that the best parameters satisfy*

$$\hat{\alpha}_{even} = \frac{-1}{\hat{\beta}_{odd}}, \quad \hat{\beta}_{even} = \frac{-1}{\hat{\alpha}_{odd}}.$$

4.3.4 An Optimal WR Algorithm with Overlap

The new WR algorithm with overlap at an even row, using the new transmission conditions

$$u_1^{k+1} + \alpha u_0^{k+1} = w_1^k + \alpha w_0^k, \quad w_0^{k+1} + \beta w_{-1}^{k+1} = u_0^k + \beta u_{-1}^k, \tag{4.124}$$

is given by

$$
\begin{aligned}
\dot{\boldsymbol{u}}^{k+1} &= \begin{bmatrix} \ddots & \ddots & \ddots & \\ & -c & 0 & c \\ & & a & b+a\alpha \end{bmatrix} \boldsymbol{u}^{k+1} + \begin{pmatrix} \vdots \\ f_{-1} \\ f_0 \end{pmatrix} + \begin{pmatrix} \vdots \\ 0 \\ -a(w_1^k + \alpha w_0^k) \end{pmatrix}, \\
\dot{\boldsymbol{w}}^{k+1} &= \begin{bmatrix} b-\frac{a}{\beta} & -a & & \\ -c & 0 & c & \\ & \ddots & \ddots & \ddots \end{bmatrix} \boldsymbol{w}^{k+1} + \begin{pmatrix} f_0 \\ f_1 \\ \vdots \end{pmatrix} + \begin{pmatrix} \frac{a}{\beta}(u_0^k + \beta u_{-1}^k) \\ 0 \\ \vdots \end{pmatrix}.
\end{aligned}
\tag{4.125}
$$

The same type solution as for the new WR algorithm without overlap is found. With similar manipulations to those we used before, we obtain the convergence factor of the new WR algorithm: for the case $|\lambda_+^2| > 1$ it is given by

$$\rho_{opt}(s,a,b,c,\alpha,\beta) = \frac{c(\lambda_-^2 - 1) + \alpha s}{c(\lambda_+^2 - 1) + \alpha s} \cdot \frac{\beta c(1-\lambda_-^2) + s}{\beta c(1-\lambda_+^2) + s},$$

and for the case $|\lambda_-^2| > 1$, we obtain

$$\rho_{opt}(s,a,b,c,\alpha,\beta) = \frac{c(\lambda_+^2 - 1) + \alpha s}{c(\lambda_-^2 - 1) + \alpha s} \cdot \frac{\beta c(1-\lambda_+^2) + s}{\beta c(1-\lambda_-^2) + s}.$$

Therefore, the convergence factor for the new WR algorithm with overlap at an even row is given by

$$\rho_{opt}(s,a,b,c,\alpha,\beta) = \begin{cases} \frac{c(\lambda_-^2-1)+\alpha s}{c(\lambda_+^2-1)+\alpha s} \cdot \frac{\beta c(1-\lambda_-^2)+s}{\beta c(1-\lambda_+^2)+s}, & |\lambda_+^2| > 1, \\ \frac{c(\lambda_+^2-1)+\alpha s}{c(\lambda_-^2-1)+\alpha s} \cdot \frac{\beta c(1-\lambda_+^2)+s}{\beta c(1-\lambda_-^2)+s}, & |\lambda_+^2| < 1. \end{cases} \tag{4.126}$$

From the convergence factor (4.126), the optimal values of the parameters α and β can be derived.

Theorem 4.12 (Optimal Convergence). *The new WR algorithm (4.125) converges in two iterations, independently of the initial waveforms $\hat{\boldsymbol{u}}^0$ and $\hat{\boldsymbol{w}}^0$, if*

$$\hat{\alpha}_{even} = -\frac{c(\lambda_-^2 - 1)}{s}, \quad \hat{\beta}_{even} = -\frac{s}{c(1-\lambda_-^2)}, \quad |\lambda_+^2| > 1, \tag{4.127}$$

$$\hat{\alpha}_{even} = -\frac{c(\lambda_+^2 - 1)}{s}, \quad \hat{\beta}_{even} = -\frac{s}{c(1-\lambda_+^2)}, \quad |\lambda_+^2| < 1. \tag{4.128}$$

Proof. The proof is analogous to the proof of Theorem 4.10. □

We will study now an optimal WR algorithm with overlap at an odd row. The new WR algorithm with an overlap at an odd row, using the new transmission conditions

$$u_0^{k+1} + \alpha u_{-1}^{k+1} = w_0^k + \alpha w_{-1}^k, \quad w_{-1}^{k+1} + \beta w_{-2}^{k+1} = u_{-1}^k + \beta u_{-2}^k, \tag{4.129}$$

is given by

$$\begin{aligned}
\dot{\boldsymbol{u}}^{k+1} &= \begin{bmatrix} \ddots & \ddots & \ddots & \\ & a & b & -a \\ & & -c & -c\alpha \end{bmatrix} \boldsymbol{u}^{k+1} + \begin{pmatrix} \vdots \\ f_{-2} \\ f_{-1} \end{pmatrix} + \begin{pmatrix} \vdots \\ 0 \\ c(w_0^k + \alpha w_{-1}^k) \end{pmatrix}, \\
\dot{\boldsymbol{w}}^{k+1} &= \begin{bmatrix} \frac{c}{\beta} & c & & \\ a & b & -a & \\ & \ddots & \ddots & \ddots \end{bmatrix} \boldsymbol{w}^{k+1} + \begin{pmatrix} f_{-1} \\ f_0 \\ \vdots \end{pmatrix} + \begin{pmatrix} -\frac{c}{\beta}(u_{-1}^k + \beta u_{-2}^k) \\ 0 \\ \vdots \end{pmatrix}.
\end{aligned} \tag{4.130}$$

The same type solution is found here as well, and similar computations as before show that the convergence factor ρ_{opt} of the new WR algorithm with overlap at an odd row is given by

$$\rho_{opt}(s, a, b, c, \alpha, \beta) = \begin{cases} \frac{s\lambda_-^2 + \alpha c(\lambda_-^2 - 1)}{s + \alpha c(1 - \lambda_-^2)} \cdot \frac{c(1-\lambda_-^2) + \beta s \lambda_-^2}{c(\lambda_-^2 - 1) + \beta s}, & |\lambda_+^2| > 1, \\ \frac{s\lambda_+^2 + \alpha c(\lambda_+^2 - 1)}{s + \alpha c(1 - \lambda_+^2)} \cdot \frac{c(1-\lambda_+^2) + \beta s \lambda_+^2}{c(\lambda_+^2 - 1) + \beta s}, & |\lambda_+^2| < 1. \end{cases} \tag{4.131}$$

The optimal values of the parameters α and β are given in the following theorem.

Theorem 4.13 (Optimal Convergence). *The new WR algorithm (4.130) converges in two iterations, independently of the initial waveforms $\hat{\boldsymbol{u}}^0$ and $\hat{\boldsymbol{w}}^0$, if*

$$\hat{\alpha}_{odd} = -\frac{s}{c(1-\lambda_+^2)}, \quad \hat{\beta}_{odd} = \frac{c(1-\lambda_+^2)}{s}, \quad |\lambda_+^2| > 1, \tag{4.132}$$

$$\hat{\alpha}_{odd} = -\frac{s}{c(1-\lambda_-^2)}, \quad \hat{\beta}_{odd} = \frac{c(1-\lambda_-^2)}{s}, \quad |\lambda_+^2| < 1. \tag{4.133}$$

Proof. The proof is analogous to the proof of Theorem 4.10. □

Remark 4.6. *Theorems 4.13 and 4.12 imply a relation between the optimal choices obtained with overlap at an even row and at an odd row. They imply that the best parameters satisfy*

$$\hat{\beta}_{even} = -\hat{\alpha}_{odd} - \frac{s}{c}, \quad \hat{\alpha}_{even} = -\hat{\beta}_{odd} - \frac{b}{a} + \frac{s}{a}. \tag{4.134}$$

As we have seen before for the extra small and small circuits, the optimal choices without overlap in Theorems 4.10 and 4.11, and the optimal choices with overlap in Theorems 4.12 and 4.13 are not just parameters but the Laplace transform of linear operators in time, since they depend on s. Therefore, we again propose an approximation by a constant of the best possible transmission conditions.

4.3.5 An Optimized WR Algorithm with Overlap and Constant Approximation

The fundamental optimization process is the same for the large circuit as it is for the smaller ones. We consider here the WR algorithm with overlap and not the one without overlap, since from the optimal choices in Theorems 4.10 and 4.11 with a cut at an even row and a cut at an odd row and without overlap, we have $\beta_{opt} = -\alpha_{opt} + \frac{(s-b)}{a}$ and $\beta_{opt} = -\alpha_{opt} - \frac{s}{c}$ respectively, which are again operators in s. From the optimal choices with overlap in Theorems 4.12 and 4.13, we have as before $\beta_{opt} = -\frac{1}{\alpha_{opt}}$, which will simplify the optimization process.

Remark 4.7. *The optimal convergence factor with a cut at an odd row without overlap (4.121), and with the choice of parameters $\beta = -\alpha - \frac{s}{c}$ is equal to the optimal convergence factor with overlap at an odd row (4.131), and with the choice of parameters $\beta = -\frac{1}{\alpha}$. Furthermore, the optimal convergence factor with a cut at an even row without overlap (4.114), and with the choice of parameters $\beta = -\alpha + \frac{(s-b)}{a}$ is equal to the optimal convergence factor with overlap at an even row (4.126), and with the choice of parameters $\beta = -\frac{1}{\alpha}$.*

We now look for a constant approximation of the optimal choice in (4.132) for the new WR algorithm with overlap at an odd row. From this constant approximation we can find a first order approximation of the optimal choice of the new WR algorithm with overlap at an even row using the relation in (4.134). This includes however implementations of first order derivatives in the transmission conditions to have the optimized WR algorithm with overlap at an even row.

The simplest way to obtain a constant approximation is again the low frequency approximation using a Taylor expansion about $s = 0$. However, for this infinitely large transmission line circuit there is no zeroth order low frequency approximation for $s = 0$, since we get a division by zero when we try to find a Taylor expansion of the optimal choice in (4.132) about $s = 0$.

The analyticity of the convergence factor ρ_{opt} in the right half of the complex plane, which allows us to apply the maximum principle, is shown in the following lemma.

Lemma 4.7. *Assume*

$$a > 0, \quad b < 0, \quad c < 0. \tag{4.135}$$

Then the convergence factor ρ_{opt} in (4.131) is an analytic function in the right half of the complex plane, $s = \eta + i\omega$, $\eta > 0$, if

$$\alpha < 0, \quad \beta > 0. \tag{4.136}$$

Proof. The proof is similar to the proof of Theorem 4.9. We consider the subregions of the complex plane defined in (4.106), and we define

$$g_1(s,a,b,c,\alpha,\beta) = \begin{cases} \frac{s\lambda_+^2+\alpha c(\lambda_+^2-1)}{s+\alpha c(1-\lambda_+^2)} \cdot \frac{c(1-\lambda_+^2)+\beta s\lambda_+^2}{c(\lambda_+^2-1)+\beta s}, & s \in \Omega_1, \\ \lim\limits_{\omega \downarrow \omega^*} \left(\frac{s\lambda_+^2+\alpha c(\lambda_+^2-1)}{s+\alpha c(1-\lambda_+^2)} \cdot \frac{c(1-\lambda_+^2)+\beta s\lambda_+^2}{c(\lambda_+^2-1)+\beta s}\right), & s \in \Gamma_1, \end{cases}$$

$$g_2(s,a,b,c,\alpha,\beta) = \begin{cases} \frac{s\lambda_-^2+\alpha c(\lambda_-^2-1)}{s+\alpha c(1-\lambda_-^2)} \cdot \frac{c(1-\lambda_-^2)+\beta s\lambda_-^2}{c(\lambda_-^2-1)+\beta s}, & s \in \Omega_2 \bigcup \Gamma_1, \\ \lim\limits_{\omega \downarrow -\omega^*} \left(\frac{s\lambda_-^2+\alpha c(\lambda_-^2-1)}{s+\alpha c(1-\lambda_-^2)} \cdot \frac{c(1-\lambda_-^2)+\beta s\lambda_-^2}{c(\lambda_-^2-1)+\beta s}\right), & s \in \Gamma_2, \end{cases}$$

$$g_3(s,a,b,c,\alpha,\beta) = \frac{s\lambda_+^2+\alpha c(\lambda_+^2-1)}{s+\alpha c(1-\lambda_+^2)} \cdot \frac{c(1-\lambda_+^2)+\beta s\lambda_+^2}{c(\lambda_+^2-1)+\beta s}, \quad s \in \Omega_3 \bigcup \Gamma_2.$$

The convergence factor ρ_{opt} in (4.131) for the optimized WR algorithm is now given by

$$\rho_{opt}(s,a,b,c,\alpha,\beta) = \begin{cases} g_1(s,a,b,c,\alpha,\beta), & s \in \Omega_1, \\ g_2(s,a,b,c,\alpha,\beta), & s \in \Gamma_1, \\ g_2(s,a,b,c,\alpha,\beta), & s \in \Omega_2, \\ g_3(s,a,b,c,\alpha,\beta), & s \in \Gamma_2, \\ g_3(s,a,b,c,\alpha,\beta), & s \in \Omega_3. \end{cases} \tag{4.137}$$

We showed in the proof of Theorem 4.9 that $\lambda_\pm^2$ are analytic in Ω_1, Ω_2, and Ω_3. Hence, by Theorem 1.4, it suffices to show that the denominator does not have zeros in order to prove the analyticity of g_1, g_2, and g_3 in Ω_1, Ω_2, and Ω_3 respectively. We first consider ρ_{opt} in Ω_1, and assume that $\alpha c(1-\lambda_+^2)+s=0$ to find a contradiction. This implies $\lambda_+^2 = 1+\frac{s}{\alpha c}$, but with the conditions (4.135) and (4.136), we have $|\lambda_+^2| > 1$, which is in contradiction to the fact that $|\lambda_+^2| < 1$ in Ω_1. A similar proof holds for the other quotient. Thus, there is no pole in the right half of the complex plane in Ω_1. We now consider ρ_{opt} in Ω_2. We again assume that $\alpha c(1-\lambda_-^2)+s=0$ to find a contradiction. This implies $\lambda_-^2 = 1+\frac{s}{\alpha c}$, but with the conditions (4.135) and (4.136), we have $|\lambda_-^2| > 1$, which is in contradiction to the fact that $|\lambda_-^2| < 1$ in Ω_2, and a similar proof holds for the second quotient. Therefore, there is no pole in the right half of the complex plane in Ω_2. A similar argument as the one for ρ_{opt} in Ω_1 holds for ρ_{opt} in Ω_3. The functions g_1, g_2, and g_3 are continuous in $\Omega_1 \bigcup \Gamma_1$, $\Gamma_1 \bigcup \Omega_2 \bigcup \Gamma_2$, and $\Omega_3 \bigcup \Gamma_2$ respectively. By Lemma 4.6, we have

$$\lim_{\omega \downarrow \omega^*} \left(\frac{s\lambda_+^2+\alpha c(\lambda_+^2-1)}{s+\alpha c(1-\lambda_+^2)} \cdot \frac{c(1-\lambda_+^2)+\beta s\lambda_+^2}{c(\lambda_+^2-1)+\beta s} \right) = \lim_{\omega \uparrow \omega^*} \left(\frac{s\lambda_-^2+\alpha c(\lambda_-^2-1)}{s+\alpha c(1-\lambda_-^2)} \cdot \frac{c(1-\lambda_-^2)+\beta s\lambda_-^2}{c(\lambda_-^2-1)+\beta s} \right),$$

which means $g_1(s,a,b,c,\alpha,\beta) = g_2(s,a,b,c,\alpha,\beta)$ on Γ_1, and by the same lemma we also have

$$\lim_{\omega \uparrow -\omega^*} \left(\frac{s\lambda_+^2+\alpha c(\lambda_+^2-1)}{s+\alpha c(1-\lambda_+^2)} \cdot \frac{c(1-\lambda_+^2)+\beta s\lambda_+^2}{c(\lambda_+^2-1)+\beta s} \right) = \lim_{\omega \downarrow -\omega^*} \left(\frac{s\lambda_-^2+\alpha c(\lambda_-^2-1)}{s+\alpha c(1-\lambda_-^2)} \cdot \frac{c(1-\lambda_-^2)+\beta s\lambda_-^2}{c(\lambda_-^2-1)+\beta s} \right),$$

which means $g_3(s, a, b, c, \alpha, \beta) = g_2(s, a, b, c, \alpha, \beta)$ on Γ_2. Therefore, by Theorem 4.8, ρ_{opt} is an analytic function in the right half of the complex plane, $s = \eta + i\omega$, $\eta > 0$. $\square$

We now take $s = re^{i\theta}$, $-\pi/2 < \theta < \pi/2$, to find the limit of ρ_{opt} as r goes to infinity in all directions in the right half of the complex plane. Considering ρ_{opt} in (4.131), we find that when $|\lambda_+^2| > 1$, the limit as $r \to \infty$ is zero, and the same limit also for the case when $|\lambda_-^2| > 1$. We again use the maximum principle, Theorem 1.5 to find the maximum in $|\rho_{opt}|$ for $s = \eta + i\omega$, $\eta > 0$ on the boundary. Therefore, the maximum is attained at $\eta = 0$. However, similar to the classical WR algorithm, as noted earlier, taking the limit on the boundary as ω goes to zero, we find that $|\rho_{opt}| = 1$. Therefore, as for the infinitely large RC type circuit, we will truncate the frequency range by a minimal frequency relevant for our problem.

The modulus of the convergence factor ρ_{opt} in (4.131) satisfies the following property.

Lemma 4.8. *The modulus of the convergence factor ρ_{opt} in (4.131), for $s = i\omega$, satisfies*

$$|\rho_{opt}(i|\omega|, a, b, c, \alpha, \beta)| = |\rho_{opt}(-i|\omega|, a, b, c, \alpha, \beta)|.$$

Proof. We consider $\lambda_\pm^2$ given in (4.95), where we have $z = 2 + C_1 s + C_2 s^2$, $C_1 = \frac{|b|}{\tilde{c}}$, $C_2 = \frac{1}{\tilde{c}}$, and $\tilde{c} = a|c|$. Now for $\eta = 0$, we have

$$z = x + iy = (2 - C_2\omega^2) + iC_1\omega,$$

and

$$\lambda_\pm^2 = \frac{x + iy \pm \sqrt{(x^2 - y^2 - 4) + 2xyi}}{2}.$$

We will treat several cases.

1. If $y = 0$, then from $y = C_1\omega$, we have $\omega = 0$, and hence there is nothing to show.

2. If $x = 0$, then from $x = 2 - C_2\omega^2$, we have $\omega = \pm\sqrt{\frac{2}{C_2}} = \pm\sqrt{2a|c|}$, and $\lambda_\pm$ is given by

$$\lambda_\pm = \frac{1}{2}(y \pm \sqrt{y^2+4})i.$$

As we have shown in Lemma 4.5, for $\omega = \sqrt{2a|c|}$, $\eta = 0$, we have $|\lambda_+^2| > 1$, and for $\omega = -\sqrt{2a|c|}$, $\eta = 0$, we have $|\lambda_+^2| < 1$. Therefore, we have to show that $|\rho_{opt}|$ in the region where $|\lambda_+^2| > 1$, at $\omega = \sqrt{2a|c|}$, equals $|\rho_{opt}|$ in the region where $|\lambda_+^2| < 1$, at $\omega = -\sqrt{2a|c|}$. For $|\lambda_+^2| > 1$, ρ_{opt} in (4.131) can be simplified to

$$\rho_{opt}(s,a,b,c,\alpha,\beta) = \frac{\beta\lambda_-^2 s^2 + \alpha c^2(2-\lambda_-^2-\lambda_+^2) + c(1-\lambda_-^2)(1-\alpha\beta c)s}{\beta\lambda_+^2 s^2 + \alpha c^2(2-\lambda_+^2-\lambda_-^2) + c(1-\lambda_+^2)(1-\alpha\beta c)s}, \quad |\lambda_+^2| > 1.$$

Using $\lambda_+^2 + \lambda_-^2 = \frac{s(b-s)}{ac} + 2$ from Vieta's formulas, Theorem 4.4, and with some simplification we obtain

$$\rho_{opt}(s,a,b,c,\alpha,\beta) = \frac{a\beta\lambda_-^2 s^2 + \alpha cs(s-b) + ac(1-\lambda_-^2)(1-\alpha\beta c)s}{a\beta\lambda_+^2 s^2 + \alpha cs(s-b) + ac(1-\lambda_+^2)(1-\alpha\beta c)s}, \quad |\lambda_+^2| > 1. \tag{4.138}$$

For the case $|\lambda_+^2| < 1$, we have

$$\rho_{opt}(s,a,b,c,\alpha,\beta) = \frac{a\beta\lambda_+^2 s^2 + \alpha cs(s-b) + ac(1-\lambda_+^2)(1-\alpha\beta c)s}{a\beta\lambda_-^2 s^2 + \alpha cs(s-b) + ac(1-\lambda_-^2)(1-\alpha\beta c)s}, \quad |\lambda_+^2| < 1. \tag{4.139}$$

For $s = i\bar{\omega}$, where $\bar{\omega} = \sqrt{\frac{2}{C_2}} > 0$, ρ_{opt} is given by

$$\begin{aligned}&\rho_{opt}(i\bar{\omega},a,b,c,\alpha,\beta)\\ &\quad= \frac{-\beta a\bar{\omega}\bar{y} + \beta a\bar{\omega}\sqrt{\bar{y}^2+4} + 2ac - 2ac^2\alpha\beta - 2\alpha cb + i(ac\sqrt{\bar{y}^2+4} - ac\bar{y} + ac^2\alpha\beta\bar{y} - ac^2\alpha\beta\sqrt{\bar{y}^2+4} + 2\alpha c\bar{\omega})}{-\beta a\bar{\omega}\bar{y} - \beta a\bar{\omega}\sqrt{\bar{y}^2+4} + 2ac - 2ac^2\alpha\beta - 2\alpha cb + i(-ac\sqrt{\bar{y}^2+4} - ac\bar{y} + ac^2\alpha\beta\bar{y} + ac^2\alpha\beta\sqrt{\bar{y}^2+4} + 2\alpha c\bar{\omega})},\end{aligned}$$

and $\bar{y} = C_1\bar{\omega}$. Now, for $s = -i\bar{\omega}$, and $y = -\bar{y} = -C_1\bar{\omega}$, ρ_{opt} is given by

$$\begin{aligned}&\rho_{opt}(-i\bar{\omega},a,b,c,\alpha,\beta)\\ &\quad= \frac{-\beta a\bar{\omega}\bar{y} + \beta a\bar{\omega}\sqrt{\bar{y}^2+4} + 2ac - 2ac^2\alpha\beta - 2\alpha cb - i(ac\sqrt{\bar{y}^2+4} - ac\bar{y} + ac^2\alpha\beta\bar{y} - ac^2\alpha\beta\sqrt{\bar{y}^2+4} + 2\alpha c\bar{\omega})}{-\beta a\bar{\omega}\bar{y} - \beta a\bar{\omega}\sqrt{\bar{y}^2+4} + 2ac - 2ac^2\alpha\beta - 2\alpha cb - i(-ac\sqrt{\bar{y}^2+4} - ac\bar{y} + ac^2\alpha\beta\bar{y} + ac^2\alpha\beta\sqrt{\bar{y}^2+4} + 2\alpha c\omega)}.\end{aligned}$$

Therefore,

$$|\rho_{opt}(i\bar{\omega},a,b,c,\alpha,\beta)| = |\rho_{opt}(-i\bar{\omega},a,b,c,\alpha,\beta)|.$$

3. If $x \neq 0$ and $y \neq 0$, then as in the proof of Lemma 4.5, for $x > 0$, we have the case where $-\sqrt{2a|c|} < \omega < \sqrt{2a|c|}$, and for $x < 0$, we have either $\omega < -\sqrt{2a|c|}$ or $\omega > \sqrt{2a|c|}$. We consider first the case $x > 0$, which implies $-\sqrt{2a|c|} < \omega < \sqrt{2a|c|}$. The real and imaginary parts of λ_+^2 and λ_-^2 are given by

$$\begin{aligned}
&\Re(\lambda_+^2) = \tfrac{1}{2}x + \tfrac{1}{4}\psi(x,y), \quad \Re(\lambda_-^2) = \tfrac{1}{2}x - \tfrac{1}{4}\psi(x,y),\\
&\Im(\lambda_+^2) = \tfrac{1}{2}y + \tfrac{1}{4}\tfrac{2xy}{|2xy|}\varphi(x,y), \quad \Im(\lambda_-^2) = \tfrac{1}{2}y - \tfrac{1}{4}\tfrac{2xy}{|2xy|}\varphi(x,y),
\end{aligned}$$

where

$$\psi(x,y) = \sqrt{2\sqrt{x^4 + 2x^2y^2 - 8x^2 + y^4 + 8y^2 + 16} + 2x^2 - 2y^2 - 8},$$

and

$$\varphi(x,y) = \sqrt{2\sqrt{x^4 + 2x^2y^2 - 8x^2 + y^4 + 8y^2 + 16} - 2x^2 + 2y^2 + 8}.$$

The convergence factor ρ_{opt} in (4.138) can be simplified for $s = i\omega$, with $-\sqrt{2a|c|} < \omega < \sqrt{2a|c|}$, to

$$\rho_{opt}(\omega, x(\omega), y(\omega), a, b, c, \alpha, \beta) = \frac{T_1}{T_2}, \tag{4.140}$$

where T_1 and T_2 are given by

$$\begin{aligned}
T_1 := \Big(&(-\beta a(\tfrac{1}{2}x - \tfrac{1}{4}\psi(x,y)) - \alpha c)\omega^2\\
&+(ac(\tfrac{1}{2}y - \tfrac{1}{4}\tfrac{2xy}{|2xy|}\varphi(x,y)) - ac^2\alpha\beta(\tfrac{1}{2}y - \tfrac{1}{4}\tfrac{2xy}{|2xy|}\varphi(x,y)))\omega\Big)\\
&+i\,\Big((ac^2\alpha\beta(\tfrac{1}{2}x - \tfrac{1}{4}\psi(x,y)) + ac(1-(\tfrac{1}{2}x - \tfrac{1}{4}\psi(x,y))) - ac^2\alpha\beta - \alpha cb)\omega\\
&-\beta a\omega^2(\tfrac{1}{2}y - \tfrac{1}{4}\tfrac{2xy}{|2xy|}\varphi(x,y))\Big),
\end{aligned}$$

and

$$\begin{aligned}
T_2 := \Big(&(-\beta a(\tfrac{1}{2}x + \tfrac{1}{4}\psi(x,y)) - \alpha c)\omega^2\\
&+(ac(\tfrac{1}{2}y + \tfrac{1}{4}\tfrac{2xy}{|2xy|}\varphi(x,y)) - ac^2\alpha\beta(\tfrac{1}{2}y + \tfrac{1}{4}\tfrac{2xy}{|2xy|}\varphi(x,y)))\omega\Big)\\
&+i\,\Big((ac^2\alpha\beta(\tfrac{1}{2}x + \tfrac{1}{4}\psi(x,y)) + ac(1-(\tfrac{1}{2}x + \tfrac{1}{4}\psi(x,y))) - ac^2\alpha\beta - \alpha cb)\omega\\
&-\beta a\omega^2(\tfrac{1}{2}y + \tfrac{1}{4}\tfrac{2xy}{|2xy|}\varphi(x,y))\Big),
\end{aligned}$$

where $x = 2 - C_2\omega^2$ and $y = C_1\omega$. Now, for $\omega > 0$, since $y = C_1\omega$, $C_1 > 0$, we have $y > 0$, and for $\omega < 0$, $y < 0$. Therefore, for the case where $\omega < 0$ and $y < 0$, we have, using the fact that we are in the region where $x > 0$,

$$\begin{aligned}
T_1 &= (-\beta a(\tfrac{1}{2}x - \tfrac{1}{4}\psi(x,-|y|)) - \alpha c)|\omega|^2 \\
&\quad +(ac(\tfrac{-1}{2}|y| + \tfrac{1}{4}\tfrac{2x|y|}{|2xy|}\varphi(x,-|y|)) - ac^2\alpha\beta(\tfrac{-1}{2}|y| + \tfrac{1}{4}\tfrac{2x|y|}{|2xy|}\varphi(x,-|y|)))(-|\omega|) \\
&\quad +i\Big((ac^2\alpha\beta(\tfrac{1}{2}x - \tfrac{1}{4}\psi(x,-|y|)) + ac(1-(\tfrac{1}{2}x - \tfrac{1}{4}\psi(x,-|y|))) - ac^2\alpha\beta - \alpha cb)(-|\omega|) \\
&\quad -\beta a|\omega|^2(\tfrac{-1}{2}|y| + \tfrac{1}{4}\tfrac{2x|y|}{|2xy|}\varphi(x,-|y|))\Big) \\
&= (-\beta a(\tfrac{1}{2}x - \tfrac{1}{4}\psi(x,-|y|)) - \alpha c)|\omega|^2 \\
&\quad +(ac(\tfrac{1}{2}|y| - \tfrac{1}{4}\varphi(x,-|y|)) - ac^2\alpha\beta(\tfrac{1}{2}|y| - \tfrac{1}{4}\varphi(x,-|y|)))|\omega| \\
&\quad -i\left((ac^2\alpha\beta(\tfrac{1}{2}x - \tfrac{1}{4}\psi(x,-|y|)) + ac(1-(\tfrac{1}{2}x - \tfrac{1}{4}\psi(x,-|y|))) - ac^2\alpha\beta - \alpha cb)|\omega|\right. \\
&\quad \left. -\beta a|\omega|^2(\tfrac{1}{2}|y| - \tfrac{1}{4}\varphi(x,-|y|))\right).
\end{aligned}$$

Now, for $w > 0$ and $y > 0$, we have

$$\begin{aligned}
T_1 &= (-\beta a(\tfrac{1}{2}x - \tfrac{1}{4}\psi(x,|y|)) - \alpha c)|\omega|^2 \\
&\quad +(ac(\tfrac{1}{2}|y| - \tfrac{1}{4}\varphi(x,|y|)) - ac^2\alpha\beta(\tfrac{1}{2}|y| - \tfrac{1}{4}\varphi(x,|y|)))|\omega| \\
&\quad +i\left((ac^2\alpha\beta(\tfrac{1}{2}x - \tfrac{1}{4}\psi(x,|y|)) + ac(1-(\tfrac{1}{2}x - \tfrac{1}{4}\psi(x,|y|))) - ac^2\alpha\beta - \alpha cb)|\omega|\right. \\
&\quad \left. -\beta a|\omega|^2(\tfrac{1}{2}|y| - \tfrac{1}{4}\varphi(x,|y|))\right),
\end{aligned}$$

and a similar argument holds for T_2.

Since $\varphi(x,-|y|) = \varphi(x,|y|)$ and $\psi(x,-|y|) = \psi(x,|y|)$, the modulus of T_1 and T_2 for $\omega > 0$ equals the modulus of T_1 and T_2 for $\omega < 0$ respectively, and hence the convergence factor in (4.140) satisfies

$$|\rho_{opt}(|\omega|, a, b, c, \alpha, \beta)| = |\rho_{opt}(-|\omega|, a, b, c, \alpha, \beta)|.$$

For the case $x < 0$, where we have $|\lambda_+^2| < 1$, and the region where $\omega < -\sqrt{2a|c|}$ or $\omega > \sqrt{2a|c|}$, a similar argument holds.

□

Therefore, by Lemma 4.8, we can optimize for positive frequencies, $\omega > 0$, and we get the min-max problem

$$\min_{\alpha<0,\beta>0}\left(\max_{0<\omega_{min}\leq\omega\leq\omega_{max}}|\rho_{opt}(i\omega,a,b,c,\alpha,\beta)|\right), \tag{4.141}$$

where we truncated the frequency range by minimal and maximal, practically relevant frequencies for our problem, as we did for the infinitely large RC circuit, where we used $\omega_{min} = \frac{\pi}{T}$ and $\omega_{max} = \frac{\pi}{\Delta t}$ as estimates for the lowest and highest numerical frequencies.

We assume $\beta = -\frac{1}{\alpha}$ as we did for the extra small and small circuits, motivated by the optimal choice, which will simplify the optimization process.

Extensive numerical experiments show that the solution of the min-max problem (4.141) with the choice $\beta = -\frac{1}{\alpha}$ occurs when the convergence factor at $\omega = \omega_{min}$ and at $\omega = \overline{\omega}$ are balanced, where ω_{min} is small and $\overline{\omega}$ is the interior maximum of $|\rho_{opt}|$. Therefore, we use the equation

$$R_0(\omega_{min}, a, b, c, \alpha^*) = R_0(\overline{\omega}, a, b, c, \alpha^*), \tag{4.142}$$

where $R_0(\omega, a, b, c, \alpha) = |\rho_{opt}|$, and ρ_{opt} is given in (4.131) for $s = i\omega$, to determine the best constant α^*. With this choice of α^*, $R_0(\omega, a, b, c, \alpha^*) \leq R_0(\omega_{min}, a, b, c, \alpha^*) := \bar{R}_{O0}$ for all $\omega \geq \omega_{min}$. We show on the top of Figure 4.20 the convergence factor as a function of the frequency ω and the optimization parameter α. We observe that the solution of the min-max problem (4.141) occurs when the convergence factor at $\omega = \omega_{min}$ and at $\omega = \overline{\omega}$ are balanced. In this example where we take $\omega_{min} = 0.00001$, the optimized constant α is equal to $\alpha^* = -2.3938$, and this leads to the convergence factor shown at the bottom of Figure 4.20.

To obtain an explicit formula for the optimized parameter we again use asymptotics. We assume $\omega_{min} = \epsilon$, and look for a solution for ϵ small. To see that there is a solution for equation (4.142) for ϵ small, we use the ansatz $\alpha = C_\alpha\epsilon^{\gamma_1}$, and $\overline{\omega} = C_\omega\epsilon^{\gamma_2}$.

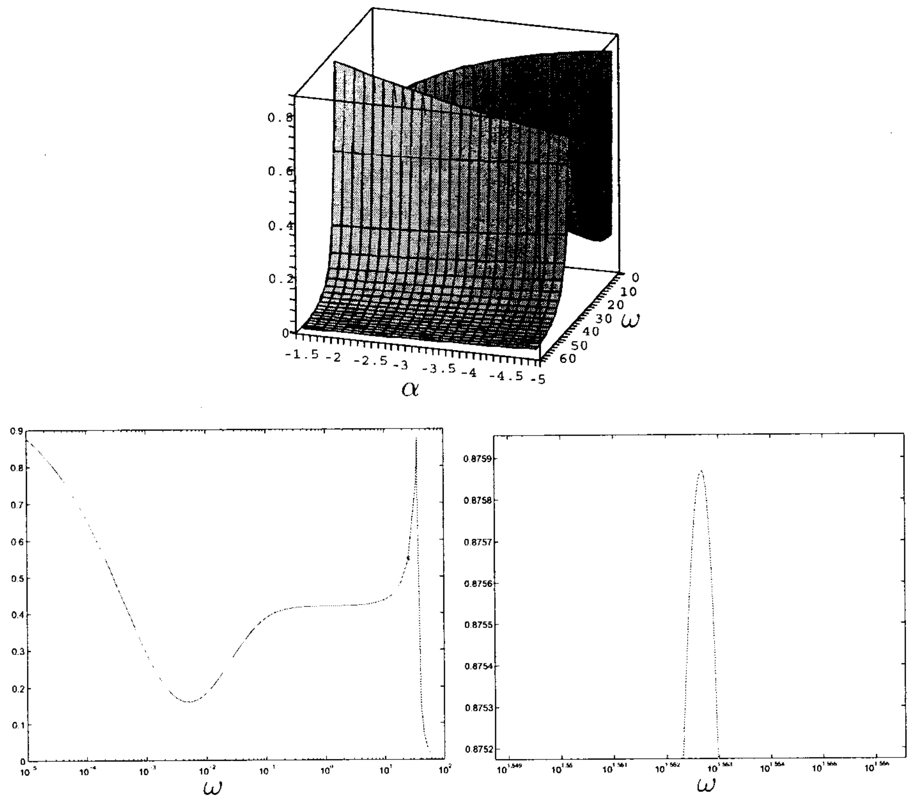

Figure 4.20: Top: convergence factor $|\rho_{opt}(\omega, \alpha)|$. Bottom: optimized convergence factor $|\rho_{opt}(\omega, \alpha^*)|$ and a zoom around the maximum. The asterisk in the figure is the point where we change from the case $|\lambda_+^2| > 1$ to $|\lambda_+^2| < 1$.

The leading asymptotic terms as ϵ goes to zero of the polynomial $P(\omega)$, which we obtain from the partial derivative of $R_0 = |\rho_{opt}|$ with respect to ω, and giving the extrema of R_0, at the maximum $\overline{\omega}$ is given by

$$P(\overline{\omega}) = \sqrt{2abc}C_\omega^4 a^2 \epsilon^{4\gamma_2} - 2\sqrt{2abc}a^2 c C_\omega^3 C_\alpha \epsilon^{\gamma_1+3\gamma_2} + \ldots.$$

Similarly, expanding the equation (4.142) for ϵ small, we find the leading order terms

$$1 + \frac{2\sqrt{2abc}}{bcC_\alpha}\epsilon^{1/2-\gamma_1} + \cdots = 1 + \frac{\sqrt{2abc}C_\alpha}{aC_\omega^{1/2}}\epsilon^{\gamma_1-\gamma_2/2} + \frac{\sqrt{2abc}C_\omega^{1/2}}{ac}\epsilon^{\gamma_2/2} + \ldots.$$

Equating the exponents in the expansions leads to $\gamma_1 = \frac{1}{3}$, $\gamma_2 = \frac{1}{3}$. Since the constants need to mach as well, we obtain

$$C_\alpha = \frac{2^{1/3}\left(\frac{a\sqrt{2c}}{b}\right)^{2/3}}{2c}, \quad C_\omega = 2^{1/3}\left(\frac{a\sqrt{2c}}{b}\right)^{2/3},$$

which leads to the asymptotic result

$$\alpha^* = \frac{2^{1/3}\left(\frac{a\sqrt{2c}}{b}\right)^{2/3}}{2c}(\omega_{min})^{1/3}. \tag{4.143}$$

Table 4.1 gives a comparison of the optimized constant α^* with the asymptotic approximation (4.143). We choose for the circuit elements the values $R_s = 0.05$ kOhms, $R = 0.5e-3$ kOhms, $L = 4.95e-3$ μH, and $C = 0.63$ pF. One can see that the asymptotic result for α^* is very close to the optimized α^* for small ω_{min}, for which we proved the existence of the equioscillation and the asymptotic result (4.143). In the case where ω_{min} is not small, there is no equioscillation and the solution of the min-max problem is found numerically. This is indeed the case for the value of α^* in Table 4.1 for $\omega_{min} = \frac{\pi}{T}$ where $T = 2.5$ and $T = 20$. Both have the same numerically optimized constant α^* where there is no equioscillation, but the asymptotic result is quite different from the numerically optimized one.

Table 4.1: Comparison of the optimized constant α^* and its asymptotic approximation.

ω_{min}	$\frac{\pi}{2.5}$	$\frac{\pi}{20}$	0.0001	0.00001	0.000001	0.0000001	0.00000001
opt.α^*	-6.5066	-6.5066	-5.8752	-2.3938	-1.0861	-0.5019	-0.2327
asy.α^*	-116.5539	-58.2769	-5.0133	-2.3270	-1.0801	-0.5013	-0.2327

An example for the convergence factor as a function of the frequency ω and using the transmission line circuit elements used above is given in Figure 4.21, where we choose $\omega_{min} = \frac{\pi}{20}$ to compute the numerically optimized constant $\alpha^* = -6.5066$, and the asymptotic value $\alpha^*_{asy} = -58.2769$, and we plot the optimized convergence factor using both results. We also compare in Figure 4.21 the optimized convergence factor with the classical one.

4.3.6 Numerical Experiments

We show here that the optimized WR algorithm also works well for larger circuits. We first choose a transmission line circuit which consists of 150 elements similar to the two used to build the small circuit in Figure 4.8, where $L_i = 4.95e-3$ μH, $C_i = 0.63$ pF, $R_i = 0.5e-3$ kOhms, and $R_s = R_L = 0.05$ kOhms. The solution is based on the backward Euler integration technique and our transient analysis time is $t \in [0, 20]$, with a time step of $\Delta t = 0.02$ ns. The source is $I_s = 20t$ mA for $0 < t < 0.1$ ns, and $I_s = 2$ mA for $t \geq 0.1$ ns. We start with zero initial waveforms. We show the error as a function of the iterations in Figure 4.22, where we use the minimal frequency $\omega_{min} = \frac{\pi}{20}$ and the maximal frequency $\omega_{max} = \frac{\pi}{0.02}$ to find the numerically optimized constant $\alpha^* = -6.5066$, and $\omega_{min} = \frac{\pi}{20}$ is also used to find the asymptotic value $\alpha^*_{asy} = -58.2769$ from (4.143). We also choose $\beta^* = -\frac{1}{\alpha^*}$. Form Figure 4.22, one can see that the optimized WR algorithm is much better than the classical one using both values of α^*.

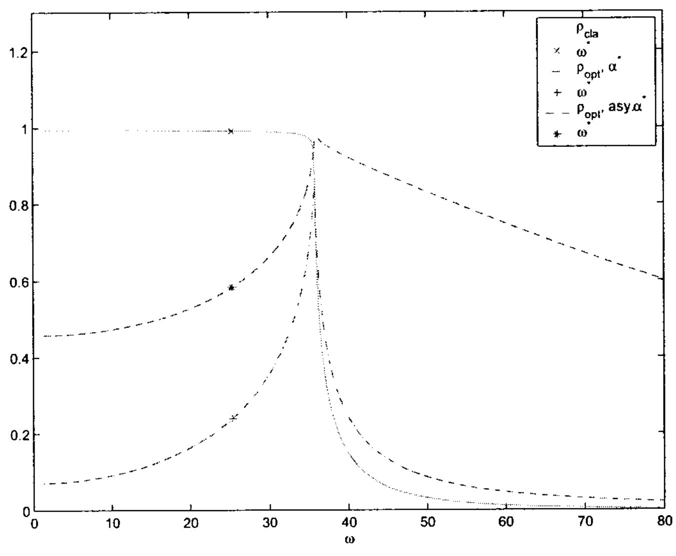

Figure 4.21: Convergence factor as a function of the frequency parameter ω for the optimized WR algorithm applied to the infinitely large circuit versus the classical one.

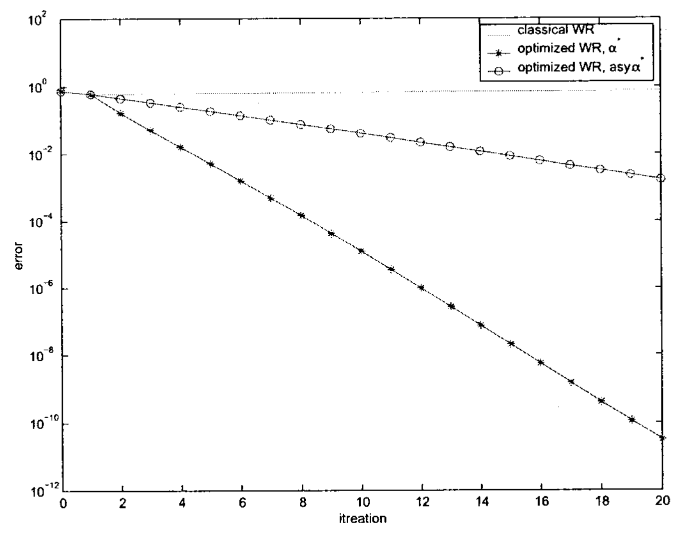

Figure 4.22: Performance of the classical versus the optimized WR algorithms for a larger transmission line circuit.

The last example is more realistic, where we choose a 5 cm TEM mode transmission line model with 150 sections and typical parameters per unit length of $L = 4.95e-3$ μH/cm, $C = 0.63$ pF/cm, $R = 0.5e-3$ kOhms/cm, and we also have $R_s = R_L = 0.05$ kOhms. Hence, for each section

$$L_i = \frac{4.95e-3}{30}\ \mu\text{H},\ C_i = \frac{0.63}{30}\ \text{pF},\ R_i = \frac{0.5e-3}{30}\ \text{kOhms}.$$

The source is $I_s = 20t$ mA for $0 < t < 0.1$ ns, and $I_s = 2$ mA for $t \geq 0.1$ ns, and the analysis time interval is $[0, T]$, with $T = 2.5$ ns. The time step that has been used is $\Delta t = 0.005$ ns. We again use the backward Euler method, and we start with zero initial waveforms. We use $\omega_{min} = \frac{\pi}{2.5}$ and $\omega_{max} = \frac{\pi}{0.005}$, which is not large enough in order to have an interior maximum for this example, to find the numerically optimized constant $\alpha^* = -11.2807$. We also choose ω_{max} to be large enough in order to have an interior maximum, and we use it together with $\omega_{min} = \frac{\pi}{2.5}$ to find the numerically optimized constant $\alpha^* = -6.5120$, which is close to the one from the previous example in which we used the maximum numerical frequency $\omega_{max} = \frac{\pi}{\Delta t}$, which was for that example large enough in order to have an interior maximum. We also use $\omega_{min} = \frac{\pi}{2.5}$ to compute the asymptotic value $\alpha^*_{asy} = -362.1601$ from (4.143) using the new circuit elements given in this example. The modulus of the convergence factor ρ_{opt} as a function of the frequency ω is given in Figure 4.23 using the above three values for α, and we also include the modulus of the classical convergence factor $|\rho_{cla}|$ as a function of ω.

In Figure 4.24 we show again the remarkable convergence of the optimized WR algorithm over the classical WR algorithm. The optimized WR using the asymptotic result is not as good as the one using the other values, since ω_{min} is not small enough to have the equioscillation and leads with the new circuit elements to a large value of α^*. Note that ω_{min} is just an estimate we choose to be $\omega_{min} = \frac{\pi}{T}$ as in Chapter 3 for the RC type circuits which might be chosen differently.

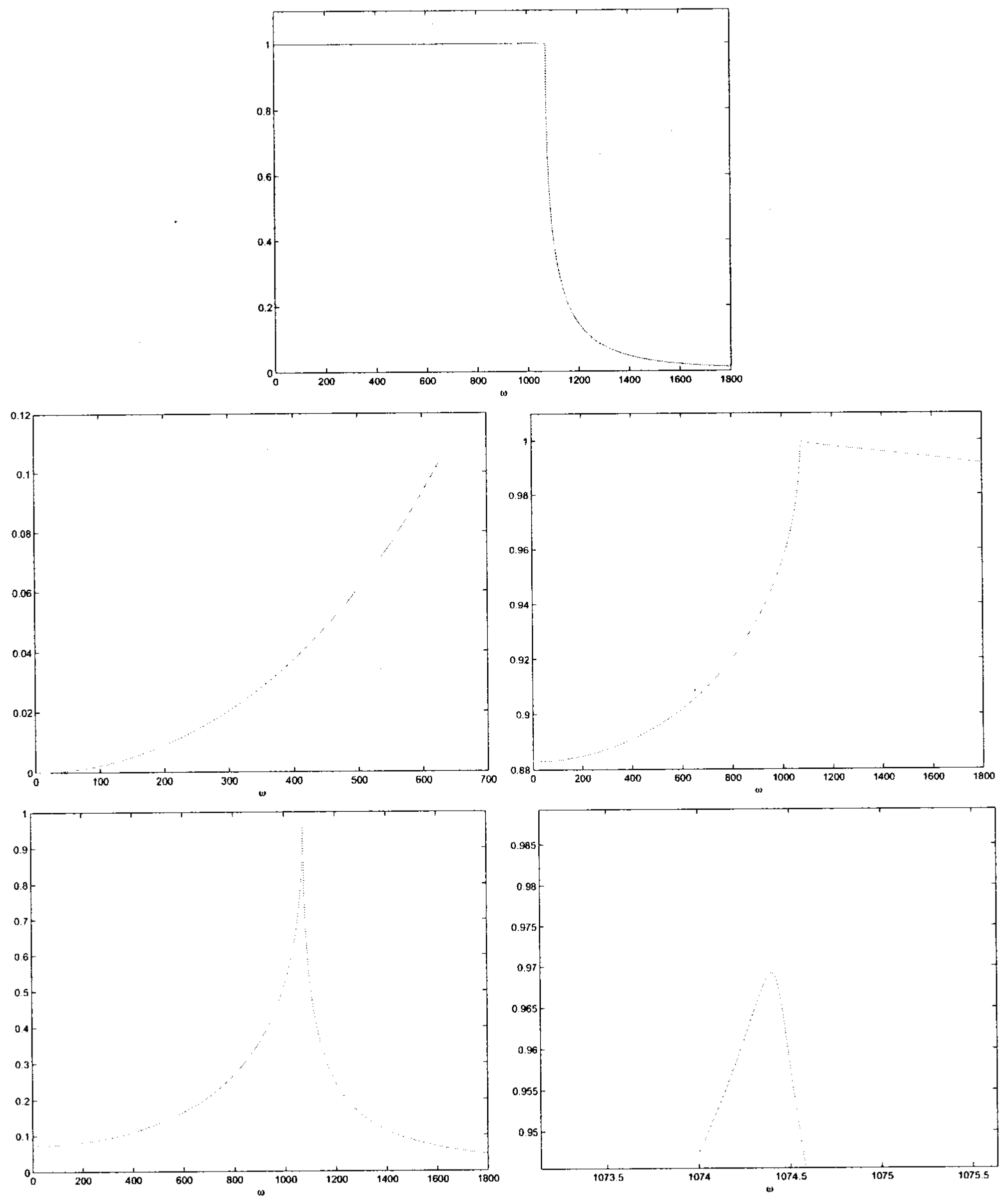

Figure 4.23: Top: $|\rho_{cla}(\omega)|$. Middle: left: $|\rho_{opt}(\omega, \alpha^* = -11.2807)|$. Right: $|\rho_{opt}(\omega, \alpha^*_{asy})|$. Bottom: left: $|\rho_{opt}(\omega, \alpha^* = -6.512)|$ and a zoom around the maximum on the right.

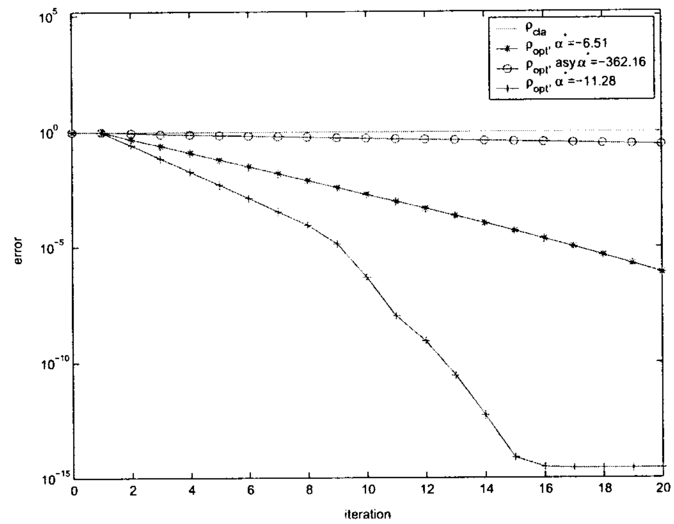

Figure 4.24: Convergence behavior of the classical versus the optimized WR algorithms.

One can also compare the result for the large subsystems with the error decay for the small ones in Figures 4.7 and 4.16, which shows that the convergence for both the classical and the optimized WR algorithms is similar, in spite of the large difference in the subsystems size.

Chapter 5

Relations Between Circuit Problems and Semi-Discretized Partial Differential Equations

In this Chapter we are looking for relations between circuit problems and semi-discretized PDEs. We show first that the RC or diffusive circuit system is indeed a semi-discretization of a particular PDE. The system of differential equations for a finite size RC circuit with n sections is given by

$$\dot{\boldsymbol{v}} = \begin{bmatrix} b_1 & c_1 & & & \\ a_1 & b_2 & c_2 & & \\ & \ddots & \ddots & \ddots & \\ & & a_{m-2} & b_{m-1} & c_{m-1} \\ & & & a_{m-1} & b_m \end{bmatrix} \boldsymbol{v} + \boldsymbol{f}, \tag{5.1}$$

where $m = n + 1$, and we need an initial condition $\boldsymbol{v}(0)$.

Note that in a fixed length of the circuit the number of sections n can be a very large number. If the total resistance is R and the total capacitance is C for the n sections, then $R_i = \frac{R}{n}$ and $C_i = \frac{C}{n}$ for each section. Hence, assuming $a := c_i = a_i$

and $b := b_i = b_1$ as before, we have $a = \frac{n^2}{RC}$ and $b = -\frac{2n^2}{RC}$ in the system representing the circuit. Now, we assume $a = n^2\tilde{a}$ and $b = n^2\tilde{b}$, where $\tilde{a} = \frac{1}{RC}$ and $\tilde{b} = -\frac{2}{RC}$, and in addition let $h = \frac{1}{n}$, where h is a small positive number. Note that the number of sections n plays a significant role in determining the number of unknowns in the system, which is the same role that is played by $\frac{1}{h}$, where h is considered as a step-size in the discretization of a PDE. The system (5.1) becomes

$$\dot{\boldsymbol{v}} = \frac{1}{h^2}\begin{bmatrix} \tilde{b} & \tilde{a} & & & \\ \tilde{a} & \tilde{b} & \tilde{a} & & \\ & \ddots & \ddots & \ddots & \\ & & \tilde{a} & \tilde{b} & \tilde{a} \\ & & & \tilde{a} & \tilde{b} \end{bmatrix} \boldsymbol{v} + \boldsymbol{f}. \tag{5.2}$$

At any row j, we have the differential equation

$$v_{tj} := \dot{v}_j = \frac{\tilde{a}}{h^2}(v_{j-1} + v_{j+1}) + \frac{\tilde{b}}{h^2}v_j + f_j.$$

Adding and subtracting the term $2\frac{\tilde{a}}{h^2}v_j$ on the right hand side leads to

$$v_{tj} = \tilde{a}\frac{v_{j-1} - 2v_j + v_{j+1}}{h^2} + \frac{(\tilde{b} + 2\tilde{a})}{h^2}v_j + f_j. \tag{5.3}$$

Equation (5.3) is a semi-discretization of the reaction diffusion equation

$$v_t - \nu v_{xx} + \bar{b}v = f, \tag{5.4}$$

where $\nu = \tilde{a} > 0$, and $\bar{b} = -\frac{(\tilde{b}+2\tilde{a})}{h^2} \geq 0$, for $\tilde{a} > 0$, $\tilde{b} < 0$, and $-\tilde{b} \geq 2\tilde{a}$, which are conditions introduced earlier in the analysis for the RC circuit in Chapter 3. The heat equation is obtained from (5.4) when $\tilde{b} = -2\tilde{a}$ which often holds for the RC type circuits. Note that otherwise we have that $\bar{b}$ depends on h.

Now, similar to the RC type circuit we will look for a semi-discretized PDE corresponding to the transmission line circuit. The system of differential equations for a finite size transmission line circuit with n sections is given by

$$\dot{\boldsymbol{x}} = \begin{bmatrix} b_1 & c_1 & & & \\ a_1 & b_2 & c_2 & & \\ & \ddots & \ddots & \ddots & \\ & & a_{m-2} & b_{m-1} & c_{m-1} \\ & & & a_{m-1} & b_m \end{bmatrix} \boldsymbol{x} + \boldsymbol{f}, \tag{5.5}$$

with the vector of unknown waveforms $\boldsymbol{x} = (v_1, i_1, v_2, i_2, \ldots, i_n, v_{n+1})^T$, which consists of nodal capacitive voltages alternating with inductance currents in the transmission line circuit, and thus $m = 2n+1$, and we also need an initial condition at time $t = 0$.

If the total resistance is R, the total capacitance is C, and the total inductance is L, then we have $R_i = \frac{R}{n}$, $C_i = \frac{C}{n}$, and $L_i = \frac{L}{n}$ for each section. Thus, with the simplifying assumptions we used in Chapter 4, we have $a = \frac{n}{L}$, $b = -\frac{R}{L}$, $b_1 = -\frac{n}{R_s C}$, and $c = -\frac{n}{C}$ in the circuit system. Assuming $a = n\tilde{a}$, $b_1 = n\tilde{b}_1$, and $c = n\tilde{c}$, where $\tilde{a} = \frac{1}{L}$, $\tilde{b}_1 = -\frac{1}{R_s C}$, and $\tilde{c} = -\frac{1}{C}$, and as before $h = \frac{1}{n}$, the system (5.5) becomes

$$\begin{pmatrix} \dot{v}_1 \\ \dot{i}_1 \\ \dot{v}_2 \\ \vdots \\ \dot{i}_n \\ \dot{v}_{n+1} \end{pmatrix} = \frac{1}{h} \begin{bmatrix} \tilde{b}_1 & \tilde{c} & & & & \\ \tilde{a} & hb & -\tilde{a} & & & \\ & -\tilde{c} & 0 & \tilde{c} & & \\ & & \ddots & \ddots & \ddots & \\ & & & \tilde{a} & hb & -\tilde{a} \\ & & & & -\tilde{c} & \tilde{b}_1 \end{bmatrix} \begin{pmatrix} v_1 \\ i_1 \\ v_2 \\ \vdots \\ i_n \\ v_{n+1} \end{pmatrix} + \begin{pmatrix} f_1^v \\ f_1^i \\ f_2^v \\ \vdots \\ f_n^i \\ f_{n+1}^v \end{pmatrix}. \tag{5.6}$$

For any index j we have two differential equations in time t,

$$i_{tj} := \dot{i}_j = -\tilde{a}\frac{v_{j+1} - v_j}{h} + bi_j + f_j^i, \quad v_{tj} := \dot{v}_j = \tilde{c}\frac{i_j - i_{j-1}}{h} + f_j^v. \tag{5.7}$$

The above two equations represent discretizations in the space variable x of the first order partial differential equations

$$i_t = -\tilde{a}v_x + bi + f^i, \quad v_t = \tilde{c}i_x + f^v. \tag{5.8}$$

Differentiating the first equation in (5.8) with respect to the time t, and the second one with respect to the space variable x, we get

$$i_{tt} = -\tilde{a}v_{xt} + bi_t + f_t^i, \quad v_{tx} = \tilde{c}i_{xx} + f_x^v.$$

Substituting the second equation into the first one, assuming $v_{xt} = v_{tx}$, we obtain the second order partial differential equation

$$i_{tt} = -\tilde{a}\tilde{c}i_{xx} + bi_t + (f_t^i - \tilde{a}f_x^v),$$

which one can write as

$$\psi_{tt} - \gamma^2\psi_{xx} + 2\delta\psi_t = g, \tag{5.9}$$

where we replaced i with ψ, and $\gamma^2 = -\tilde{a}\tilde{c} > 0$ since $\tilde{a} > 0$ and $\tilde{c} < 0$, $2\delta = -b > 0$ since $b < 0$, and we also set $g = f_t^i - \tilde{a}f_x^v$. Equation (5.9) is called the damped wave equation or the Telegrapher's equation.

We have shown above that there is a natural relationship between our circuit problems and semi-discretized PDEs. To further analyze the relationship between the circuit and the PDE problems we consider in the sequel the infinitely large RC circuit case and the reaction diffusion equation

$$\mathcal{L}v := v_t - \nu v_{xx} + \bar{b}v = f, \text{ in } \Omega \times (0, T), \tag{5.10}$$

where $\Omega = \mathbb{R}$, $\nu > 0$, and $\bar{b} > 0$, with an initial condition $v(x, 0) = v_0(x)$ in Ω.

A more general equation is the advection reaction diffusion equation

$$\mathcal{L}v := v_t - \nu v_{xx} + \bar{a}v_x + \bar{b}v = f, \text{ in } \Omega \times (0, T),$$

where $\Omega = \mathbb{R}$, $\nu > 0$, and the advection coefficient $\bar{a}$ and the reaction coefficient $\bar{b}$ are nonnegative constants which do not both vanish simultaneously. WR algorithms for this type of equations were analyzed in [41, 42]. In our case here where in equation (5.10) we have $\bar{a} = 0$ and $\bar{b} > 0$, the results from [41, 42] hold. The case of the

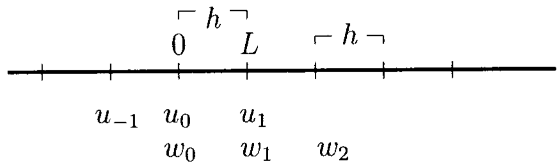

Figure 5.1: Discretization in space.

heat equation where both $\bar{a}$ and $\bar{b}$ are zero was analyzed in [43]. In [41, 42, 43] optimized WR methods are introduced for the advection reaction diffusion and the heat equations to illustrate the great improvement in convergence of the optimized WR methods over the classical ones for this type of equations. We decompose here the spatial domain $\Omega = \mathbb{R}$ into two overlapping subdomains $\Omega_1 = (-\infty, L)$ and $\Omega_2 = (0, \infty)$, $L > 0$, in a way similar to the one introduced in [41] for the advection reaction diffusion equation, and in [43] for the heat equation.

If we call the unknowns in the first subdomain u and in the second one w, then the WR algorithm, which is called Schwarz WR algorithm when the application is PDEs, is for iteration index $k = 0, 1, 2, \ldots$ given by

$$\begin{array}{ll} \mathcal{L}u^{k+1} = f, \text{ in } \Omega_1 \times (0,T), & \mathcal{L}w^{k+1} = f, \text{ in } \Omega_2 \times (0,T), \\ u^{k+1}(.,0) = u_0, \text{ in } \Omega_1, & w^{k+1}(.,0) = w_0, \text{ in } \Omega_2, \\ \mathcal{B}_1 u^{k+1}(L,.) = \mathcal{B}_1 w^k(L,.), \text{ in } (0,T), & \mathcal{B}_2 w^{k+1}(0,.) = \mathcal{B}_2 u^k(0,.), \text{ in } (0,T), \end{array} \tag{5.11}$$

where $\mathcal{B}_1$ and $\mathcal{B}_2$ are linear operators in time, possibly pseudo-differential, and an initial guess $u^0(0,t)$ and $w^0(L,t)$, $t \in (0,T)$, needs to be provided. Note that we use as transmission conditions at the interfaces $x = 0$ and $x = L$ the $\mathcal{B}_i$ applied to solutions obtained from the previous iteration.

The classical Schwarz WR algorithm is obtained by choosing $\mathcal{B}_1$ and $\mathcal{B}_2$ equal to the identity. The new Schwarz WR algorithm is obtained by using the better choice

$$\mathcal{B}_1 = \partial_x + \mathcal{S}_1, \quad \mathcal{B}_2 = \partial_x + \mathcal{S}_2, \tag{5.12}$$

where $\mathcal{S}_1$ and $\mathcal{S}_2$ are again linear operators in time, possibly pseudo-differential, see [41].

We now show that the new transmission conditions introduced for the infinitely large RC circuit in Chapter 3, which are given by

$$\begin{aligned}(u_1^{k+1} - u_0^{k+1}) + \alpha u_1^{k+1} &= (w_1^k - w_0^k) + \alpha w_1^k,\\ (w_1^{k+1} - w_0^{k+1}) + \beta w_0^{k+1} &= (u_1^k - u_0^k) + \beta u_0^k,\end{aligned} \tag{5.13}$$

can be considered as a discretization of the new transmission conditions associated with the PDE with the choice of $\mathcal{B}_1$ and $\mathcal{B}_2$ as in (5.12). The first transmission condition in (5.13) can be written as

$$h\frac{u_1^{k+1} - u_0^{k+1}}{h} + \alpha u_1^{k+1} = h\frac{w_1^k - w_0^k}{h} + \alpha w_1^k,$$

and thus we get

$$h\frac{u^{k+1}(L,.) - u^{k+1}(L-h,.)}{h} + \alpha u^{k+1}(L,.) = h\frac{w^k(L,.) - w^k(L-h,.)}{h} + \alpha w^k(L,.),$$

where the overlap L is equal to the step-size h as shown in Figure 5.1. Therefore, we obtain

$$(h\frac{\partial}{\partial x} + \alpha)u^{k+1}(L,.) = (h\frac{\partial}{\partial x} + \alpha)w^k(L,.),$$

and similarly from the second transmission condition, we have

$$(h\frac{\partial}{\partial x} + \alpha)w^{k+1}(0,.) = (h\frac{\partial}{\partial x} + \alpha)u^k(0,.).$$

Hence, the new transmission conditions at the continuous level are

$$\begin{aligned}(\tfrac{\partial}{\partial x} + \mathcal{S}_1)u^{k+1}(L,.) &= (\tfrac{\partial}{\partial x} + \mathcal{S}_1)w^k(L,.),\\ (\tfrac{\partial}{\partial x} + \mathcal{S}_2)w^{k+1}(0,.) &= (\tfrac{\partial}{\partial x} + \mathcal{S}_2)u^k(0,.),\end{aligned}$$

where $\alpha = h\mathcal{S}_1$ and $\beta = h\mathcal{S}_2$. Therefore, the new transmission conditions in (5.13) imply the new transmission conditions associated with the PDE, where $\mathcal{B}_1$ and $\mathcal{B}_2$ are chosen as in (5.12). In Table 5.1 we compare the optimized constant α_c^* obtained from the circuit with the one computed from $\alpha_c^* = h\alpha_p^*$, where α_p^* is the optimized constant from the PDE. One can see that the two values are very close for moderately small values of the overlap h.

Table 5.1: Comparison of the optimized α_c^* from the circuit with the one computed using the optimized α_p^* from the PDE.

h	0.1	0.01	0.001	0.0001
α_p^*	0.6241	0.9464	0.9898	0.9943
$\alpha_c^* = h\alpha_p^*$	0.0624	0.0095	9.898e-4	9.943e-5
α_c^* circuit	0.1032	0.0100	9.956e-4	9.947e-5

We study now the relation between the convergence factor obtained from applying the new WR algorithm to the PDE at the continuous level and the one obtained from applying the algorithm to the system of ODEs which represents the discrete problem. Assuming that $\nu > 0$ and $\bar{b} > 0$ are two arbitrary constants, the differential system that arises from the semi-discretization of the PDE in (5.10), using the centered finite difference discretization with step-size h to approximate the second partial derivative with respect to x,

$$\begin{aligned} v_{tj} &= \nu \frac{v_{j-1} - 2v_j + v_{j+1}}{h^2} - \bar{b}v_j + f_j, \\ &= \frac{\nu}{h^2} v_{j-1} - \left(\frac{2\nu}{h^2} + \bar{b}\right) v_j + \frac{\nu}{h^2} v_{j+1} + f_j, \; j \in \mathbb{Z}, \end{aligned}$$

is given by the system of ODEs

$$\dot{\boldsymbol{v}} = \begin{pmatrix} \ddots & \ddots & \ddots & & \\ & \underline{a} & \underline{b} & \underline{a} & \\ & & \underline{a} & \underline{b} & \underline{a} \\ & & \ddots & \ddots & \ddots \end{pmatrix} \boldsymbol{v} + \boldsymbol{f}, \tag{5.14}$$

and $\underline{a} = \frac{\nu}{h^2} > 0$, and $\underline{b} = -\frac{(2\nu + \bar{b}h^2)}{h^2} < 0$. Note that, using the values for ν and $\bar{b}$ obtained from the circuit system, the system in (5.14) is the same as the one in (5.2) representing the circuit, since by using those values for ν and $\bar{b}$ we get $\underline{a} = \frac{\bar{a}}{h^2}$ and $\underline{b} = \frac{\bar{b}}{h^2}$, which are the same as in (5.2).

The transmission conditions associated with the PDE (5.10) as we find above are

$$\begin{aligned}(\tfrac{\partial}{\partial x} + \mathcal{S}_1)u^{k+1}(L,.) &= (\tfrac{\partial}{\partial x} + \mathcal{S}_1)w^k(L,.),\\ (\tfrac{\partial}{\partial x} + \mathcal{S}_2)w^{k+1}(0,.) &= (\tfrac{\partial}{\partial x} + \mathcal{S}_2)u^k(0,.),\end{aligned}$$

and the discretized ones are

$$\begin{aligned}u_1^{k+1} - u_0^{k+1} + \alpha u_1^{k+1} &= w_1^k - w_0^k + \alpha w_1^k,\\ w_1^{k+1} - w_0^{k+1} + \beta w_0^{k+1} &= u_1^k - u_0^k + \beta u_0^k.\end{aligned}$$

By linearity, we will consider the homogeneous problems for the analysis below, where $f = 0$ and $v(.,0) = 0$. The solutions of the two sub-systems we obtain by decomposing the system in (5.14) into two subsystems exactly as we did in Chapter 3, using Laplace transform and boundedness at infinity, are

$$\begin{aligned}\hat{u}_j^k(s) &= C_1^k\lambda_+^j,\ j = 1, 0, -1, \ldots,\\ \hat{w}_j^k(s) &= C_2^k\lambda_-^j,\ j = 0, 1, 2, \ldots,\end{aligned}$$

where $\lambda_\pm$ are given by

$$\lambda_\pm = \frac{s - \underline{b} \pm \sqrt{(s-\underline{b})^2 - 4\underline{a}^2}}{2\underline{a}}.$$

Using the discretized transmission conditions, and taking $\beta = -\alpha$, we get

$$\rho_c(s, \underline{a}, \underline{b}, \alpha) = \left(\tfrac{\alpha+1-\lambda_+}{(\alpha+1)\lambda_+-1}\right)^2 = \left(\tfrac{\alpha+1-\lambda_+}{\alpha+1-\lambda_-}\right)^2\lambda_-^2, \tag{5.15}$$

which is the optimal convergence factor we have found for the infinitely large RC circuit in Chapter 3, and we used $\lambda_- = \frac{1}{\lambda_+}$ to get the last equality on the right. However, we have here $\underline{a}$ and $\underline{b}$ which both depend on h instead of a and b. Using the fact that $h \longrightarrow 0$, $\lambda_\pm$ are simplified to

$$\lambda_\pm = \frac{h^2(s+\bar{b}) + 2\nu \pm \sqrt{(h^2(s+\bar{b}) + 2\nu)^2 - 4\nu^2}}{2\nu}.$$

The solutions of the two homogeneous PDEs we obtain by decomposing the PDE in (5.10) as given in (5.11) are given in [41], where the Fourier transform is used to obtain the solutions. Similarly, we apply instead here the Laplace transform in time to (5.11), and we use boundedness at infinity to get the solutions. Therefore, we will have the same solutions but in terms of the Laplace parameter $s = \eta + i\omega$ instead of the Fourier parameter ω. The solutions are given by

$$\hat{u}^k(x,s) = \tilde{C}_1^k e^{r^+(x-L)}, \ x \in (-\infty, L),$$
$$\hat{w}^k(x,s) = \tilde{C}_2^k e^{r^- x}, \ x \in (0, \infty),$$

where

$$r^{\pm} = \pm\sqrt{\frac{s+\bar{b}}{\nu}}. \tag{5.16}$$

Using the continuous transmission conditions, we obtain the convergence factor

$$\rho_p(s, \bar{b}, \nu, \sigma_1, \sigma_2) = \frac{\sigma_1 - r^+}{\sigma_1 - r^-} \cdot \frac{\sigma_2 - r^-}{\sigma_2 - r^+} e^{2r^- L}.$$

Since the convergence factor above vanishes if we insert $\sigma_1 = r^+ = -r^-$ and $\sigma_2 = r^-$ into ρ_p, these values are indeed the optimal values, and moreover, $\sigma_2 = -\sigma_1$. Thus assuming $\sigma_2 = -\sigma_1$, as above for the discrete case, the convergence factor is

$$\rho_p(s, \bar{b}, \nu, \sigma_1) = \left(\frac{\sigma_1 - r^+}{\sigma_1 - r^-}\right)^2 e^{2r^- L},$$

where $r^{\pm}$ are given in (5.16).

We consider below the solutions in Ω_2, i.e. $x \in (0, \infty)$ and $j = 0, 1, \ldots$. If we assume $x = jh$, then $j = \frac{x}{h}$, and as $h \to 0$ we want to show the following limits:

$$\lambda_-^{\frac{x}{h}}(h) \to e^{r^- x},$$

$$\rho_c \longrightarrow \rho_p.$$

The Taylor expansion of $\lambda_-^{\frac{x}{h}}$ for small h is given by

$$\begin{aligned}\lambda_-^{\frac{x}{h}} = & \left(e^{-x\sqrt{\frac{\bar{b}+s}{\nu}}}\right) + \left(e^{-x\sqrt{\frac{\bar{b}+s}{\nu}}}\right)\frac{x(\bar{b}+s)\sqrt{\nu(\bar{b}+s)}}{24\nu^2}h^2 \\ & + \left(e^{-x\sqrt{\frac{\bar{b}+s}{\nu}}}\right)\frac{x(\bar{b}+s)^2(-27\sqrt{\nu(\bar{b}+s)}+5x\bar{b}+5xs)}{5760\nu^3}h^4 \\ & + \left(e^{-x\sqrt{\frac{\bar{b}+s}{\nu}}}\right)\dots h^6 + O(h^8).\end{aligned}$$

Therefore, as $h \to 0$, $\lambda_-^{\frac{x}{h}}$ converges to $e^{r^- x} = e^{-x\sqrt{\frac{\bar{b}+s}{\nu}}}$. For the other limit, we first note that

$$\lambda_- \to e^{r^- L}, \text{ as } h \to 0,$$

which can be seen by taking $x = h$ in the previous limit we have shown, i.e. $\lambda_-^{\frac{h}{h}}$ will converge to $e^{r^- L} = 1$, where the overlap L equals the step-size h. Next, we substitute $\alpha = h\sigma_1$ into the convergence factor ρ_c given in (5.15), and hence we need to show that

$$\left(\frac{h\sigma_1 + 1 - \lambda_+}{h\sigma_1 + 1 - \lambda_-}\right) \to \left(\frac{\sigma_1 - r^+}{\sigma_1 - r^-}\right),$$

which is obtained as follows:

$$\begin{aligned}\lim_{h\to 0}\left(\frac{h\sigma_1+1-\lambda_+}{h\sigma_1+1-\lambda_-}\right) &= \lim_{h\to 0}\frac{-2h\sigma_1\nu+\bar{b}h^2+sh^2+\sqrt{(\bar{b}+s)h^2(sh^2+4\nu+\bar{b}h^2)}}{-2h\sigma_1\nu+\bar{b}h^2+sh^2-\sqrt{(\bar{b}+s)h^2(sh^2+4\nu+\bar{b}h^2)}} \\ &= \lim_{h\to 0}\frac{-2\sigma_1\nu+\bar{b}h+sh+\sqrt{(\bar{b}+s)(sh^2+4\nu+\bar{b}h^2)}}{-2\sigma_1\nu+\bar{b}h+sh-\sqrt{(\bar{b}+s)(sh^2+4\nu+\bar{b}h^2)}} \\ &= \frac{\sigma_1\nu-\sqrt{\nu(s+\bar{b})}}{\sigma_1\nu+\sqrt{\nu(s+\bar{b})}} \\ &= \frac{\sigma_1\sqrt{\nu}-\sqrt{s+\bar{b}}}{\sigma_1\sqrt{\nu}+\sqrt{s+\bar{b}}} \\ &= \frac{\sigma_1-r^+}{\sigma_1-r^-}.\end{aligned}$$

Therefore, we have $\rho_c \to \rho_p$ as $h \to 0$.

We have shown above that $\rho_c \to \rho_p$, and that the solution of the second differential subsystem obtained from the partitioning of the differential system that arises from the semi-discretization of the PDE converges to the solution of the PDE in Ω_2, i.e. $\hat{w}_j \to \hat{w}(x)$ as the step-size h goes to zero. In other words, the discrete case converges to the continuous one as the step-size h goes to zero, and the same can be shown for the solutions in Ω_1 similarly.

Similar arguments can also be found for the other PDE obtained for the transmission line circuit using similar work and analysis.

Conclusions

We have shown that the classical WR algorithm has difficulties to converge for many circuit problems. Much better convergence in the sense of being more uniform and faster, can be obtained by improving the information exchange between the decomposed subsystems. This has been achieved by new transmission conditions that exchange a combination of voltages and currents rather than just voltages or just currents from one subsystem to its neighboring subsystems as in the classical WR algorithm. Optimal transmission conditions are in general nonlocal and thus less convenient to use. The constant and first order approximations proposed instead lead to practical optimized WR algorithms, which are not complicated and can be easily implemented by only changing the few lines in the WR code responsible for the transmission conditions. In addition, we have demonstrated for the RC circuits that taking first order approximation for the optimal symbols in the transmission conditions leads to a faster and more uniform convergence than the constant approximation.

By considering the general circuit, we have shown that the optimized WR works for general systems of ODEs, and by considering the infinitely large circuits, we have shown that the size of the circuit does not have a major impact on the convergence of the optimized WR methods. Numerical experiments given confirm the theoretical results.

Future work could involve:

- Analyzing a general transmission line circuit of size n.
- Other possible asymptotics for the infinitely large transmission line circuit. Indeed, the asymptotics introduced for the infinitely large transmission line circuit seem to be not the right one with minimal frequency estimate $\omega_{min} = \frac{\pi}{T}$, and thus we are working on expansions about the circuit elements instead, which are similar to those used for the very small and small transmission line circuits case.
- Different ansatz to find the first order approximation for the small RC circuit, where we will use the ansatz $\tilde{p} = C_p \epsilon^{\gamma_1} + \tilde{C}_p \epsilon^{\tilde{\gamma}_1}$ instead, and find the exponents and match the constants in the expansions to get a better result.
- Applying the WR algorithms to the Telegrapher's equation in a similar way to the advection reaction diffusion equation, and studying the relations between the transmission line circuit and this PDE.
- Working on new expansions and asymptotics based on h from the relationship between the PDEs and the circuit problems and their optimal parameters as a new approach to get approximations of the optimal parameters for the circuit problems.
- Proofs of optimality for the zeroth order approximations proposed for the transmission line circuits, and the first order approximations proposed for the small and infinitely large RC circuits.
- Extending the results shown in this thesis to other types of circuits such as high pass, transmission line with delays, and resistive circuits.
- Parallel implementation.

Appendix A

Polynomials and Expansions

The polynomial P in Theorem 3.8 is given by

$$\begin{aligned}P(\tilde{x}) = {} & -2c^2(1+2q+2q\tilde{p}^2+64c^6\tilde{p}^3+16c^4\tilde{p}^4+24qc^4-8c^2\tilde{p}-24c^4q^2 \\ & -512q^3c^{12}-64q^3c^8+256c^{12}q^4-256c^{12}-128c^8\tilde{p}^2q^2-192c^8q-256c^{10}\tilde{p} \\ & +512qc^{12}-16c^8q^4-32c^4+176c^8+24c^4\tilde{p}^2+96c^8q^2+128c^6\tilde{p}+128qc^8\tilde{p}^2 \\ & +512qc^{10}\tilde{p}-256c^{10}q^2\tilde{p}+q^2-192qc^6\tilde{p}-64c^6\tilde{p}q^2-16c^4\tilde{p}^2q \\ & -\tilde{p}^4+4c^2\tilde{p}q^2+8c^4\tilde{p}^2q^2+24c^2\tilde{p}q)\tilde{x}^4-2c^2(-96c^4\tilde{p}q \\ & -384q^3c^{10}-96c^6\tilde{p}^2+96qc^6\tilde{p}^2-64c^6\tilde{p}^2q^2-16c^6q^4-192c^8\tilde{p} \\ & -16c^4\tilde{p}^3-8qc^2\tilde{p}^2-64q^3c^6+112c^6q^2-128c^{10}q^2+256c^{10}q^4-128c^{10}+16c^4\tilde{p} \\ & -192c^8\tilde{p}q^2+32c^6+384qc^8\tilde{p}+384c^{10}q-64qc^6-8qc^2-8c^2q^2+4c^2\tilde{p}^2q^2)\tilde{x}^3 \\ & -2c^2(64c^8q^4+32qc^8\tilde{p}^2-32c^8q+32c^8+16c^6\tilde{p}^3+4c^4\tilde{p}^4+128qc^{12}-128q^3c^{12} \\ & -64c^{10}\tilde{p}+32c^6\tilde{p}q^2+16qc^4+128qc^{10}\tilde{p}-4c^4q^4-64c^8q^2+20c^4q^2-16q^3c^4 \\ & -64c^{10}q^2\tilde{p}-64c^{12}+16c^4\tilde{p}^2q-32c^8\tilde{p}^2q^2+64c^{12}q^4-4c^4 \\ & +16c^6\tilde{p})\tilde{x}^2-2c^2(64c^{10}q^4+64c^{10}q^2-128q^3c^{10}-16c^6\tilde{p}^2q^2-32c^6q^2 \\ & +32q^3c^6)\tilde{x}-2c^2(16c^8q^4+16c^8q^2-32q^3c^8).\end{aligned} \tag{A.1}$$

The polynomial Q in Theorem 3.8 is given by

$$
\begin{aligned}
Q(\tilde{x}, c, \tilde{p}, q) = {} & 4\tilde{x}c^2(1+2\tilde{x}c^2)(-16c^8+128\tilde{x}^2c^8-32c^{10}\tilde{x}-64\tilde{x}^4c^8-64\tilde{x}^3c^6 \\
& +2\tilde{x}^3c^2+4\tilde{x}^4c^4+128c^{10}\tilde{x}^3-16\tilde{x}^2c^4+32\tilde{x}c^6)q^2+4\tilde{x}c^2(1+2\tilde{x}c^2) \\
& (-64\tilde{x}^4c^6\tilde{p}-32\tilde{x}c^6+128\tilde{x}^4c^8-128\tilde{x}^3c^8\tilde{p}+20\tilde{x}^2c^4 \\
& -256c^{10}\tilde{x}^3+16c^8-128\tilde{x}^2c^8+128\tilde{x}^3c^6+\tilde{x}^4+4\tilde{x}^4c^2\tilde{p}-24\tilde{x}^4c^4+32c^8\tilde{x}\tilde{p} \\
& +64c^{10}\tilde{x}-8\tilde{x}^3c^2)q+4\tilde{x}c^2(1+2\tilde{x}c^2)(12\tilde{x}^4c^2\tilde{p}+16\tilde{x}^2c^4+\tilde{x}^4 \\
& +32\tilde{x}^2c^6\tilde{p}+\tilde{x}^4\tilde{p}^2+4\tilde{x}^4c^4-8\tilde{x}c^6-64\tilde{x}^4c^8-32c^{10}\tilde{x}-32\tilde{x}^3c^4\tilde{p}-8\tilde{x}^3c^2 \\
& +128c^{10}\tilde{x}^3+128\tilde{x}^3c^8\tilde{p}+32\tilde{x}^3c^6\tilde{p}^2+16\tilde{x}^2c^4\tilde{p}^2-16\tilde{x}^4c^4\tilde{p}^2 \\
& -8c^6\tilde{x}\tilde{p}^2-32c^8\tilde{x}\tilde{p}-64\tilde{x}^4c^6\tilde{p}-8\tilde{x}^3c^2\tilde{p}^2).
\end{aligned}
\tag{A.2}
$$

The leading asymptotic terms in (3.104) are given by

$$
\begin{aligned}
P_{Expan} = {} & -30C_p^4C_1^4\epsilon^{4\gamma_1+4\delta}-8C_p^4C_1^2\epsilon^{4\gamma_1+2\delta}-146C_1^4C_q^2\epsilon^{4\delta+2\gamma_2}+64C_q^2C_1^2C_p\epsilon^{2\delta+2\gamma_2+\gamma_1} \\
& +72C_1^2\epsilon^{2\delta}-688C_1^4C_pC_q\epsilon^{4\delta+\gamma_1+\gamma_2}+352C_1^3C_p\epsilon^{3\delta+\gamma_1}+222C_1^4\epsilon^{4\delta} \\
& -176C_p^2C_1^3C_q\epsilon^{3\delta+2\gamma_1+\gamma_2}+192C_1^3\epsilon^{3\delta}+64C_q^3\epsilon^{3\gamma_2}-32C_p^3C_1^2\epsilon^{3\gamma_1+2\delta} \\
& +632C_1^4C_pC_q^2\epsilon^{4\delta+\gamma_1+2\gamma_2}-228C_1^4C_qC_p^2\epsilon^{4\delta+\gamma_2+2\gamma_1}-224C_1^2C_q\epsilon^{2\delta+\gamma_2} \\
& -692C_1^4C_q\epsilon^{4\delta+\gamma_2}+96C_1^2C_p\epsilon^{2\delta+\gamma_1}-256C_1^2C_qC_p\epsilon^{2\delta+\gamma_1+\gamma_2}-480C_q^4C_1^3\epsilon^{4\gamma_2+3\delta} \\
& -32C_q^4\epsilon^{4\gamma_2}+896C_q^3C_1^3\epsilon^{3\gamma_2+3\delta}+384C_q^2C_1^3C_p\epsilon^{3\delta+2\gamma_2+\gamma_1}-96C_1^2C_qC_p^2\epsilon^{2\delta+\gamma_2+2\gamma_1} \\
& -48C_1^4C_p^2\epsilon^{2\gamma_1+4\delta}+288C_1^2C_q^3\epsilon^{2\delta+3\gamma_2}+192C_1C_q^3\epsilon^{\delta+3\gamma_2}+64C_p^2C_1^2C_q^2\epsilon^{2\delta+2\gamma_1+2\gamma_2} \\
& +88C_1^2C_q^2\epsilon^{2\delta+2\gamma_2}-128C_q^4C_1\epsilon^{4\gamma_2+\delta}-576C_1^3C_qC_p\epsilon^{3\delta+\gamma_1+\gamma_2}-624C_1^3C_q\epsilon^{3\delta+\gamma_2} \\
& +48C_1^3C_q^2\epsilon^{3\delta+2\gamma_2}+1152C_1^4C_q^3\epsilon^{4\delta+3\gamma_2}+32C_p^3C_1^3\epsilon^{3\gamma_1+3\delta}-32C_q^2\epsilon^{2\gamma_2} \\
& -248C_q^4C_1^2\epsilon^{4\gamma_2+2\delta}+192C_1^3C_p^2\epsilon^{3\delta+2\gamma_1}+240C_p^2C_1^4C_q^2\epsilon^{2\gamma_1+4\delta+2\gamma_2} \\
& +120C_p^2C_1^3C_q^2\epsilon^{3\delta+2\gamma_1+2\gamma_2}+272C_1^4C_p\epsilon^{4\delta+\gamma_1}-64C_1C_q^2\epsilon^{\delta+2\gamma_2} \\
& +32C_p^2C_1C_q^2\epsilon^{\delta+2\gamma_1+\gamma_2}-128C_1^4C_p^3\epsilon^{4\delta+3\gamma_1}+\ldots,
\end{aligned}
$$

$$
\begin{aligned}
Q_{Expan} = {} & 1160C_1^4C_q^2\epsilon^{4\delta+2\gamma_2}+288C_1^5C_q^2\epsilon^{5\delta+2\gamma_2}+840C_1^6C_q\epsilon^{6\delta+\gamma_2}-160C_1^2\epsilon^{2\delta} \\
& -128C_1^3C_p\epsilon^{3\delta+\gamma_1}+608C_1^4\epsilon^{4\delta}-256C_1^3\epsilon^{3\delta}-472C_1^6\epsilon^{6\delta}-416C_1^6C_p\epsilon^{6\delta+\gamma_1} \\
& +132C_1^5C_p^2\epsilon^{5\delta+2\gamma_1}-1408C_1^4C_q\epsilon^{4\delta+\gamma_2}-128C_1^2C_p\epsilon^{2\delta+\gamma_1}-32C_1^2C_p^2\epsilon^{2\delta+2\gamma_1} \\
& -668C_1^5C_q\epsilon^{5\delta+\gamma_2}+560C_1^5C_p\epsilon^{5\delta+\gamma_1}+128C_1^2C_pC_q\epsilon^{2\delta+\gamma_1+\gamma_2}
\end{aligned}
$$

$$+224C_1^4C_p^2\epsilon^{2\gamma_1+4\delta} - 120C_1^6C_p^2\epsilon^{6\delta+2\gamma_1} - 64C_1C_q^2\epsilon^{\delta+2\gamma_2} - 128C_1^2C_q^2\epsilon^{2\delta+2\gamma_2}$$
$$+256C_1^3C_pC_q\epsilon^{3\delta+\gamma_1+\gamma_2} - 176C_1^3C_q\epsilon^{3\delta+\gamma_2} + 448C_1^3C_q^2\epsilon^{3\delta+2\gamma_2}$$
$$+640C_1^4C_p\epsilon^{4\delta+\gamma} + 724C_1^5\epsilon^{5\delta} - 480C_1^6C_q^2\epsilon^{6\delta+2\gamma_2} - 480C_1^6C_qC_p\epsilon^{6\delta+\gamma_1+\gamma_2}$$
$$-512C_1^4C_qC_p\epsilon^{4\delta+\gamma_1+\gamma_2} + 256C_1^2C_q\epsilon^{2\delta+\gamma_2} + 64C_1C_q\epsilon^{\delta+\gamma_2}$$
$$-1264C_1^5C_pC_q\epsilon^{5\delta+\gamma_1+\gamma_2} + \dots,$$

$$R_{1\tilde{x}_0Expan} = \frac{1+4C_p\epsilon^{\gamma_1}+4C_p^2\epsilon^{2\gamma_1}}{16+24C_p\epsilon^{\gamma_1}+9C_p^2\epsilon^{2\gamma_1}} + \dots,$$

$R_{1\bar{\tilde{x}}Expan} = \frac{P_1}{P_2} + \dots,$ where

$$P_1 = 8C_1^2C_q^2\epsilon^{2\delta+2\gamma_2} - 12C_1^2C_q\epsilon^{2\delta+\gamma_1} + 4C_1^3C_p\epsilon^{3\delta+\gamma_1} + 8C_1^3C_q\epsilon^{3\delta+\gamma_2} + 4C_1\epsilon^{\delta}$$
$$-2C_1^2C_p^2\epsilon^{2\delta+2\gamma_1} + 4C_1^2\epsilon^{2\delta} + 4C_1C_q^2\epsilon^{\delta+2\gamma_2} - 8C_1C_q\epsilon^{\delta+\gamma_2} - 7C_1^3\epsilon^{3\delta},$$

$$P_2 = -2C_1^2\epsilon^{2\delta} - 56C_1^3C_p\epsilon^{3\delta+\gamma_1} - 52C_1^3\epsilon^{3\delta} + 16C_1C_p\epsilon^{\delta+\gamma_1} + 12C_1^2C_q\epsilon^{2\delta+\gamma_2}$$
$$-4C_1^2C_p^2\epsilon^{2\delta+2\gamma_1} + 8C_1C_q\epsilon^{\delta+\gamma_2} + 4C_1C_p^2\epsilon^{\delta+2\gamma_1} - 8C_1C_q^2\epsilon^{\delta+2\gamma_2} + 46C_1^2C_q^2\epsilon^{2\delta+2\gamma_2}$$
$$-8C_1^3C_q\epsilon^{3\delta+\gamma_2} + 60C_1^3C_q^2\epsilon^{3\delta+2\gamma_2} - 8C_q^2\epsilon^{2\gamma_2} + 16C_1\epsilon^{\delta} - 15C_1^3C_p^2\epsilon^{3\delta+2\gamma_1}$$
$$-8C_1^2C_p\epsilon^{2\delta+\gamma_1}.$$

The polynomial P in Theorem 3.10 is given by

$$P(\tilde{x}) = -4(q^4c^2 - 2q^3c^2 + 4qc^2 - 2q^2c^2 - \tilde{p}q^2 + 2\tilde{p}q)\tilde{x}^8$$
$$-4(12q^2c^4\tilde{p} + 8q^4c^2 - 6c^2\tilde{p}^2 - 16q^3c^2 - \tilde{p}^3 + 8c^2 - 12c^4\tilde{p} - 40qc^6$$
$$-8c^6 + 4\tilde{p}q^2 + 4\tilde{p} - 8q^4c^6 - 8\tilde{p}q - 8q^2c^2 + 32c^6q^2 - 2c^2\tilde{p}^2q^2 - 8qc^4\tilde{p}$$
$$+6qc^2\tilde{p}^2 + 8q^3c^6 + 8qc^2)\tilde{x}^6$$
$$-4(32qc^2 - 16c^2 - 32c^6 - 16c^4\tilde{p} - 128qc^6 + 160c^6q^2 + 48\tilde{p}^2c^6 + 48c^{10}$$
$$+160qc^{10} - 160q^2c^{10} + 80\tilde{p}c^8 + 12c^4\tilde{p}^3 - 56qc^6\tilde{p}^2 - 32qc^8\tilde{p} - 48c^8\tilde{p}q^2$$
$$+8qc^2\tilde{p}^2 + 16q^2\tilde{p}^2c^6 - 8c^2\tilde{p}^2q^2 - 32q^3c^2 + 32q^3c^{10} + 64qc^4\tilde{p}$$
$$-32q^4c^6 + 16q^4c^{10} + 16q^4c^2 + \tilde{p}^4c^2)\tilde{x}^4$$
$$-4(-64qc^6\tilde{p}^2 + 256q^2c^{14} + 128qc^{12}\tilde{p} + 256c^6q^2 + 64c^{12}\tilde{p}q^2 - 128c^{10}$$
$$-64\tilde{p}c^8 + 256q^3c^{10} + 640qc^{10} - 32q^2c^{10}\tilde{p}^2 - 256qc^6 - 384qc^{14} - 96c^{10}\tilde{p}^2$$
$$-128qc^8\tilde{p} - 48c^8\tilde{p}^3 - 8\tilde{p}^4c^6 + 128c^6 + 32q^2\tilde{p}^2c^6 + 160qc^{10}\tilde{p}^2 - 128q^3c^6$$
$$-512q^2c^{10} - 64c^{12}\tilde{p} - 64c^8\tilde{p}q^2 - 128q^3c^{14})\tilde{x}^2$$

$$+1024c^{10} - 2048qc^{10} + 512qc^{14}\tilde{p}^2 + 4096qc^{14} - 2048qc^{18} - 1024c^{12}\tilde{p}$$
$$-256c^{12}\tilde{p}^3 + 1024c^{16}\tilde{p} - 2048c^{14} + 1024c^{18} - 512qc^{10}\tilde{p}^2 - 64c^{10}\tilde{p}^4. \quad \text{(A.3)}$$

Bibliography

[1] M. Al-Khaleel. Optimized waveform relaxation methods for RC type circuits. Master's thesis, McGill University, Montreal, QC, Canada, 2002.

[2] W. T. Weeks, A. J. Jimenez, G. W. Mahoney, D. Mehta, H. Quassemzadeh, and T. R. Scott. Algorithms for ASTAP - a network analysis program. *IEEE Trans. on Circuit Theory*, CT(20):628–634, November 1973.

[3] C. W. Ho, A. E. Ruehli, and P. A. Brennan. The modified nodal approach to network analysis. *IEEE Trans. on Circuits and Systems*, CAS-22:504–509, June 1975.

[4] J. M. Ortega and W. C. Rheinboldt. *Iterative solution of nonlinear equations in several variables*, volume 30 of *Classics in Applied Mathematics*. Society for Industrial and Applied Mathematics (SIAM), Philadelphia, PA, 2000. Reprint of the 1970 original.

[5] J. White, A. Sangiovanni-Vincentelli, F. Odeh, and A. Ruehli. Waveform relaxation: theory and practise. *Trans. Soc. Computer Simulation*, 2:95–133, 1985.

[6] J. White and A. Sangiovanni-Vincentelli. Relax 2.1 - a waveform relaxation based circuit simulation program. *In Proc. Int. Custom Integ. Circ. Conf.*, June 1984.

[7] E. Picard. Sur l'application des méthods d'approximations successives à l'étude de certaines équations différentielles ordinaires. *J. de Math. Pures et Appl.*, 4e série, 9:217–271, 1893.

[8] E. Lindelöf. Sur l'application des méthods d'approximations successives à l'étude des intégrales réelles des équations différentielles ordinaires. *J. de Math. Pures et Appl.*, 4e série, 10:117–128, 1894.

[9] E. Lelarasmee. *The waveform relaxation method for the time domain analysis of large scale nonlinear dynamical systems.* PhD thesis, University of California, Berkeley, CA, 1982.

[10] E. Lelarasmee, A. E. Ruehli, and A. L. Sangiovanni-Vincentelli. The waveform relaxation method for time-domain anaylsis of large-scale integrated circuits. *IEEE Trans. on CAD of Integrated Circuits and Systems*, CAD-1(3):131–145, July 1982.

[11] C. H. Carlin and C. Vachoux. On partitioning for waveform relaxation time-domain analysis of VLSI circuits. In *Proc. of Int. Conf. on Circ. and Syst.*, 1984. Held in Montreal, 1984.

[12] T. J. Cockerill, H. Y. Hsieh, J. LeBlanc, D. Ostapko, A. E. Ruehli, and J. K. White. Toggle: A circuit analyzer for MOSFET VLSI. In *Proc. Int. Conf. VLSI and Computers (COMP - EURO'87)*, 1987. Held in Hamburg, Germany, May 1987.

[13] J. White and A. Sangiovanni-Vincentelli. *Relaxation techniques for the simulation of VLSI circuits.* Kluwer Academic Publishers, Boston, 1987.

[14] U. Miekkala and O. Nevanlinna. Convergence of dynamic iteration methods for initial value problems. *SIAM J. Sci. Statist. Comput.*, 8:459–482, 1987.

[15] U. Miekkala and O. Nevanlinna. Sets of convergence and stability regions. *BIT*, 27:554–584, 1987.

[16] O. Nevanlinna. Remarks on Picard-Lindelöf iteration. I. *BIT*, 29(2):328–346, 1989.

[17] O. Nevanlinna. Remarks on Picard-Lindelöf iteration. II. *BIT*, 29(3):535–562, 1989.

[18] O. Nevanlinna. Linear acceleration of Picard-Lindelöf iteration. *Numer. Math.*, 57(2):147–156, 1990.

[19] K. Burrage. *Parallel and sequential methods for ordinary differential equations.* Oxford Science Publications, 1995.

[20] R. Jeltsch and B. Pohl. Waveform relaxation with overlapping splittings. *SIAM J. Sci. Comput.*, 16(1):40–49, 1995.

[21] C. Lubich and A. Ostermann. Multi-grid dynamic iteration for parabolic equations. *BIT*, 27(2):216–234, 1987.

[22] S. Vandewalle and G. Horton. Fourier mode analysis of the multigrid waveform relaxation and time-parallel multigrid methods. *Computing*, 54(4):317–330, 1995.

[23] J. Janssen and S. Vandewalle. Multigrid waveform relaxation on spatial finite element meshes: the continuous-time case. *SIAM Journal on Numerical Analysis*, 33(2):456–474, 1996.

[24] J. Janssen and S. Vandewalle. Multigrid waveform relaxation on spatial finite element meshes: the discrete-time case. *SIAM J. Sci. Comput.*, 17(1):133–155, 1996.

[25] M. J. Gander and A. M. Stuart. Space-time continuous analysis of waveform relaxation for the heat equation. *SIAM Journal on Scientific Computing*, 19(6):2014–2031, 1998.

[26] E. Giladi and H. B. Keller. Space time domain decomposition for parabolic problems. *Numerische Mathematik*, 93(2):279–313, 2002.

[27] M. J. Gander, L. Halpern, and F. Nataf. Optimal Schwarz waveform relaxation for the one dimensional wave equation. *SIAM Journal on Numerical Analysis*, 41(5):1643–1681, 2003.

[28] P. Debefve, F. Odeh, and A. Ruehli. *in Circuit Analysis, Simulation and Design, Ruehli Ed.* Part II, Elseviers, North-Holland, New York, Amsterdam, 1987.

[29] V. B. Dmitriev-Zdorov and B. Klaassen. An improved relaxation approach for mixed system analysis with several simulation tools. In *Proc. of EURO-DAC'95, IEEE Comp. Soc. Press*, 1995.

[30] V. B. Dmitriev-Zdorov. Generalized coupling as a way to improve the convergence in relaxation-based solvers. In *Design Automation Conference, 1996, with EURO-VHDL '96 and Exhibition, Proceedings EURO-DAC '96, European*, 1996. Held in Geneva, Switzerland, Sept. 1996.

[31] M. J. Gander and A. Ruehli. Optimized waveform relaxation methods for RC type circuits. *IEEE Transaction on Circuits and Systems*, 51(4):755–768, April 2004.

[32] M. J. Gander and A. Ruehli. Solution of large transmission line type circuits using a new optimized waveform relaxation partitioning. *IEEE International Symposium on Electromagnetic Compatibility*, 2:636–641, August 2003.

[33] J. W. Nilsson and S. A. Riedel. *Electric circuits.* Addison-Wesley Publishing Company, fifth edition, 1996.

[34] P. Henrici. *Applied and computational complex analysis*, volume 2. John Wiley & Sons, NewYork, 1991.

[35] Serge Lang. *Complex analysis.* Springer-Verlag, New York, second edition, 1985.

[36] W. Lepage. *Complex variables and the Laplace transform for engineers.* McGraw-Hill, United State of America, 1961.

[37] F. Zhang, T. Ando, C. Brezinski, R. Horn, C. Johnson, J.-Z. Liu, S. Puntanen, R. Smith, and G.P.H. Steyn. *The Schur complement and its applications.* Springer, New York, 2005.

[38] N. M. Nakhla, A. E. Ruehli, M. S. Nakhla, and R. Achar. Simulation of coupled interconnects using waveform relaxation and transverse partitioning. *IEEE Transactions on Advanced Packaging*, 29:78–87, Feb 2006.

[39] A. I. Kostrikin. *Introduction to Algebra.* Springer-Verlag, New York, 1982.

[40] M. J. Ablowitz and A. S. Fokas. *Complex Variables, Introduction and Applications.* Cambridge University Press, 2 edition, 1997.

[41] M. J. Gander and L. Halpern. Optimized Schwarz waveform relaxation methods for advection reaction diffusion problems. *to appear in SIAM J. Numer. Anal.*, 2007.

[42] D. Bennequin, M. J. Gander, and L. Halpern. A homographic best approximation problem with application to optimized Schwarz waveform relaxation. *submitted*, 2007.

[43] M. J. Gander and L. Halpern. Methodes de relaxation d'ondes pour l'equation de la chaleur en dimension 1. *C. R. Acad. Sci Paris, Série I*, 336(6):519–524, 2003.